MODIFICATION OF LEFT VENTRICULAR GEOMETRY AND FUNCTION DURING HEALING AFTER ACUTE MYOCARDIAL INFARCTION

Bodh I. Jugdutt, MBChB, MSc

A thesis submitted in fulfillment of the requirements

for the degree of Doctor of Medicine (MD),

FACULTY OF MEDICINE, UNIVERSITY OF GLASGOW

The research was conducted in the Division of Cardiology,

Department of Medicine, Faculty of Medicine, University of Alberta,

Edmonton, Alberta, T6G 2R7, CANADA.

Submitted December 2004

Revised January 2006

ProQuest LLC.
789 East Eisenhower Parkway
P.O. Box 1346
Ann Arbor, MI 48106 – 1346

Modification of left ventricular geometry and function during healing after acute myocardial infarction

MD dissertation

Faculty of Medicine, University of Glasgow

ABSTRACT

Increased left ventricular (LV) size and deformation of LV geometry are associated with LV dysfunction. Regional shape distortion (RSD), detected on two-dimensional echocardiography (2D-Echo) after acute myocardial infarction (MI), is associated with poor outcome.

Two hypotheses were tested: i) early RSD of the asynergic infarct zone after MI is followed by progressive global LV dilatation, remodelling towards a spheroidal shape, and more LV dysfunction; and ii) the progressive remodelling of LV geometry spans the phases of early infarction and healing and may be modified by early and prolonged therapies applied over the phases of infarction and healing.

A bench to bedside approach was used, with concurrent studies in a dog model of healing over 6 weeks after MI and patients with first MI's. Computer-assisted analysis of the 2D-Echo images with 3D reconstruction was used to quantify LV asynergy (akinesis + dyskinesis), LV volumes, LV ejection fraction, RSD bulge and global LV shape.

The animal studies showed that collagen deposition during healing after MI increases progressively, reaching a plateau around 2 weeks, and deposition of collagen in already dilated infarct zones is followed by late thinning and further RSD associated with LV aneurysms. Importantly, serial 2D-Echo tracked the in-vivo changes in LV geometry and function and showed greater RSD and LV dysfunction with anterior than inferior MI, and with transmural MI than non-transmural MI. Other studies showed: i) lower LV resistance to distension and rupture in infarcted hearts; ii) marked extracellular matrix (ECM) disruption and RSD in transmural MI; iii) delayed effects on LV remodelling after infarct-limiting therapies given during acute MI; iv) loss of beneficial effects of the vasodilator nitroglycerin (NTG) with hypotension induced by high doses during acute MI; v) decreased wall stress by prolonged LV unloading after MI, with nitrates (eccentric dosing) and angiotensin-converting enzyme (ACE) inhibitors, limited early RSD

and progressive LV remodelling and dysfunction; this effect was greater with therapy over 6-weeks than just over the first 2 weeks; vi) late reperfusion limited early RSD and adverse LV remodelling, and preserved ECM in the epicardial rim; vii) the resistance of the healed left ventricle to distension and rupture was further reduced by prolonged anti-inflammatory therapy (ibuprofen); viii) prolonged ACE inhibitor therapy decreases infarct collagen, which may be harmful under certain conditions.

The clinical studies with serial 2D-Echo showed that systematic tomographic imaging could provide quantitative data on regional and global LV geometry and function including the degree of RSD (depth, area, and volume). An early 2D-Echo not only provided diagnostic data on LV thrombi and complications of MI, but the extent of LV asynergy on the initial 2D-Echo predicted outcome at 3 months and 1 year. Importantly, the degree of RSD on the initial 2D-Echo predicted patients at high risk of adverse remodelling with infarct expansion, greater LV dysfunction, progressive LV dilatation, and poor outcome at 1 year. Survivors of MI with > 18% LV asynergy and significant RSD on a baseline 2D-Echo were at increased risk of topographic deterioration on exercise programs. Anti-inflammatory therapy after MI resulted in more RSD and adverse remodelling. Short-term LV unloading with low-dose intravenous NTG therapy during the acute MI, as well as prolonged nitrate (eccentric dosing) and captopril therapy during healing over 6 weeks after MI, improved 2D-Echo indexes of LV geometry and function, decreased complications and improved outcome. Acute thrombolytic therapy also limited LV remodelling after MI. In all these studies, the degree of RSD and severity of LV dysfunction were greater with anterior than inferior MI, and with Q-wave than non-Q wave MI.

In Conclusion, the overall results indicate that early RSD in the infarct zone leads to progressive global LV dilatation, LV dysfunction and poor outcome and the changes in LV geometry and function can be quantified by serial quantitative 2D-Echo imaging. Marked RSD is associated with early ECM disruption and aneurysm formation after transmural MI. During healing, infarct zones may be thinned and dilated before the collagen plateau, and collagen deposition into these zones result in further RSD and chronic aneurysms. Prolonged anti-remodelling therapy during healing, with agents that decrease wall stress without damaging the ECM, or decreasing infarct collagen, or causing infarct thinning, or impairing healing, might be more effective for reducing RSD, LV aneurysm, global

dilatation and poor outcome. The 2D-Echo measurement of RSD early after MI might be potentially important for stratifying patients according to their topographic status and for the objective assessment of the effects of anti-remodelling strategies during healing after MI.

ACKNOWLEDGEMENTS

I wish to express my gratitude to several individuals and agencies along the road leading to the completion of this thesis:

1. Three teachers during my MBChB studies in Glasgow, namely Drs. Ross Lorimer, David McCall and Ian Hutton, who were my first models of clinician-scientists.
2. Dr. Robert S. Fraser, Chairman of Medicine, and Dr. Richard E. Rossall, Director of Cardiology, for offering me a Residency in Medicine and Cardiology at the University of Alberta Hospital in 1971, when I moved to Edmonton for family reasons and to pursue higher studies in Cardiology. It was Dr. Rossall and Dr. Fraser who introduced me to clinical follow-up studies after cardiovascular surgery during my postgraduate training in Edmonton (1971-1974). These led to my first publications in medical journals.
3. Dr. Simon J.K. Lee who, as my mentor during my formal research training in Edmonton (1974-1976), introduced me to invasive and non-invasive methodologies in Clinical Cardiology research, including cardiac catheterization and coronary angiography, M-mode echocardiography, precordial ST-segment mapping using electrocardiography (ECG), and exercise- and pacing-induced stress in patients with coronary artery disease. More importantly, Dr. Lee supported my studies on the protection of ischaemic myocardium using intravenous propranolol in patients with acute myocardial infarction (MI) in the Coronary Care Unit (CCU). In these studies, I systematically applied state-of-the-art tools available at the time, such as haemodynamic recordings for arterial and pulmonary capillary wedge pressures, precordial ST-segment mapping for ischaemic injury, M-mode echocardiography for left ventricular (LV) dimensions and function, creatine kinase for infarct size, and continuous ECG monitoring for arrhythmias. These studies led to my first papers in Circulation, a major journal of the American Heart Association.
4. Drs Lewis C. Becker, Bernadine H. (Bulkley) Healy, Grover H. Hutchins and Myron L. Weisfeldt, for mentoring me during 3 additional years of training as a clinical research fellow and instructor at the Johns Hopkins Hospital (1976-1979). While there, I contributed to the development of a conscious canine model for assessing the effect of therapeutic interventions in early MI and the concept of expressing infarct size relative to the size of the risk region. I

subsequently evaluated various therapies (e.g. indomethacin, ibuprofen, nitroglycerin, dipyridamole, prostaglandins and prostacyclin) in that model. Importantly, I collaborated with two colleagues, Drs Allan N. Lieberman and James L. Weiss, in applying two-dimensional echocardiography (2D-Echo) to assess myocardial infarct size in the canine model. These studies led to key publications in Circulation, Circulation Research and the American Journal of Cardiology. I also observed two colleagues, Drs Leland W. Eaton and Jay A. Erlebacher, apply 2D-Echo to assess infarct expansion at the bedside.

5. My mentors at the Johns Hopkins Hospital for teaching me two lessons: first, the clinician-scientist was but one individual in a larger group of researchers with diverse expertise, and second, applied, translational research involved to-and-fro activity between the bench and the bedside.
6. Dr. Rossall, Director, Division of Cardiology, the successive Chairs of Medicine (Drs R.S. Fraser, George D. Molnar and Brian J. Sproule), and the successive Deans of Medicine (Drs D.F. Cameron and R.S. Fraser) at the University of Alberta for their support, following my return to the University of Alberta Hospital in 1979, of my efforts to set up my research program and a postgraduate degree program in Cardiology.
7. Several collaborators at the University of Alberta Hospital for their advice, critiques, time and skills in the multidisciplinary research. Foremost among the collaborators were the successive CCU directors, Drs J. Wayne Warnica and Wayne J. Tymchak, who were supportive of my enrolling patients into the clinical studies. Also, Dr. Gordon E. Blinston provided advice regarding the information systems, computer programming and statistical methods throughout the research (1985-1992).
8. My mentors and professional friends, Drs Marc A. Pfeffer and Martin St. John Sutton, for their encouragement between 1986 and 1992, during my son's prolonged illness with acute myeloid leukemia and his death after a failed bone marrow transplant at age 19.
9. Dr. Ross Lorimer, for letting me discuss the topic of the MD thesis with him in 1985, and agreeing to act as adviser when the University of Glasgow approved the proposal for the thesis in 1990.
10. The University of Glasgow, for granting an extension following the delay in submission due to difficult personal circumstances.

11. My peers, for their critiques of my presentations between 1985 and 1990, especially those on:
    i) The long-term effects of early intravenous nitroglycerin (NTG) after acute MI, at the American College of Cardiology meeting of March 1985, later published in Circulation in 1988.
    ii) The effects of prolonged nitrate therapy over 6 weeks after MI and follow-up to one year, at the American Heart Association meeting of 1987, with longer follow-up at the American College of Cardiology meeting of March 1990.
    iii) The effects of prolonged captopril therapy for 6 weeks after MI in a dog model, at international meetings in 1986, 1987 and 1990, and the effects of prolonged captopril for 6 weeks after MI with the follow-up for one year in humans, at plenary sessions of the European Congress of Cardiology and the American Heart Association meeting of 1990.
    iv) The 2D-Echo approach for quantifying LV remodelling and function at the American College of Cardiology meeting of March 1990.
12. To several extramural granting agencies for partial funding of my salary at the University of Alberta Hospital. First, the Heart and Stroke Foundation of Canada (HSFC), Ottawa, Ontario and the provincial branch in Alberta (HSFA) provided awards as Fellow (1975-1978) and Senior Clinical Investigator (1980-1986). Second, the Alberta Heritage Foundation for Medical Research (AHFMR) provided awards as Senior Scholar and Scientist (1986-1997). Third, the Medical Research Council of Canada (MRC), now the Canadian Institutes of Health Research (CIHR), Ottawa, Ontario provided a Distinguished Scientist award (1999-2004).
13. To these agencies for partial funding of the research projects, fellows, sonographers, nurse assistants, students and technicians in my laboratory.
14. To my fellows, sonographers, nurse assistants, students and technicians for their dedication.

Finally, I am indebted to my wife Catherine and daughter Bernadine, for their patience, understanding and support throughout this project.

DEDICATION

I would like to dedicate this work to

Sunil Keith Jugdutt

(1972 – 1992)

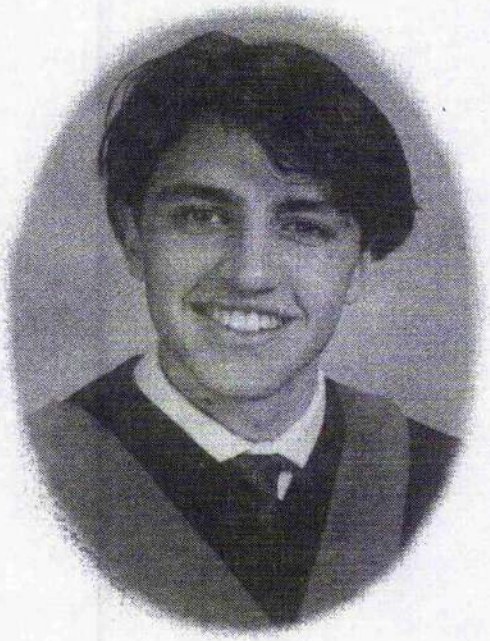

TABLE OF CONTENTS

1. Jugdutt BI, Cahn RL, Basualdo CA, Rossall RE. Measurement of left ventricular shape distortion. In, Ripley, KL, editor. Computers in Cardiology. Los Angeles: IEEE Computer Society Press, 1984:47-52. (**citation # 19**)

2. Jugdutt BI, Michorowski BL. Role of infarction expansion in rupture of the ventricular septum after acute myocardial infarction. A Two-Dimensional Echocardiographic study. Clin Cardiol 1987;10: 641-652. (**citation # 20**)

3. Jugdutt BI. Identification of patients prone to infarct expansion by the degree of regional shape distortion on an early two-dimensional echocardiogram after myocardial infarction. A prospective study. Clin Cardiol 1990;13: 28-40. (**citation # 21**)

4. Jugdutt BI. Prevention of ventricular emodeling post myocardial infarction: Timing and duration of therapy. Can J Cardiol 1993;9: 103-114. (citation # 22)

5. Jugdutt BI. Ventricular remodeling postinfarction and the extracellular collagen matrix. When is enough enough? Circulation 2003;108:1395-1403. (**citation # 27**)

6. Jugdutt BI, Warnica JW. Intravenous nitroglycerin therapy to limit myocardial infarct size, expansion and complications: effect of timing, dosage and infarct location. Circulation 1988;78:906-919. (**citation # 28**)

7. Maidens JM, Blinston GE, Jugdutt BI. Computer-assisted measurement of regional and global left ventricular shape distortion after myocardial infarction. In, Computers in Cardiology. Los Angeles: IEEE Computer Society Press, 1987:413-416. (**citation # 33**)

8. Jugdutt BI, Michorowski BL, Kappagoda TC. Exercise training after anterior Q wave myocardial infarction: importance of regional left ventricular function and topography. J Am Coll Cardiol 1988;12: 362-372. (**citation # 34**)

9. Jugdutt BI, Basualdo CA. Myocardial infarct expansion during indomethacin and ibuprofen therapy for symptomatic post-infarction pericarditis: Effect of other pharmacologic agents during early remodelling. Can J Cardiol. 1989;5:211-221. (**citation # 35**)

10. Johnston BJ, Blinston GE, Jugdutt BI. Overestimation of myocardial infarct size on two-dimensional echocardiograms due to remodeling of the infarct zone. Can J Cardiol 1994;10:77-86. (**citation # 36**)

11. Jugdutt BI. Prevention of ventricular remodeling after myocardial infarction and in congestive heart failure. Heart Failure Reviews 1996;1:115-129. (**citation # 37**)

12. Jugdutt BI, Amy RW. Healing after myocardial infarction in the dog: changes in infarct hydroxyproline and topography. J Am Coll Cardiol 1986;7:91-102. (**citation # 41**)

13. Jugdutt BI, Khan MI, Jugdutt SJ, Blinston GE. Impact of left ventricular unloading after late reperfusion of canine anterior myocardial infarction on

remodeling and function using isosorbide-5-mononitrate. Circulation 1995;92:926-934. (**citation # 48**)

14. Jugdutt BI. Effect of reperfusion on ventricular mass, topography and function during healing of anterior infarction. Am J Physiol 1997;272: H1205-1211. (**citation # 49**)

15. Jugdutt BI, Schwarz-Michorowski BL, Tymchak WJ, Burton JR. Prompt improvement of left ventricular function and topography with combined reperfusion and intravenous nitroglycerin in acute myocardial infarction. Cardiology 1997;88:170-179. (**citation # 50**)

16. Jugdutt BI. Delayed effects of early infarct-limiting therapies on healing after myocardial infarction. Circulation 1985;72: 907-914. (**citation # 55**)

17. Michorowski B, Senaratne PJM, Jugdutt BI. Myocardial infarct expansion. Cardiovasc Rev Rep 1987;8: 42-47. (**citation # 63**)

18. Michorowski B, Senaratne PJM, Jugdutt BI. Deterring myocardial infarct expansion. Cardiovasc Rev Rep 1987;8: 55-62. (**citation # 67**)

19. Jugdutt BI, Khan MI. Impact of increased infarct transmurality on remodeling and function during healing after anterior myocardial infarction in the dog. Can J Physiol Pharmacol 1992;70:949-958. (**citation # 73**)

20. Jugdutt BI, Tang SB, Khan MI, Basualdo CA. Functional impact on remodeling during healing after non-Q-wave versus Q-wave anterior myocardial infarction in the dog. J Am Coll Cardiol 1992;20:722-731. (**citation # 74**)

21. Jugdutt BI. Intravenous nitroglycerin unloading in acute myocardial infarction. Am J Cardiol. 1991;68:52D-63D. (**citation # 100**)

22. Jugdutt BI. Effect of nitroglycerin and ibuprofen on left ventricular topography and rupture threshold during healing after myocardial infarction in the dog. Can J Physiol Pharmacol 1988;66:385-395. (**citation # 102**)

23. Jugdutt BI, Khan MI. Effect of prolonged nitrate therapy on left ventricular remodeling after canine acute myocardial infarction. Circulation 1994;89:2297-2307. (**citation # 103**)

24. Jugdutt BI, Michorowski BL, Tymchak WJ. Improved left ventricular function and topography by prolonged nitroglycerin therapy after acute myocardial infarction. Z Kardiol 1989;78: Suppl 2; 127-129. (**citation # 105**)

25. Jugdutt BI, Tymchak W, Humen D, Gulamhusein S, Hales M. Prolonged nitroglycerin versus captopril therapy on remodeling after transmural myocardial infarction. (Abstract) Circulation 1990;82 (Suppl III):III-442. (**citation # 108**)

26. Jugdutt BI, Michorowski BL, Tymchak WJ. Improved left ventricular geometry and function by prolonged nitroglycerin therapy after acute myocardial infarction. In, Lewis BS and Kimchi A, editors. Chronic Heart Failure - Mechanisms and Management. I. Quality of Life, II Nitrate Therapy. New York: Springer-Verlag, 1990:266-271. (**citation # 109**)

27. Jugdutt BI, Warnica JW. Tolerance with low dose intravenous nitroglycerin therapy in acute myocardial infarction. Am J Cardiol 1989;64:581-587. (**citation # 118**)

28. Jugdutt BI. Myocardial salvage by intravenous nitroglycerin in conscious dogs: loss of beneficial effect with marked nitroglycerin-induced hypotension. Circulation 1983;68:673-684. (**citation # 122**)

29. Jugdutt BI, Michorowski BL, Khan MI. Effect of long-term captopril therapy on left ventricular remodeling and function during healing of canine myocardial infarction. J Am Coll Cardiol 1992;19:713- 723. (**citation # 126**)

30. Jugdutt BI, Khan MI, Jugdutt SJ, Blinston GE. Effect of enalapril on ventricular remodeling and function during healing after anterior myocardial infarction in the dog. Circulation 1995;91:802-812. **(citation # 127)**

31. Jugdutt BI. Effect of captopril and enalapril on left ventricular geometry, function and collagen during healing after anterior and inferior myocardial infarction in the dog. J Am Coll Cardiol 1995;25:1718-1725. (**citation # 128**)

32. Jugdutt BI, Lucas A, Khan MI. Effect of angiotensin-converting-enzyme inhibition on infarct collagen and remodeling during healing after transmural canine myocardial infarction. Can J Cardiology 1997;13:657-668. (**citation # 129**)

33. Jugdutt BI, Khan MI, Jugdutt SJ, Blinston GE. Combined captopril and isosorbide dinitrate during healing after myocardial infarction. Effect on remodeling, function, mass and collagen. J Am Coll Cardiol 1995;25:1089-1096. (**citation # 131**)

34. Jugdutt BI. Different relations between infarct size and occluded bed size in barbiturate-anesthetized versus conscious dog. J Am Coll Cardiol 1985;6:1035-1046. (**citation # 227**)

35. Jugdutt BI. Difference in the relation between infarct and occluded bed in pentobarbital-anesthetized and conscious dogs. Can J Physiol Pharmacol 1986;64: 254-262. (**citation # 228**)

36. Jugdutt BI, Sussex BA, Warnica JW, Rossall RE. Persistent reduction in left ventricular asynergy in patients with acute myocardial infarction by intravenous infusion of nitroglycerin. Circulation 1983;68:1264-1273. (**citation # 232**)

37. Jugdutt BI. Intravenous nitroglycerin infusion in acute myocardial infarction: myocardial salvage. Cardiovasc Rev Rep 1984;5:1145-1163 and Master Teacher Award 1990;11:53-67. (**citation # 250**)

38. Jugdutt BI, Khan MI, Johnston BJ, Jugdutt SJ, Blinston GE. Progressive changes in regional and global left ventricular dilation during remodeling post-myocardial infarction. (Abstract) J Am Coll Cardiol 1994;23:269A. (**citation # 274**)

39. Jugdutt BI. Remodeling of the myocardium and potential targets in the collagen degradation and synthesis pathways. Current Drug Targets, Cardiovascular & Haematological Disorders 2003;3:27-56. (**citation # 278**)

40. Jugdutt BI. Left ventricular rupture threshold during the healing phase after myocardial infarction in the dog. Can J Physiol Pharmacol 1987;65:307-316. (**citation # 283**)

41. Jugdutt BI, Balghith M. Diastolic dysfunction during remodeling after myocardial infarction: Natural history and effect of prolonged ACE inhibition and nitrate therapy. (Abstract) Circulation 2001;104:II-430. (**citation # 298**)

42. Balghith M, Jugdutt BI. Assessment of diastolic dysfunction after acute myocardial infarction using Doppler Echocardiography. Can J Cardiol 2002;18:69-77. (**citation # 315**)

43. Jugdutt BI, Humen DP, Khan MI, Schwarz-Michorowski BL. Effect of left ventricular unloading with captopril on remodelling and function during healing of anterior transmural myocardial infarction in the dog. Can J Cardiol 1992;8:151-163. (**citation # 318**)

44. Jugdutt BI. Nitrates as anti-ischemic and cardioprotective agents. In: Singh BN, Dzau VJ, Vanhoutte P, Woosley RL, editors. Cardiovascular Pharmacology and Therapeutics. New York: Churchill Livingston, 1993:449-465. (**citation # 333**)

45. Jugdutt BI. Angiotensin II receptor blockers. In M.H. Crawford, editor. 1998 Cardiology Clinics Annual of Drug Therapy. Philadelphia: W.B. Saunders Publishers, 1998;Vol 2:1-17. (**citation # 363**)

46. Jugdutt BI. Nitric oxide and cardioprotection during ischemia-reperfusion. Heart Failure Reviews 2002;7:391-405. (**citation # 433**)

LIST OF TABLES

LIST OF FIGURES

ABBREVIATIONS

2D	two-dimensional
3D	three-dimensional
99m-Tc	99m-technetium
ACE	angiotensin-converting enzyme
A-HeFT	African American Heart Failure Trial
AIRE	Acute Infarction Ramipril Efficacy
ALDH	aldehyde dehydrogenase
ARBs	angiotensin II type 1 receptor blocker
AT_1	angiotensin II type 1 receptor
AT_2	angiotensin II type 2 receptor
ATP	adenosine triphosphate
BNP	brain natriuretic peptide
CATS	Captopril and Thrombolysis Study
CCS	Chinese Captopril Study
CCU	coronary care unit
cGMP	cyclic guanosine 3′ 5′ monophosphate
CHARM	Candesartan in Heart failure: Assessment of Reduction in Mortality and morbidity
CK	creatine kinase
CK-MB	CK-myocardial B fraction
CONSENSUS-I	Cooperative New Scandinavian Enalapril Survival Study
COX	cyclooxygenase
CRP	C-reactive protein
CTGF	connective tissue growth hormone
ECG	electrocardiography, electrocardiographic or electrocardiogram
Echo	two-dimensional echocardiography, echocardiographic or echocardiogram
ECM	extracellular matrix
ELITE	Evaluation of Losartan in the Elderly
eNOS	endothelial nitric oxide synthase
G-CSF	granulocyte-colony-stimulating factor
GISSI	Gruppo Italiano per lo Studio della Sopravivvenza nell' Infarcto Miocardico

ABBREVIATIONS continued

HEART	Healing and Early Afterload Reducing Therapy
HOPE	Heart Outcomes Prevention Evaluation
iNOS	inducible nitric oxide synthase
ISDN	isosorbide dinitrate
ISIS 4	Fourth International Study of Infarct Survival
ISMN	isosorbide-5-mononitrate
LAD	left anterior descending
LCX	left circumflex
LV	left ventricular
MI	myocardial infarction
MIAMI	Metoprolol In Acute Myocardial Infarction
MMP	matrix metallo-proteinase
MRI	magnetic resonance imaging
NADPH	nicotinamide adenine dinucleotide phosphate, reduced
nNOS	neuronal nitric oxide synthase
NO	nitric oxide
NOS	nitric oxide synthase
NSAID	non-steroidal anti-inflammatory agents
NTG	nitroglycerin
NYHA	New York Heart Association
OHP	hydroxyproline
$ONOO^{\bullet}$	peroxynitrite
OPTIMAAL	Optimal Therapy in Myocardial Infarction with the Angiotensin II Antagonist Losartan
PCI	percutaneous coronary intervention
PEACE	Prevention of Events With Angiotensin-Converting Enzyme Inhibition
PG	prostaglandin
PKC	protein kinase C
PKCε	protein kinase Cε, epsilon isoform
PTCA	percutaneous transluminal coronary angioplasty
RAAS	renin-angiotensin-aldosterone system
RSD	regional shape distortion
SD	standard deviation

ABBREVIATIONS continued

SEM	standard error of the mean
SMILE	Survival of Myocardial Infarction Long-term Evaluation
SOLVD	Studies of Left Ventricular Dysfunction
SPECT	single-photon emission computed tomography
STEMI	ST-segment elevation MI
TAMI	Transmural anterior myocardial infarction
TGFβ	tissue growth factor β
TIMP	tissue inhibitor of matrix metalloproteinase
Tl-201	thallium-201
TOSCA	Total Occlusion Study of Canada
t-PA	tissue plasminogen activator
TRACE	Trandolapril Cardiac Evaluation
TTC	triphenyl tetrazolium chloride
Val-HeFT	Valsartan Heart Failure Trial
VALIANT	Valsartan In Acute Myocardial Infarction
VEGF	vascular endothelial growth factor
V-HeFT	Veterans Administration Cooperative Vasodilator-Heart Failure Trial

SUMMARY

Background. This dissertation summarizes studies carried out between 1980 and 1988 on the modification of left ventricular (LV) geometry and function during healing after acute myocardial infarction (MI). A review of pertinent knowledge before, during, and after 1980 places the work in perspective and covers the following topics: LV geometry and function after MI; healing and remodelling; the application of two-dimensional echocardiography (2D-Echo) to quantify LV geometry and function and assess temporal changes; detection of early infarct expansion and regional shape distortion (RSD) of asynergic zones by 2D-Echo; the anti-remodelling effects of infarct-limiting therapies; the protective role of the extracellular matrix (ECM); the potential adverse effects of anti-remodelling therapies on the ECM in infarct zones; and the value of non-invasive quantitative 2D-Echo imaging in assessing the effects of anti-remodelling therapies on regional and global LV geometry and function.

Hypotheses. Two main hypotheses were addressed: i) MI results in early RSD followed by progressive global LV dilatation and a more spheroidal shape, and more LV dysfunction during and after healing; and ii) the remodelling of LV geometry and structure after MI is a dynamic process that spans the early infarction and healing phases, and is largely driven by increased wall stress. Mechanical forces acting on the infarct and non-infarct zones, as well as other factors, play significant roles in the remodelling of these regions. Progressive remodelling occurring during and after healing impacts negatively on outcome and may be modified by early and prolonged therapies.

Methods and Results. A multidisciplinary bench to bedside approach was used, with concurrent studies in a chronic dog model of healing over 6 weeks after MI and patients with a first MI. Computer-assisted analysis of the 2D-Echo images with 3D reconstruction was used to quantify LV asynergy (akinesis + dyskinesis), LV volumes, LV ejection fraction, RSD in short-axis images using novel indices [such as the peak (P_k) and depth (r_d) of the bulge], RSD in diastolic images, and global LV shape.

Animal studies. These showed that collagen deposition increases progressively during healing, reaching a plateau around 2 weeks, and is associated with

significant remodelling such that collagen deposition in already expanded infarct zones and late thinning lead to permanent RSD associated with LV aneurysms. Importantly, serial 2D-Echo tracked the topographic and functional changes and showed greater RSD and dysfunction with anterior than inferior MI, and with transmural than non-transmural MI. Transmural MI showed marked ECM disruption and RSD. Infarct-limiting therapies, such as nitroglycerin (NTG) and the anti-inflammatory drug ibuprofen, produced delayed effects on LV remodelling. Vasodilator-induced hypotension during acute MI paradoxically negated the beneficial effects on collateral blood flow, infarct size and LV geometry seen with low-dose NTG. Decreased wall stress by prolonged LV unloading with nitrates (eccentric dosing) and angiotensin-converting enzyme (ACE) inhibitors during healing after MI limited RSD, progressive LV remodelling and dysfunction. Importantly, this effect was greater when given over 6 weeks than just over the first 2 weeks. Late reperfusion, made 2 hours post-occlusion, limited RSD, adverse LV remodelling and dysfunction during healing and this effect was enhanced by nitrates. The resistance of the healed left ventricle to distension and rupture, which was lower for infarcted than normal hearts, was further reduced by prolonged therapy with ibuprofen over 6 weeks but was preserved by prolonged nitrate. Prolonged ACE inhibitor therapy decreased infarct collagen. Combined captopril and nitrate therapy showed similar beneficial effects on LV remodelling as compared to monotherapy.

Clinical studies. Serial 2D-Echo studies showed that systematic tomographic imaging was feasible and provided reproducible diagnostic and quantitative data on regional and global LV geometry and function. Strong correlations were shown between 2D-Echo LV volumes and those by biplane LV angiography, LV asynergy as percent LV circumference or endocardial surface area and CK infarct size, and the degree of RSD and infarct expansion or ventricular septal rupture. An early 2D-Echo detected thrombi and other complications. In follow-up studies after first anterior MI's, the extent of LV asynergy on the initial 2D-Echo predicted outcome at 3 months and 1 year. In a larger study, the degree of RSD on the initial 2D-Echo predicted patients likely to develop adverse remodelling with infarct expansion and greater LV dysfunction, in-hospital complications and deaths, progressive LV dilatation, and poor outcome at 1 year. In a study of MI survivors started on exercise programs, those with > 18% LV asynergy and significant RSD

were at increased risk of topographic deterioration. Indomethacin therapy for post-MI pericarditis resulted in more RSD and infarct expansion. 2D-Echo indexes of LV geometry and function correlated with decreased complications and improved outcome after short-term low-dose intravenous NTG therapy during the acute MI, and prolonged nitrate (eccentric dosing) and captopril therapy during healing over 6 weeks after MI. Acute thrombolytic therapy also limited remodelling. In all studies, the degree of RSD and severity of LV dysfunction were greater with anterior than inferior MI, and with Q-wave than non-Q wave MI. The degree of early RSD (area, depth or volume) correlated with the severity of subsequent LV dilatation and the degree of overestimation of regional LV dysfunction.

Conclusion. The overall results indicated that progressive topographical and functional changes occur during healing after MI and can be quantified by serial 2D-quantitative Echo. Early RSD that develops in the infarct zone leads to progressive global LV dilatation involving both the infarct and non-infarct zones and is associated with LV dysfunction and poor outcome. Importantly, RSD, LV dilatation and LV function can be measured by 2D-Echo. Marked RSD is associated with early ECM disruption and aneurysm formation after transmural MI. Collagen deposition into thinned and dilated infarct zones during healing seems to result in permanent RSD found with chronic aneurysms. Prolonged therapy, with anti-remodelling agents that decrease wall stress but do not damage the ECM, or decrease infarct collagen, or cause infarct thinning, or impair healing, might be more effective for reducing RSD, LV aneurysm, global dilatation and poor outcome. The 2D-Echo measurement of RSD might be potentially important for assessing the effects of anti-remodelling strategies during healing after MI.

1. INTRODUCTION

This dissertation for the degree of MD is submitted in the form of an essay entitled **'Modification of left ventricular geometry and function during healing after acute myocardial infarction (MI)'**. The work was conducted at the University of Alberta Hospital between 1980 and 1988, following the completion of post-doctoral training and clinical fellowships in cardiovascular research at the University of Alberta Hospital (1974-1976) and the Johns Hopkins Hospital (1976-1979). In this essay, I have endeavoured to 'show the relationship between the various published papers' and abstracts relating to the topic, and 'place the whole work critically into perspective with the general state of knowledge' in this area of investigation.

2. REVIEW OF BACKGROUND LITERATURE

In order to place the work in perspective, the background knowledge section summarizes the pertinent findings from studies that I conducted on the subject during the period between 1980 and 1988 in my laboratory, and those in reports from other laboratories before 1980 and after 1988. I have highlighted the progress made in my field during the study period and the major advances made in subsequent years. For reference, I have included, in the bibliography, published papers and some pertinent abstracts of papers that have not yet been published.

2.1. Left ventricular geometry and function

The left ventricle, the main pumping chamber of the beating heart, occupies a key position in the cardiovascular system as it generates the stroke output critical for survival. Since the 1960's, left ventricular (LV) geometry, which refers to the shape, size and structure of the left ventricle, was becoming recognized as an important determinant of LV function (1). The normal LV geometry is considered to be a prolate ellipsoid, that is elliptical in the long-axis and circular in the short-axis (2). Deformation of LV geometry, with a departure from an ellipsoidal to a spheroidal configuration, was subsequently shown to be associated with LV dysfunction (3-5). Several authors suggested that changes in global LV shape and size might influence clinical outcome (1,4,6-12).

Studies since the mid 1970's suggested that dramatic regional deformation of LV geometry may occur after acute myocardial infarction (MI) (13-

18,19[**Appendix 1**],20-22) and have a profound negative impact on LV function and outcome (20[**Appendix 2**],21[**Appendix 3**]). Studies in the mid 1980's indicated that these negative effects were evident on both the short-term and long-term (21,22:**Appendix 4**), and depended largely on the initial myocardial infarct size (21) as well as the subsequent processes of infarct healing and LV remodelling (22).

In general, the term remodelling refers to changes in structure and shape. The Oxford and Webster's English dictionary definitions of "remodel" emphasize three-dimensional (3D) reconstruction and shape, while definitions of repair emphasize restoration of shape and function (Table 1).

TABLE 1. Definitions

Remodel
Webster's dictionary: to alter the structure of; remake
The Oxford dictionary: to model again or differently; to reconstruct or reorganize (model n: representation in 3 dimensions of proposed structure; vb: fashion, shape)
Repair
Webster's dictionary: vb: to restore, fix, renew, make good, mend, remedy; n: replacement of destroyed cells or tissues by new formations
The Oxford dictionary: vb: to restore to good condition after damage or wear, to set right, to fix, renovate, refix

After MI, LV remodelling refers to the changes in the geometry, shape, structure, architecture and topography of the infarcted left ventricle. Collective evidence, mostly over the last two decades, has strengthened the hypothesis that these LV remodelling changes after MI have profound negative effects on LV function and survival (22-26,27[**Appendix 5**],28[**Appendix 6**],29,30). This has led to efforts to develop therapeutic strategies for limiting, preventing and even reversing adverse remodelling after MI (22-30).

An important aspect of the assessment of therapeutic interventions to limit adverse remodelling is the ability to reliably quantify LV shape, size, structure and function in repeated studies before, during and after therapy (21,28-30). Since the early 1980's, two-dimensional echocardiography (2D-Echo) has emerged as a practical tool for the non-invasive quantification of in-vivo LV remodelling and function after MI in research studies at the bedside and in the laboratory (16,19-21,28-32,33[**Appendix 7**],34[**Appendix 8**],35[**Appendix 9**],36[**Appendix 10**],37). However, only a few of these studies have applied 2D-Echo with 3D reconstruction for quantifying LV size and regional dysfunction (21,28,30-34) or

2D-Echo for quantifying early regional shape distortion (RSD) of the infarct zone (13-16,31-36).

2.2. Healing after acute myocardial infarction

The healing process after acute MI attempts to repair the damaged LV wall, preserve its integrity and restore function. Clearly, the healing process is not ideal since LV dysfunction usually persists. This topic has been previously reviewed (22,37[**Appendix 11**],38-40).

The collective evidence indicates that healing after MI is a dynamic and time-dependent process (22,23). Pathophysiologically, it involves acute and chronic inflammation followed by collagen deposition and scar formation. Histopathological studies have shown an early inflammatory component after both animal and human MI. Thus, early pathophysiological events in the occluded region during acute MI closely resemble events during acute inflammation (40,41: **Appendix 12**). These include trapping of leucocyte and inflammatory cells, lysosomal membrane breakdown and release of lysosomal enzymes, cellular membrane breakdown, release of prostaglandins (PGs), red blood cell sludging, blood platelet trapping and aggregation leading to release of granular products, hemorrhage, oedema, myocardial tissue necrosis, and necrosis of intramyocardial blood vessels (38). The granular products, released by platelet aggregation into the ischaemic tissue, appear to lead to a vicious cycle of platelet plugging, vasoconstriction, thrombosis, increased vascular permeability, more tissue oedema and injury, and more necrosis, especially in the marginal zones of the infarcts.

In both animals and humans, acute inflammation is followed by chronic inflammation, connective tissue proliferation and collagen deposition until healing is completed by formation of a firm, contracted and inelastic scar (40,41). In humans, acute inflammation predominates in the first week, chronic inflammation in the second week, and collagen deposition from the third week onwards (40). The timing of these sequential events during healing might be highly pertinent when using agents that impair acute or chronic inflammation and collagen deposition during healing after MI (Table 2) (22).

Evidence indicates that the duration of healing of the infarct zone after MI differs among species (Figure 1), being longer in humans than dogs and rodents (42). Thus, the interval from the onset of an MI to the formation of the final scar

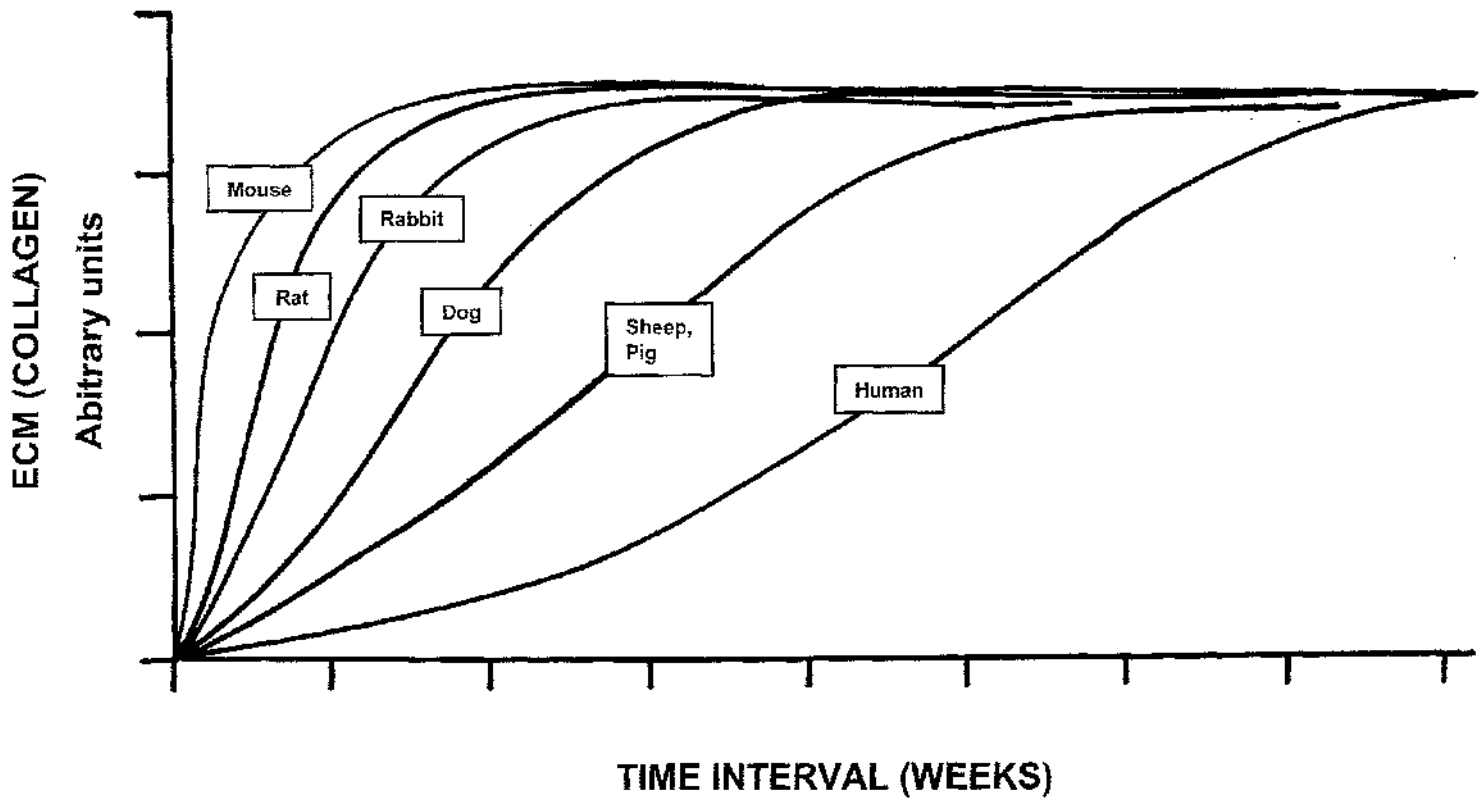

Fig 1. Effect of species on time to collagen plateau

Duration of healing measured by time to collagen plateau for moderate myocardial infarct size. The duration of healing is shorter in smaller animals. ECM, extracellular matrix. Modified from Jugdutt (42)

ranges between two and three weeks in rats (43), four and six weeks in dogs (41), and between six weeks and six months in humans depending on infarct size (40,44). The slower rate of healing in humans compared to dogs and rats is therefore pertinent when determining the optimal timing and duration of therapeutic interventions on the basis of animal data, so as to avoid confounding effects on healing.

TABLE 2. Temporal staging of left ventricular remodelling after myocardial infarction: A guide for the timing of therapy

Timing	Pathophysiological process
Very early: First 24 hours	Acute evolution and completion of myocardial infarction
Early: Day 2 to 2 weeks	Healing before infarct collagen plateau
Late: 3 to 6 weeks (up to 6 months)	Healing after infarct collagen plateau
Very late: After 1.5 months (up to 12 months)	Late postinfarct healing

From Jugdutt (22[Appendix 2])

As noted above, several pathophysiological studies have documented that the rate of healing depends on infarct size, such that the larger the infarct, the slower the rate (40,41,43). The rate of healing also depends on cellular, metabolic and biochemical factors and the adequacy of nutrient blood flow (22,37,39). It follows that therapies that are likely to impair healing may need to be delayed for longer in patients with large MI compared to those with small MI.

The possibility that certain interventions may accelerate or delay healing also needs to be considered when applying therapy. Thus, reperfusion after MI has been shown to be associated with decreased infarct size (45), more rapid healing (46) and less adverse remodelling in animals (47,48[**Appendix 13**],49[**Appendix 14**]) and humans (50:**Appendix 15**).

Collective evidence indicates that LV remodelling and healing after MI are highly dynamic processes that run in parallel (22,23) and significant regional remodelling of the infarct zone occurs during the healing phase (22). It follows that therapies that modify healing may significantly influence LV remodelling after MI (22,23).

Several experimental studies in the early 1980's addressed the hypothesis that administration of drugs that decrease the inflammatory response, collagen

deposition and collateral blood flow during healing after MI may promote adverse LV remodelling. Thus, anti-inflammatory agents, such as glucocorticoids and non-steroidal anti-inflammatory drugs (NSAIDs) given during healing after MI consistently induced more thinning of the infarct zone in the dog model (51-54). However, these agents did not significantly reduce the collagen content in the infarct scar (51-54). Importantly, the NSAIDs caused infarct zone thinning and expansion even in small infarcts in dogs (55:**Appendix 16**). Furthermore, these agents exerted different effects on infarct size and remodelling. Thus in the infarction phase, indomethacin was shown to increase (56) and ibuprofen to decrease (57) infarct size, while both agents increased remodelling of the infarct zone (52,54). Interestingly, aspirin did not cause infarct thinning or expansion (54), suggesting that it might be safe during healing after MI. In contrast to studies with ibuprofen in the dog (54,55), one study of ibuprofen during healing after MI in rats suggested it may increase infarct collagen by delaying proteolysis and, in that setting, did not cause significant infarct thinning (58). Moreover, in the clinical setting, therapy with ibuprofen or indomethacin for post-infarction pericarditis in patients resulted in enhanced infarct thinning and expansion, and increased prevalence of LV aneurysm (35).

2.3. Two-dimensional echocardiography after myocardial infarction and the recognition of infarct expansion

Following the introduction of 2D-Echo in the mid 1970's, several investigators recognized the importance of RSDs following MI and the importance of tomographic imaging in multiple planes (5). Others systematically applied 2D-Echo to study LV aneurysm (13), LV asynergy (14-17) and regional dilatation in acute MI (18). The latter study led to the first description of clinically significant and often fatal myocardial infarct expansion after acute MI (18).

However, Hutchins and Bulkley (now Healy) first described the pathological correlates of clinically significant and fatal infarct expansion after MI in 1978 (59). They defined infarct expansion pathologically, as an increase in the proportion of the surface area of the left ventricle occupied by necrotic myocardium with concomitant thinning of the infarcted wall, dilatation of the LV cavity and distortion of LV topography that was not explained by new necrosis. They found that the majority of patients dying within 30 days of an acute MI had infarct expansion. Thus, within six days of transmural (Q-wave) MI, about 17% developed infarct

extension with further new necrosis while about 59% developed infarct expansion but no new necrosis. This marked and fatal expansion was associated with abrupt or insidious disruption of necrotic myocytes where acute inflammatory cells were disintegrating. It was compared to an 'intramural tearing of necrotic muscle'. Removal of necrotic cells or mural collapse did not appear to play a significant role during the early stages of healing.

In that study (59), Hutchins and Bulkley also graded the severity of infarct expansion pathologically. They compared the relative position of internal ventricular landmarks such as the papillary muscles and junctions of the right and LV free walls with the septum. They found that marked expansion tended to develop 5 days or more after acute MI, and was more frequent with first infarctions that were large and transmural. They also found that wall thinning was greater with marked expansion in these large transmural infarcts but was less with small and subendocardial infarcts.

Clinically, infarct extension in that study was defined as the syndrome consisting of new ischaemic chest pain, ST-segment elevation on electrocardiography (ECG), rise in serum creatine kinase (CK) levels, and increasing congestive heart failure within 10 days of the indexed MI. Pathologically, extension was defined as new necrosis around the area of previous acute infarction. However, of the 14 patients who were clinically diagnosed as having extension, only two (14%) had isolated extension while as many as nine patients (65%) had extension plus expansion, and 3 patients (21%) had isolated expansion.

More importantly in that study, the next clinical event associated with the syndrome of recurrent chest pain, worsening congestive heart failure, hypotension and ST-T wave changes after an acute MI, was more likely to be due to infarct expansion than infarct extension. This fatal syndrome occurred in 70% of patients with marked morphologically defined expansion, in 38% with moderate expansion, but in none of the patients with mild expansion.

Several mechanisms for components of the clinical syndrome were postulated (59). The chest pain was explained by the acute dilatation of the LV wall and stretching of the overlying pericardium, which is often involved in the inflammatory process associated with transmural infarcts. Reflection of the expanded infarct surface area over a greater number of praecordial leads was suggested to explain new changes on ECG. A tearing of necrotic myocardium

and new necrosis secondary to adverse haemodynamic consequences of expansion (increased wall stress; increased myocardial oxygen demands and hypotension; decreased diastolic perfusion, ischaemia and infarction) was postulated to result in secondary elevation of serum CK levels or accelerate enzyme release.

Thus, this carefully conducted and small clinico-pathological study drew attention to the critical role of early infarct expansion in early remodelling after acute MI and underscored the need to recognize significant infarct expansion clinically. Subsequent clinical studies using 2D-Echo confirmed that infarct expansion with marked acute LV dilatation was associated with moderate to large areas of myocardial necrosis and dyskinesis and resulted in acute congestive heart failure and hypotension (18,21,28,31,32). Several of these longitudinal clinical studies applied 2D-Echo to establish the central role of early infarct expansion in early and late stages of remodelling after acute MI (21,28,31,32). Thus, these studies indicated that early infarct expansion in humans plays a role in acute LV enlargement (32), accelerated aneurysm formation (21), cardiac rupture (20,60), and progressive LV enlargement (31).

The early detection of infarct expansion therefore became important. Although several clinical features may lead one to suspect infarct expansion, definitive diagnosis has been difficult. Although praecordial ST-segment mapping on ECG permits the non-invasive diagnosis of infarct extension (61), it is not helpful in the diagnosis of infarct expansion. Several studies suggested that an early non-invasive diagnosis of infarct expansion can be made by means of 2D-Echo at the bedside (21).

Eaton et al. (18) first reported the recognition of regional LV dilatation or infarct expansion by serial 2D-Echo imaging over the first two weeks after anterior Q-wave MI in 8 of 28 patients. They assessed infarct expansion on end-diastolic outlines of short-axis 2D-Echo images by means of a computer-aided semi-automated contouring system. They measured: i) the length of the infarct-containing segment between anterior and posterior papillary muscle markings; ii) the average thickness of the segments; and iii) the total LV circumference. They were able to make a retrospective diagnosis of expansion in 8 patients (29%) who showed evidence, between initial and final echocardiograms, of an increase in the infarct-containing segment length by 48% (range, 26% to 108%), marked infarct thinning by 26% (range 17% to 44%) and an increase in LV circumference by

25%. These expanders represented a high-risk group and showed greater functional deterioration and higher eight-week mortality compared to non-expanders (50% versus 0%).

Subsequent studies with serial 2D-Echo after MI (20,21,28,31,32,34,35) used two more variables to quantify infarct expansion on 2D-Echo: i) expansion index or ratio of the length of the infarct-containing endocardial segment to the length of the non-infarct containing endocardial segment; ii) thinning ratio or ratio of the average thickness of the infarct zone to the average thickness of the non-infarct zone. In all these studies, the infarcted zone was defined as the zone containing asynergy, usually defined as akinesis plus dyskinesis. The relationship between asynergy and myocardial necrosis was established in an earlier study (62). Erlebacher et al. (31) found that at 10 to 21 days after MI, an anterior infarct-containing segment length of more than 11.0 cm indicated anterior infarct expansion.

It is important to note that these five measurements allowed the diagnosis of expansion to be made after the event, or retrospectively, after repeated studies. There was still a need in the mid 1980's to identify expanders on the initial 2D-Echo. My laboratory therefore attempted to quantify the regional diastolic bulge, or RSD, of asynergic zones on short-axis 2D-Echo images (19,20,21,34). In a large prospective study of 244 consecutive patients with a first Q-wave MI, the degree of RSD on an early 2D-Echo within 2 days of the MI was found to identify potential expanders (21). Specifically, 50 of 51 expanders, compared to 3 of 193 non-expanders, had a peak regional shape distortion index (P_k) or depth of outward bulging (r_d) of more than 10 mm on the initial 2D-Echo.

The ability to predict which patients are likely to develop infarct expansion on an initial 2D-Echo is of considerable clinical importance if timely therapy is to be applied to attenuate remodelling. The prospective evaluation of several predictive indexes has been a prime objective in my laboratory. In two recent large prospective clinical studies (28,35), prospective diagnosis of the infarct expansion syndrome was made possible, at 40 hours or more, when the acute event was associated with the following two sets of criteria:

i) **clinical**: acute hypotension (systolic blood pressure <90 mm Hg and peripheral hypoperfusion), LV failure with pulmonary congestion, evidence of LV dilatation with or without further chest pain, no new ECG changes of injury,

no significant new plasma CK elevation (<100 IU/L) suggesting new necrosis; and

ii) **2D-Echo**: evidence of marked regional diastolic stretching (>25% increase in asynergy-containing endocardial segment length), marked thinning (>25% decrease in thickness of asynergic wall), and dilatation (>25% increase in diameter, area and volume) compared to the initial recording.

In summary, acute infarct expansion is now recognized as the cornerstone of remodelling after MI. The topic has been previously reviewed (63[**Appendix 17**],64). The determinants of infarct expansion and early remodelling are summarized in Table 3. The overall findings suggest that, within the first few hours to days after an acute MI, early remodelling with expansion of the infarcted segment involves acute outward bulging of the infarct zone, with stretching, thinning and dilatation of that zone, resulting in RSD that can be detected on end-diastolic 2D-Echo images.

TABLE 3. Determinants of myocardial infarct expansion and early remodelling

Physical characteristics of the infarct

- Size of the infarction
- Transmurality of infarction
- Location of infarction
- Type of infarction
- Age of infarction

Efficacy of the healing processes

- Inflammatory response
- Collagen deposition
- Collateral circulation
- Reperfusion

Mechanical forces (strength, duration and frequency of application)

- Intracavitary distending forces (Push)
  - Preload
  - Afterload
  - Wall stress (dimension dependent, Laplace effect)
- Intramural forces (Stretch and Pull)
  - Contractility
  - Heart rate:
    - Treppe effect (increased contractility)
    - Increased frequency of contraction
- External restraining forces
  - Pericardium and fluid
  - Pericardial pressure
  - Extracardiac structures

From Jugdutt (67[Appendix 18])

2.4. Changes in left ventricular geometry and function during healing after myocardial infarction

It is well known that most acute infarcts bulge out during systole. In 1935, Tennant and Wiggers first reported systolic expansion of the cyanotic zone after acute coronary artery ligation in the dog (65). However, with infarct expansion, outward bulging is also present in diastole, implying more profound shape deformation and architectural change in the left ventricle (41). Initially, the increase in cavity area, and therefore the diameter, is confined to the zone with regional bulging. Subsequently, further progressive remodelling takes place and the end-result is global LV cavity dilatation, with generalized increase in LV cavity area and diameter (21,28), and a more spherical LV shape (7-12).

Experimental studies suggested that the early thinning in the infarct zone is due to a slippage between muscle bundles so that the number of myocytes across the thickness of the infarct zone is reduced (66). It was reasonable to suggest that the necrotic myocardium during the early stage of healing after MI, when inflammation is active, might be more susceptible to shape deformation due to distending intracavitary forces, such as high preload and afterload, and intramural traction, or pull, of the adjacent non-infarcted myocardium (63,67:**Appendix 18**).

It appears that RSD results in increased regional wall stress and the associated gradient in wall stress may drive the remodelling of LV shape in an attempt to normalize wall stress, thereby resulting in the spherical LV shape. Several forces at work in every individual case, and at different stages of healing, appear to influence the final outcome.

Before 1980, it was known that infarcted hearts often underwent marked dilatation associated with dilated cardiomyopathies (7), lengthening of the non-infarct segment played a role in the late LV dilatation (7,68), and healed scars were less distensible and more resistant to deformation (69). However, the mechanisms were not known and it was not clear whether significant late remodelling of the infarct scar occurred consistently after the healing phase.

In the 1980's, my laboratory proposed a sequence of changes during early and late stages of remodelling during healing after MI (Figure 2). Theoretically, the early infarct expansion and RSD that develop after acute MI initiate a vicious cycle of ineffective cardiac contraction, decreased systolic ejection, decreased cardiac output, increased systolic and diastolic volumes, which in turn lead to more LV enlargement, LV dysfunction, physical disability and death.

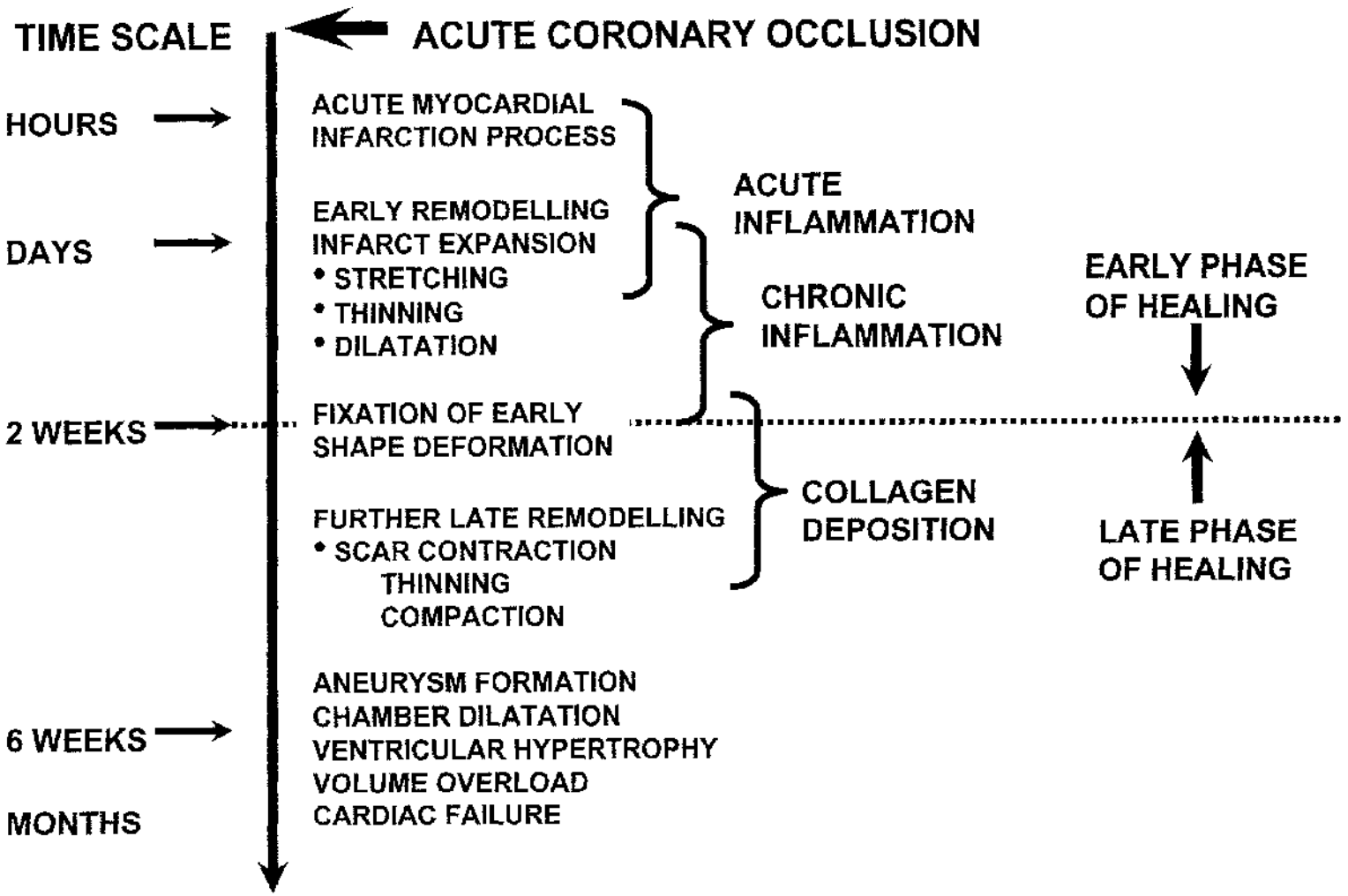

Figure 2. Early and late stages of remodelling after canine myocardial infarction
(Modified from Jugdutt (22; Appendix 4)

Within the first few hours to days after acute MI, the infarcted wall undergoes regional expansion, with stretching, thinning and dilatation; this results in early RSD, with outward bulging in diastole and ballooning in systole. The acute remodelling of LV shape and structure after acute MI undergoes further alterations during subsequent healing and may, under certain conditions, trigger the vicious cycle of progressive global LV dilatation, LV failure, LV rupture, and death.

Major forces in the development of early infarct expansion and RSD include: i) physical characteristics of the infarct such as infarct size and location; ii) other factors relating to the efficacy of early healing such as cellular infiltration, fibroblast activity and collagen deposition, metabolism and nutrient collateral blood flow; and iii) haemodynamic factors, such as the magnitude, duration and frequency of mechanical forces acting on the infarct zone, such as afterload, preload, wall stress, heart rate and contractile pull of the adjacent normal myocardium (22,37,39,63) (Table 3).

During healing, collagen deposition into the already thinned and stretched infarct segment fixes or 'cements' the early RSD, resulting in the permanent RSD associated with aneurysm formation (41). The permanent scars that develop in thinned infarct tend to be thin and weak, ballooning out during contraction, thereby leading to incomplete emptying of the pumping chamber and permanent disability.

Further late remodelling, with compaction of the infarct scar and lengthening and hypertrophy of the non-infarcted segment, may initially provide some some compensation but is eventually followed by LV dilatation and dysfunction.

Several studies have documented the importance of infarct size and location on the severity of infarct expansion and the degree of RSD. All pathologic studies have suggested that first, large and transmural infarcts are prone to expansion (18,59,60,70-72,73[**Appendix 19**],74[**Appendix 20**]). Clinical studies have confirmed that first, large, 'transmural' or 'Q-wave' infarcts are prone to expand (21,28). The reason why nontransmural or subendocardial infarcts do not expand might be because the subepicardial rim of normal myocardium provides a buttress or scaffold that protects against the distending forces. Small infarcts, that tend to be subendocardial, are less likely to expand (21). The critical infarct size for expansion to occur was found to be 11% of the LV weight in the dog heart (70) and 17% in the rat heart (71). However, there was no strong

correlation between infarct size and the degree of infarct expansion in these studies, suggesting that other factors are involved. In the rat model, infarct size was found to influence LV function (75), dilatation (76) and survival (77).

Although the frequency and severity of infarct expansion did not differ between anterior and posterior infarcts in the dog (70), all clinical studies indicate that topographic deterioration is greater with anterior infarcts (18, 20,21,28,78). In a clinico-pathologic study, Pirolo et al. (79) also found that patients with transmural infarction of the LV antero-apical area are more likely to develop expansion. This might be due to the fact that this region of the left ventricle is the thinnest, has the greatest curvature and is under more stress (1,80). The greater restraining effect of the posterior pericardium and adjacent extracardiac structures might explain why topographic deterioration is less with infarction at the inferior than the antero-apical location. Pirolo et al (79) also found in their study that hearts with prior LV hypertrophy are less prone to develop infarct expansion.

Other factors, such as prior collagen content, infarct age, the patient's age, presence of multivessel disease, collateral reserve and concomitant drugs also appear to be important (63). The importance of nutrient flow during healing after acute MI is becoming recognized. In antero-apical infarcts of fixed size and produced by left anterior descending (LAD) coronary artery ligation and collateral obliteration, expansion was more severe than with coronary ligation alone (73,74).

Factors that increased wall stress, such as hypertension (32) and exercise (34,81-83), were shown to increase expansion in animals and humans. An acute increase in afterload and wall stress with methoxamine was found to increase expansion in dogs (84). Conversely, an acute decrease in afterload and wall stress with intravenous nitroglycerin (NTG) and intra-aortic counterpulsation was shown to reduce LV dilatation in humans (85). Venodilatation, decreased blood volume and preload with long-term treatment with captopril, an angiotensin-converting enzyme (ACE) inhibitor, was shown to be an important mechanism for attenuation of LV dilatation in rats (86).

2.5. Effect of potential infarct-limiting therapies on healing and left ventricular geometry and function after myocardial infarction

In the mid 1970's, a major goal of therapy after MI was to reduce infarct size (87,88). Around the early 1980's, several experimental studies using the rat model of MI showed a negative relation between myocardial infarct size and LV

function (75), LV dilatation (76), and survival (77). However, those studies did not address infarct expansion or RSD or topographic changes during infarct healing. Early scepticism about infarct-limiting therapies and the potential for limiting remodelling was rooted mainly in the lack of robust in-vivo quantitative methodology.

Subsequent experimental and clinical studies over the 1980's provided further evidence in support of the idea that infarct size is a major determinant of the degree of LV remodelling and dysfunction after MI (18,21,26,34-36,60,70-75). Several of these studies assessed infarct expansion (21,34-36,60,70-75) or both infarct expansion and RSD (21,34-36,73,74), and many used 2D-Echo clinically (18,21,34-36,89) or in the dog model (70,73,74).

Three other clinical studies in the early 1980's supported the idea that infarct size was a major determinant of outcome. First, one study confirmed that acute extension of infarct size is associated with a high mortality (90). Second, another study showed the 21 day mortality after acute MI was higher with transmural than non-transmural MI (23 % versus 10 %, $P<0.01$) and early infarct recurrence had an additional adverse effect on survival (91). Third, a study using equilibrium radio-nuclide angiocardiograms, confirmed that early functional aneurysms in patients after anterior MI carries a high-risk of death within one year that is independent of LV ejection fraction and its absence identified a group with low mortality despite impaired ejection fraction (92).

Other studies documented early and late topographic changes after MI in the rat model ex-vivo (93,94). One study addressed healing and repair after MI in the rabbit model and suggested that LV rupture was more common 1-4 days after MI and collagen content was a determinant of infarct stiffness and the resistance of the left ventricle to rupture (95). In a comparative study of healing after MI in the dog and rat models, healing was shown to be more rapid and LV remodelling more severe in the rat than the dog (96).

In the mid 1980's, a novel concept was that limitation of infarct size and preserving ventricular muscle might be the most effective means of limiting LV remodelling, dilatation and dysfunction, and thereby improving survival. I therefore embarked, as others did, on studies of the limitation of LV remodelling via limitation of infarct size. I pursued the hypothesis that therapy given during healing after MI, using agents that decrease afterload, preload, chamber size, heart rate, contractility and wall stress without impairing healing, decreasing

infarct collagen, or causing infarct thinning, might reduce the extent of RSD and thereby improve myocardial performance and have a positive impact on overall outcome. Furthermore, the potential beneficial effects of such agents on scar topography and collagen deposition might be expected to enhance the mechanical strength of the scar and thereby limit LV distension and aneurysm formation, and prevent LV rupture. However, on the basis of my findings in on-going studies of healing after MI (55) and those from other laboratories (51-54), I considered it was pertinent to address the issue of potential effects of infarct-limiting therapies on the healing phase during which significant LV remodelling occurred.

By the mid 1980's, three categories of infarct-limiting therapy were becoming available for testing: i) non-thrombolytic pharmacological therapy; ii) pharmacologically-mediated thrombolysis with or without coronary angioplasty; and iii) the combination of thrombolytic and non-thrombolytic therapies.

2.5.1. Anti-inflammatory agents

The effects of methyl prednisolone on infarct size have been controversial (51). However, methyl prednisolone delayed inflammation and disintegration of necrotic myocytes, decreased infarct collagen, and impaired healing after MI in the rat (43). It also caused infarct thinning, infarct expansion and LV dilatation despite a decreased infarct size in the rat model (97). Furthermore, short-term methyl prednisolone given after MI in the dog induced marked infarct thinning and regional dilatation although collagen did not change (51).

As mentioned previously, the NSAID ibuprofen decreases infarct size (55) but also aggravates thinning and expansion during early healing of the infarct without altering the collagen content of the infarct scar (54). However, one study in the rat model, where ibuprofen was given at 1, 6 and 18 hours after MI did not detect infarct thinning but found increased infarct collagen (58). Since a randomized clinical study of the effect of ibuprofen after MI could not be ethically justified, the effects of ibuprofen and indomethacin (another NSAID) therapy on LV remodelling and function was studied in patients given these drugs for pericarditis associated with acute transmural MI and both agents were shown to enhance LV aneurysm formation (35).

2.5.2. Nitroglycerin, prostaglandins, and ibubrofen

Several therapies that are potentially infarct-limiting when given during the infarction phase over the first few hours after acute MI, such as NTG (98) and prostacyclin or prostaglandin (PG) I_2 (99), were shown to result in delayed beneficial effects on infarct collagen and LV geometry at 7 days post MI in the dog model (55). In that study, ibuprofen given after acute MI decreased infarct size and the infarct expansion index, did not decrease infarct collagen, but induced infarct wall thinning (55). Interestingly, NTG therapy was associated with increased infarct collagen and no infarct expansion or thinning (55).

The effects of long-term NTG therapy (100**[Appendix 21]**,101) during healing after MI were subsequently tested in the dog model (48,102**[Appendix 22]**,103**[Appendix 23]**,) and in patients (104,105**[Appendix 24]**,106,107,108 **[Appendix 25]**,109**[Appendix 26]**). Briefly, these studies demonstrated beneficial effects of NTG on LV geometry and function as well as clinical outcome (104-109). The potential mechanisms of benefit with nitrates after MI are summarized in Table 4.

TABLE 4. Potential mechanisms for benefit with low-dose intravenous nitroglycerin therapy in acute myocardial infarction

1. Improved haemodynamics
   - Decreased preload; increased venous capacitance
   - Decreased afterload and impedance
2. Improved flow and perfusion
   - Increased collateral blood flow
   - Decreased coronary artery spasm
   - Increased diameter of epicardial arteries and stenoses
   - Increased endothelial relaxation factor activity
   - Increased prostacyclin activity
   - Decreased platelet adhesiveness and plateau plugs
   - Increased coronary vein and lymphatic flow
   - Increased removal of noxious metabolites of ischaemia
3. Decreased ischaemic injury and infarct size
4. Improved cardiac geometry
   - Decreased chamber size and wall stress
   - Decreased deformation forces
   - Decreased regional dilatation and expansion
   - Decreased global dilatation
   - Decreased aneuysm formation
5. Improved regional and global ventricular performance
6. Decreased infarct related complications
7. Improved survival

Modified from Jugdutt (22[Appendix 4])

2.5.3. The RAAS and ACE-inhibition

During the early 1980's, interest in the role of the renin-angiotensin-aldosterone system (RAAS) in heart failure after MI was increasing. Collective evidence indicated that cardiac failure from myocardial loss, or other causes, is associated with excessive rise in preload, systemic vascular resistance and afterload, heart rate, catecholamines and activation of the RAAS (110). This leads to angiotensin-mediated vasoconstriction and aldosterone-mediated sodium retention result (111). The end-result of significant myocardial loss is congestive heart failure (Table 5). Various factors in congestive heart failure lead to the release of renin, the rate-limiting enzyme for the generation of angiotensin II and aldosterone. Several compensatory mechanisms become activated in the very early stages of heart failure (Table 5).

TABLE 5. **Pathophysiology of congestive heart failure after myocardial infarction**

Special features
Loss of ventricular mass
Ischaemia in adjacent regions
Aneurysm (regional shape distortion)
- paradoxical systolic expansion
- diastolic expansion
- increased wall stress
Increased wall stress in normal muscle
Decreased ventricular compliance
Global ventricular dilatation
Ventricular volume overload hypertrophy
General features
Pressure overload
Volume overload
Further loss of ventricular muscle
Decreased systolic contractile function
Restricted diastolic filling
Potentially deleterious compensatory mechanisms
Increase in renin-angiotensin-aldosterone
Increase in circulating catecholamines
Increase in preload
Increase in systemic vascular resistance
Increase in heart rate

It has been shown that neurohumoral activation is present after acute MI (112,113), even in haemodynamically compensated patients (114). Neurohumoral activation results in increased vasoconstrictor activity and retention of sodium and water, due mainly to the effect of angiotensin II, norepinephrine and

vasopressin (110,111). This is only partially counter-balanced by the vasodilator and natriuretic actions of atrial natriuretic peptide. Activation of the RAAS is the dominant feature of congestive heart failure. Angiotensin II contributes to the excessive rise in systemic vascular resistance, increased sympathetic outflow and increased levels of circulating catecholamines, and increased release of aldosterone which promotes more salt and water retention. Although compensatory mechanisms initially serve to maintain cardiac performance, they can potentially overshoot and produce deleterious effects, with excessive rise in preload, systemic vascular resistance and heart rate (115).

Although pharmacological inhibition of the RAAS may be produced at several points along the hormonal pathway (111), a practical and effective means of blocking the renin-angiotensin axis is by angiotensin-converting enzyme (ACE)-inhibition. ACE-inhibition was suggested for preventing the haemodynamic and metabolic changes, and thereby decreasing preload, afterload, and leading to improved cardiac output (111,116). I therefore pursued the hypothesis that ACE-inhibition might potentially limit infarct expansion, RSD, LV dilatation and aneurysm formation after MI. Long-term treatment with ACE inhibitors might be more effective than NTG alone because of their combined metabolic and haemodynamic effects and the fact that continuous NTG administration might be complicated by nitrate tolerance (117,118:**Appendix 27**).

In the early 1980's, ACE inhibitors, like captopril and enalapril, had been shown to effectively decrease preload and afterload, reduce cardiac size, and improve cardiac output in patients with severe and refractory heart failure (111,116). The ACE inhibitor captopril was also shown to reduce infarct size in rats (119). In 1985, Pfeffer et al. first reported the beneficial effects of 3 to 4 months of captopril therapy, begun 2 and 21 days after MI, on LV dilatation, cardiac output, and chamber stiffness after MI in the rat (120). The groups with initiation of treatment at 2 and 21 days after MI did not differ in that study (120). In a later study, Pfeffer et al. showed that captopril therapy prolonged survival in the rat model when begun 14 days after MI, after the early healing phase was mostly over (76). However, infarct expansion, RSD and infarct collagen were not evaluated in those studies.

By 1988, two randomized, double-blind clinical trials reported the beneficial effects of prolonged captopril therapy after acute MI, on LV size and function (29,30). First, Sharpe et al. (29) showed that captopril therapy (25 mg t.i.d.), in 60

patients with one-week old Q-wave MI but no heart failure prevented the increase in LV diastolic volume, reduced the LV systolic volume, increased stroke volume index, and improved LV ejection fraction after one month and up to one year by quantitative 2D-Echo. Second, Pfeffer et al. (30) showed that captopril therapy decreased LV diastolic volume, decreased filling pressure and increased exercise capacity during one year of follow-up in 59 patients with 11-day to 31-day old anterior MI and radio-nuclide ejection fractions of 45% or less but no heart failure.

The subsequent 'Survival and Ventricular Enlargement' (SAVE) trial showed beneficial effects of prolonged captopril therapy, started between 3 and 14 days (mean 11) after acute MI, on mortality and morbidity after MI (121). The effect on prolongation of survival in the patients with objective evidence of LV dysfunction on 2D-Echo was sustained for 3.5 years.

Because of fear that clinically significant vasodilator-induced hypotension during acute MI might increase infarct size and potentially result in more infarct expansion, as reported with NTG from my laboratory (122:**Appendix 28**), ACE inhibitors were avoided in the very early stage of MI. The relatively long half-lives of ACE inhibitors suggested the need for caution when used in that setting since timely withdrawal of the drug effect following a hypotensive event might not be possible. This possibility was expressed in the 'Cooperative New Scandinavian Enalapril Survival Study II' (CONSENSUS II) trial, where the ACE inhibitor was initiated intravenously on day 1 after MI and followed by oral therapy for 6 months (123).

The subsequent 'Healing and Early Afterload Reducing Therapy' (HEART) trial evaluated the effect of early (day 1 onwards) or delayed (day 14 onwards) ACE-inhibition with ramipril on LV enlargement by 2D-Echo in patients after acute anterior Q-wave MI (124,125). In this study, LV enlargement on quantitative 2D-Echo was used as a surrogate marker for the risk of clinical events (125). The results showed that early ACE-inhibition attenuated LV remodelling, assessed by the LV area, and resulted in earlier recovery of LV ejection fraction (124). The HEART trial was terminated early, because the results of the concurrent trials evaluating early ACE inhibitor therapy begun within 24 hours after MI indicated that substantial lives were saved by early therapy (124).

Meanwhile, studies from my laboratory in the canine model of relatively small MI suggested that long-term ACE inhibitor therapy during healing after MI limited LV remodelling and dysfunction (126[**Appendix 29**],127[**Appendix 30**],

128:**Appendix 31**) but also decreased infarct collagen (127-129), which was harmful in some cases (129:**Appendix 32**). The beneficial effects of ACE-inhibition of LV geometry and function were also confirmed in patients during healing after Q-wave MI (130). The combination of captopril and isosorbide dinitrate (ISDN) therapy during healing did not prevent the decrease in infarct collagen seen with captopril alone in the dog model (131:**Appendix 33**). In a parallel randomized double-blind clinical study that compared prolonged therapy with buccal nitrate (eccentric dosing, allowing a daily nitrate-free interval), oral captopril, or both given between 48 hours and 6 weeks after Q-wave MI, all three active treatments preserved LV function and equally attenuated LV remodelling and LV aneurysm (108).

In all these studies from my laboratory, the evaluation of LV geometry included 3D-reconstruction and assessment of RSD and infarct expansion on 2D-Echo. In contrast, the evaluation of LV geometry by 2D-Echo in the large clinical trials were somewhat limited and did not include 3D reconstruction and assessment of RSD or infarct expansion (132). Nevertheless, the finding of decreased infarct collagen is difficult to reconcile (27,133) with the overwhelming evidence in favour of the use of ACE inhibitors after MI (134). It is possible that pleiotropic effects of ACE inhibitors are involved in the overall benefits. The potential mechanisms of benefit from ACE inhibitors after MI are summarized in Table 6.

TABLE 6. **Potential mechanisms for benefit from ACE-inhibition therapy after acute myocardial infarction**

1. Improved haemodynamics
   - Decreased preload; increased venous capacitance
   - Decreased afterload and impedance
2. ACE-inhibition
   - Decreased renin-angiotensin-aldosterone system
   - Decreased catecholamine secretion
   - Decreased inotropic stimulation
   - Decreased systemic vascular resistance
   - Decreased vasoconstrictor tone
   - Improved collateral blood flow
   - Decreased heart rate
   - Decreased salt retention
3. Kininase inhibition
4. Improved cardiac geometry
   - Decreased chamber size and wall stress
   - Decreased deformation forces
   - Decreased regional dilatation and expansion
   - Decreased global ventricular dilatation
5. Improved regional and global ventricular performance
6. (Improved survival)

Modified from Jugdutt (22[Appendix 4])

The short-term trials of early ACE inhibitor therapy, initiated within 24 hours of MI, included the 'Fourth International Study of Infarct Survival' (ISIS 4) study (135), the 'Gruppo Italiano per lo Studio della Sopravivvenza nell' Infarcto Miocardico' (GISSI-3) study (136), the 'Chinese Captopril Study' (CCS-1) (137), and the 'Survival of Myocardial Infarction Long-term Evaluation' (SMILE) study (138). In addition, the 'Acute Infarction Ramipril Efficacy' (AIRE) study initiated ACE inhibitor therapy 3 to 10 days after MI in patients with congestive symptoms (139) and the 'Trandolapril Cardiac Evaluation' (TRACE) study began ACE inhibitor therapy 2 to 7 days after MI (140). The 'Captopril and Thrombolysis Study' (CATS) began the ACE inhibitor within 6 hours of MI (141). Of note, although these trials were conducted in the thrombolytic era, the SMILE study patients did not receive thrombolytic therapy (138).

Previous trials of ACE inhibitors in heart failure, including the 'Cooperative New Scandinavian Enalapril Survival Study' (CONSENSUS-I) (142), the 'Studies of Left Ventricular Dysfunction' (SOLVD treatment) with enalapril (143), the 'Veterans Administration Cooperative Vasodilator-Heart Failure Trial' (V-HeFT) (144) and SOLVD prevention trial with enalapril (145), were all beneficial but did not include detailed evaluation of regional infarct expansion, RSD or global LV shape on 2D-Echo.

2.5.4. Reperfusion

By the 1980's, several key studies in the dog model had demonstrated that acute coronary artery occlusion renders myocardium in the distal coronary bed at risk of infarction (146-148), and a gradient of nutrient flow from the central to border regions and from the endocardium to the epicardium is a major determinant of infarct size (149). Biochemical abnormalities that ensue in the ischaemic zone, such as increased lactate, acidosis, ionic pump failure and adenosine triphosphate (ATP) depletion, were postulated to set in motion a chain of events that lead to rapid loss of cellular homeostasis and progression to cell death (150). The biochemical studies suggested that the march to cell death is modulated by the severity of ischaemia and the levels of calcium ions, reactive oxygen species and ATP (150).

In the dog model of reperfused MI, Reimer et al. showed that necrosis marches from the endocardium to the epicardium as a wavefront between 40 minutes and 3-6 hours post-occlusion, and the march can be interrupted by

reperfusion (151). Furthermore, the transmural extent of necrosis in that study was 38% after 40 minutes, 57% after 3 hours, 71% after 6 hours and 85% after 24 hours, suggesting that the therapeutic time window for myocardial salvage was 3-6 hours in the dog (151). These findings continue to provide the rationale for early reperfusion to reduce infarct size (152).

The timing of therapy has been shown to be a critical factor for salvage of muscle, geometry and function after MI following permanent occlusion or post ischaemic reperfusion. It was recognized that the interval between the onset and completion of myocardial necrosis provides time for applying protective therapy to limit infarct size. Collective evidence suggests that this interval might be longer in humans than dogs or rodents (Figure 3). Thus, interventions applied 9 hours after coronary artery occlusion did not decrease infarct size in the dog model (153) while several studies in humans demonstrated salvage beyond 6 hours from the onset of MI (28,154). For example, Flaherty et al. (154) demonstrated that NTG therapy, given within 10 hours (range 6 to 13.5) after MI, improved thallium-201 scintigrams in patients and suggested that the 'cut-off' for reversibility was about 14 hours. In a subsequent study from my laboratory, NTG therapy given within 12 hours of onset of MI was associated with beneficial effects on clinical and laboratory parameters of myocardial necrosis and remodelling (28).

Several factors may explain the slower march to necrosis in humans compared to smaller animals (Figure 3). These include: i) the larger heart size and the slower heart rate in humans; ii) a more gradual occlusion process, involving thrombus formation on long-standing atheromatous plaques and/or spasm, and often subtotal in humans compared to the sudden and complete total occlusion induced in animal experiments. Evidence in the early 1980's suggested that the syndrome of severe chest pain associated with ECG changes signals the onset of the infarction process, and both occlusion and necrosis are not completed for several hours. This concept was supported by findings of the prolonged release of CK enzyme over 16 to 60 hours (155) and myoglobin over 2 to 3 days (156), or prolonged ST-segment elevation for several days (157), or improvement in multiple clinical and laboratory indicators of infarction in patients given therapy later than 6 hours after onset of chest pain (154). Other possibilities were also considered: i) that slow enzyme or protein release might merely reflect poor perfusion of the central core of necrosis rather than continued cell death; and

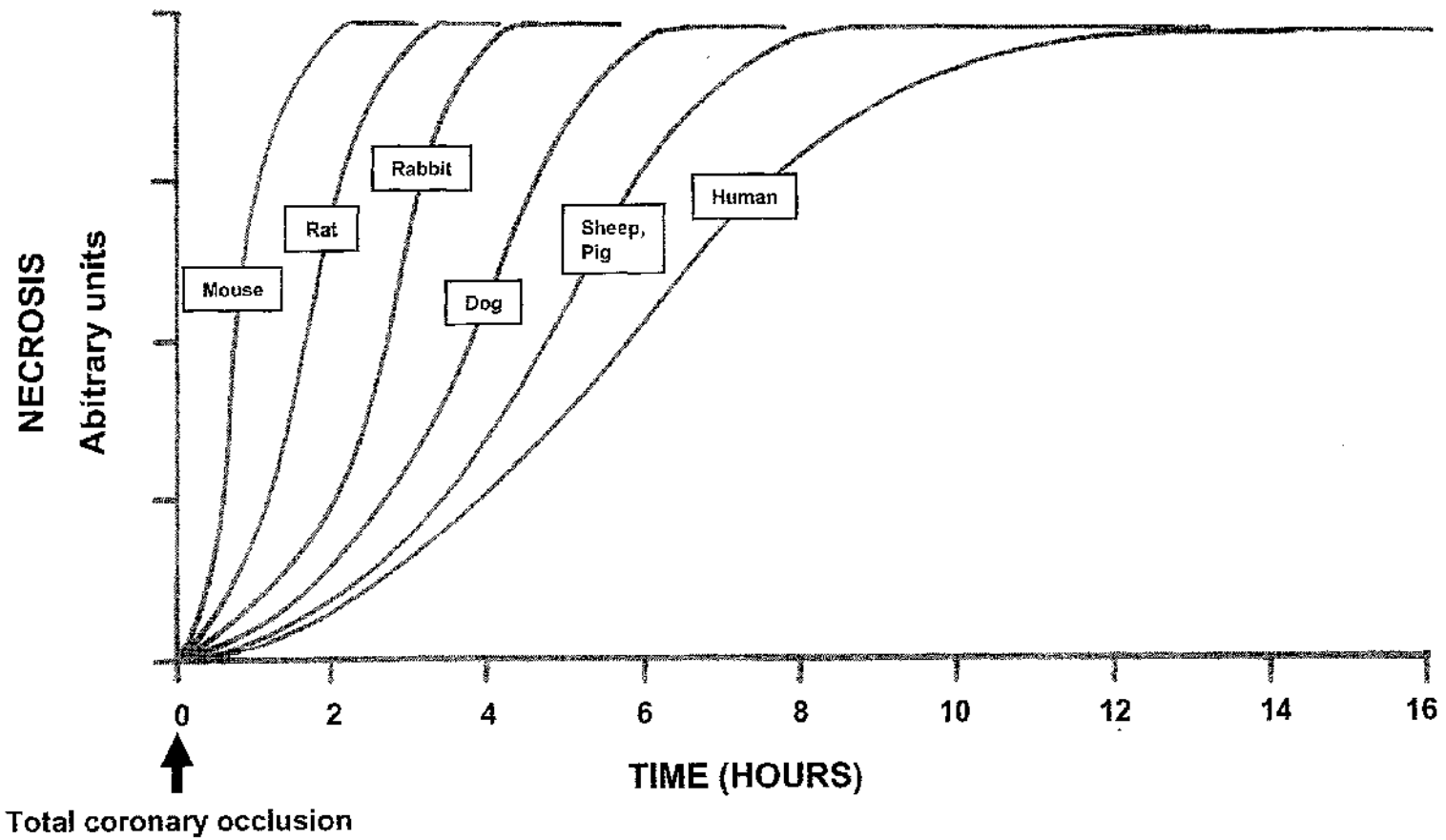

Fig 3. Rate of progression of necrosis in different species

The concept of slower progression of ischaemic injury to necrosis in humans compared to smaller animals. The interval between coronary occlusion and completion of necrosis is longer in humans with larger hearts and areas at risk than in dog, sheep, rabbits, rats and mice.

ii) that early therapy might prolong the interval to completion of necrosis by delaying its evolution, and this prolongation may be longer in man than dogs.

Although a slower march to necrosis might apply to permanent occlusion, subsequent data indicated that reperfusion, with thrombolytic therapy and/or percutaneous transluminal coronary angioplasty (PTCA), is most beneficial if performed very early (152). This led to the concept that other factors might be associated with the sudden restoration of flow to ischaemic myocardium by reperfusion. Thus, reperfusion may be associated with 'myocardial stunning' and reperfusion injury (158-162), resulting in mismatches between restoration of flow and salvage of muscle, LV geometry or LV function.

The mechanisms of reperfusion injury have been reviewed (158,163). Even successful reperfusion, that does not result in coagulative necrosis, may cause persistent mechanical dysfunction for 1 week or more. This delayed recovery of function, termed 'myocardial stunning', is associated with delayed recovery of adenosine triphosphate (ATP) (80% within 3 days). Other prolonged biochemical abnormalities include: increased oxygen-free radicals, calcium overload, interrupted creatine phosphate shuttle, cardiac sympathetic nerve dysfunction, and vascular 'no reflow'. Reperfusion itself can cause paradoxical injury and 'necrosis' that is predominantly of the contraction band type and may be potentially reversible. Reperfusion also causes extracellular collagen matrix (ECM) disruption, which may lead to disruption of mechanical coupling and contribute to dysfunction (164-166).

Evidence in the early 1980's suggested that late reperfusion, beyond 2 hours and up to a maximum of 6 hours in the dog (151,162), and probably 14 hours in humans (154), might result in significant reperfusion injury. Although late reperfusion results in persistent and prolonged mechanical dysfunction and ECM disruption (164-166), it still seemed to preserve LV geometry and limit acute expansion (47,167). Whether this beneficial effect might persist throughout the healing phase was controversial.

Three experimental studies in the rat model confirmed the benefits of very early reperfusion. First, late reperfusion made 2 hours post-occlusion did not limit infarct size or transmurality but reduced infarct expansion (47). Second, early reperfusion made 1 hour post-occlusion reduced infarct size and expansion while late reperfusion at 6 hours did not limit infarct size or expansion but accelerated healing (168). Third, late reperfusion made 6-8 hours post-occlusion did not limit

infarct size as seen with early reperfusion after 1-2 hours but limited infarct expansion and accelerated healing, with more rapid removal of dead myofibrils and increased myocytolysis (46).

Eight studies in the dog model supported the idea of greater overall benefits with very early rather than late reperfusion. These studies were:

First, reperfusion made 2 hours after left circumflex (LCX) coronary artery occlusion was associated with decreased tissue loss but delayed improvement of regional LV function over 4 weeks (169).

Second, reperfusion made 3 hours after LAD or LCX coronary artery occlusion showed little evidence of myocardial salvage (170).

Third, LV function at 4 weeks improved with reperfusion made 2 hours after LAD occlusion but not with reperfusion made 4 hours after LAD occlusion despite similar infarct sizes in the two groups (171).

Fourth, reperfusion made 90-120 minutes after LCX occlusion resulted in late recovery of function and hypertrophy of salvaged cardiomyocytes in the border regions at 3 weeks (172).

Fifth, reperfusion made at 2 hours after LAD occlusion resulted in delayed recovery of global LV function without change in regional LV asynergy, attenuation of global and regional dilatation, less infarct expansion and thinning during healing over 6 weeks despite decreased infarct collagen (49).

Sixth, reperfusion made 6 hours after LCX occlusion did not decrease infarct or scar size but still increased the rate of healing over 6 weeks (173).

Seventh, reperfusion after 4 hours, in a mid-LAD and LCX branch occlusion model, was associated with significant intra-myocardial haemorrhage in necrotic areas, decreased early granulocyte response, suggesting impaired early healing, and no decrease in infarct size (174).

Eighth, very late reperfusion, made at 1 day or 7 days after completion of necrosis from an LAD occlusion, had no effect on infarct size, transmurality, collagen, haemorrhage, calcification or inflammation, suggesting that there was no effect on healing in that setting (175).

A study of the mechanical properties of the infarcted left ventricle following reperfusion, made 1-3 hours after coronary occlusion in the rabbit model, demonstrated that the reperfused scars had lower collagen content and lower tensile strength and ruptured more easily at high stresses (176). The late group in

that study also showed lower collagen cross-linking density in the 3-week-old scars.

A clinical study assessed the effect of time to reperfusion on infarct size by imaging with thallium-201 (Tl-201) single-photon emission computed tomography (SPECT) and LV function by LV angiography in patients with anterior MI (177). Compared to non-reperfused patients, reperfusion decreased infarct size and improved global LV ejection fraction in early (within 3 hours of the onset of pain) and intermediate (3-6 hours) groups but not the late (>6 hours) group. Importantly, reperfusion limited LV dilatation in all three groups (177).

Several studies addressed the effect of adjunctive therapies after reperfusion. In the dog model of reperfusion made 4 hours after LAD occlusion for 2 hours, methyl prednisolone decreased infarct size but did not improve function on 2D-Echo (178).

In the dog model of reperfusion for 2 days after 90 minutes of LAD occlusion, the diffusible anti-oxidant and hydrogen peroxide scavenger N-(2-mercaptopropionyl)-glycine, given between 30 minutes and 4 hours after reperfusion, decreased infarct size (179). Data in a clinical study from my laboratory indicated that early and prolonged intravenous low-dose NTG therapy (>24 hours) during and after late reperfusion (at 4 hours) was associated with prompt improvement of LV function and a decrease in infarct expansion that persisted up to 6 months on serial 2D-Echo (50,180).

In the dog model, the oxygen free radical scavenger, superoxide dismutase, given for 1 hour from the time of reperfusion made at 90 minutes post-occlusion, reduced infarct size (159). In the same model, superoxide dismutase given for 2 hours from the time of reperfusion made 2 hours post-occlusion, reduced infarct size and infarct expansion and improved LV function beyond that achieved with reperfusion alone (181). The overall findings suggest that myocardial stunning and reperfusion injury can be prevented by early reperfusion and adjunctive therapy (182).

There is now general agreement that greatest success is achieved when reperfusion is established within 2 hours after MI in humans (152). Although this is not always clinically possible, aggressive approaches to abbreviate the interval between the onset of pain and therapy have been beneficial (183). Reperfusion therapy alone, with coronary angioplasty and thrombolysis (184) or in combination with other pharmacological agents such as NTG (50), has been shown to limit

infarct expansion. Thrombolytic therapy has already been shown to improve survival in both the GISSI trial (185) and the international ISIS-2 trial (186,187).

Recent studies in the rat model have suggested that early cell death after coronary occlusion involves apoptosis, a form of genetically programmed cell death, followed by necrosis (188). After reperfusion in the rat, early cell death has been suggested to also involve oncosis (cell swelling) together with nuclear changes seen with apoptosis (189). The topics of apoptotic and oncotic cell death in acute coronary syndromes have been reviewed (190). Imaging of apoptotic cell death after reperfused MI has confirmed that very early cell death occurs within the 2-hour time window in mice (191) and within the 6-hour time window in patients (192,193). In one clinical study, 99m-technetium (99m-Tc)-labeled annexin-V uptake reflecting cardiomyocyte apoptosis increased between early (3.4 hours) and late (20.5 hours) on SPECT images, and 99m-Tc –sestamibi imaging at 6-8 weeks confirmed defects seen at the earlier annexin-V uptake sites (192). In the other clinical study, 99m-Tc-sestamibi imaging showed perfusion defects that decreased in size between baseline and 5-19 day studies and all patients showed 99m-Tc-annexin-V-positive cardiomyocytes in the infarct zone (193). The overall findings support the concept of reversible myocardial damage being present beyond 6 hours after the onset of MI in humans.

After 1985, several laboratories applied imaging techniques to study LV remodelling after MI in patients with or without reperfusion. Of eight reported studies, none addressed RSD and LV remodelling in a systematic fashion. These studies were:

First, a study of 30 patients receiving thrombolysis after a first Q-wave MI (15 anterior, 15 inferior) showed, by serial M-mode echocardiography and LV angiography over 2 weeks, that early infarct expansion and global LV dilatation correlated with the extent of wall motion abnormality on the baseline study (194).

Second, a study of 54 patients with a first MI (29 anterior, 25 inferior) and no thrombolysis, showed evidence of early LV dilatation which was more marked in anterior MI, and LV diastolic dysfunction even in patients with preserved LV systolic function using serial blood pool radio-nuclide (99m-Tc) angiography over 10 days (195).

Third, in a randomized study of 99 patients with acute MI (50 placebo, 49 captopril; 12 previous MI; 76 with new Q waves; 59 anterior; 40 infero-posterior; no thrombolysis), serial 2D-Echo over 2 months documented evidence of early

infarct expansion which was attenuated by captopril (196). However, that study did not show improvement of exercise capacity or attenuation of LV dilatation with captopril (196).

Fourth, a study of 56 patients with acute MI using 2D-Echo over 6 months, confirmed that successful reperfusion preserves LV systolic volumes and regional function (197).

Fifth, a study of 14 patients with a first acute MI (12 anterior, 2 inferior) and receiving reperfusion therapy with PTCA and rt-PA (recombinant tissue-type plasminogen activator) used 99m-Tc-sestamibi for measuring infarct size and electron beam computed tomographic imaging for LV volumes and function (198). This study showed significant LV dilatation over 1 year and correlation between infarct size and LV volume and function at 1 year (198).

Sixth, in a study of 233 patients with a first anterior MI treated with thrombolysis, the baseline wall motion score index was shown to predict LV dilatation and mortality (199). The enzymatic infarct size, which is not available until 3 days after MI, also predicted LV dilatation in that study (199).

Seventh, in a study of 53 patients after a first anterior MI treated with PTCA, angiographic dye intensity in the myocardial risk area correlated with the reduction in LV volume (200).

Eighth, in a randomized study of 352 patients with anterior Q-wave MI treated with reperfusion and the ACE inhibitor ramipril for 90 days, serial 2D-Echo confirmed myocardial stunning and delayed recovery and the predictive value of CK for functional recovery (201). This study noted that the baseline LV function was not a predictor of LV functional recovery after reperfusion (201).

2.5.5. Importance of collateral blood flow in remodelling and healing after MI

In the 1980's, there was continuing controversy about the existence of intramural coronary collaterals in the normal human heart and their functional significance in patients with coronary artery disease (For review see Gregg, 202). Post-mortem studies (203,204) had demonstrated inter-coronary arterial collateral channels, measuring 20 to 350 μm and more prevalent in the endocardium, in both normal and diseased human hearts. Blumgart had pointed out that the majority of intramural collaterals were too small to be visualized on routine coronary angiography (205). It was postulated that chronic ischaemia stimulates the

development of collateral channels, thereby resulting in greater increase in their size in the subendocardium than subepicardium.

The pattern of collateral anastomoses in dogs is somewhat similar to that in human hearts with chronic coronary artery disease (203,205), but there are important differences. Dog hearts have a more abundant collateral supply and the network is predominantly sub-epicardial (204). Furthermore, the time required for inter-coronary collaterals to develop in man in response to ischaemia is not known. After abrupt coronary occlusion in dogs, there is a small collateral inflow which often doubles in the first 24 hours (206) and increases considerably during the first 4 days. In contrast, gradual coronary occlusion in the dog results in a large increase in collateral function within days (202,207). Thus, it was postulated that chronic ischaemia in man may stimulate enlargement of collaterals and development of muscle bundles in their walls within days to weeks (204), and blood flow via collaterals into ischaemic areas was possible (208).

In patients with MI, the degree of collateral development and the amount of collateral reserve might differ depending on such factors as duration and severity of coronary artery disease, presence of multi-vessel involvement, type of occlusion and a history of previous angina pectoris and/or infarction. Characterization of coronary anatomy and collateral circulation before and after infarct-limiting therapy such as NTG have not been done for practical, ethical and technical reasons.

In the pig heart, collaterals are sparse (and concentrated toward the endocardium) so that infarcts are predominantly transmural (204). In a dog model of collateral obliteration and more LV aneurysms (Figure 4), the infarcts are consistently transmural and show greater LV remodelling (73,74).

Attenuation of remodelling might be greater in patients with developed collaterals and a patent infarct-related artery (209,210) during healing after MI. Collaterals also appear to influence recovery of function after reperfusion (23). Thus, collaterals contribute flow not only for salvage of ischaemic myocardium, resulting in small subendocardial infarcts that are less prone to adverse LV remodelling, but also provide nutrient flow which likely promotes normal healing, thereby limiting remodelling. In the recent Total Occlusion Study of Canada (TOSCA), the restoration of flow in the non-acute occluded arteries resulted in a small improvement in LV regional and global function (211). However, the effects on LV remodelling or RSD were not assessed in that study.

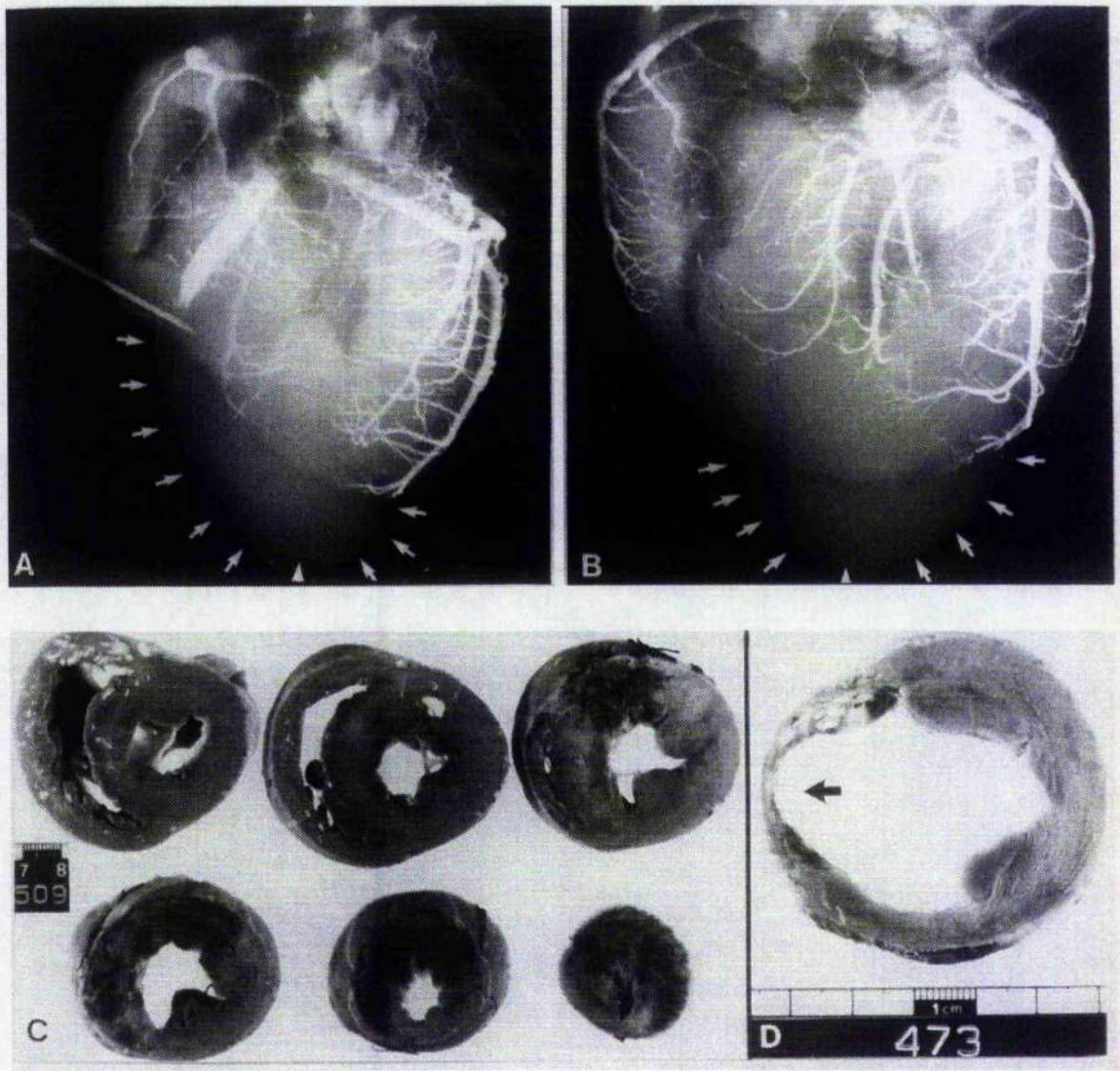

Figure 4. Transmural infarction and aneurysm in the dog induced by collateral obliteration.

A, B. Radiographs showing an LV apical aneurysm and patent coronary vessels by post-mortem arteriography. Note the avascular LV apex.

C, D. Transmural infarction produced by mid-LAD ligation (arrow), barium-gelatin-polymer injection into distal LAD, and running suture around the occluded bed. All myocardium within the ligated bed shows infarction, with no sparing.

Jugdutt (74[Appendix 20])

2.5.6. Beta-adrenergic blockade and calcium channel blockade

Experimental (212) and clinical (213) studies in the mid 1970's showed that beta-adrenergic blockade with propranolol after MI decreased infarct size (212) and improved LV function (213). Beta-adrenergic blockade with metoprolol, given over the first 15 days after acute MI in the large Metoprolol In Acute Myocardial Infarction (MIAMI) trial, showed positive effects on CK infarct size in patients treated within 7 hours but no survival benefit (214-216). Acute improvement in LV function with intravenous metoprolol after MI was seen in patients with pre-formed collaterals to the infarct zone (217). In the dog model of MI, intravenous metoprolol initiated before thrombolytic therapy, increased infarct limitation partly by increasing collateral flow (218). In the rat model, propranolol, given over 5 weeks after MI, decreased myocyte dimensions, and wall thicknesses, and increased LV dimensions (219).

In theory, decreased inotropism and heart rate with beta-adrenergic blockade would be expected to decrease the strength and frequency of the contractile pull of the non-infarct zone on the infarct zone and thereby reduce infarct expansion. However, this beneficial effect may be offset by any increase in LV volume secondary to decreased contractility.

The effect of beta-adrenergic blockade on LV function and topography by 2D-Echo was studied in 63 MI patients randomized to metoprolol (15 mg intravenously initially, given as 5 mg intravenously every 2 minutes for a total of 3 injections, followed by 100 mg orally twice day trial for 15 days and maintenance for 90 days) or placebo (220). Metoprolol decreased early rate-pressure product and CK infarct size, and persistently decreased LV asynergy and increased LV ejection fraction on serial 2D-Echo over 24 weeks (220). However, serial 2D-Echo revealed similar mean expansion index and thinning ratio in the two treatment groups (220). Thus, it is very likely that the beneficial effect of metoprolol on infarct size, rate-pressure product and contractile pull was offset by the effect on chamber size, which was similar to that in the placebo group.

The effect of the calcium-channel blocker nifedipine on LV function, infarct size and infarct expansion was studied in a prospective double-blind, placebo-controlled trial of 132 low-risk MI patients randomized to nifedipine (120 mg/day) or placebo (89). The patients were treated within 12 hours of symptom onset and had initial LV ejection fractions more than 35% and clinical Killip classes of less than II. Therapy was continued for 6 weeks, and evaluations made before

treatment and at 10 days. There was no effect on clinical outcome or infarct size with nifedipine, although mean blood pressure decreased by 10% over the 10 days. However, nifedipine limited infarct expansion on 2D-Echo. In a study of 424 patients with successful reperfusion, within 12 hours of symptoms of acute MI, a possible survival benefit was shown with beta-adrenergic antagonist but not calcium-antagonist therapy taken before reperfusion (221).

2.5.7. Digoxin

In theory, prolonged inotropic stimulation and increased contractility of the non-infarct area after MI would be expected to promote infarct expansion by increasing intra-mural traction on the infarct zone. The effect of digoxin therapy during healing over 6 weeks after MI was therefore studied in the dog model of MI (222). In this model of predominantly small infarcts, digoxin therapy increased infarct expansion, thinning and bulging as well as the frequency of LV aneurysms on 2D-Echo (222). Digoxin also reduced global LV dilatation but preserved LV mass, global LV systolic function and infarct collagen (222).

2.6. Development of a chronic large animal model for studies of left ventricular remodelling during healing after myocardial infarction

Prior to 1980, there were no well-defined chronic large animal models for quantifying infarct size and remodelling or studying the long-term effects of interventions on LV function and remodelling during healing after MI. Variability of coronary anatomy in dogs resulted in variable infarct size despite occlusions at a fixed anatomic site. Between 1976 and 1979, a chronic canine model was therefore developed for studying the effects of early interventions on the size of the infarct relative to that of the occluded bed 48 hours after LCX occlusion as well as regional collateral blood flow and haemodynamic variables (147). This model allowed the mapping of infarcts, occluded beds and regional blood flows from the base to apex of the left ventricle (147,149). The potential for pharmacological agents to modify the relation between the mass of the infarct and occluded bed was initially studied using vasodilators, such as NTG and prostaglandin (PG) inhibitors (which were also anti-inflammatory agents), in the conscious dog model (56,57,98,99). The end-points included haemodynamics, collateral blood flow and pathologic infarct size (56,57,98,99).

The analysis of infarct size relative to occluded bed size at 2 days post MI had at least 5 advantages (56,57,98,99,147). **First**, it provided a reliable baseline for studying the effect of therapies on infarct size. **Second**, it made allowance for the variation in coronary anatomy which leads to variation in infarct size despite occlusions made at a fixed site. **Third**, it allowed comparison of treatment groups using linear regressions showing the direct relation of infarct size to the occluded bed size. **Fourth**, it recognized the fact that no infarcts result with occluded beds smaller than 20% of the LV weight; this factor resulted in a dilution effect in studies that expressed the infarct weight in grams or as percent of LV weight, necessitating large numbers of dogs to detect significant differences with interventions. **Fifth**, it permitted the detection of increased or decreased infarct size using relatively small numbers of animals, by comparing the slopes of the linear regressions between infarct size and occluded bed size for treatment groups. Similar relationships between infarct size and occluded bed size were found in humans dying soon after acute MI.

Post-mortem coronary arteriography had been used previously to visualize the coronary anatomy by Fulton in Glasgow (223) and Schaper in Mannheim (204). This technique was applied in the 2-day infarct model to measure the occluded bed size, which was defined as the boundary between the anatomic locations of epicardial and transmural vessels recorded on stereoscopic radiographs of transverse sections, after permanent opacification by a barium sulphate-gelatin mixture containing pigments (224). This method was shown to be reproducible and allowed the mapping of collateral blood flow relative to an anatomic reference base that was considered to remain fairly fixed over the first 48 hours after MI (225).

In 1980, I set up the first laboratory for studying LV function and remodelling after MI at the University of Alberta. I introduced the chronic dog model that was developed at the Johns Hopkins Hospital (147) and adapted it for studying cardiac function and remodelling over several weeks after MI rather than just 2 days (41,55). Since several studies suggested that anterior MI had a worse prognosis that inferior MI, I performed both LAD and LCX occlusions. Infarct size was quantified and topography was mapped using computerized planimetry (Hewlett Packard digitizer and computer, Seymour, Connecticut) (Figure 5). Regional myocardial blood flow was measured by the radioactive microsphere method using a flow program for multiple isotopes rather than just six (Tracor

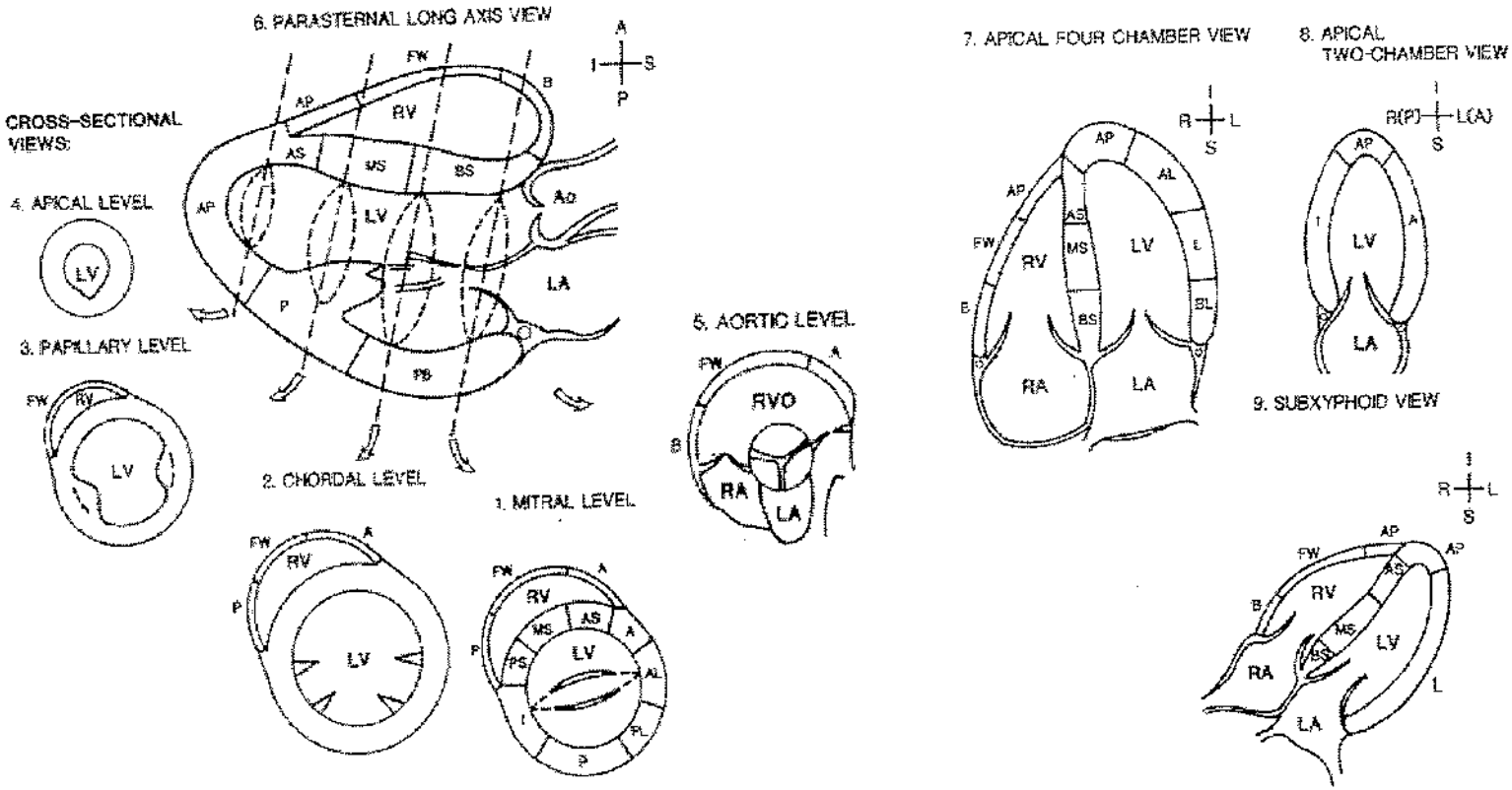

Figure 5. Systematic tomographic imaging protocol using 2D-Echocardiography.

Tomographic images in 9 planes used systematically in our laboratory for studies of ventricular function and geometry. Outlines based on the first 500 studies.
A, anterior; Ao, aorta; AL, anterolateral; AP, apical; AS, anteroseptal; B, basal; BL, basal lateral; BS, basal septal; FW, free wall; I, inferior; LA, left atrium, LV, left ventricle; MS, mid septal; P, posterior; PB, posterior basal; PL, posterior lateral; PS, posterior septal, RA, right atrium, RV, right ventricle; RVO, right ventricular outflow.

From Jugdutt (247)

Northern 2250 gamma scintillation counter). Post-mortem coronary arteriography was used for quantifying the occluded bed size (Figure 6). Systematic pathological assessment of the post MI hearts was carried out for infarction, cardiac dilatation, aneurysm formation, rupture, geometric variables and correlation with ante-mortem 2D-Echo imaging. Computer programs were developed (Hewlett Packard) for statistical analysis, the analysis of large volumes of haemodynamic, angiographic, pathological and CK infarct size, 2D-Echo, and clinical data.

The model of mid-LCX occlusions and 2-day infarcts was validated in a study of the effects of PGE_1, PGE_2, and PGI_2 (or prostacyclin) and drugs acting via apparently different mechanisms such as NTG and ibuprofen, on infarct size, collateral blood flow and post-infarction arrhythmias (226). Decreased infarct size as percent of the risk region was demonstrated with PGI_2, NTG, PGE_1 and ibuprofen but not with PGE_2. Interestingly, this beneficial effect was associated with decreased infarction arrhythmias and was more marked with PGI_2, NTG and PGE_1, which also increased collateral blood flow, but was trivial with ibuprofen which did not increase flow. In addition, PGE_2 exerted an anti-arrhythmic effect independent of beneficial effects on infarct size or flow (226).

The model was then modified by using i) arteriographic injections distal and proximal to the occlusion site instead of relying on filling via collateral channels, and ii) 10 LV sections instead of 5, in order to reduce the error in marking the boundaries to 1±1 mm (SD). Collateral blood flows were mapped within the occluded bed from the base to apex of the heart. This approach allowed definition of a functional risk region based on regional blood flows.

Using this modified model, the effect of mid-LCX and mid-LAD occlusions on infarct size was studied in conscious and barbiturate-anesthetized dogs (227[**Appendix 34**],228[**Appendix 35**]). The results showed that for similar occluded bed sizes, I) LAD infarcts were larger than LCX infarcts (227,228), and ii) infarcts were larger for anesthetized compared to conscious dogs (227,228). The overall findings suggest that this effect was due to tachycardia in the anesthetized model (227,228). In a previous study, a single dose of thiopental to 'conscious' dogs resulted in increased heart rate and bigger infarcts after LCX occlusions (229). Two conclusions were drawn from these studies. First, cardiac patients who receive barbiturate anesthesia and develop peri-operative MI may be at increased risk for larger infarcts. Second, intervention studies should analyze

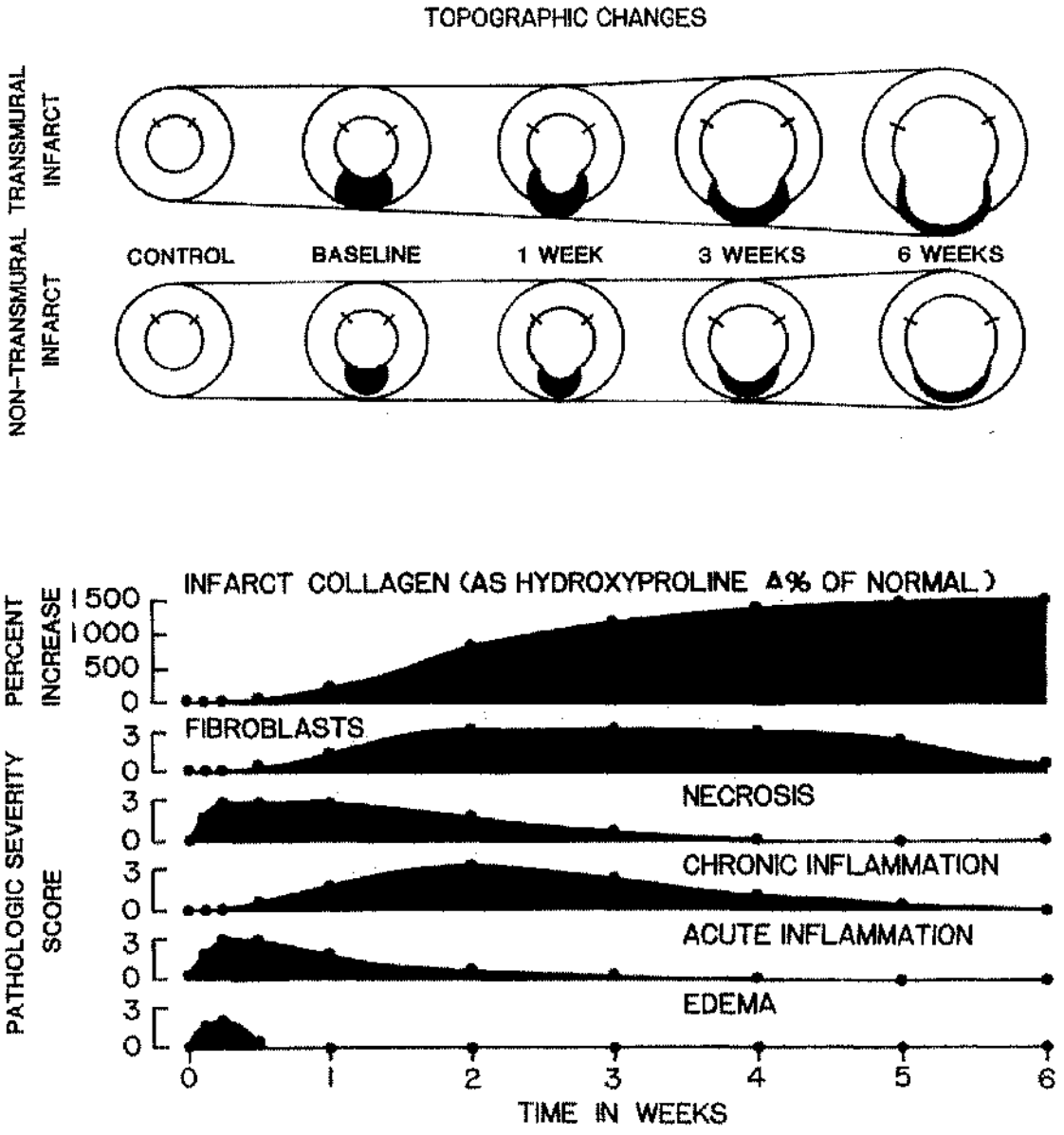

Figure 6. Histopathological and topographical changes during infarct healing

A. A schematic of topographical changes from average maps of the transmural and non-transmural infarcts among those hearts for five selected time intervals.

B. The dynamic nature of histological changes in the infarct substrate during healing over 6 weeks in the dog model of myocardial infarction. Data from 194 canine hearts.

From Jugdutt (22[Appendix 4])

infarct size data after LAD or LCX occlusions separately and pooling of infarct size data from anterior and inferior MI should be avoided.

Subsequent studies tested various vasodilator therapies in the model of anterior MI after LAD occlusion. The concern that excessive afterload reduction with vasodilator therapy after acute MI might decrease perfusion pressure below a critical level and offset previously noted beneficial effects was first investigated. In the previous study, 6 hour intravenous infusion of the vasodilator NTG after LCX occlusion, in low-dose to decrease mean arterial pressure (an index of afterload) by less than 10% but not below 80 mm Hg, was demonstrated to decrease pathologic infarct size (98). This beneficial effect was associated with a marked increase in collateral blood flow and a marked decrease in LV filling pressure, an index of preload. In the new LAD occlusion model, collateral flow did not increase and no myocardial salvage was found when mean arterial pressure decreased by 20% or more with higher NTG dosage (123), suggesting a narrow therapeutic margin for benefit with vasodilator therapy, such as intravenous NTG, in acute MI. In the same conscious dog model, prolonged therapy after MI with NTG (48,102,103), captopril and enalapril (126-129,131) were shown to further limit remodelling during healing after transmural MI and improve LV function.

2.7. Assessment of left ventricular geometry and function during healing after myocardial infarction

Since 1980, I focused studies in my laboratory on the natural history of LV geometry and function during healing after MI using 2D-Echo and the effects of early infarct-limiting therapies on subsequent healing, LV geometry and LV function by 2D-Echo, and clinical outcome.

Since 2D-Echo provided tomographic images of the heart in real-time (230) and permitted repeated examinations to be made non-invasively, it became an effective tool for research studies in the early 1980's. Between the mid 1970's and the mid 1980's, 2D-Echo was successfully applied to estimate regional LV function and LV asynergy (16,17,231,232:**Appendix** 36) despite some technical limitations (233), to estimate infarct size (62), to detect LV aneurysms (15,234), to detect post MI complications (235), to measure LV volumes (236), to measure regional LV shape distortion (19,21,34), infarct expansion and remodelling in general (18,20,21,31,32), and LV hypertrophy (102,237).

The relationship between LV asynergy on 2D-Echo and myocardial necrosis was validated in an earlier study in the dog model (62). The ability to quantify LV volumes by tomographic imaging using 2D-Echo was also validated in the dog model (238). Significant resolution of LV dyskinesis on 2D-Echo after LAD or LCX occlusion with normalization of transmural blood flow over 6 weeks was demonstrated in a small study of 13 dogs (239). This recovery of regional function was later ascribed to scar contraction during healing after MI (240). Several studies applied 2D-Echo to measure the endocardial surface area of LV asynergy after MI (21,28,34,36,241-243) and demonstrated its expansion after MI (244). Quantitative 2D-Echo was used to assess LV thrombi after MI (245) and later to predict apical thrombus formation (246). The application of 2D-Echo to detect the viability of dysfunctional myocardium has been recently reviewed (247). Quantitative 2D-Echo has confirmed greater LV dilatation after anterior than inferior MI (28) that was previously documented by echoventriculography (248). Quantitative 2D-Echo has also confirmed that LV ejection fraction may improve and the extent of LV asynergy may decrease in some survivors after MI (21,28,34), as suggested in a previous study using gated blood pool scanning (249).

2.7.1. Assessment of infarct or scar size and remodelling in humans versus animals

In animal studies, direct ex-vivo demonstration of myocardial protection and reduction of ultimate necrosis and remodelling is possible. In contrast, clinical studies have had to rely on indirect methods that are often frustrating because of the lack of a single reliable standard for infarct size and difficulties in obtaining serial measurements before and after therapy. Multiple non-invasive techniques that permit serial measurements of different indicators of the extent of ischaemic injury have therefore been used to assess effects of therapy but each technique has its limitations (250:**Appendix 37**).

Because of the possibility that therapy merely delays the evolution of necrosis and prolongs the interval to its completion, assessment of infarct size needed to be repeated over several days to demonstrate persistent benefit. Quantitative 2D-Echo was therefore an attractive tool for quantifying LV geometry and function during healing after MI in the dog model (102) and in patients (21,28,34,35,132).

2.7.2. Preliminary studies: validation of quantitative 2D-Echo for left ventricular remodelling and function

Although there was a paucity of information in the literature on the application of 2D-Echo for repeated studies, beginning at the bedside in acutely ill or acute MI patients in the early 1980's, my laboratory validated the method in the first 500 patients over the first 2 years and had performed over 1500 research studies by 1985. As there was no standard protocol for quantifying wall motion abnormalities in acute MI and to allow the application of repeated 2D-Echo imaging for assessing the effect of therapies in early MI in 1980, a systematic approach for tomographic 2D-Echo imaging using a strict protocol (Figure 5), was applied both for studies at the bedside and in the laboratory (21,28,34,35). Against prevailing scepticism over the applicability of quantitative 2D-Echo in acute MI studies, the necessary computer software programmes were developed for these studies in my laboratory (19-21,28,34,35,232). This innovative research approach in patients with acute MI, while in the coronary care unit (CCU), revealed unsuspected complications on 2D-Echo imaging such as right ventricular infarction (251-253), LV thrombi and embolization (245), early RSD and infarct expansion (19-21,33-36), cardiac rupture (20), as well as large pericardial effusions and cardiac tamponade, and papillary muscle rupture.

The advantage of quantitative 2D-Echo studies using a strict systematic protocol, both for initial studies at the bedside and subsequent follow-up studies in the laboratory, with recording of patient positioning and angulation as well as transducer positions for repeated studies, has been confirmed in many laboratories (31,32,132). The ability to perform serial, non-invasive estimation of LV asynergy and RSD using quantitative 2D-Echo in experimental and clinical studies made it possible to objectively assess the effect of therapies on these parameters. Such studies contributed to the development of practical therapeutic strategies to preserve ischaemic myocardium as well as geometry and function in survivors, and thereby reduce morbidity and mortality post MI (23). Systematic application of 2D-Echo in bedside studies in acute MI patients between 1980 and 1985 demonstrated the limitation of LV asynergy (232) and infarct expansion (28) by NTG.

2.7.3. Assessment of global left ventricular shape and regional shape distortion

The shape, size and structure of the normal left ventricle appear to reflect an adaptation to the dynamic requirements during systole and diastole. Adjustments ensure the optimal conversion of energy during contraction to the development of pressure and systolic ejection. Heart size has been shown to be directly related to its work load (254). Ventricular wall thickness is directly related to ventricular radius, and the ratio of wall thickness is directly related to systolic pressure (1). The Law of Laplace (255), which is crucial for understanding LV shape relative to LV load, states that wall stress (S) is proportional to pressure (P) and the radius of the curvature (r) for thin walled spheres. Thus, for wall thickness (t), the Law of Laplace states:

$$S = Pr / 2t$$

Clearly, this only provides an approximation as the left ventricle is not a thin-walled sphere with uniform radius. Other investigators have modelled LV shape on a spheroid (256) or an ellipsoid (2,257), or on an egg shell with its top cut off (258), close to a truncated ellipsoid. More than 100 years ago, the LV wall was modelled on a curved membrane with two principal radii of curvature and a finite thickness (259). Modern cardiac imaging techniques, including 2D-Echo, support the idea of the normal LV shape being circular in the short-axis and close to a truncated ellipse in the long-axis (2).

It is important to note that mathematical models assume uniform LV shape and, often, uniform wall thickness as well. Calculations of LV wall stress are therefore flawed by over-simplified assumptions (260). Various mathematical approaches have been proposed for calculating wall stress (10,261,262). In pressure- and volume-overload hearts with LV dysfunction and LV dilatation, the transition from the normal ellipsoidal shape to a spheroidal shape represents an adaptation towards normalized wall stress (263-266). Global shape has been measured by a variety of indexes: the eccentricity index (267), Gibson index (268), shape-power index from Fourier analysis (269), curvature index based on quantitative regional curvature analysis (270), global LV shape index based on the ratio of major axis to minor LV axis at end-systole and end-diastole (271), a shape index based on the short- to long-axis ratio on 2D-Echo (265), a shape index based on width, length and area on 2D-Echo (266) and a sphericity index based

on the long-axis length (12). Although these indexes were useful predictors, none involved left ventricles with marked regional shape distortions associated with MI.

Numerous reports have described RSD of asynergic zones on end-diastolic short-axis and long-axis images on 2D-Echo, with further dilatation on end-systolic images (15-21,33-36,272). Several investigators have attempted to measure the areas and volumes of large chronic LV aneurysms on 2D-Echo. In patients with LV aneurysms, a residual myocardial index derived from 2D-Echo was shown to identify survivors after LV aneurysectomy (273).

I quantified RSD directly on short-axis 2D-Echo images in patients after MI and showed that the degree of early diastolic RSD predicted subsequent outcome (21). In another study, I demonstrated that significant RSD preceded ventricular septal rupture after MI (20). Importantly, the degree of RSD on the baseline 2D-Echo correlated with the degree of LV dilatation at follow-up, suggesting its role in progressive LV enlargement (274:**Appendix 38**). It is possible that increased wall stress in the border zone (275), especially in the presence of RSD, drives the progression to global LV dilatation and a global LV shape with normalized wall stress. Moreover, in 40 patients with LV dysfunction after anterior MI, the sphericity index on LV angiography was elevated at a baseline study between 2 and 4 weeks (12). In a study of 30 patients with anterior or inferior MI from the SOLVD study (11 placebo, 19 enalapril), follow-up between about 1 year and 2 years showed evidence of increased wall stress and progression of LV dilatation (276). In a subsequent study of 70 patients with anterior and inferior MI, progressive dilatation was detected over 3 years after MI (26). However, these studies did not assess RSD and the populations were fairly heterogeneous.

The collective evidence suggests that measurement of diastolic RSD in asynergic zones after acute MI may identify a high-risk group of patients who might benefit from aggressive therapy.

2.8. The concept of adverse remodelling after myocardial infarction and anti-remodelling therapy

The concept of infarct size limitation implies existence of a functional border zone in the ischaemic region (88). In that concept, myocardium within the border zone is at jeopardy because of reduced flow but has sufficient flow for immediate survival. Subsequent increase in collateral flow, natural or drug-induced, provides

for ultimate survival of this tissue. Flow in other areas is so low that necrosis results despite therapeutic efforts.

One major factor for survival of ischaemic myocardium is collateral flow, and this was confirmed in a previous study (149). It appears that during the early hours after coronary occlusion, there are varying amounts of normal, ischaemic and dead myocardial cells depending on a gradient of collateral flow from the peripheral to more central regions of the occluded bed (149). Other factors are also important, such as the myocardial oxygen demands and various cellular and metabolic factors (87). However, these are also linked to flow. Well-timed restoration of flow by reperfusion of the ischaemic myocardium may arrest the progression to necrosis (148). The timing of therapy is therefore critical and the early hours are of pivotal importance in therapeutic efforts to modify the extent of ultimate necrosis. This was also confirmed in experimental (153) and clinical (152) studies.

As discussed before, MI is followed by adverse LV remodelling which contributes significantly to LV dilatation, LV dysfunction, disability and death (21-27). The aim of anti-remodelling therapy after MI is therefore to prevent, limit, or reverse adverse structural remodelling and thereby interrupt the sequence of LV dilatation, LV dysfunction, disability and death (22).

As for the protection of ischaemic myocardium, the early hours are critical for therapy to limit early LV remodelling after MI. The timing of anti-remodelling therapy after MI may be staged to span the acute infarction phase, the healing phases, and the post-healing phase (Table 2) (22,37,39). Longitudinal studies have suggested that timing and duration of therapy are critical (22). Sequential changes during LV remodelling post MI (Figure 6) span the phases of acute MI, healing and repair over weeks to months (Figure 2), and beyond (22,23).

Since mechanical deformation forces and increased wall stress act on the infarct and non-infarct zones throughout these phases (Figure 7), thereby promoting progressive LV dilatation (22,23,277) and stimulating fibrosis (277,278: **Appendix 39**), early and prolonged anti-remodelling therapy is favoured. Some potential anti-remodelling therapies based on the determinants (Table 3) are listed (Table 7). Since several of the anti-remodelling therapies exert pleiotropic effects, some of which may potentially impact on the supporting ECM and infarct healing, the assessment of regional remodelling in the infarct zone throughout infarct healing after MI, using such tools as 2D-Echo, is highly pertinent.

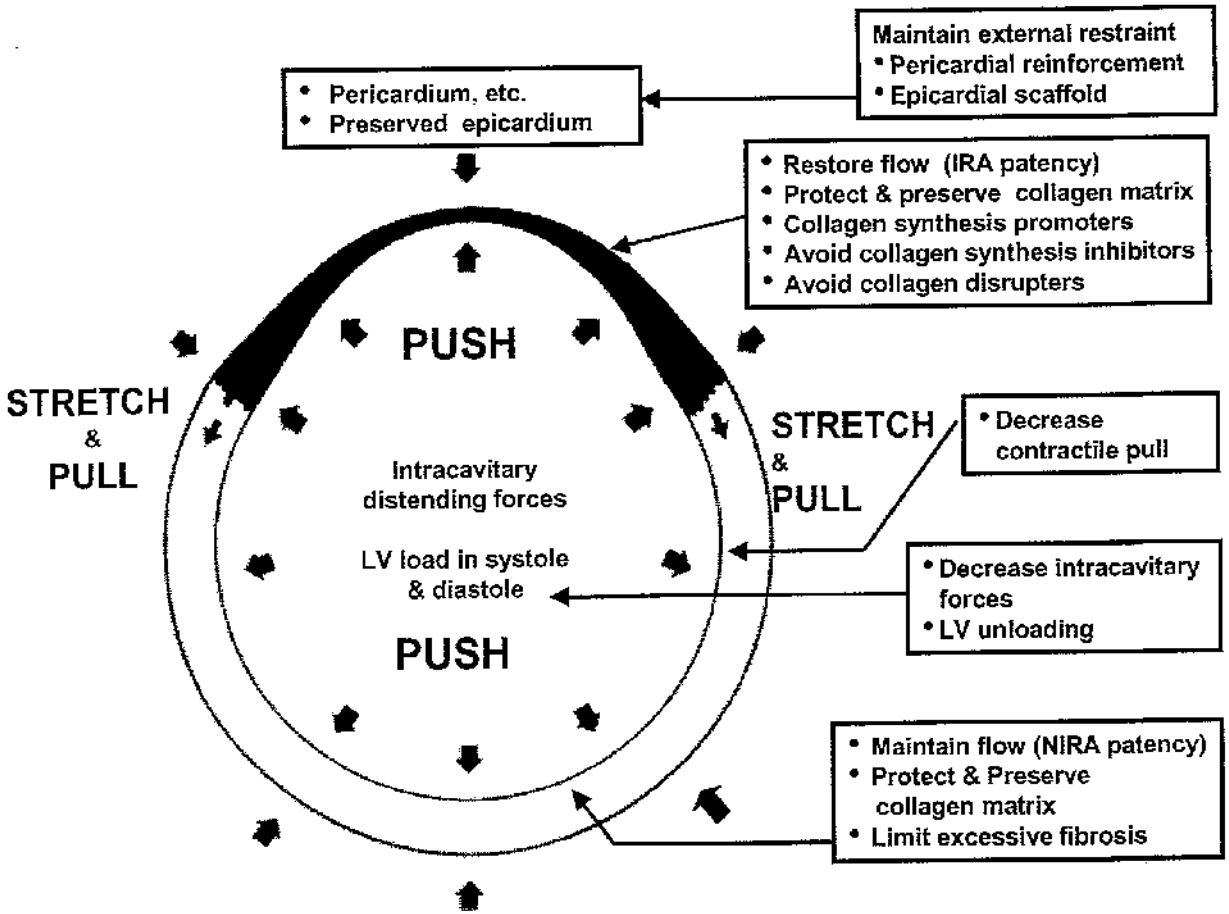

Figure 7. Remodelling of infarct and non-infarct zones.

Mechanical forces acting on the infarct and non-infarct zones on a beat-to-beat basis and approaches for prevention. IRA, infarct-related artery; NIRA, non-infarct-related artery.

Jugdutt (278; Appendix 39)

TABLE 7. **Potential pharmacological therapies for limiting remodelling after acute myocardial infarction**

Mechanism	Therapeutic intervention
Decrease infarct size	Nitroglycerin, Reperfusion (thrombolysis and/or mechanical)
Decrease preload	Nitroglycerin, ACE inhibitors
Decrease afterload	Nitroglycerin, nifedipine, ACE inhibitors
Decrease chamber size	Nitroglycerin, ACE inhibitors
Decrease heart rate	Beta-adrenergic blockers, calcium channel blockers
Decrease contractility	Beta-adrenergic blockers, calcium channel blockers
Increase collateral flow	Nitroglycerin

Modified from Jugdutt (22[Appendix 4])

2.9. Role of the extracellular collagen matrix during healing and left ventricular remodelling after myocardial infarction

During the 1980's, several investigators have drawn attention to the ECM (see 27,277,278 for review). A large body of evidence supports the role of an organized, intricate network of ECM in mediating several important functions in the normal heart, including mechanical support, coupling of cardiomyocytes, mechanical strength and resistance to distension (279). During early healing after MI, the loss of the 3D organization of the matrix (74,280), mediated by matrix metallo-proteinases (MMPs), was postulated to result in cardiomyocyte disarray (281), which might explain why cardiac ruptures occur spontaneously (282,283:**Appendix 40**) or during acute pressure loading (283), infarct distension (284), and early aneurysm formation (74). Several studies support the concept that ECM dissolution promotes dilatation (279,285-289). Loss of ECM 1-2 hours after MI in the dog is associated with regional dilatation of the infarct zone (290). Several studies have linked extracellular strut rupture (Figure 8) and cardiomyocyte slippage to early infarct dilatation post infarction (66,73,74) and progressive global LV dilatation in heart failure (291). Others have linked collagen loss to cardiac rupture (292,293).

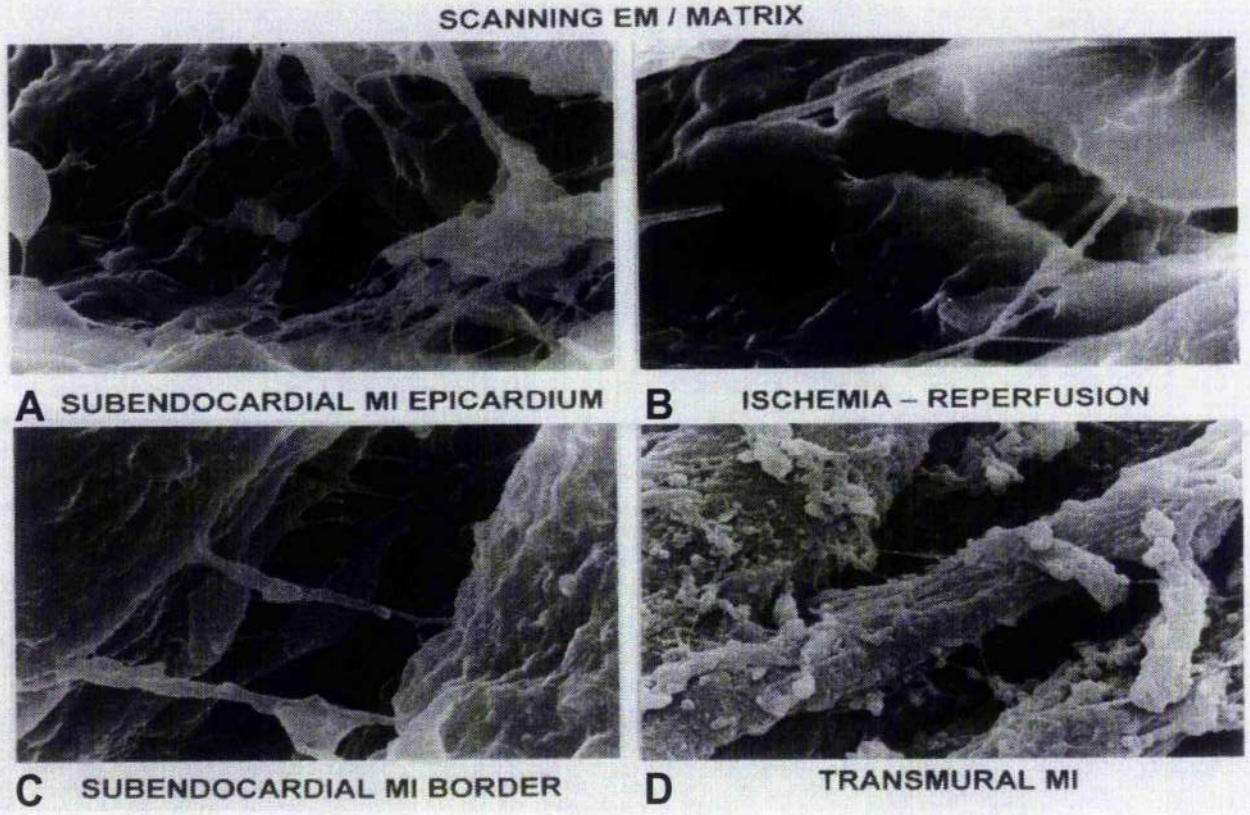

Figure 8. Extracellular matrix disruption after myocardial infarction and reperfusion

Extracellular matrix (ECM) disruption after transmural myocardial infarction (MI) or reperfused MI using scanning electron microscopy (EM) after 48 hours in dog hearts. **A.** Mild ECM disruption in the epicardium with rupture of intermyocyte struts and strands. **B.** Significant ECM disruption with ischemia-reperfusion. **C.** Mild ECM disruption in the border of subendocardial MI. **D.** Severe ECM disruption in transmural MI.

2.9.1. MMP and TIMP balance in remodelling post MI

During the early hours after MI, ECM degradation, mediated by MMPs (294), follows early rapid activation of latent MMPs and exceeds synthesis. Since degradation occurs rapidly and synthesis slowly (0.56% per day in dog left ventricle), replacement after degradation is slow (295). This implies that the early ECM degradation results in a window of increased susceptibily for adverse remodelling that may last for weeks after the acute event, so that its prevention is imperative (277). Once activated, MMP-1 degrades fibrillar collagen into fragments, and MMP-2 and MMP-9 degrade these fragments into smaller fragments (294). Within hours of MI in rats, collagen content decreases (165) and MMPs increase (296). The tissue inhibitors of MMPs (TIMPs), which neutralize MMPs, also increase after MI (296). A balance between MMPs and TIMPs appears to be necessary for normal ECM remodelling and function (296).

Since replacement of the ECM after damage is slow, it is doubtful whether therapy targeted on MMP/TIMP balance, given after the damage in the acute setting of acute post-ischaemic reperfusion or reperfused MI, can significantly reduce or reverse the early disruption of the ECM after acute ischaemia-reperfusion and thereby improve LV geometry and function.

The mechanical and other forces that alter regional and global shape and function during structural LV remodelling after MI (Figure 7) have been reviewed (22,37,39). Sequential changes (e.g. matrix disruption, LV dilatation, hypertrophy and fibrosis) span the phases of acute injury and subsequent healing (Figure 6).

Since early expansion of the infarct zone contributes to regional dilatation and RSD that precede global dilatation (21), early anti-remodelling therapy is needed. Since mechanical forces ("push, pull and stretch") that increase wall stress influence remodelling throughout its course (Figure 7) (22,28), it follows that therapy should be continued for a prolonged period.

Several studies over the 1980's have shown that the in-vivo changes in LV remodelling and function during post MI healing (22) and beyond can be tracked using 2D-Echo in-vivo (21,26,130,132). These studies indicated that timing and duration of therapy are critical (22). Susceptibility to deformation has been shown to depend on characteristics of the substrate, stage of healing, the status of the ECM and the pharmacological milieu (21,22,60,73,74,297). Transmural infarction is especially prone to expansion and rupture (64,78,81,87-89). Long-term studies that tracked in-vivo changes in LV remodelling using 2D-Echo have shown that

therapy with overall beneficial effects on global LV remodelling could also modify infarct collagen matrix and infarct zone remodelling (103,126,127,129). In addition, these studies showed that therapy targeted at one mechanism might be unsuitable for another and produce potentially harmful effects, such as those seen with nitrates (122), ACE inhibitors (123,129,276), and anti-inflammatory agents (35). Clinical studies using 2D-Echo after MI have shown progressive LV dilatation up to 1 year (28,105,132), or 3 years (26), or 10 years (298:**Appendix 41**). In rats with moderate infarct size, LV dilatation, assessed ex-vivo, progressed over months (120,299).

After acute MI, regional mural damage provides the basic substrate for remodelling by mechanical forces (Figure 7). Early reperfusion therapy, which effectively reduces the transmural extent of damage (148), also impacts positively on overall LV remodelling after MI (22). Paradoxically, this occurs despite ECM damage (164-166). Moreover, morphological evidence of irreversible injury has been shown to increase between 5 and 90 or 180 minutes of post-ischaemic reperfusion in the dog model, suggesting that late reperfusion is less beneficial (162). Studies in the 1990's have shown that apoptosis contributes significantly to cell death in early MI (188) and reperfused MI (189), suggesting that apoptosis may also contribute to acute LV dysfunction and remodelling (190). Apoptosis has recently been implicated in long-term LV remodelling after MI (300).

Cumulative evidence also suggests that reperfusion injury associated with post-ischaemic coronary reperfusion involves damage to the ECM, besides calcium overload, oxygen free radicals, microvascular obstruction, neutrophil leucocytes and peroxynitrite (ONOO) (163). Thus, in the dog, myocardial stunning is associated with ECM disruption, complete loss of the collagen weave and increased MMP activity (164,165). In the pig model of 90 minutes of ischaemia and 90 minutes of reperfusion without infarction or inflammatory cell infiltration, MMP-9 increased and MMP-2 did not change (301). MMP-9 is also increased in the pig model of acute MI (302). In other animal models, MMP-9 deletion (303) and MMP inhibition (304) were shown to limit global LV dilatation after MI.

In transmural MI without reperfusion, the concept that extensive early damage to the ECM (Figure 8) results in rapid aneurysm formation (285) was confirmed (Figure 4). Early inflammation and the cellular responses after acute MI and reperfusion (297) were linked with increased MMPs and collagen degradation by others (294). That non-transmural damage achieved by early reperfusion (148)

is associated with less ECM damage in the spared epicardial rim of the myocardium (Figure 8), less infarct expansion when made 2 hours post occlusion in dogs (49), and better overall long-term prognosis in humans (21,28) and dogs (73,74), were confirmed. However, myocardial stunning with persistent LV dysfunction is still a common clinical problem after reperfused MI (50). Although late reperfusion produces several important overall benefits in animal models, including non-transmural damage, less infarct zone remodelling and less global dilatation (49), and accelerated healing (43), it also results in decreased infarct collagen (49). In reperfused infarcts in the rat, the density of collagen cross-links (168) is reduced and ECM disruption is greater than in non-reperfused MI (160). Clinically, late reperfusion is associated with persistent LV dysfunction (305), earlier ruptures (282), and increased ruptures when made after 17 hours of onset of MI (306). Thrombolytic therapy with streptokinase after MI was also associated with decreased myocardial collagen (307).

2.9.2. Effects of anti-remodelling therapies on the ECM and collagen

The aim of anti-remodelling therapy after MI is to prevent and limit adverse remodelling, and thereby interrupt the sequence of LV dilatation, LV dysfunction, disability and death (22). An important aspect of this goal is to protect the ECM during remodelling after MI (27,279).

However, several of the anti-remodelling strategies currently used after MI exert pleiotropic effects that can potentially affect ECM turnover in both the infarct and non-infarct zones (27,278). Thus, ACE inhibitors, angiotensin II type 1 receptor blockers (ARBs) and aldosterone blockers decrease ECM (278, 295) and the aldosterone blocker spironolactone decreases collagen turnover (308). Angiotensin receptor blockers (ARBs) also decrease proline-4-hydroxylase, the major enzyme involved in synthesis of collagen, the major protein of the ECM (27,278). As discussed above, reperfusion disrupts ECM (27,278), increases MMPs and collagen degradation (294), decreases infarct collagen (49), and decreases collagen cross-links (168). Unloading with the LV assist device (LVAD) results in a down-regulation of MMPs, increased TIMPs, decreased collagen damage and increased collagen cross-links (278). Beta-blockers decrease MMPs (278). Nitrates preserve IZ collagen and prevent the decrease in collagen after reperfusion (278). Digitoxin increases proline-4-hydroxylase activity although digoxin does not alter IZ collagen (278). Endothelins increase collagen synthesis

and decrease MMPs (278) while endothelin blockade impairs healing after MI (309). Bradykinin increases MMPs and decreases collagen (278). Agents such as adenosine, which elevate cAMP, nitric oxide (NO) and cGMP, decrease fibrosis (278).

Several studies in the 1980's suggested potentially harmful effects of some post-MI therapies (26,35,49,122,123,129,278), supporting caveats against inducing very early hypotension with vasodilators (122,123), or impairing early healing with powerful anti-inflammatory drugs post MI (35). Other studies demonstrated progressive LV enlargement over 1 year (21) or 3 years (26) despite optimal post-MI therapy, and morbidity and mortality remain high (310). In addition, cardiac rupture remains a major cause of death after reperfused MI (311) and the number of post-MI patients needing LV assist devices or awaiting transplantation is increasing, suggesting that additional protection against LV dilatation, adverse ECM remodelling, lowering of infarct collagen, and impaired healing is needed.

2.10. Epidemiology and relevance of ventricular remodelling after myocardial infarction

In 1970, acute MI was the major cause of mortality and morbidity in North America (312). Without therapy, 40% of patients died in the first few hours of onset of symptoms, a further 20% in the first 30 days and another 10% within the first year. Pump failure, cardiogenic shock, and cardiac rupture were major causes of death within the first month. Congestive heart failure was a major cause of suffering and death in early survivors. Since these complications were directly related to total infarct size, therapeutic strategies in the mid 70's were aimed at limiting infarct size (88). Remodelling during healing in survivors of acute MI received little attention.

During the mid 1980's, it became increasingly clear that complications after acute MI were not only related to the total infarct size but also, to a large extent, on the severity of LV remodelling, dilatation and shape deformation that took place during healing and beyond, and in turn adversely affected LV function and outcome (18,20,22,23, 59,63). It was hypothesized that the profound changes in LV architecture and structure that occurred during remodelling contributed to LV aneurysm formation and set the stage for congestive heart failure (41,102,283). Several studies indicated that the severity of topographic deterioration was greater for large, anterior transmural AMI (18,21,23,28,35,78). Cardiovascular research

was therefore aimed at developing therapeutic strategies directed not only at salvaging LV muscle but also at preserving LV geometry and function, especially in high-risk patients with large, anterior transmural MI. Two pharmacological therapies were suggested to be potentially promising for limiting remodelling after acute MI, namely the vasodilator NTG (28) and the ACE inhibitor captopril (29,30).

In the mid 1980's, coronary heart disease and congestive heart failure became recognized as major public health problems in North America. In the United States, coronary heart disease was responsible for more than 550,000 deaths per year (313). This translated to at least 1 death per minute. In perspective, it exceeded deaths from all types of cancer combined, which amounted to less than 500,000 persons per year. Coronary heart disease also resulted in as many as 1.5 million heart attacks per year or 2.9 per minute.

By the late 1980's, at least 5.4 million North Americans had symptomatic coronary disease. Nearly 2 million had congestive heart failure and approximately 250,000 new cases were diagnosed each year (314). Direct and indirect costs in the United States exceeded 60 billion dollars per year. Despite a steady decrease in the incidence of coronary heart disease since the late 1960's, deaths from coronary disease still exceeded those from cancer. In 1968 and 1982, death rates from the following were, respectively: cardiovascular diseases, 54.3 versus 49.0%; coronary heart disease, 35.0 versus 27.9%; stroke, 11.0 versus 8.0%; cancer, 16.5 versus 21.9%. While the exact figures might be different in other countries, it became apparent that the application of potentially successful preventive therapy after MI might have considerable impact on the work force and the cost of continuing health care.

By the 1990's, it was apparent that limitation of LV remodelling after MI was likely to have important world-wide epidemiological and public health implications (23). This approach offered the potential for prevention by reducing the risk from infarct-related complications, especially aneurysm formation and congestive heart failure. An ultimate goal of translational, pre-clinical and clinical research became the prevention of adverse LV remodelling and dysfunction after MI. In theory, therapy to limit LV remodelling should improve LV function, increase survival and decrease morbidity after MI. However, the objective application of therapy to limit remodelling and salvage function not only requires an understanding of the pathophysiology of the substrate being remodelled but also how it changes in composition during healing after MI (24,25,27). Since the remodelling process is

progressive, it follows that therapy should be applied throughout its duration. An important prerequisite is the availability of a reliable and readily available tool such as 2D-Echo for repeated non-invasive evaluations of LV geometry and function over time.

In the 2000's, anti-remodelling therapy is still far from ideal, as progressive LV enlargement, morbidity and late mortality remain significant despite improved therapy. Post MI survivors who develop heart failure and need LV assist devices and transplantation are increasing.

3. STATEMENT OF THE PROBLEM AND HYPOTHESES

3.1. The problem

In the early 1980's, myocardial infarction (MI) was recognized as a major killer world-wide. Left ventricular (LV) myocardial infarct size and cardiogenic shock were the major contributors to mortality and morbidity after MI. Early deformation of LV geometry, associated with early expansion of the infarct zone, was becoming recognized as a major contributor to early mortality and morbidity after MI. Subsequent LV enlargement, with a departure from the normal global ellipsoidal to a more spheroidal shape, was becoming recognized as a major contributor to persistent LV dysfunction and late mortality and morbidity after MI. Potential new therapies were being targeted mainly on the reduction of infarct size but progress was hindered by the lack of a quantitative non-invasive method for assessing effects of therapy on regional and global LV geometry and dysfunction. 2D-Echo was just emerging as a potential tool for assessing changes in LV geometry and function after MI but imaging protocols and quantitative methodologies had not yet been defined. The importance of healing after MI and harmful effects of potentially beneficial therapies on LV geometry and function were just becoming recognized but the underlying pathophysiological mechanisms were unclear and the role of the ECM was not fully appreciated.

3.2. Hypotheses:

i) Myocardial infarction (MI) results in early regional distortion of LV geometry and LV dysfunction during the early infarction phase. This early regional shape distortion (RSD) is followed by progressive global LV dilatation, development of a more spheroidal shape and more LV dysfunction during and after the subsequent healing phase.

ii) The remodelling of LV geometry and structure after MI is a dynamic process that spans the early infarction and healing phases, and is largely driven by increased wall stress as a consequence of the RSD and increased LV size. Mechanical forces acting on the infarct and non-infarct zones during healing, and other factors, play a significant role in the remodelling of these regions. Progressive LV remodelling, during and after healing post MI, impacts negatively on outcome after MI and may be modified by early and prolonged anti-remodelling therapies applied during the phases of infarction and post-infarction healing.

These can be more simply stated as follows: since early RSD and thinning and subsequent scar formation are gradual processes, prolonged LV unloading during the healing phase or reduction of the pounding of mechanical forces should reduce the degree of thinning and bulging until the scar is formed. This scar should be thicker, stronger, less deformed. Pumping action of the heart should improve.

Conversely, agents that impair healing and decrease or adversely modify infarct collagen and the ECM, cause thinning, increase preload and afterload, increase contractile pull of the non-infarcted segment, increase wall stress and heart rate might enhance adverse remodelling, increase RSD and decrease performance.

3.3. Objectives

The main goal, between 1980 and 1988, was to gain better understanding of pathophysiological mechanisms of LV remodelling during healing after MI and determine the effects of potential anti-remodelling therapies using non-invasive quantitative 2D-Echo imaging. A secondary goal was to determine the effects of therapies on the ECM and possible accentuation of adverse remodelling during healing after MI.

The proposed algorithm was as follows:

salvage ischaemic myocardium and maintain normal healing → preserve LV structure, geometry and shape→ improve LV systolic squeeze → improve outcome and survival.

4. METHODS AND PROCEDURES

Due to the complex nature of the field of research, it was necessary to take a multidisciplinary approach, involving biochemistry, pharmacology, physiology, histopathology, computing, imaging, radiation physics and biomedical engineering.

A bench to bedside approach was used, with animal and human studies being carried out in parallel. Both sets of studies involved two phases:

- **phase 1**, focused on validations and the natural history, and
- **phase 2**, focused on modification by pharmacological agents.

4.1. Animal studies

The studies were approved by the institutional animal welfare committee and conformed with the guiding principles of the American Physiological Society, the "Position of the American Heart Association on Research in Animal Use" as adopted by the Association on November 11, 1884, and the Canadian Council on Animal Care guidelines on the use of animals in research. Animals were purchased initially through the institutional Medical and Surgical Research Institute and later through the new institutional Health Sciences Laboratory Animal Services.

A previously validated chronic dog model (62,147) was modified for studying healing over 6 weeks after acute MI and established, standard and published methods were used (41,48,49,55,102,103,122,126). Mongrel dogs (18-20 kg) were surgically instrumented under general anesthesia (intravenous sodium pentobarbital, 30 mg/kg; endotracheal intubation; ventilation with room air enriched with oxygen) and sterile thoracotomy. In studies performed after 1988, general anesthesia with isofluorane was used to avoid tachycardia associated with barbiturates (227,228).

Polyethylene catheters were inserted in the jugular vein, carotid artery and right and left atria, filled with heparinized saline, and the distal ends exteriorized behind the neck. An occluding snare was inserted around the mid-LAD or mid-LCX coronary artery and the chests closed. All animals were given 1 million units of penicillin and 1 gram of streptomycin intramuscularly and returned to their cages.

A warm blanket was used during recovery and supplementary antibiotics administered as necessary. Post-operative monitoring and follow-up care were carried out in the institutional animal facility and included regular clinical assessment,

catheter care, haemodynamic and 2D-Echo recordings for assessing LV function and remodelling over 6 weeks.

The coronary artery snare was pulled in the sedated but conscious animals 2 days after the surgical preparation. In reperfusion experiments, the snare was released 90- to 120 minutes post-occlusion, while still anesthetized before chest closure and by random allocation. With late reperfusion, infarct sizes in this model averaged 25 ± 3% (SEM) LV mass and 49 ± 6% occluded bed mass at 7 days.

Although high LAD and LCX occlusions were used in anesthetized animals for some experiments focused on infarct limitation in 2-day infarcts, mid-LAD or mid-LCX occlusions were used in subsequent long-term studies focused on remodelling during healing in survivors post MI. This was necessary because the high occlusions were associated with greater mortality compared to mid-coronary occlusions (30 % versus 10 %). The risk regions with the mid-LAD or mid-LC occlusions averaged 25 % of the left ventricles.

Serial 2D-Echo (either Diasonics V3400 R, or Toshiba SSH-65A or Hewlett Packard Sonos 1000; 3.5 or 5 MHz transducer) was recorded in-vivo, using the established protocol for obtaining tomographic images (Figure 5) and techniques in the mildly sedated but conscious animals (Figure 9). Standard views included: parasternal long-axis; five parasternal short-axis from base to apex at mitral, chordal, mid-papillary, low-papillary and apical levels; the apical four- and two-chamber views. Recordings were made before surgery, at baseline before occlusion, and again post-occlusion and/or reperfusion for up to 7 weeks, with careful attention to transducer position and angulation.

Sterile echo-opaque beads were sutured on the anterior and posterior LV surfaces at 3 levels from base to apex for better 2D-Echo orientation and consistent imaging post MI. Although 2D-Echo image analyses routinely used anatomic landmarks, such as the papillary muscle, to identify the levels for measuring infarct segment lengths and infarct wall thickness, and shape changes during remodelling (Figure 10), repeated comparisons of the same area was often difficult. The opaque beads were therefore useful for regional comparisons of serial 2D-Echo data post MI in animal studies. Pilot serial 2D-Echo studies in 30 infarcted dogs with sutured epicardial beads confirmed consistent 2D-Echo imaging (103,283).

In studies after 1985, 2D-Echo guided pulsed Doppler recordings of the mitral inflow velocity at the level of the mitral annulus were made concurrently with

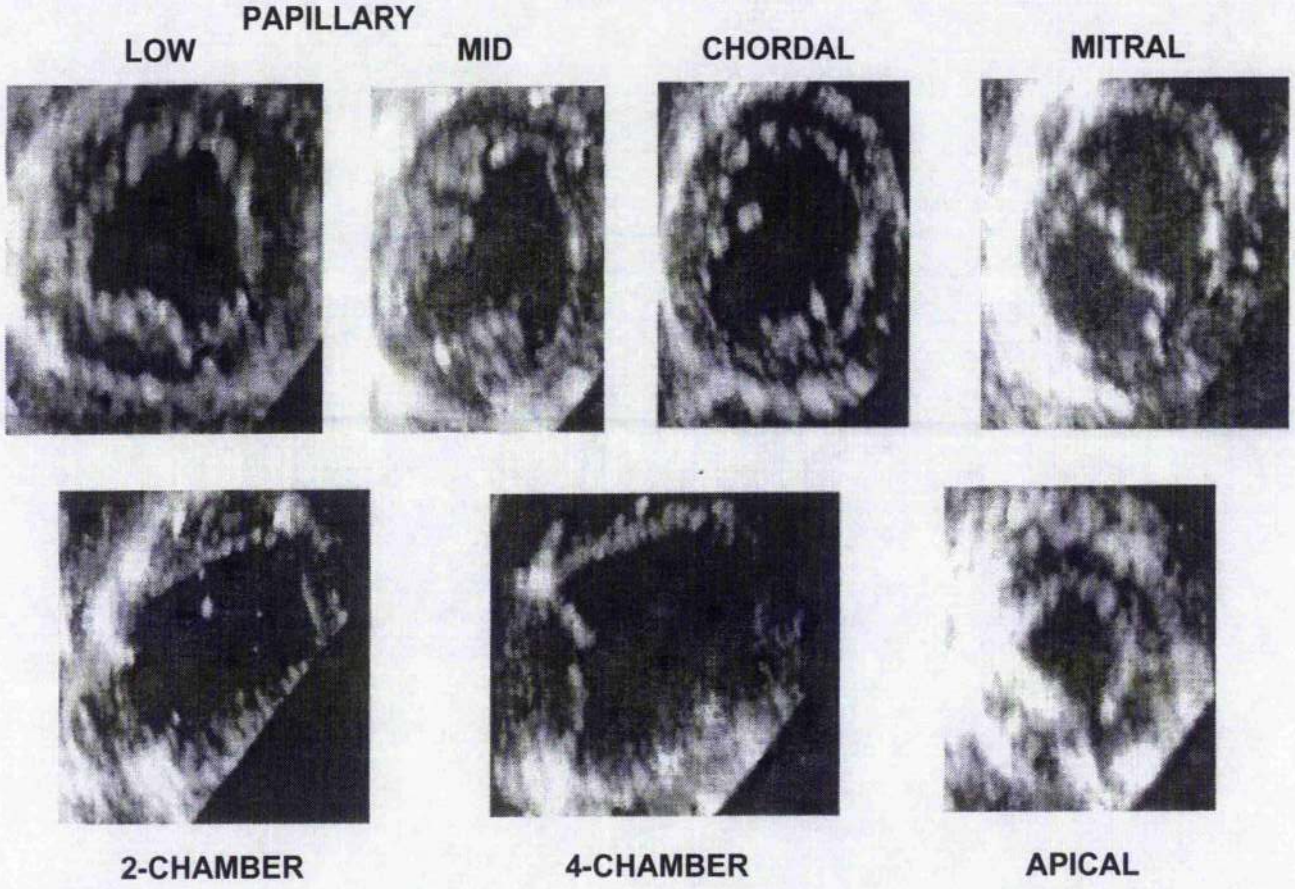

Figure 9. Tomographic 2D-Echo imaging for 3D-reconstruction

Scanned from frozen frames at 7 planes

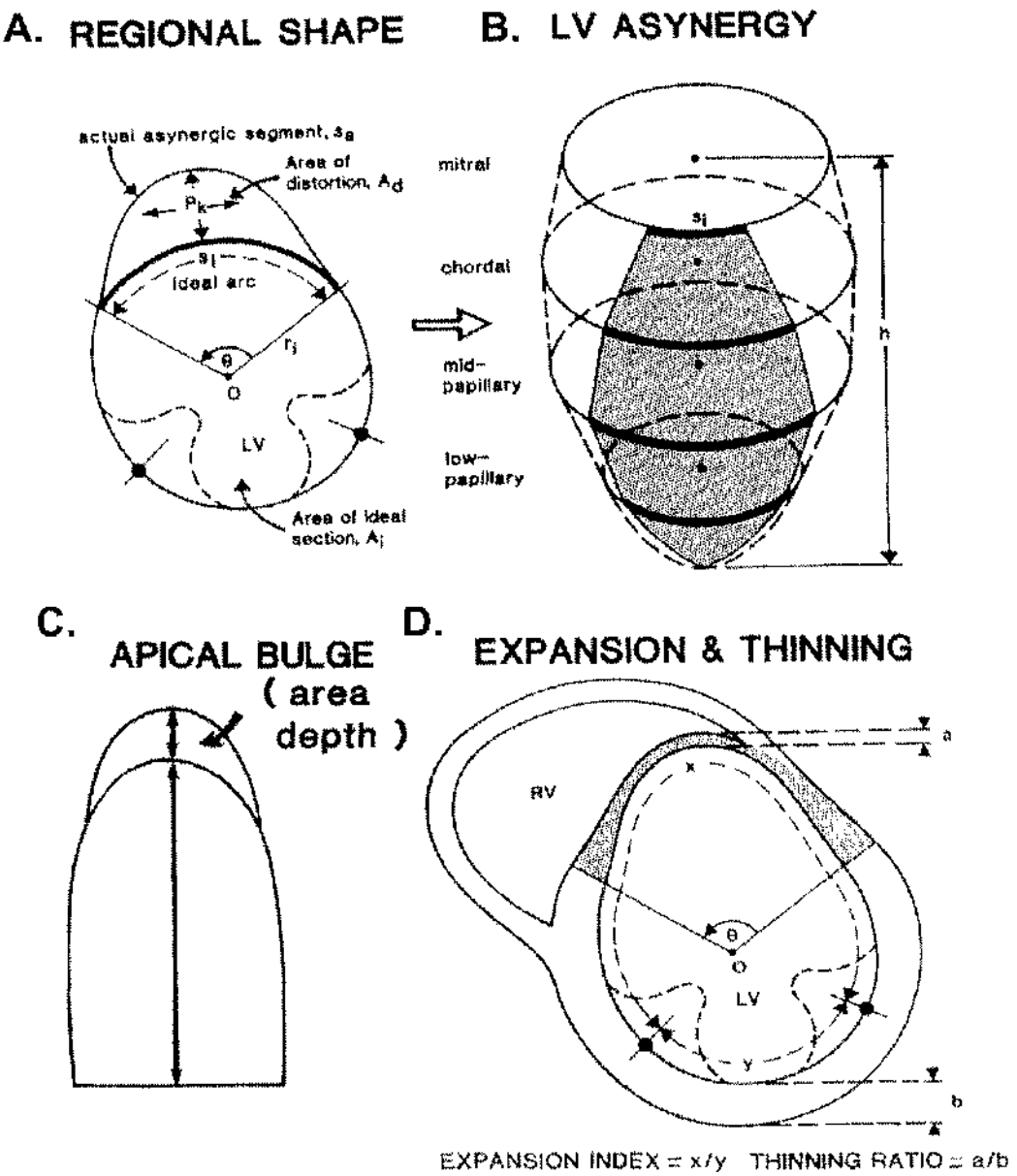

Figure 10. Quantitative analysis of echocardiographic images

Computer assisted measurements of:
A. circumferential extent of asynergy (Si) and regional bulging;
B. endocardial surface area of LV asynergy and volume from 3D reconstruction;
C. bulge of the asynergic zone,LV apical view;
D. the expansion index (x/y) and thinning ratio (a/b) from the papillary short-axis.

From Jugdutt (21[Appendix 3])

2D-Echo recordings (315:**Appendix 42**), as previously described in the dog (316) from the apical-2 or -4 chamber view parallel to flow, with optimal definition of the spectral envelope and a sample volume size of 3 to 6 mL. Three to five cycles were manually digitized and averaged for peak velocities and integrals of the LV inflow in early and late diastole. The 4 main parameters were the rapid filling velocity (E), the atrial filling velocity (A) and the atrial filling fraction (E/A) and the deceleration time (DT) (Figure 11).

In all dogs, serial haemodynamics were recorded on a Gould Recorder (Cleveland, Ohio), as described previously (122,126), and included: right atrial pressure (index of right ventricular filling pressure and hydration), left atrial pressure (index of LV end-diastolic pressure or filling pressure); phasic and mean arterial pressures (index of afterload), and ECGs (for heart rate, rhythm, and evidence of ischaemic injury and infarction).

After the final recordings, the dogs were re-anesthetized. In order to study LV topography, the hearts were arrested in diastole (1 molar potassium chloride intravenously), removed, washed in normal saline, and filled with gelatin to preserve diastolic relations before formalin fixation (41). The hearts were sectioned systematically along the transverse axis from base to apex after formalin fixation in distension to preserve diastolic relations and at the same planes where 2D-Echo images were obtained (41). Occluded bed size was measured by post-mortem coronary arteriography before formalin fixation (Figures 4 and 12).

Improved computerized planimetry techniques with recordings of all anatomic landmarks was used for more accurate definition of the location of infarcts and shape distortion, measurements of wall thickness (41) and correlation with 2D-Echo images (Figure 13). A successfully developed and validated computer program, executed on a Hewlett Packard 9835A computer and 9874A digitizer interfaced with a VAX 750 computer, was used for measuring RSD on LV short-axis 2D-Echo images (Figures 13 and 14) and similarly on pathologic transverse sections in the dog hearts.

Myocardial samples (100 to 200 mg) were taken from the infarct, border and non-infarct zones for assays of hydroxyproline (OHP), a marker of collagen content and histopathology (41), and immuno-histopathology for collagen subtypes I, III and IV (129), after making tracings of the weighed transverse sections, infarcts or scars, and occluded bed for computerized planimetry (Figure 13). Histology and

SYSTOLIC FUNCTION

Offline analysis (Disc method) versus automatic edge detection for volumes

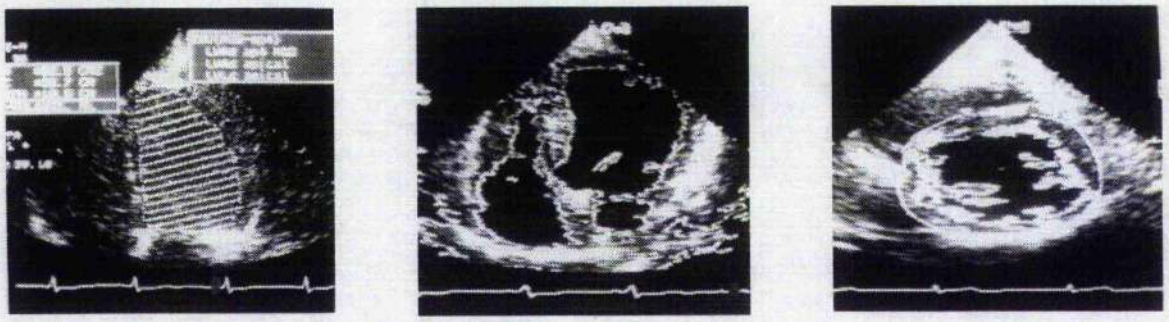

DIASTOLIC FUNCTION

Transmitral Doppler for E and A integrals

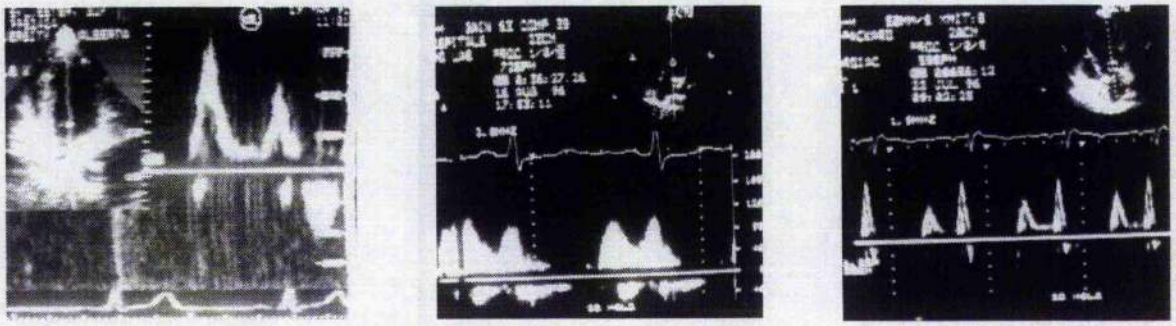

Normal E and A | **E and A equalization** | **E and A reversal**

Figure 11. Computer assisted quantification of LV global systolic and diastolic function by 2D-Echo

Upper panel: LV volumes (end-diastole shown) by the offline Disc method versus the automatic edge detection method for systolic and diastolic volumes and global LV ejection fraction. **Lower panel:** Typical recordings of transmitral Doppler velocity integrals for diastolic function. The early (E) amplitude exceeds the late atrial (A) amplitude in normals. The waves become equalized or reversed post MI. In large MI and severe diastolic dysfunction, the E wave is taller and the deceleration time (DT) is decreased (not shown).

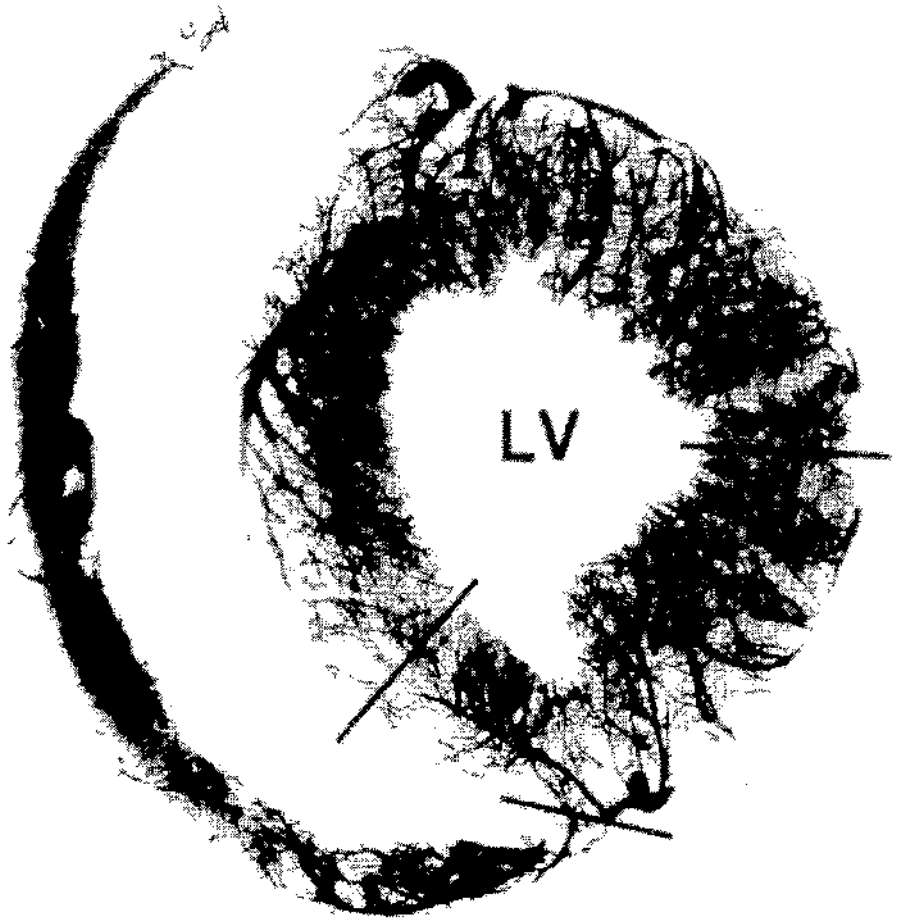

Figure 12. Delineation of the anatomic boundaries of the occluded bed or risk region

Black lines indicate occluded bed boundaries on an LV section radiograph.

Jugdutt, Can J Physiol & Pharmacol 1986;64:254-262.

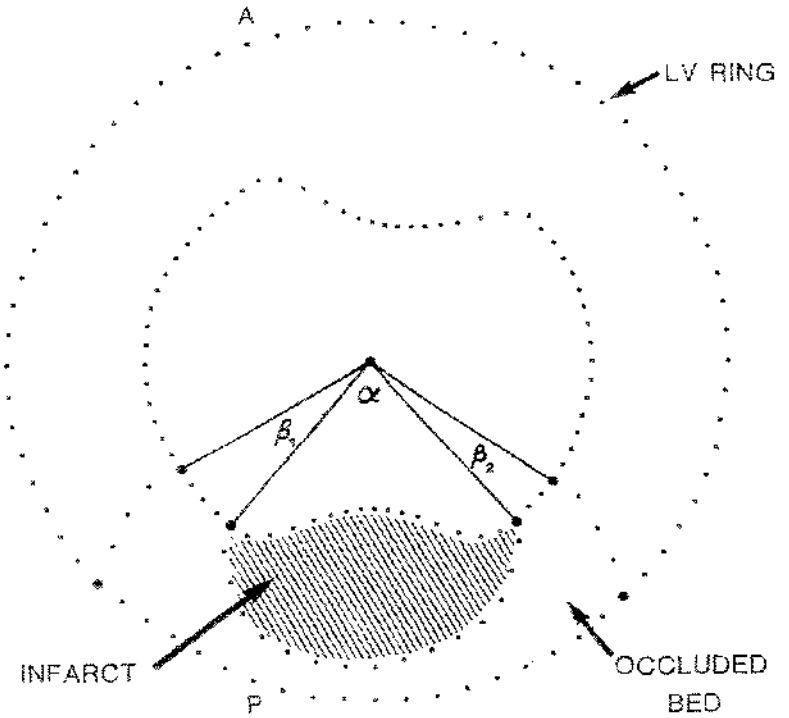

Figure 13. Actual computer map of the infarct, occluded bed and LV ring at the papillary muscle level

The center of the inner endocardial contour was computed. Points along inner and outer contours are at 5° intervals. Linear measurements were made along or between selected radii and appropriate pairs of points in the occluded bed. Radii were drawn at intersections of the inner perimeter with the infarct and occluded bed (large dots) so that angular extents of the infarct (α) and lateral rims of the uninfarcted myocardium within the occluded bed (β_1 and β_2) could be measured. Intersections of the occluded bed boundaries with the outer perimeter (large dots) and the right ventricle with the LV ring (A and P) were also recorded. Data from corresponding rings of all hearts within a group were used to compute the average map for that group.

From Jugdutt (55; Appendix 15)

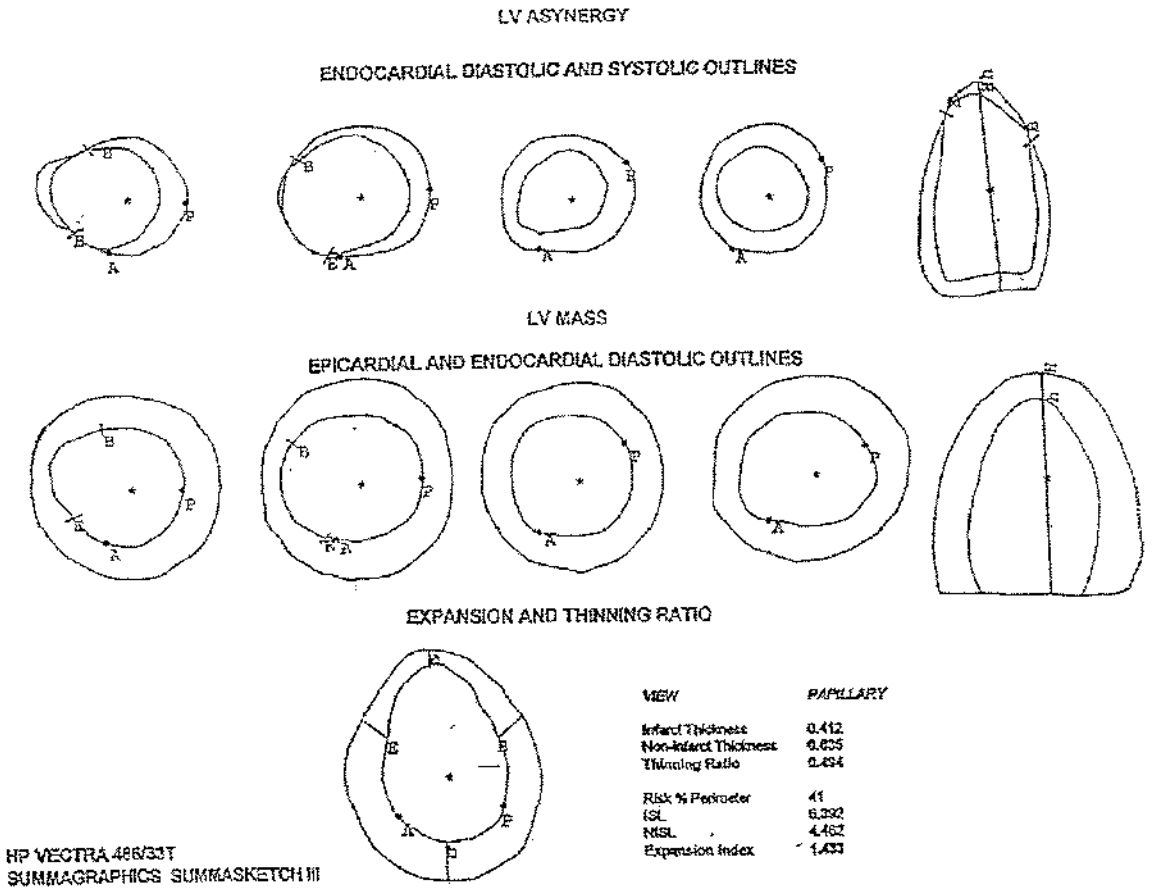

Figure 14. Outputs from new computer software

Typical computer generated outputs of endocardial and epicardial contours from end-diastolic images with data on LV asynergy, volume, LV mass, expansion index and thinning ratio.

morphometric analysis was done on 5 mm slices from the middle of the occluded bed. Thin 5-µm sections taken in triplicate were stained with hematoxylin and eosin, Mallory's stain, or Masson's trichrome, respectively, and examined for infarction and collagen. The concentration of OHP, as mg/g of dry weight, was measured using spectroscopy, as described by Bergman and Loxley (317). Scanning electron microscopy for extracellular matrix evaluation was performed on fresh samples (74, Figure 8).

In animals undergoing reperfusion and sacrificed within 2 days, infarct size was measured using the triphenyl tetrazolium chloride (TTC) method and planimetry. Sections were incubated in TTC (1% in 0.09 molar phosphate buffered saline, pH 7.4) for 30 minutes at 37°C to delineate infarct tissue. In those animals, the LAD was re-occluded at the same site after final recordings and the left atrium injected with monastral blue to define the risk region.

Because infarcts in the dog are rarely 100% transmural, small transmural apical infarcts (< 25% LV mass) were produced by ligating the collateral feeders from the LCX into the bed below the standard mid-LAD ligation (73,74,318:**Appendix 43**). This results in marked remodelling with antero-apical aneurysm formation, avascularity and collagen matrix disruption (Figures 4 and 8). The finding lends support to the concepts that collateral flow protects ischaemic myocardium (203,204) and the ECM framework (279), ECM is disrupted during post-MI remodelling (284) thereby contributing to LV dysfunction (277) and shape deformation (22,73,74). Because healing takes 6 weeks in dogs and mortality from large infarcts is high over that time (about 35 %), we produced infarcts that are about 25% LV for ensuring survival to 6 weeks. This modified model is closer to the "collateral-poor human model" (203,204) and shows more ECM disruption, regional bulging (RSD) and global LV dilatation than the standard model (73,74).

All data were coded for analysis and observers were blinded with respect to the details of the protocols and the treatment groups, as described in extensively published methods from my laboratory. Randomization into treatment groups was done by opening a sealed envelope that contained the pre-assigned group.

4.1.1. Analysis of echocardiograms for remodelling and functional data

As described previously (103,126), coded echocardiograms were analyzed double-blind on video playback (0.5 inch tapes) by two independent observers for standard in-vivo 2D-Echo parameters of mechanical function, such as regional LV asynergy

and global LV ejection fraction, and topographic parameters such as expansion index, cavity areas, volumes, segment lengths, thinning ratios, and the area (A_d) and depth (r_d) of RSD (Figures 10 and 14). Differences were resolved by consensus.

Briefly, endocardial and epicardial outlines of the LV images at end-diastole and end-systole were traced with a light pen (Diasonics CardioRevue Center), corrected over at least three consecutive cycles and copied on plastic overlays. Anatomic landmarks, such as papillary muscles and right and left ventricular junctions, were indicated on the tracings. Markings of asynergy, defined as akinesis (no systolic inward motion and thickening) or dyskinesis (systolic outward motion and thinning), or both, were made on each endocardial diastolic outline by careful visual assessment of motion and thickening on repeated video playbacks. Circumferential extents of asynergy on each short-axis view were then digitized and used to compute total endocardial surface area asynergy by a 3D reconstruction algorithm. Outlines from five short-axis and two long-axis views were also used to compute volumes by means of a modified Simpson's rule algorithm. Global ejection fraction was calculated as end-diastolic volume minus end-systolic volume divided by end-diastolic volume. The inter-observer error was less than 5% in marking asynergy, segment length, wall thickness and areas of outlines (103,126). As for post-mortem hearts, topographic measurements were made on end-diastolic outlines of short-axis images at the papillary level, and the expansion index (ratio of the lengths of the asynergy containing and the non-asynergy containing segments), thinning ratio (ratio of the average thicknesses of the asynergic and non-asynergic zones) and regional area ejection fraction (end-diastolic area minus end-systolic area divided by end-diastolic area) were computed.

The degree of regional bulging, or RSD, in the asynergic zone was characterized by its area (A_d) and depth (r_d), as described previously (19,21,103,126,318). LV aneurysm was defined as the presence of a bulge in diastole and further bulging in systole. LV mass was calculated from the volume of myocardium (difference in volumes of epicardial and endocardial shells at end-diastole) multiplied by an assumed specific gravity of 1.05 g/ml (319). The LV mass and the RSD indices (Figures 10 and 14) for each set of 2D-Echo and heart-section outlines were compared using linear regression analysis. Wall thicknesses on 2D-Echo and heart sections were also compared at 5° angular intervals.

4.1.2. Post-mortem measurement of scar size and geometry

As described previously (103,126), the risk region was measured on post-mortem coronary arteriograms. These were made by simultaneous pressure-controlled injections of the coronary arteries of fresh hearts with a mixture of barium sulfate and gelatin, followed by fixation of the hearts in distension (15 cm pressure head; 10% phosphate-buffered formalin solution or gelatin for 48 hours) to preserve diastolic proportions. Radiographs of the whole heart (in two perpendicular planes) and transverse sections (five equally spaced sections, 1-1.5 cm thick) were then made.

Boundaries of the risk region were then marked on section radiographs, by consensus, at the water-shed between the adjacent beds. The LV rings were weighed and outlines of the rings, occluded zones and infarct scars were made on plastic overlays. Computerized planimetry was then performed to measure infarct or scar size (masses and volumes of infarct, risk region, non-infarct myocardium) and ex-vivo topographic parameters, including "thinning" ratio (ratio of average thickness of infarcted wall to average thickness of the normal wall) and "expansion" index (ratio of endocardial lengths of infarct to non-infarct containing segments demarcated by papillary muscle landmarks) and generate average short-axis topographic maps for each treatment group (Figure 13).

Average maps of long-axis contours of the LV epicardium and endocardium were also made for each treatment group from digitized whole heart radiographs and direct measurements of the area and depth of the apical bulge or RSD (Figure 15).

4.1.3. Sample size.

Calculation of sample sizes considering beta error was done for all remodelling experiments. Thus, defining a significant change in RSD as a 50% decrease, a doubly significant sample size (N) was calculated by Feinstein's method (320; Clinical Biostatistics, St. Louis, Mosby, 1977; p 329) as N=16 for $\alpha = 0.05$ and $\beta = 0.20$. With N=16 in each group, a negative result would be associated with a 20% chance of falsely accepting the null hypothesis due to a sampling error. With this correction, n=10 for $\alpha = 0.05$, $\beta = 0.1$. An increase in LV mass of greater than 7% was considered to be an indicator of significant LV hypertrophy (103,127,128,131). A mortality rate of 10% for mid-LAD occlusions was factored in.

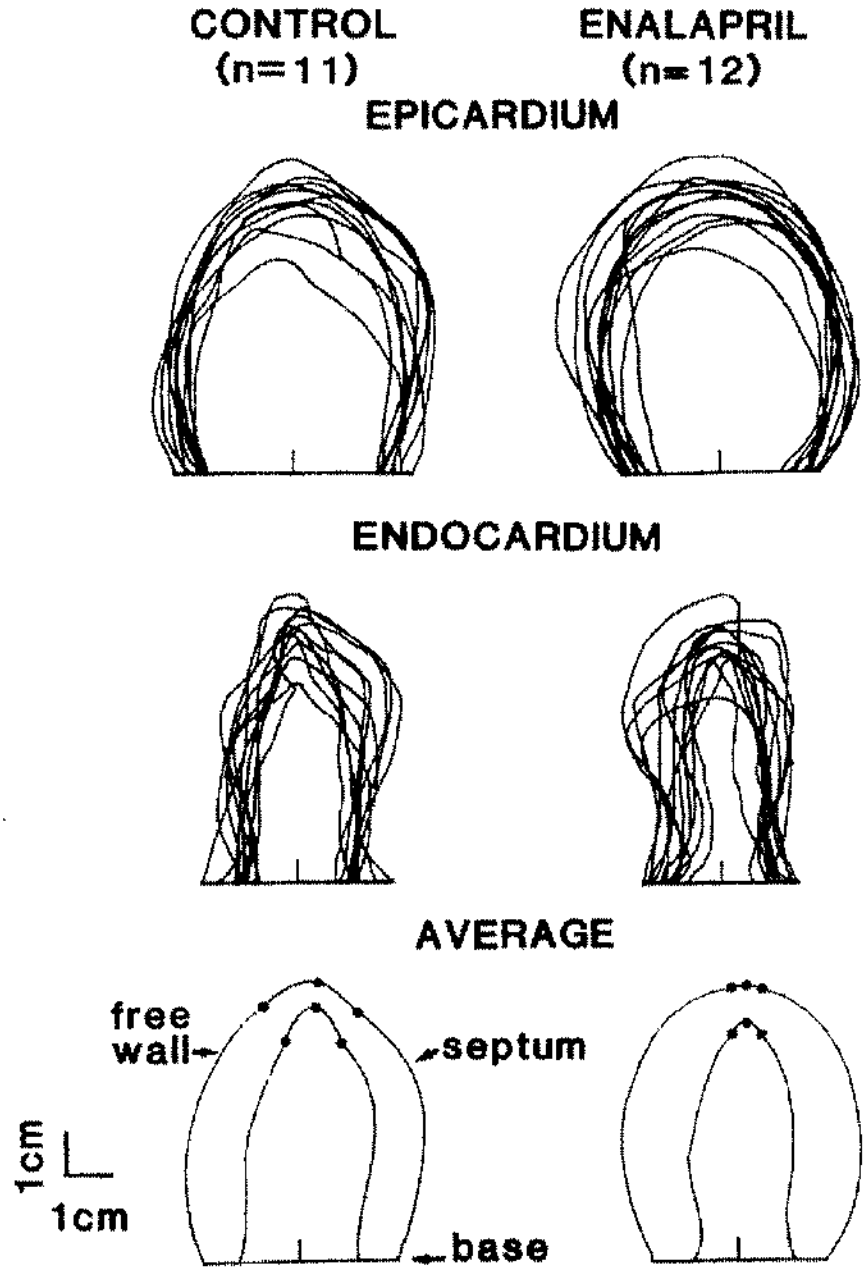

Figure 15. Computerized topographic maps: Long-axis remodeling (anterior MI).

Postmortem maps of diastolic ventricular topography in the long-axis. Digitized epicardial and endocardial contours and average maps in the long-axis plane. Dots on the average contours indicate landmarks for quantifying the apical bulge. The maps show less apical bulging and smaller cavities in the enalapril group.

Jugdutt et al. (127[Appendix 25])

4.2. Clinical studies

All protocols were reviewed and approved by the institutional ethics committees and informed consents were obtained from all patients for the studies. The methodology for non-invasive assessment of regional and global LV function before and after therapy using 2D-Echo was developed in 3 stages:

First, the facility was developed for performing tomographic imaging by means of 2D-Echo in acutely ill MI patients at the bedside in the CCU and follow-up 2D-Echo recordings in the step-down cardiac recovery wards and the 2D-Echo Laboratory. Two 2D-Echo machines were acquired (Diasonics 3400) for the studies; one was dedicated for studies in the CCU and the adjoining step-down ward and another for laboratory studies. The laboratory personnel in the early 1980's consisted of two sonographers, three fellows and a computer programmer.

Second, the methodology was developed for systematic 2D-Echo studies and computer-assisted quantification of right ventricular and LV asynergy (wall motion and wall thickening abnormalities), wall thicknesses, and LV shape at multiple short-axis levels from the base to the apex of the heart and multiple long-axis planes (251-253; Figures 10,14,16). As mentioned above, the computer software needed for the above was developed. Manually contoured LV endocardial and epicardial outlines were digitized for analysis using a Hewlett-Packard computer and digitizer as described for the animal studies. Computer programs were developed for measuring the circumferential extent and location of LV asynergy using a radial coordinate system (21) and for quantifying LV regional and global function (21,28,34,35).

Third, all 2D-Echo studies were performed systematically, according to a strict imaging protocol (Figure 5) to permit non-invasive evaluation of cardiac function and follow changes by repeated studies focused on LV remodelling and myocardial protection.

In addition, the following methodologies for the measurement of multiple indexes of infarct size were implemented:

i) Praecordial ST-segment and R/Q-wave mapping using ECG.

ii) Haemodynamic measurements of pulmonary capillary wedge pressure and cardiac output using the Swan-Ganz catheter with the thermodilution technique, and arterial blood pressure via arterial lines in the CCU.

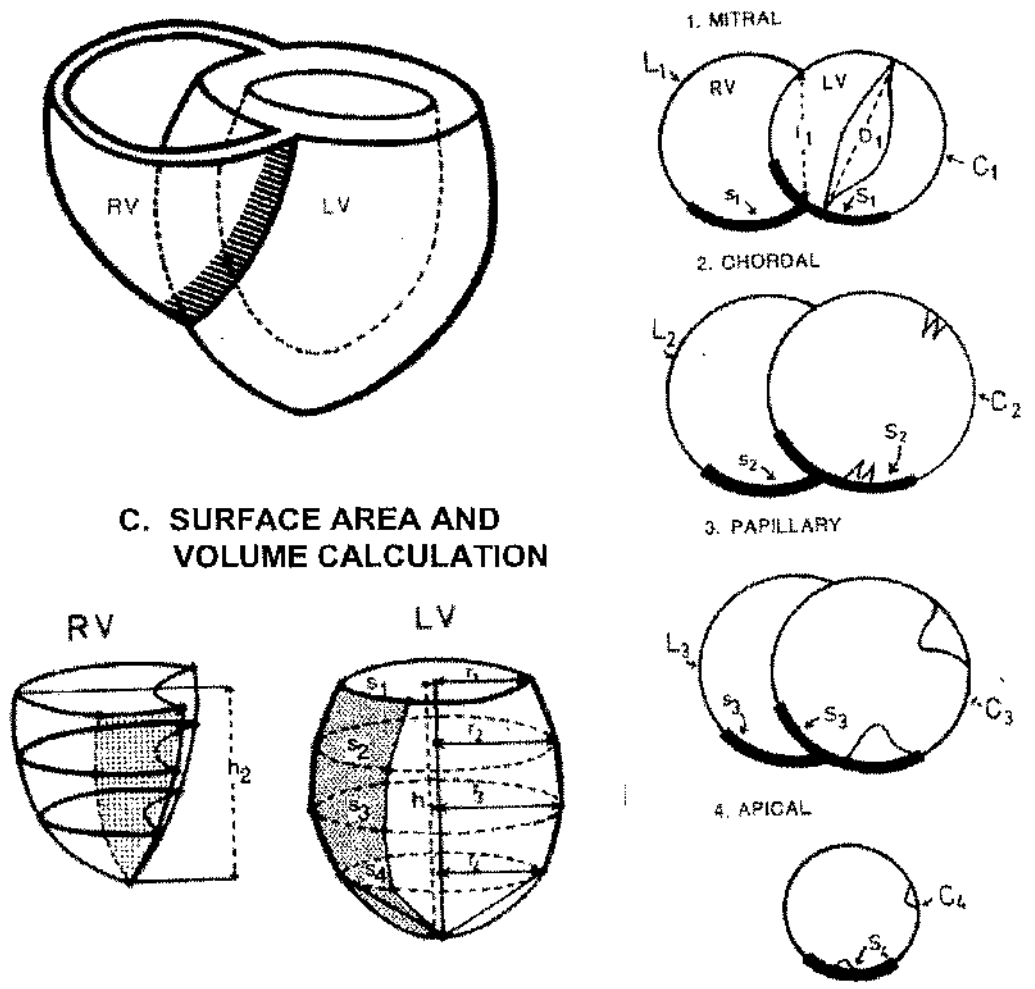

Figure 16. 2D-Echo evaluation of right ventricular infarction

A. Right ventricle (RV) is a crescent shaped appendage attached to the more conical left ventricle (LV).
B. Extents of abnormal wall motion (AWM) in 4 short-axis sections (*thick lines*) were expressed as ratios of circumferences for LV (S_1/C_1 to S_4/C_4) and as ratios of the arc lengths for RV (S_1/L_1 to S_3/L_3). LV diameters (D_1 to D_4) and RV septal chord lengths (l_1 to l_4) were measured.
C. Surface area of AWM (*stippled*) in endocardial shells was computed from AWM in 4 serial short-axis views at the mitral, chordal, papillary and apical levels. Long-axis lengths (h_1, h_2) of RV and LV were measured in the apical 4-chamber views and slices assumed to be of equal thickness. Total LV AWM area was computed for conical shapes. The RV was opened out into 2 trapezoids and a triangle to compute the total RV AWM area. Volumes were computed from areas and thicknesses of sections.

Jugdutt et al. (253)

iii) Serial CK and CK-MB enzyme assays for cumulative CK infarct and CK-MB-infarct sizes in gram-equivalents based on method of Shell and Sobel (321), using customized computer software (Hewlett Packard).

iv) Thallium-201 myocardial scintigraphy and other radio-nuclide cardiac imaging.

v) The procedure for preparation of NTG solutions for intravenous infusions in acute MI in initial studies, before commercial preparations became available, using glass bottles, special tubings and infusion sets in the CCU.

vi) Use of computer for rapid statistical analysis, analysis of large volumes of haemodynamic, angiographic, CK and 2D-Echo data.

4.3. Statistics

Data were analyzed in blinded fashion. Stringent methodology was used (320-322). The statistical tests included: 1) analysis of variance (univariate) for differences within and between separate or combined groups; 2) repeated measures analysis of variance with orthogonal contrast for comparing serial data within groups and a multigroup repeated measures design for overall differences between groups; 3) multiple comparisons analysis of variance and the Student Newman-Keuls test for the significance between placebo and separate or combined therapy groups; and 4) chi-square and Fisher's exact tests for the significance of difference in event frequency among groups. Results are presented as mean values ± standard deviation (SD) or standard error of the mean (SEM) as stated. Statistical significance was set at $P < 0.05$ (two-tailed).

5. RESULTS

5.1. ANIMAL STUDIES: NATURAL HISTORY

5.1.1. Temporal changes in infarct collagen and left ventricular topography during healing after myocardial infarction in the dog (41: Appendix 12)

Background: Healing after acute MI takes places over weeks. Collagen deposition in expanded and thinned infarct segments during healing might contribute to permanent RSD associated with ventricular aneurysms. The changes in collagen content in the infarcted and non-infarcted zones during healing over 6 weeks after MI were studied in 132 hearts of untreated or control dogs with LAD or LCX occlusions between 1980-1983 (41).

Methods/Results: Hydroxyproline (OHP) was used as a biochemical marker for collagen. Over the 6 weeks, OHP content did not change significantly in normal non-infarcted regions but increased progressively in infarct zones (Figure 17). The data indicated that, compared to the non-infarct zone, the increase in OHP content in infarct zones became detectable by 7 days [9.94 ± 0.67 (SEM) versus 4.38 ± 0.18 mg/g dry weight, n=25, $P<0.001$] and peaked by 6 weeks (55.55 ± 3.27 versus 4.06 ± 0.20 mg/g dry weight, n=17, $P<0.001$). In contrast, over the 6 weeks in sham-operated dogs and dogs with no infarcts, OHP content in the two regions remained normal and similar (4.41 ± 0.25 versus 4.06 ± 0.18 mg/g dry weight, n=21, P=NS). The changes in OHP were similar for LAD and LCX infarcts.

Importantly, significant ex-vivo changes ($P<0.05$) in LV geometry accompanied the changes in infarct collagen and included increased LV cavity area (5.0 versus 3.9 cm^2), endocardial circumference (8.8 versus 7.4 cm) and expansion index (1.21 versus 1.02) by 7 days, and decreased thinning ratio (0.71 versus 0.98). Compared to 2-day infarcts, the infarct area decreased by 6 weeks (1.8 versus 3.4 cm^2) and the non-infarcted length increased (6.9 versus 5.4 cm). The overall findings indicated that healing over 6 weeks in the dog model is associated with infarct expansion and LV dilatation within 7 days, before significant collagen deposition occurs, and this is followed by infarct scar contraction and thinning at 6 weeks.

The findings suggested that collagen deposition in already expanded and thinned infarct zones might explain the permanent RSD associated with LV aneurysms. The peak RSD index, P_k, for the infarct zone in the LV apical section at 6 weeks in that study, was significantly greater in infarcted than non-infarcted or

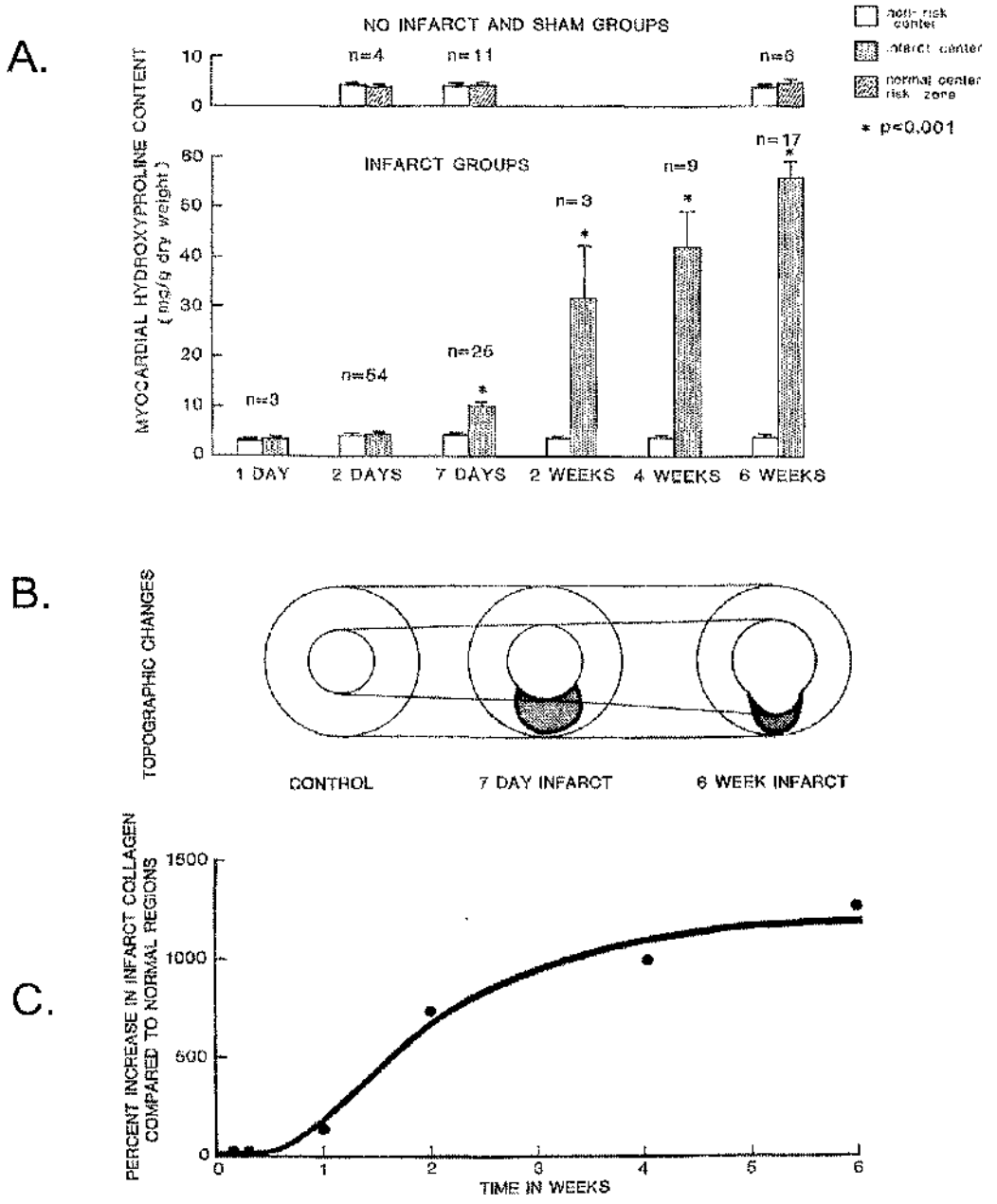

Figure 17. Temporal changes in myocardial hydroxyproline

A. Temporal changes in myocardial hydroxyproline content.
B. Summary of changes in topography (*top panel*) and percent increase in infarct collagen (*bottom panel*) during healing in the canine model. Stippled area indicates infarct.

From Jugdutt (41: Appendix 12)

sham hearts (4.57 ± 0.06 versus 1.12 ± 0.04, n=21, P<0.001) and greater for LAD than LCX infarcts (5:62 ± 0.05 versus 2. 13 ± 0.06, P<0.05).

Relevance: In applying these results, it is important to remember five points with respect to the duration of therapeutic interventions to modify remodelling in humans.

First, the infarcts in the dog model were not all 100 % transmural, although this was apparent at the LV apex for the posterior MI after LCX occlusion shown in Figure 17C.

Second, the duration of healing of the infarct zone after MI, from the time of an acute coronary occlusion to formation of the final scar, differs among species (Figure 1) and takes place over a period of two to three weeks in rats (43,96), four to six weeks in dogs (41,96) and between six weeks and six months in humans depending on infarct size (40,44). Thus, the slower rate of healing in humans compared to rats and dogs should be taken into consideration.

Third, the rate of healing also depends on infarct size (44), in addition to other cellular, metabolic and biochemical factors involved in the healing process. It was also apparent, in this study, that the time to the collagen plateau was longer with large than small infarcts.

Fourth, further late remodelling takes place after collagen deposition has plateaued. This involves compaction of the infarcted segment, hypertrophy of the non-infarcted segment, and global LV dilatation due mainly to dilatation of the non-infarct segment (41) as confirmed by others (71,72,93,94). As shown in Figure 17C, the infarct scar at 6 weeks shows evidence of both endocardial and epicardial RSD, suggesting that collagen deposition fixes the endocardial and epicardial RSD associated with early infarct expansion before the collagen plateau. A subsequent report has confirmed an acute increase in both endocardial and epicardial surface areas with infarct expansion (323). The early window after infarct expansion and before the collagen plateau leaves the infarct zone vulnerable to adverse remodelling.

Fifth, late thinning of the infarct zone, with compaction of the scar after collagen deposition has plateaued at about 3 weeks in the dog, is associated with increased LV chamber distensibility which appear to contribute further to LV chamber and aneurysmal dilatation (102,283). However, the subsequent normally healed scar is relatively less distensible and more resistant to deformation (69).

This resistance to further stretch appears to be related to connective tissue cells entering the myocyte compartment and connecting disrupted myocyte fibers (324). Since the infarct scar has now been recognized as a living structure containing myofibroblasts with contractile ability (325), some infarct remodelling may continue for years beyond the initial healing phases. Several studies have confirmed that lengthening of the non-infarcted segment plays a major role in the late cavity dilatation (7,31,68,194). Progressive LV dilatation has also been correlated to infarct size and continues long after the healing process is completed (26,76,298,299). In the rat model, a further 30% increase in LV volume occurred between 3 weeks and 3 months (77).

5.1.2. Two-dimensional echocardiographic characterization of topographic changes after transmural and non-transmural infarcts during healing after myocardial infarction in the dog

5.1.2.1. Transmurality (73: Appendix 19)

Background: The subepicardial rim of spared myocardium after subendocardial MI might protect against infarct remodelling whereas its absence in transmural MI might allow unrestricted infarct bulging and thereby contribute to LV dysfunction.

Method/Results: The effect of infarct transmurality on adverse in-vivo and ex-vivo LV remodelling during healing over 6 weeks after MI was studied systematically in the dog model (73). Serial topographic and functional parameters on 2D-Echo and haemodynamics as well as post-mortem topography were measured in dogs randomized to standard LAD ligation (group 1) or a modified lower LAD ligation plus collateral obliteration to decrease collateral inflow and increase infarct transmurality (group 2). Compared to group 1 at 6 weeks, group 2 had similar infarct weight [5.5 ± 2.0 (SD) g versus 4.7 ± 2.9 g] and slightly less infarct collagen (36.1 ± 7.7 versus 43.1 ± 17.1 mg/g dry weight, $P<0.05$). In contrast, group 2 had greater transmurality (94.8 ± 6.7% versus 66.6 ± 23.7%, $P<0.001$) (Figure 18) and was associated with more necrosis relative to the area at risk (54.9 ± 11.5% versus 35.3 ± 17.4%, $P<0.001$), Q-waves (86% versus 36%, $\chi^2=12.88$, $P<0.0005$), infarct expansion, infarct thinning, regional bulging or RSD (depth: 0.96 ± 0.15 versus 0.57 ±0.14 cm, $P<0.001$, and LV dilatation. At 6 weeks on 2D-Echo, group 2 showed more infarct expansion (2.59 ± 0.32 versus 2.30 ± 0.25, $P<0.001$), more late thinning (0.56 ± 0.15 versus 0.72 ± 0.13, $P<0.001$) and RSD in the short-axis

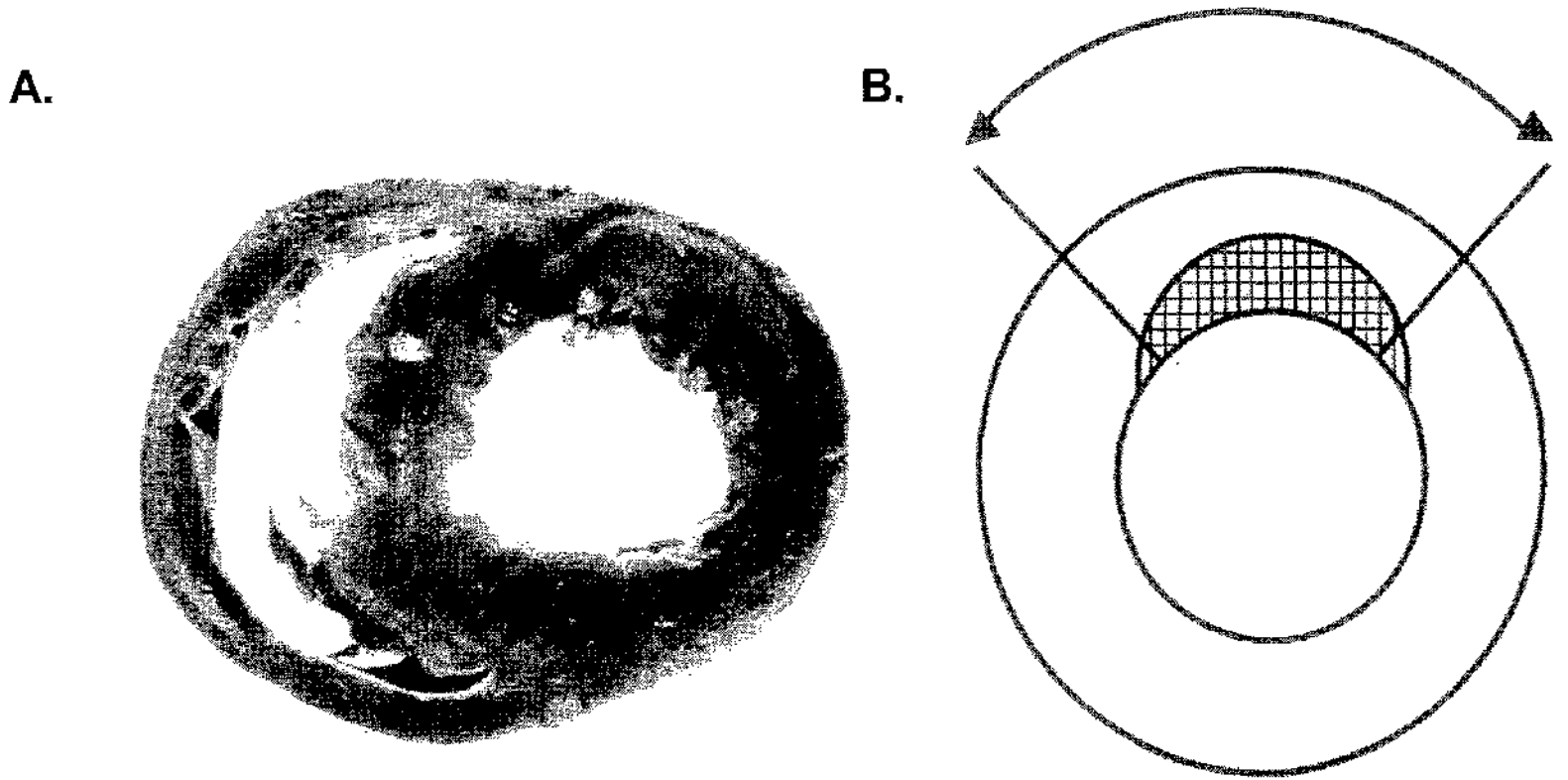

Figure 18. Infarct transmurality.

A. Well demarcated infarction at 2 days after permanent coronary ligation in the dog. A transverse section at the high papillary level is shown. This infarct is nearly transmural at that level, with less than 10% epicardial sparing, and results in segmental akinesis. **B.** Subendocardial infarction with about 50% transmural extent. The segment subtended by more than 20% transmural infarction (cross-hatched) results in dyskinesis (with systolic thinning) despite significant sparing in the midwall and epicardium. Since the epicardium contributes little to systolic thickening, epicardial salvage may not result in improved regional systolic function with reperfusion. Jugdutt (247)

(Figure 18), larger LV diastolic (82 ± 10 versus 75 ± 11 mL, P<0.05) and systolic (53 ± 14 versus 42 ± 11 mL, P<0.05) volumes, and more LV apical aneurysms and RSD (Figure 18) in the long-axis, reflecting greater topographic deterioration. Group 2 also showed more LV thrombi (79% versus 55%, χ^2=2.70, P<0.01), ventricular arrhythmias, and deaths (36% versus 12%, P<0.001). Infarct transmurality correlated with the severity of LV remodelling and dysfunction.

Also in that study, mean left atrial pressure was higher in group 2 but heart rate and blood pressure were not significantly different. Collateral blood flow was less in all regions of the risk region for group 2, infarct center flows being 0.05 ± 0.01 versus 0.29 ± 0.10 mL/min/g (P<0.001). Importantly in group 2, 66% of the infarct expansion occurred by 2 days while 84% of the infarct thinning occurred late, after the second week. The ECGs showed a greater frequency of pathological Q-waves in group 2, the frequencies at 6 weeks being 33% versus 0% (χ^2=10.18, P<0.005). Premature ventricular contractions at 2 days were more frequent in group 2, 63% versus 24% (χ^2=6.93, P<0.01). The Lown score of arrhythmias at 6 weeks was also greater for group 2 (1.8 ± 1.2 versus 0.5 ± 0.7, P<0.001). The overall findings indicated that infarct transmurality is a major determinant of LV remodelling and dysfunction during healing after MI (73).

Relevance: Since infarct transmurality is a major determinant of the severity of adverse LV remodelling and dysfunction during healing after anterior MI, early therapeutic interventions aimed at decreasing transmurality might limit remodelling. Furthermore, stratification on the basis of initial infarct transmurality might be useful in selecting high-risk patients for aggressive anti-remodelling therapy during healing after MI.

5.1.2.2. Q-wave and non-Q-wave MI (74: Appendix 20)

Background: The presence of anterior Q waves on the ECG might identify a group at high risk for adverse LV remodelling and severe LV dysfunction after MI.

Methods/Results: Whether LV remodelling is more severe after anterior Q-wave than non-Q-wave MI was addressed in another report (74). This study confirmed that the Q-wave group had greater infarct transmurality (88% versus 58%, P<0.001), higher left atrial pressures, more infarct expansion, more infarct thinning, greater LV dilatation, more LV apical bulging (depth of RSD: 4.9 versus

1.9 mm, P<0.001), more LV asynergy (18% versus 7%, P<0.001), lower global ejection fraction (40% versus 48%, P<0.001), more LV apical aneurysms (82% versus 36%, P<0.001), more LV thrombus (64% versus 0%, P<0.0005) and ventricular arrhythmias.

Importantly, this study provided insight into the relation between infarct transmurality and the presence of Q waves over 6 weeks after MI (74). The presence of Q waves correlated with greater transmurality at 2 days (87% versus 52%), 7 days (88% versus 53%) and 6 weeks (88% versus 15%). The values of transmurality that separated the Q-wave from the non-Q-wave group were close at the three time intervals and averaged 76.6%.

Relevance: The association of anterior Q waves on ECGs with greater infarct transmurality and more adverse LV remodelling and dysfunction during healing after MI suggests that the finding of an anterior Q wave on the initial ECG might be used to select high-risk patients after MI.

5.1.2.3. Resistance to distension and rupture (283: Appendix 40)

Background: Healing after MI is associated with progressive ECM and collagen remodelling. These may lead to changes in the distensibility and mechanical strength of the infarcted LV. The LV rupture threshold might provide a global measure of the mechanical strength of the infarcted heart.

Methods/Results: The mechanical resistance of the infarcted left ventricle to rupture, or rupture threshold, was measured using the balloon technique (Figure 19) between 1 and 2 days in 70 fresh post-mortem hearts from dogs with LAD occlusion (283). The rupture threshold in infarcted hearts was lower than in non-infarcted hearts (754 ± 223 (SD) mm Hg versus 1168 ± 165 mm Hg, P<0.001).
Over 6 weeks after MI, the rupture threshold did not change in non-infarcted hearts but decreased after 14 days in infarcted hearts, the average value being less between 21-42 days than 1-14 days (577 ± 140 versus 867 ± 191 mm Hg, P<0.001). Passive LV stiffness before rupture also decreased after 14 days in infarcted hearts. Infarct OHP increased during healing and 2D-Echo confirmed evidence of early infarct expansion and late infarct thinning. The late decrease in rupture threshold and pre-rupture stiffness of the infarcted left ventricle and late

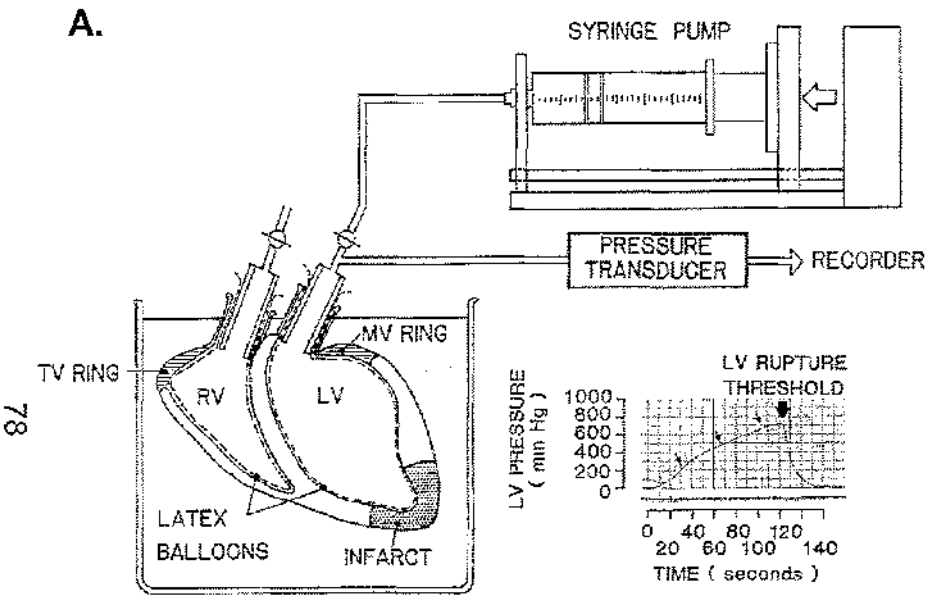

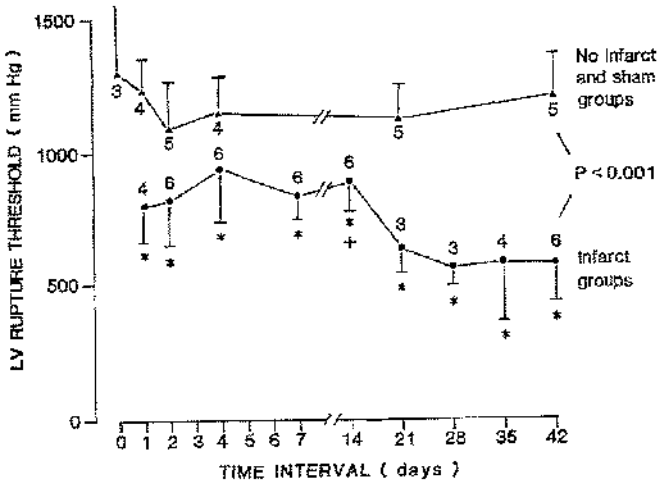

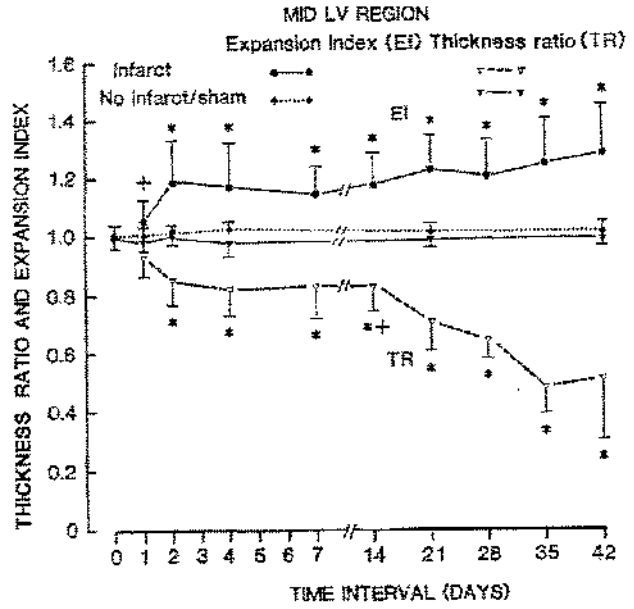

Figure 19. Measurement of the left ventricular rupture threshold during healing of canine myocardial infarction

A. Measurement of the left ventricular (LV) rupture threshold using the balloon technique.
B. Changes in the LV rupture threshold during healing
C. Changes in infarct thinning and expansion during healing
From Jugdutt (283; Appendix 40)

scar thinning suggests there is a late decrease in the mechanical strength and resistance of the infarcted left ventricle to distension during healing after MI.

Relevance: The time-dependent changes in collagen content (and remodelling) and LV structural remodelling during healing after MI are associated with changes in global LV distensibility and resistance to rupture. High, "non-physiologic", LV pressures like those in this study can develop during activities such as heavy lifting and snow shovelling.

The overall findings of the first two studies (73,74) underscore 5 points:

First, anterior Q-wave MI is associated with greater infarct transmurality, LV remodelling and dysfunction in the dog model.

Second, transmural or Q-wave MI does not simply imply more than 50% transmural extent as previously assumed but about 77%. This implies that Q-wave infarcts may also have a subepicardial buttress of 23% or less. This factor contributes to heterogeneity in clinical studies.

Third, subendocardial or non-Q-wave MI may be buttressed by a more significant subepicardial rim than Q-wave MI. While this may be an advantage in preventing infarct expansion (Figure 20), an increase in this area due to myocardial salvage after reperfusion therapy may not be reflected in improved regional function on 2D-Echo. This is because systolic thickening is due mainly to thickening of the endocardium and to a lesser extent to thickening of the mid-myocardium, but very little to thickening of the epicardium (326).

This factor is compounded by the fact that restoration of flow to near normal levels in epicardial vessels may not achieve 100% transmural reperfusion because of reperfusion injury associated with microvascular injury and "no reflow" (305). The mismatch between restoration of flow and recovery of function has been an active area of study in several laboratories since the mid 1980's.
Contrast 2D-Echo has been applied to better define the area at risk and the role of microvascular injury (327-331).

Fourth, it follows from the first two studies (73,74) that a significant number of patients who have non-Q-wave or subendocardial MI may be expected to have significant necrosis between 21% and 75% in transmural extent and significant akinesis and dyskinesis. Furthermore, as post-MI survivors show loss of Q-waves and heterogeneity in the severity of LV dysfunction over time on serial 2D-Echo (21,35,74,75), the timing of the measurements after MI becomes pertinent.

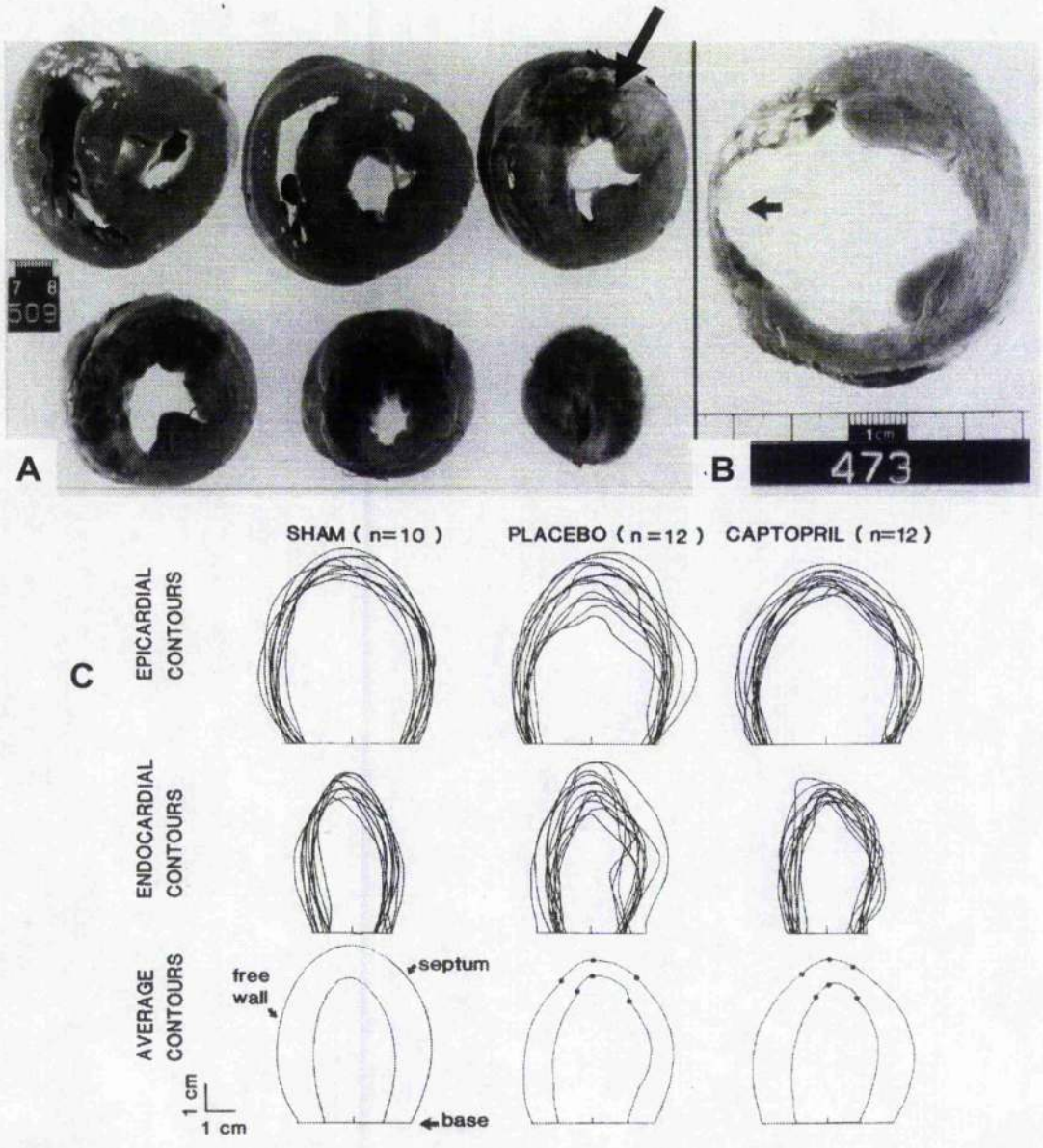

Figure 20. Transverse sections for measurement of infarct size, expansion, thinning and bulging in anterior MI.

A, B. Transmural infarction produced by mid-LAD ligation (arrow), barium-gelatin-polymer injection into distal LAD, and running suture around the occluded bed. All myocardium within the occluded bed below the ligation shows transmural infarction, with no sparing.

C. Computer-generated LV endocardial and epicardial contours from radiographs in the long-axis plane for the infarction and sham groups. Group 1, standard LAD occlusion. Group 2, LAD occlusion with collateral obliteration and increased transmurality. Points on the average contours indicate landmarks for quantifying the bulge.

From Jugdutt et al. (318; Appendix 43)

Fifth, the third study (283) suggests that the infarcted left ventricle after 6 weeks is weaker than the non-infarcted left ventricle, and the resistance to distension is diminished. It follows that the healing heart is vulnerable even in the late phase of healing after the collagen plateau has been reached.

The overall findings suggest that the infarcted left ventricle is susceptible to early regional dilatation and RSD during the first 2 weeks after MI, before the collagen plateau, and significant progressive dilatation involving both the infarct and the non-infarct segment in the later phase of healing, after the collagen plateau and in part due to late infarct scar thinning.

5.2. ANIMAL STUDIES ON MODIFICATION BY PHARMACOLOGICAL AGENTS

5.2.1. Effect of infarct-limiting therapies on infarct collagen, LV geometry and LV function during healing after MI in the dog (55: Appendix 16)

Background: Before embarking on clinical studies, it was necessary to determine whether infarct-limiting therapies (Table 7) applied during acute MI might influence early healing after MI. Effects of LV unloading with NTG and ACE-inhibition were first studied (Figure 21).

Methods/Results: The hypothesis that early short-term therapy with 3 infarct-limiting drugs, given only during the first 6 hours of acute MI might produce persistent or delayed effects on LV remodelling during early infarct healing over 1 week was tested in the dog model (55). Measurements of regional OHP content, wall thicknesses, segment lengths and infarct size were made at 7 days in left ventricles from 69 animals with LAD ligation and 7 sham animals. The animals were randomized after LAD occlusion to 6 hour infusions of intravenous saline (controls, n=29), NTG (low-dose to decrease mean arterial pressure by 10% but not below 80 mm Hg, n=13), PGI_2 (low-dose, 10% decrease in mean arterial pressure, n=13), or ibuprofen (low-dose, 4 mg/kg/hour, n=14). Infarct size, measured by computerized planimetry of weighed LV rings, was less in therapy groups compared to saline, as percent of occluded bed size ($P<0.001$) and as percent of the left ventricle ($P<0.005$). Infarct expansion was less with NTG and PGI_2 compared to saline and ibuprofen. However, infarct thinning was greater with ibuprofen compared to the other groups. Thus, the ratios of the infarct to the normal wall thickness were similar for saline, NTG and PGI_2 groups [0.92 ± 0.02

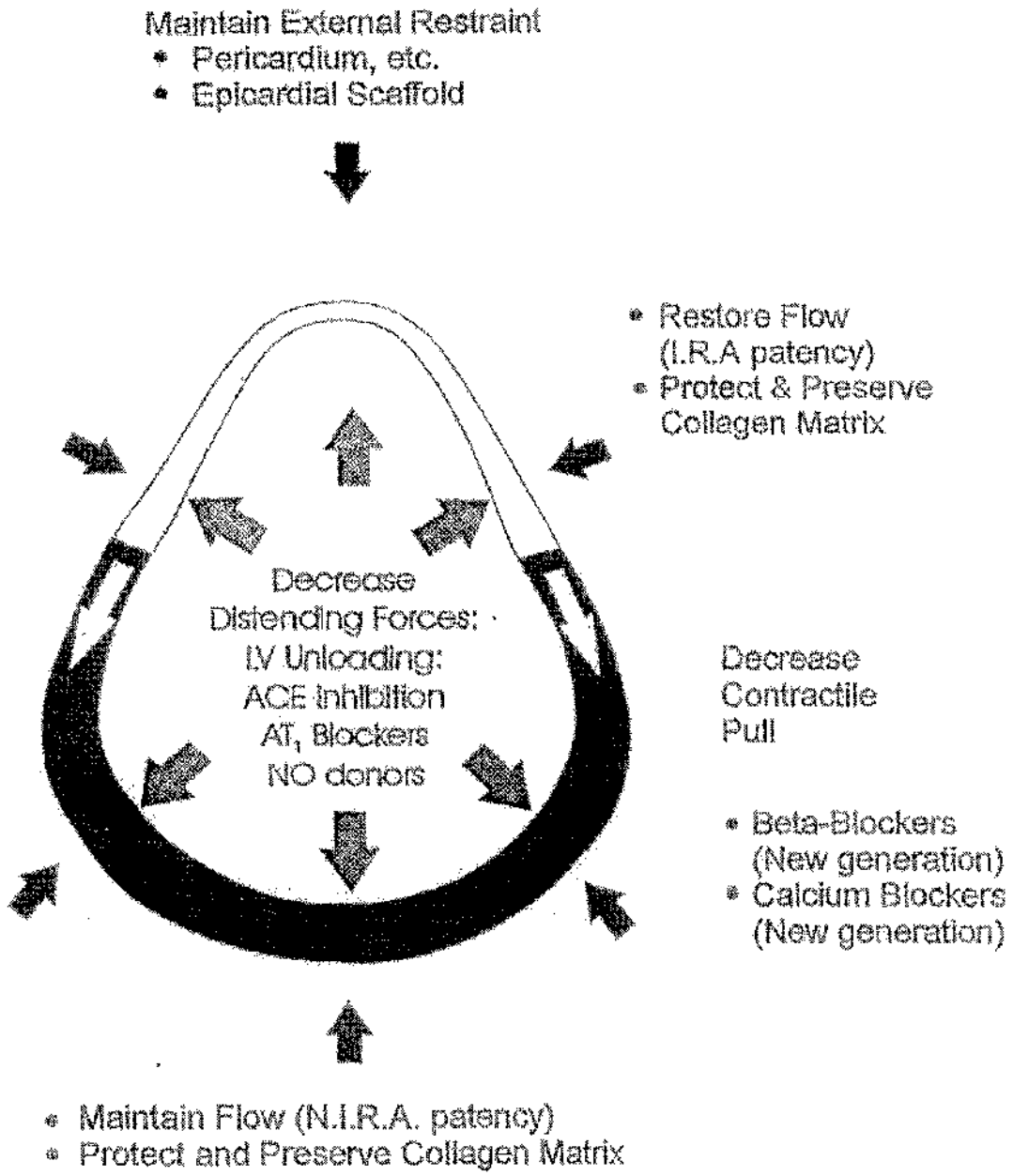

Figure 21. Determinants and therapeutic approaches in the remodelling of infarct and non-infarct zones

Potential therapeutic approaches. IRA = infarct related artery, NIRA = non-infarct related artery. White arrows = intramural contractile pull, stipples arrows = intracavitary distending forces, dark arrows = restraining forces opposing distension.

(SEM) versus 0.94 ± 0.02 versus 0.96 ± 0.01, respectively] but significantly lower in the ibuprofen group (0.80 ± 0.02, P<0.001). The OHP contents (mg/g dry weight) were higher (P<0.001) in the infarct than normal zones in all 4 groups (saline: 9.9 ± 0.7 versus 4.4 ± 0.2; NTG: 14.9 ± 1.9 versus 5.2 ± 0.3; PGI_2: 12.9 ± 0.9 versus 5.3 ± 0.6; ibuprofen: 10.6 ±1.4 versus 4.2 ± 0.2), and higher with NTG compared to saline (14.9 ± 1.9 versus 9.9 ± 0.7 mg/g, P<0.02). The degree of RSD measured on short-axis outlines of sections and long-axis radiographic outlines was less (P<0.001) with NTG and PGI_2 compared to saline and ibuprofen. The rupture thresholds were less in ibuprofen than NTG or PGI_2 or saline groups (397 ± 37 versus 720 ± 67 mm Hg, P<0.005). There was no difference among the NTG or PGI_2 or control groups.

These results indicated that early therapy with NTG, PGI_2 or ibuprofen reduced infarct size but did not reduce infarct collagen by 1 week. NTG increased infarct collagen while ibuprofen increased infarct thinning, and NTG and PGI_2 limited infarct expansion and RSD.

Relevance: The overall findings support the concept that the application of short-term infarct-limiting therapy during acute MI may exert delayed, and sometimes unexpected effects and influence LV remodelling during the very early phase of healing, before significant collagen deposition. Appropriate therapies might have greater potential for limiting remodelling and aneurysm formation when administered early after MI. This was subsequently confirmed in a study at the bedside (28**: Appendix 6**).

5.2.2. Effect of vasodilator-induced hypotension on infarct size, collateral blood flow, and LV geometry and function in 7-day old anterior infarcts in dogs (122: Appendix 28)

Background: The hypothesis that vasodilator therapy, previously shown to be beneficial in MI in dogs (98) and humans (232**: Appendix 36**), might be deleterious and lead to adverse remodelling was tested in the dog model when given in excess (122). NTG therapy was delayed 2 hours post-occlusion to mimic the clinical scenario.

Methods/Results: The effect of NTG-induced decreases in mean arterial pressure on myocardial salvage was studied in 65 lightly sedated conscious dogs

that were randomized 2 hours after LAD occlusion to receive 4-hour intravenous infusions of saline (group 1, n=19), or NTG in doses to decrease mean arterial pressure by 10% (group 2, n=18), 25% (group 3, n=14), and 50% (group 4, n=14), respectively. At 7 days, infarct size and occluded bed size (post-mortem coronary arteriography) were measured in 41 dogs using computerized planimetry. Over the first 6 hours, regional blood flow was measured using 7 to 10 μm radioactive microspheres in 24 dogs (98). Compared to saline infusions in group 1, NTG infusions produced sustained reductions ($P<0.001$) in mean left atrial pressure and mean arterial pressure in all dogs, but heart rate was unchanged. The decreases in mean arterial pressure achieved in groups 2, 3, and 4 were 10% (range, 5% to 19%), 23% and 39%, respectively, with average levels of 96 (range, 83 to 113), 83, and 64 mm Hg, respectively. Infarct size was significantly smaller ($P<0.025$) in group 2 compared to groups 1, 3, or 4, expressed both as percent of the left ventricle (6% versus 14% versus 13% versus 15%) and as percent of the occluded bed (13% versus 37% versus 34% versus 44%) (Figure 22). Myocardial salvage (expressed as percent of the occluded bed) with NTG correlated inversely with the percent of decrease in mean arterial pressure ($r = -0.77$, $P<0.001$). Collateral blood flow increased ($P<0.005$) throughout the occluded bed in group 2 compared to group 1 but was unchanged in groups 3 and 4. In contrast, coronary vascular resistance decreased ($P<0.025$) in all NTG groups. These results suggested that perfusion pressure is an important determinant of myocardial salvage during vasodilator therapy such as NTG. An increase in the dose of NTG to decrease mean arterial pressure by more than 10%, and to levels below 96 mm Hg, might offset its potential for myocardial salvage in the dog.

Relevance: The overall findings suggest the need for a caveat on avoiding hypotension during vasodilator therapy after acute MI. The paradoxical J-curve effect (Figure 22C), whereby reduction in perfusion pressure beyond a critical level leads to more necrosis instead of salvage, can occur with other vasodilators (100). In this study, marked NTG-induced hypotension negated the beneficial effects on infarct size and collateral blood flow (122). This underscores the need for extreme caution and titration of the drug to a suitable haemodynamic end-point in the setting of acute MI. The risk is further amplified in the presence of multivessel disease and coronary vasodilators that can potentially cause 'coronary artery steal'. The short half-life of intravenous NTG and its rapid onset and offset

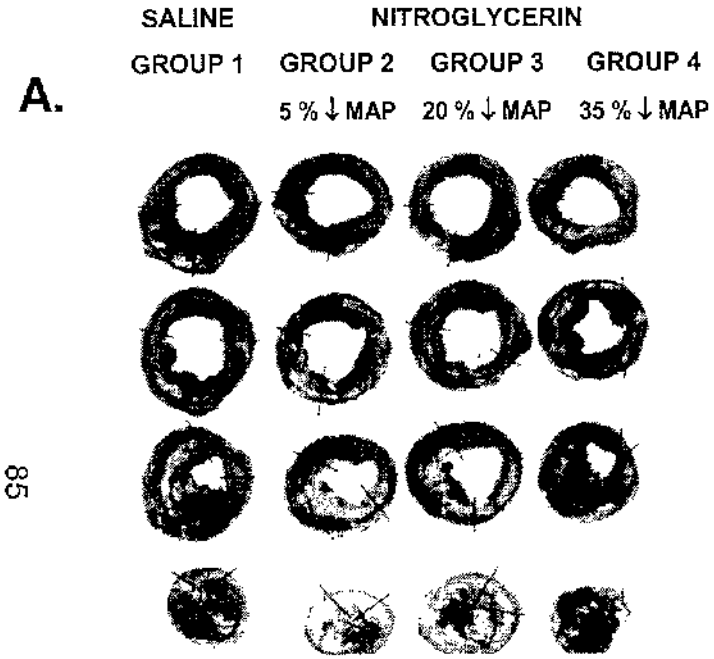

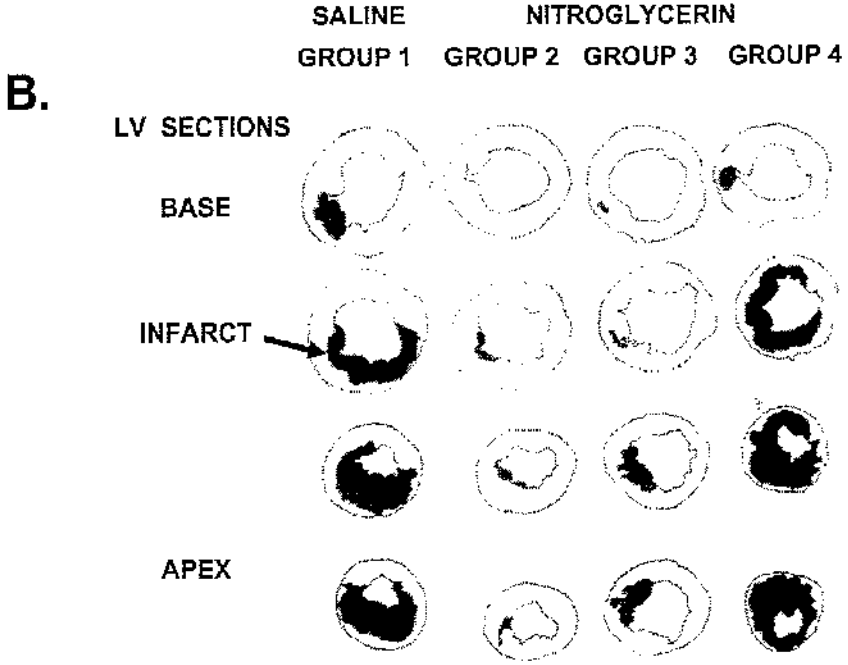

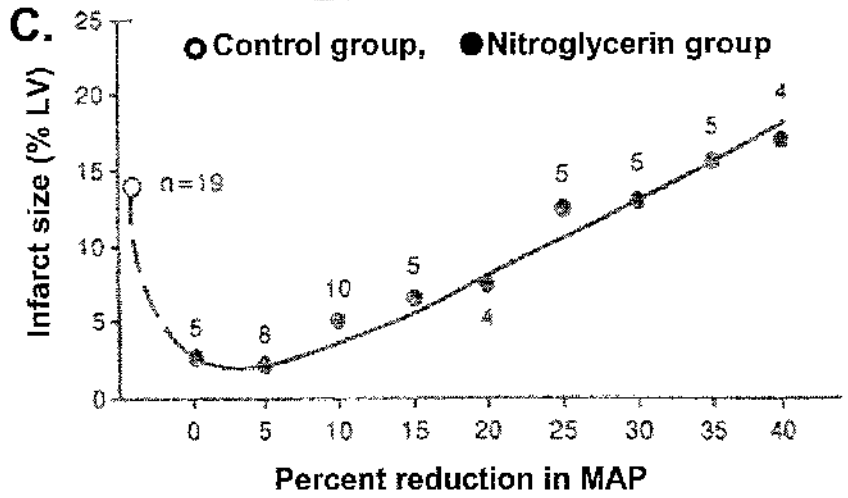

Figure 22. Examples of infarcts in LV sections

A. Representative examples of infarcts in LV sections from base (top) to apex (bottom) of 4 hearts treated with saline (group 1) or nitroglycerin in increasing doses (groups 2, 3, 4).

B. Corresponding outlines of infarcts and LV rings for the same hearts.

C. Paradoxical J-curve with progressive afterload reduction by nitroglycerin infusions in acute MI.

From Jugdutt (100:Appendix 21, 122: Appendix 28)

of action makes the drug suitable for use in acute MI (250). Long-acting nitrate preparations, such as ISDN, may be problematic if hypotension develops during infusions in acute MI.

5.2.3. Effect of prolonged vasodilator and anti-inflammatory treatment on LV remodelling and LV rupture threshold during healing after MI in the dog

The hypothesis that prolonged therapy during healing after MI significantly modifies LV geometry and function was addressed in 3 studies using the dog model (48,102,103).

5.2.3.1. Effect of prolonged isosorbide dinitrate and ibuprofen on LV topography and rupture threshold during healing after MI (102: Appendix 22)

Background: Short-term pharmacological interventions applied during healing after MI might modify LV remodelling during healing and the mechanical resistance of the healed infarcted LV to distension and rupture threshold. Although acute administration of nitroglycerin and ibuprofen has been shown to reduce infarct size, prolonged treatment with ibuprofen was reported to produce adverse infarct remodelling (54).

Methods/Results: The effect of ISDN and ibuprofen, given between 2 and 7 days after LAD ligation, on the mechanical resistance of the infarcted left ventricle to rupture or the rupture threshold (balloon technique) and LV topography (computerized planimetry) and function (2D-Echo) at 7 days (n=32) and 42 days (n=34) post-ligation was studied in 66 dogs (102). The animals were randomly allocated to sham (no infarction, n=22) and infarction sub-groups (15 controls; 15 ISDN, 30 mg b.i.d. orally at 08:00 and 14:00 hours, followed by 10 mL of water at 22:00 hours so as to allow a washout period of about 12 hours and avoid development of nitrate tolerance (332); 14 ibuprofen, 200 mg t.i.d. orally). ISDN decreased mean arterial and left atrial pressures, decreased diastolic cross-sectional area, and improved LV systolic function, while ibuprofen increased diastolic area. Infarction subgroups showed infarct shrinkage and more infarct OHP at 6 weeks. Compared to sham animals, all infarct subgroups showed early expansion and thinning, with further marked late thinning in controls. ISDN

produced less expansion and thinning both at 1 and 6 weeks, while ibuprofen produced marked early thinning. Rupture threshold was less at 6 weeks than 1 week with controls and ibuprofen but remained unchanged with ISDN. Passive pre-rupture stiffness was less at 6 weeks than 1 week with controls but remained unchanged with ISDN and ibuprofen.

The overall results indicated that reduced expansion and thinning with ISDN during the first week after MI was associated with improved LV function, mechanical strength, and resistance to distension at 6 weeks.

Relevance: The finding of beneficial effects of short-term nitrate therapy, given using an eccentric dosing schedule and allowing a nitrate-free interval during the first week after MI, on LV remodelling, LV function, mechanical strength and distensibility measured at 6 weeks supported the concept that short-term therapy may have long-term benefits. Another pertinent finding was that therapy given before infarct collagen reaches a plateau (before significant fibroblast activity develops) did not seem to lead to a detectable difference in the collagen content of the healed infarcts. This finding suggests that drugs that inhibit collagen synthesis may not significantly affect infarct collagen during that time window.

Erratum: An error appears in the title of this publication in reference #102 (**Appendix 22**); 'nitroglycerin' should be 'ISDN' as stated in the text.

Both ISDN and NTG are denitrated to release NO (333: **Appendix 44**). While NTG is short-acting, ISDN is long-acting (334). ISDN is denitrated at a much slower rate than NTG (334). In fact, ISDN is a prodrug that is denitrated in the liver (first pass) to liberate NO, which then stimulates guanylyl cyclase leading to the conversion of cGMP (guanosine triphosphate to cyclic guanosine 3′,5′-monophosphate) which causes vasodilatation. ISDN is metabolized to isosorbide 2- and 5-mononitrrate. The latter is the primary metabolite that is commercially available as ISMN. NTG, on the other hand, is metabolized to 1,3- and 1,2-glyceryl dinitrate, which are active metabolites with lower potency than NTG (334). Inactive metabolites are also produced. Further metabolism yields glycerol and carbon dioxide. Unlike NTG, ISDN and ISMN do not cause spontaneous release of NO and are less effective in raising platelet cGMP (333,335,336).

5.2.3.2. Effect of prolonged 2-week versus 6-week nitrate therapy regimens on LV remodelling after MI in the dog (103; Appendix 23)

Background: Although the beneficial effects of LV unloading with low-dose NTG in acute MI (limitation of infarct size) (123) and ISDN during short-term therapy before the infarct collagen plateau (limitation of LV remodelling and dysfunction) (102) had been demonstrated, the effect of long-term nitrate throughout post-MI healing had not been determined. This study tested the hypothesis that long-term therapy, given throughout healing over 6 weeks after MI, might be more beneficial than short-term therapy given over the first 2 weeks after MI (103).

Methods/Results: The effect of prolonged nitrate therapy between 2 days and 6 weeks during healing after MI on serial parameters of LV remodelling (scar expansion, scar thinning, LV dilatation, and hypertrophy) and LV function (asynergy or akinesis plus dyskinesis and ejection fraction) by serial 2D-Echo, haemodynamics, post-mortem topography (computerized planimetry, geometric maps, and radiographs), and collagen content (OHP) was studied in 64 dogs. The animals were randomized 2 days after LAD ligation to various nitrate regimens (n=32) over the first 2 weeks: sub-group 1, 2% transdermal NTG at 8 AM and 4 PM (n=6); sub-group 2, 2% transdermal NTG plus 2.6 mg of sustained release oral NTG at 8 AM, 3 PM, and 10 PM (n=5); sub-group 3, oral ISDN, 30 mg at 8 AM and 4 PM (n=11) or 6 weeks: sub-group 4, ISDN (n=10); and matching controls (n=32).

Nitrate therapy reduced left atrial pressure, mean arterial pressure, and the rate-pressure product compared to controls over the 6 weeks. Post-mortem scar mass and OHP were similar in control and nitrate groups. However, scar stretching and thinning, cavity dilatation, non-infarct wall hypertrophy, and apical bulging (RSD) were less with nitrates, especially in the long-term sub-group 4. In-vivo remodelling parameters between 2 days and 6 weeks after ligation showed that, compared to controls, nitrate therapy prevented further stretching of the asynergic segment, decreased the expansion index, decreased further scar thinning, prevented the increase in LV volumes, reduced the frequency of LV aneurysm, prevented the increase in LV mass, reduced the extent of asynergy, and improved ejection fraction. Although the beneficial effect on topography and function was seen in all nitrate sub-groups, the overall benefit was greater with

long-term therapy over 6 weeks (sub-group 4) than short-term therapy confined to the first 2 weeks (sub-groups 1, 2, and 3).

The overall results indicated that prolonged nitrate therapy, in various regimens during healing after infarction, effectively reduced LV loading and prevented infarct thinning, further infarct expansion, progressive LV dilatation, and the increase in mass. These effects were associated with decreased LV asynergy and improved LV ejection fraction. The beneficial effects were greater with long-term therapy over 6 weeks than short-term therapy over the first 2 weeks.

Relevance: The benefits of long-term nitrate therapy given in an eccentric dosing schedule in this study supported the concept that prolonged LV unloading can limit adverse LV remodelling and dysfunction after MI.

5.2.3.3. Impact of LV unloading after late reperfusion of canine anterior MI on remodelling and function using isosorbide-5-mononitrate (48: Appendix 13)

Background: Late coronary artery reperfusion was being reported to result in a mismatch with delayed recovery of function despite re-established perfusion (158). However, late reperfusion was also reported to limit infarct expansion independent of reduction of infarct size (83). Whether prolonged LV unloading after late reperfusion might improve recovery of LV function and limit remodelling during healing after anterior MI had not been determined.

Methods/Results: The hypothesis that late reperfusion combined with prolonged unloading with isosorbide-5-mononitrate (ISMN) might produce greater functional recovery and less remodelling than late reperfusion alone was tested in the dog model (48). The rationale was that late reperfusion during acute MI results in delayed recovery of LV function and less remodelling, whereas LV unloading with nitrates improves function and attenuates remodelling.

In-vivo LV function and topography (2D-Echo), post-mortem topography (planimetry), and collagen content (OHP) were measured in dogs that were randomized to reperfusion 2 hours after LAD ligation plus ISMN (n=12) or placebo (n=12) given as 25 mg intravenously over 4 hours followed by 50 mg q.i.d. for 6 weeks. ISMN had been reported to be associated with less nitrate tolerance (337). Compared to placebo, the ISMN group had similar heart rate but lower left

atrial pressure, mean arterial pressure, and rate-pressure products. Although in-vivo remodelling and functional parameters were similar in the two groups, by 6 weeks the ISMN group had smaller ($P \leq 0.05$) infarct and non-infarct segment lengths, ventricular volumes, and mass; less ($P<0.001$) asynergy; and greater ($P<0.001$) volume ejection fraction. More importantly, by 2 days, ejection fraction was 18% greater ($P<0.025$) and asynergy 26% less ($P<0.05$) with ISMN. At 6 weeks, the ISMN group showed less ($P \leq 0.05$) scar size, scar collagen, cavity dilatation, non-infarct wall thickness, and apical bulging than the placebo group. In another 4 dogs, ISMN given acutely produced less improvement in LV function and remodelling than prolonged ISMN.

The overall results suggested that late reperfusion of acute anterior MI combined with prolonged ISMN unloading results in greater and earlier recovery of LV function and less remodelling than late reperfusion alone.

Relevance: Prolonged LV unloading with ISMN (once daily) after late reperfusion results in earlier recovery of LV function and less remodelling.

The overall findings of the three studies (48,102,103) underscore 3 important points.

First, both the timing and duration of interventions after MI are important. It is evident that certain factors such as mechanical forces are operative throughout the period after MI (Figures 7 and 21). It follows that prolonged application of an appropriate intervention throughout healing might be more effective than early or late therapy alone. These principles have been tested and found to be true with agents that: i) reduce preload and afterload, such as NTG (48,102,103,104-109), and captopril or enalapril (108,126-131); ii) increase contractile pull, such as digoxin (222); and iii) decrease contractility and heart rate, such as metoprolol (220).

Second, therapy during the healing phase with an agent such as NTG, which does not decrease infarct collagen, does not cause thinning, but decreases preload and afterload, would be expected to reduce the extent of RSD and improve myocardial performance after acute MI. The effect of prolonged NTG therapy during the healing phase in the studies described above confirm beneficial effects on LV geometry, RSD and LV function after MI with or without reperfusion in the dog model (48,102,103).

Third, the long-acting nitrate, ISDN, proved to be safe and produced benefits when given during the period after completion of MI, between 2 days and 7 weeks and allowing a daily nitrate-free interval. Thus, the ISDN was administered using an eccentric dosage schedule to avoid the development of nitrate tolerance (332). It is possible that the healing infarct is less susceptible to the harmful effects of hypotension than the acutely infarcting myocardium.

5.2.4. Effect of agents that decrease infarct collagen on LV remodelling during healing after MI in the dog

The hypothesis that prolonged therapy with ACE inhibitors, that produce LV unloading and inhibition of angiotensin II formation, might limit LV remodelling and dysfunction after MI was tested in the dog model (126-129,131). The effect of ACE inhibitors on collagen synthesis was not known at the time that the studies were done in the mid 1980's. This unexpected finding led to additional studies with ACE-inhibition.

5.2.4.1. Effect of long-term captopril therapy on LV remodelling and function during healing after MI in the dog (126: Appendix 29)

Background: The effect of prolonged LV unloading with an ACE inhibitor on LV remodelling, function and infarct collagen during healing after anterior MI in the dog model had not been determined.

Methods/Results: The effect of long-term reduction of preload and afterload by captopril during healing after MI on LV remodelling and function was studied in 30 chronically instrumented dogs with LAD ligation (126). The animals were randomized 2 days after MI to oral therapy with placebo (n=15) or captopril, 50 mg t.i.d. (n=15), for 6 weeks. Serial haemodynamic as well as topographic and functional variables (2D-Echo) were measured over 6 weeks. Scar topography (planimetry), occluded bed size (coronary arteriography) and collagen (OHP) content were measured at 6 weeks. Between 2 days and 6 weeks, captopril decreased ($P<0.001$) mean arterial pressure and mean left atrial pressure more than placebo, but did not influence heart rate. Infarct scar mass, transmurality and collagen content at 6 weeks were similar in the two groups but scars showed less ($P<0.001$) thinning and expansion with captopril than with placebo. The infarct scar weights were consistent with small infarcts (control, 5.7 ± 2.7 g;

captopril, 6.4 ± 3.5 g). Echocardiograms showed similar infarct expansion and thinning in the two groups at 2 days but less aneurysm with captopril at 6 weeks. Between 2 days and 6 weeks, the expansion index (infarct-/non-infarct-containing segment length) decreased ($P<0.001$) with captopril but increased ($P<0.001$) with placebo. Also, thinning ratio (infarct/normal wall thickness) decreased ($P<0.001$) with placebo but did not change (P=NS) with captopril. By 6 weeks, LV asynergy and volumes showed a greater decrease ($P<0.01$) and global ejection fraction a greater increase ($P<0.05$) with captopril.

The results suggested that captopril therapy during healing after canine anterior infarction limits LV remodelling and improves LV function in a dog model of small infarcts.

Similar benefit was seen with captopril in the canine model of small transmural MI (318: **Appendix 43**). Transmural MI was induced by mid-LAD ligation plus a circumferential running silk suture around the central cyanotic zone (not penetrating more than 50% of the LV wall thickness and not applied with excessive tension that might distort or tear the wall) and, as added precaution, ligation of visible collateral feeders (318). The captopril-induced attenuation of RSD in that study was dramatic in some hearts (Figure 23).

Relevance: The findings established that the ACE-inhibitor captopril limits LV remodelling and dysfunction in small transmural MI. Beneficial effects of captopril on LV remodelling and survival were previously reported in rats with small and moderate MI (75-77). Captopril in that study did not significantly decrease collagen in the infarct center region (126). Of note, the dose of captopril in that study decreased both afterload and preload (126).

5.2.4.2. Effect of enalapril on LV remodelling and function during healing after anterior MI in the dog (127: Appendix 30)

Background: In view of the results of the CONSENSUS II study (123), the hypothesis that prolonged ACE-inhibition with enalapril might produce similar benefits as found with captopril (77) was tested. The effect of prolonged ACE-inhibition with enalapril, given in a dose that does not produce prolonged decrease in blood pressure, on LV remodelling, function and infarct collagen during healing after anterior MI in the dog model had not been determined.

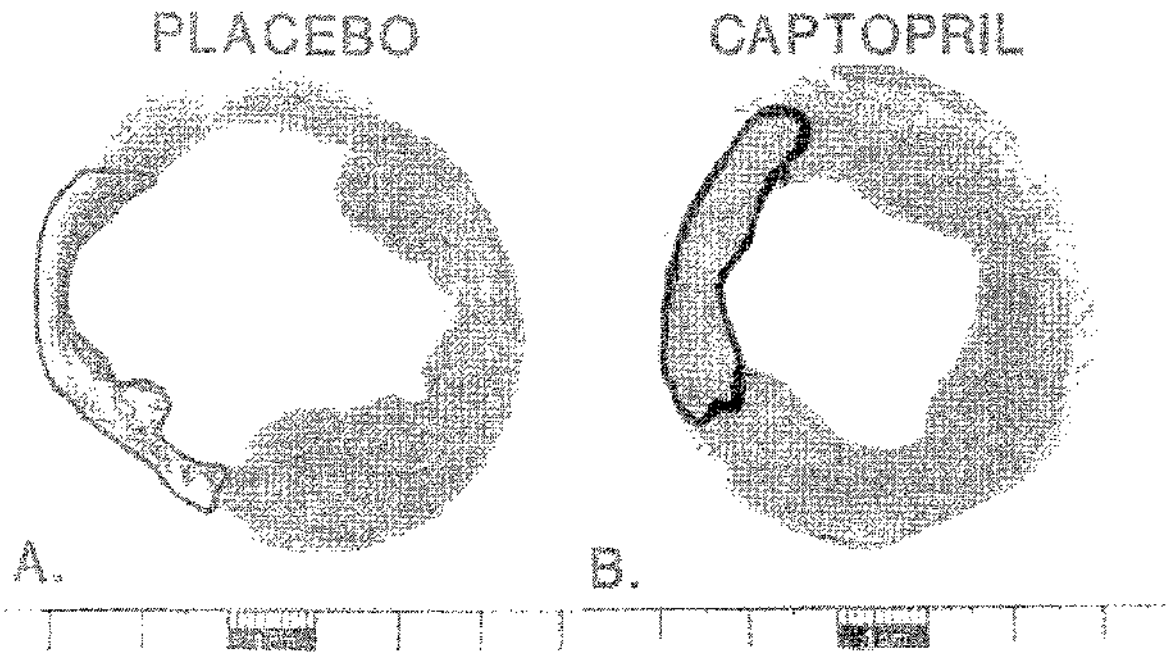

Figure 23. Effect of captopril on remodelling post-infarction

Thin transverse sections at the papillary level. Dog hearts were arrested in diastole. Pale scar zones are contoured. Risk regions were similar in the two hearts.
A. Expansion with regional bulging and thinning plus cavity dilatation in a placebo-treated dog.
B. Preservation of geometry with attenuation of expansion, thinning and dilatation in a captopril-treated dog.

From Jugdutt et al. (318: Appendix 43)

Methods/Results: The effect of enalapril, during healing between 1 day and 6 weeks after MI, on in-vivo changes in LV size, shape, mass and function (asynergy, or akinesis and dyskinesis, and ejection fraction) as determined by serial 2D-Echo, haemodynamics, post-mortem topography (planimetered short- and long-axis ventricular contours), and collagen content (determined by levels of OHP) was measured in 25 instrumented dogs (127). The dogs were randomized 1 day after LAD ligation to a control group (no treatment) and a group receiving oral enalapril (2.5 mg b.i.d.). Compared to controls, enalapril produced a sustained lowering of left atrial pressure but no difference in heart rate and mean blood pressure over the 6 weeks.

Also compared to controls, enalapril modified in-vivo remodelling parameters between 1 day and 6 weeks, with less elongation of the asynergy containing segment, lower expansion index (ratio of endocardial lengths of infarct to non-infarct containing segments demarcated by papillary muscle landmarks), less scar wall thinning, lower thinning ratio (ratio of average thickness of infarcted wall to average thickness of the normal wall), smaller LV volumes, less regional bulging and aneurysm frequency, prevention of the increase in LV mass, less total extent of asynergy, and higher LV volume ejection fraction.

At post-mortem examination, scar mass was similar in the two groups, but topographic maps with enalapril revealed less infarct bulging, flatter infarct scars and less non-infarct wall thickness. In addition, post-mortem collagen was similar in the non-infarct zones of the two groups but lower in the infarct zones of the dogs given enalapril.

The overall results indicated that prolonged enalapril therapy, in a dose that did not lower blood-pressure, during healing after anterior MI produced prolonged reduction of LV preload in dogs. This diastolic unloading was associated with limitation of remodelling parameters (infarct expansion and thinning, progressive LV dilatation and hypertrophy, regional bulging), less total asynergy and improved LV ejection fraction. Although ACE-inhibition was associated with lower infarct collagen and altered scar topography, these effects did not impact negatively on overall remodelling and function in the model of small infarcts.

Relevance: The findings established that the ACE-inhibitor enalapril, in a dose that produced prolonged reduction of preload but not blood pressure, limited LV remodelling and dysfunction in small transmural MI. However, beneficial effects of

this non-blood-pressure lowering dose of enalapril on LV remodelling were associated with less infarct collagen and flatter scars (127). These findings suggested that the effects on collagen might be due to an inhibition of collagen at the tissue or cellular level.

5.2.4.3. Effect of combined captopril and isosorbide dinitrate during healing after MI (131: Appendix 33)

Background: Because i) ACE-inhibition was suggested to decrease infarct collagen (127), ii) captopril can donate sulfhydryl radicals that are depleted during chronic nitrate therapy, iii) nitrates did not decrease infarct collagen (103), and iv) both nitrate and ACE-inhibition limit remodelling and exert local vascular effects, it was reasonable to suggest that the combination of a nitrate and captopril might be more beneficial than either given alone. The effect of prolonged ACE-inhibition and a nitrate on LV remodelling, function and infarct collagen during healing after anterior MI in the dog model had not been determined.

The hypothesis that combination therapy with captopril and ISDN might be more beneficial than monotherapy in limiting LV remodelling and dysfunction during healing after MI was therefore studied (131).

Methods/Results: In-vivo remodelling variables and function (2D-Echo), haemodynamics, post-mortem topography (planimetry) and collagen (OHP) were measured in 48 chronically instrumented dogs that were randomized 2 days after LAD ligation to 6 weeks of therapy with captopril, ISDN, captopril plus ISDN, or placebo. Compared to placebo, the three active therapies decreased blood pressure and left atrial pressure, limited infarct expansion, infarct thinning, non-infarct wall stretching and thickening, limited LV dilatation and the increase in LV mass, and decreased regional bulging, aneurysm frequency and LV dysfunction. However, the decrease in asynergy and increase in volume ejection fraction were less with captopril alone or captopril plus ISDN than ISDN alone. Infarct thinning and bulging at 6 weeks was also less with ISDN than captopril. Although initial LV asynergy, final scar sizes and non-infarct collagen at 6 weeks were similar among the groups, collagen in the center of the infarct scar was less with captopril or captopril plus ISDN compared to placebo and ISDN.

The results suggested that monotherapy with captopril or ISDN, or the combination improved all remodelling parameters but ISDN improved function more

than captopril or captopril plus ISDN. Inhibition of infarct collagen content by captopril suggests that benefits with captopril represent a balance between positive and negative effects, and combination with ISDN might be advantageous.

Interestingly, the 6-week old scar weights in the four groups in this study (6.0 ± 2.1 (SD) g, 4.0 ± 3.6 g, 5.9 ± 4.5 g and 4.8 ± 2.0) were all small (131) and similar to those in other studies with captopril (126,318).

Relevance: The overall findings supported the concept of added benefits of combination therapy and synergism between ACE-inhibitor and nitrate therapy with respect to LV function. However, the captopril-induced decrease in infarct collagen detected in this study was not attenuated by addition of the nitrate (131).

5.2.4.4. Effect of captopril and enalapril on LV geometry, function and collagen during healing after anterior and inferior MI in the dog (128: Appendix 31)

Background: The effect of prolonged ACE-inhibition on LV remodelling, function and infarct collagen during healing after anterior and inferior MI in the dog model had not been determined. The hypothesis that the beneficial effect of prolonged ACE inhibitor therapy on remodelling during healing after MI might be greater in anterior than inferior infarction and with captopril than enalapril was tested in the dog (128). This was based on the findings that LV remodelling is more marked after anterior MI (21,28,35) and enalapril decreased infarct collagen (127).

Methods/Results: The effect of 6 weeks of therapy with captopril (50 mg b.i.d.), enalapril (2.5 mg b.i.d.), or placebo on in-vivo parameters of LV remodelling, function and mass (2D-Echo), haemodynamic function, post-mortem topography (planimetry) and collagen (OHP) was studied in 36 instrumented dogs randomized to therapy 48 hours after LAD or LCX occlusion. Compared to placebo, both captopril and enalapril decreased infarct expansion, infarct thinning, progressive LV dilatation, LV mass and asynergy, and infarct collagen in anterior and inferior infarction. Despite similar small scar sizes, the effects on remodelling and dysfunction were greater in anterior than inferior infarction. In addition, captopril produced greater attenuation of infarct expansion and LV enlargement, greater improvement in volume ejection fraction, and less decrease in infarct collagen than enalapril.

Relevance: The overall results of that study (128) indicated, that on balance, captopril and enalapril attenuated LV remodelling and preserved function in small anterior and inferior infarction despite differences in the effects of the drugs on individual remodelling variables. The results also suggested that further studies were needed to determine whether inhibition of infarct collagen might be harmful, or differences between captopril and enalapril therapy might be important in large transmural infarctions.

5.2.4.5. Effect of ACE-inhibition on infarct collagen deposition and remodelling during healing after transmural MI in the dog (129: Appendix 32)

Background: The effects of the ACE-inhibitors captopril and enalapril on the temporal changes in infarct collagen during healing after transmural anterior MI in the dog had not been determined. In view of the previous findings with captopril and enalapril in small and predominantly non-transmural MI (127,128,131), this study focused on small but transmural anterior MI.

The hypothesis that prolonged ACE-inhibition for 6 weeks after transmural MI lowers the collagen content of infarct scars was studied in dogs (129). Since collagen deposition increases progressively during healing, the temporal changes in collagen content of the infarct zone with ACE-inhibition during healing over 6-7 weeks and their possible relation to infarct remodelling was also addressed (129).

Methods/Results: Infarct collagen (OHP) content was measured over 6-7 weeks in dogs treated with captopril (50 mg b.i.d.), enalapril (2.5 mg b.i.d.) or placebo, beginning on day 2 after transmural anterior MI or sham. In-vivo changes in the infarct and global LV remodelling, mass and function (2D-Echo) and haemodynamics among 6-week survivors were also measured. Compared to placebo over the 7 weeks, both inhibitors decreased infarct collagen ($P<0.001$). Among the 6-week survivors, both inhibitors lowered infarct collagen ($P\leq0.001$) and increased the collagen type I/III ratio, but preload was lower, increase in diastolic volume and mass were less, and systolic function improved. Although the doses of captopril (but not enalapril) decreased afterload, inhibition of infarct collagen was less, infarct bulging and global LV dilatation were less and systolic function was better with captopril than enalapril (Figure 24). Apical aneurysm frequency at 6 weeks was similar ($P=0.9$) for enalapril (13/18) and controls (31/40)

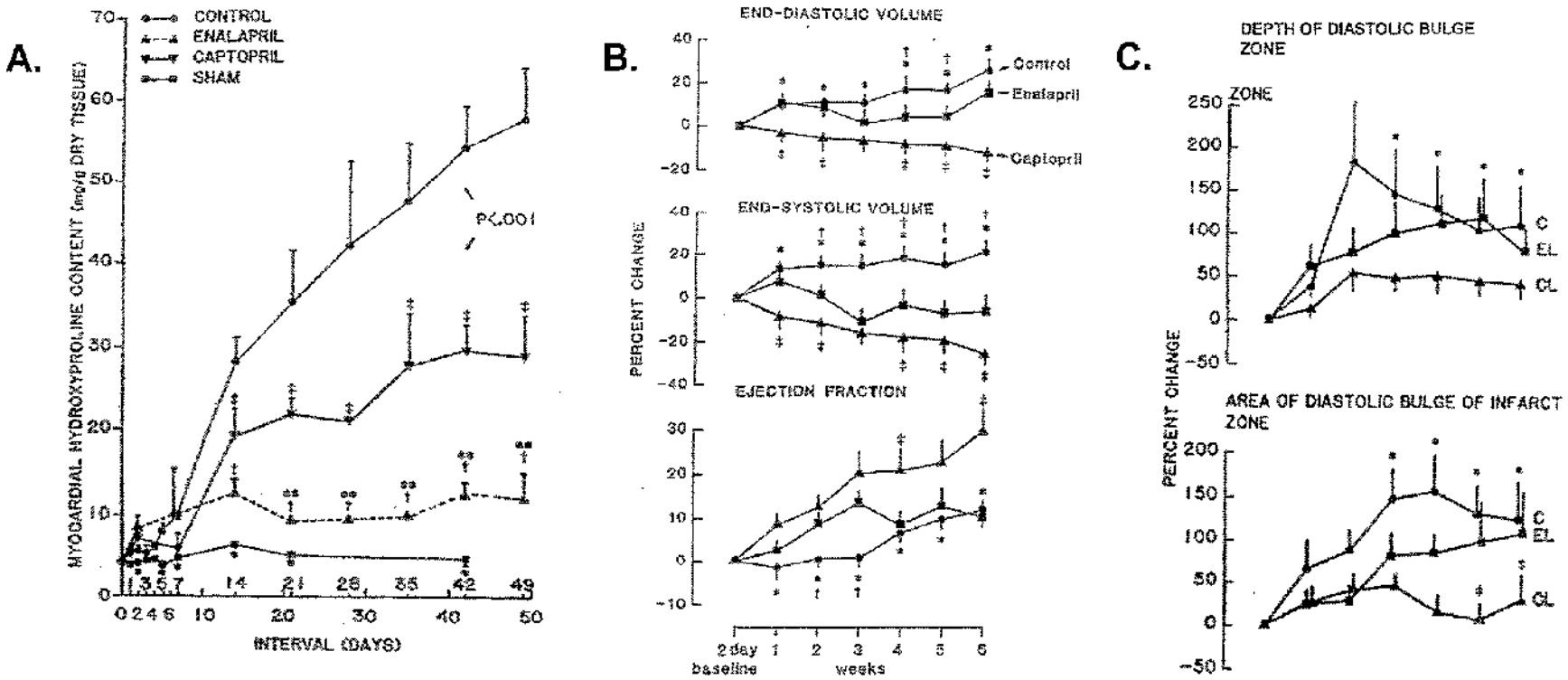

Figure 24. Effect of ACE-inhibition on infarct collagen and remodelling

A. Hydroxyproline content of the infarct center region during healing after MI. P≤0.05, *control versus sham, †controls versus enalapril, ‡ controls versus captopril, ** enalapril versus captopril groups. P<0.001 (arrows) , overall P value, control versus ACE-inhibitor groups at 6 weeks. Values as mean ± SEM.

B. Changes in left ventricular volumes and ejection fraction. *P≤0.05, control versus captopril; †P≤0.05, control versus enalapril; ‡P≤ 0.05, enalapril versus captopril at timed intervals.

C. Changes in diastolic bulging of the infarct zone. *P≤0.05, control (C) versus captopril (CL) at timed intervals; ‡P≤0.05, enalapril (EL) versus captopril at timed intervals.

From Jugdutt et al. (129: Appendix 32)

but less with captopril (6/23) than controls (χ^2 = 6.9, P=0.0002) and less with captopril than enalapril (χ^2 = 13.9, P=0.0002). In all 3 MI groups, deaths over the 7 weeks correlated with greater infarct size, LV volume and dysfunction, and lower infarct collagen.

The overall findings suggested that ACE-inhibition suppresses the temporal increase in infarct collagen and attenuates infarct expansion, thinning and bulging, LV enlargement and aneurysm formation during healing after MI.

Relevance: In light of the overwhelming evidence from clinical trials that ACE-inhibition decreases mortality in survivors after MI (134), one must conclude that the benefits outweighed potential disadvantages in the study patients.

However, the effects of ACE-inhibition on collagen in the infarct zone during healing of transmural MI observed in the last study (129), suggests the possibility that long-term inhibition of collagen deposition and hypertrophy may be excessive and allow more LV distension, dilatation and dysfunction. This may be especially true after large transmural MI. The findings in this study may explain the persistent LV dysfunction after early ACE-inhibition observed in rats (338). However, large transmural MI as found in rats could not be studied in the dog model for logistic reasons. Since the patient population with heart failure and marked cardiac enlargement has been increasing in the ACE inhibitor era, inhibition of collagen deposition may be an important factor to consider.

The dose of captopril and enalapril used in the canine model (126,127,129,131) deserves comment. As a general rule, doses of drugs used in animals should not be extrapolated to humans. The 50 mg BID dose of captopril in dogs weighing about 20 kilograms (126,129,131) translates to 5 mg/kg daily. This is higher, on a milligram per kilogram basis, than the final dose used in patients in the SAVE trial: escalation from 6.25 mg to 50 mg TID or 1.42 mg/kg for the 70 kg human (121). The 2.5 mg BID dose of enalapril used in the approximately 20 kg dogs (127,129) would translate to 0.25 mg/kg daily, which is similar to the final dose used in the SOLVD and CONSENSUS trials: escalation from 2.5 mg BID to 20 mg QD or 0.29 mg/kg for the 70 kg human (123,142, 143,145). A major focus of the study was on the tissue effect of ACE-inhibition on infarct collagen. A higher dose of captopril relative to that used in humans was chosen so as to offset a possible bias against enalapril. Furthermore, a non-hypotensive dose of enalapril was used for the same reason.

5.3. CLINICAL STUDIES: VALIDATION AND NATURAL HISTORY

5.3.1. Preliminary clinical research studies: Feasibility and validation

5.3.1.1. Phase 1: Reproducibility and angiographic correlation

Background: Although 2D-Echo was an attractive clinical tool for the non-invasive assessment of the effect of pharmacological interventions on adverse LV remodelling and dysfunction in repeated studies on the long-term, this was a novel application and there was a paucity of data on feasibility and reproducibilty. Publications on these applications of 2D-Echo were just beginning to appear (15-17,230,231,235-238,241,242).

Methods/Results: The first priority was to determine the inter-observer and intra-observer variability in quantifying wall motion abnormalities and global function in human MI by contouring endocardial outlines and marking asynergic boundaries. These errors were found to be minimal, between 5 and 10% depending on the level of training of the observers and whether or not hypokinesis was included or excluded. Asynergic areas at 48 hours in 89 patients post-MI correlated with peak serum CK levels ($r=0.88$, $P<0.001$), in agreement with a report from Visser et al. (231) and other publications from my laboratory (232: **Appendix 36**; 251-253).

Correlative studies of LV volumes by 2D-Echo and biplane LV angiography in 31 patients, using 4 models (Figure 25) and the modified Simpson's rule, were in agreement with observations of others (236). Results of correlative studies of LV asynergy on 2D-Echo and biplane LV angiography in 30 patients were in agreement with those reported by Kisslo et al. (16) and Gibson et al. (339) using smaller groups of patients. Early correlative studies between LV asynergy and LV ejection fraction calculations in patients with remote MI by LV angiography (biplane) and 2D-Echo were also done and published in several abstracts as well as papers (251-253). Inter-observer reproducibility of 2-Echo steered M-mode measurements in infarct patients, positioning the M-mode beam perpendicular to the region of interest, was reasonable (error < 5 %). Although 2D-Echo and LV biplane angiographic estimates of ejection fraction were very good ($r=0.91$ to 0.96, $P<0.001$), attempts at quantifying LV volumes using 2D-Echo in patients with MI uncovered the major problem of RSD in diastole and becoming more marked in systole (21: **Appendix 3**). It therefore became necessary to quantify RSD after MI (19: **Appendix 1**; 33: **Appendix 7**).

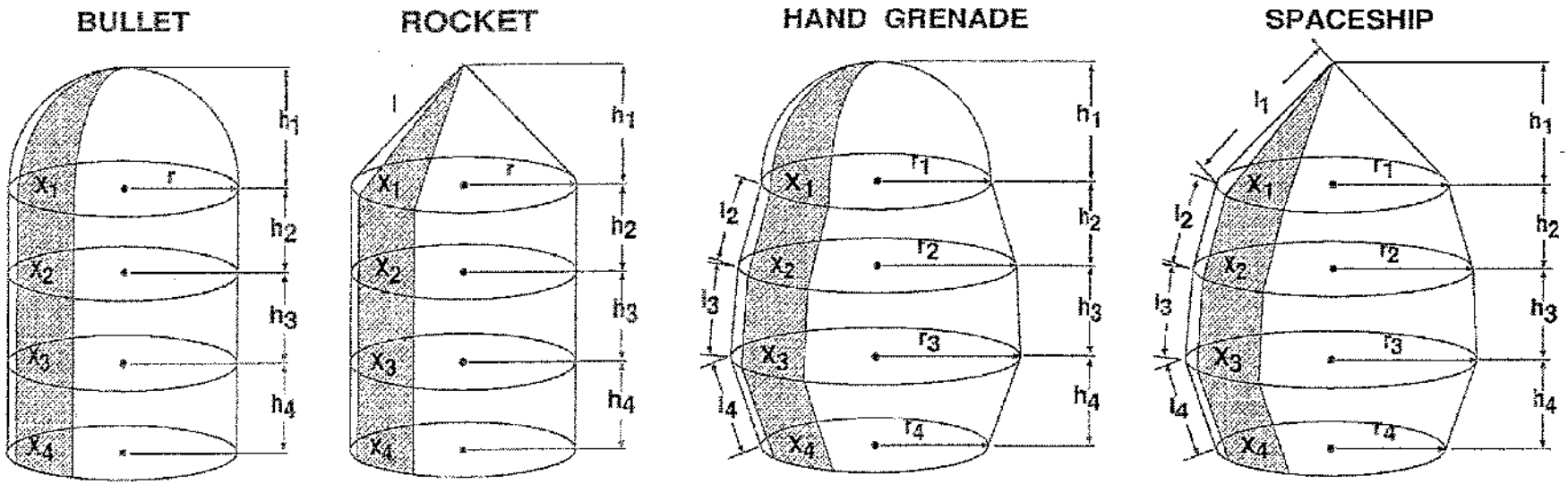

Figure 25. Schematic representations of four algorithms

These were used for LV volumes and endocardial surface areas after 3D-reconstruction of short-axis tomographic images on 2D-Echo. $x_1 \ldots x_4$ = circumferential extents of LV asynergy; $r_1 \ldots r_4$ = radii of short-axis contours; $h_1 \ldots h_4$ = vertical spacing of sections from long-axis lengths in apical-4-chamber and apical-2-chamber views; $l_1 \ldots l_4$ = oblique spacings from apical views. The 'hand grenade' most closely approximated volumes from gelatin casts of LV chambers in infarcted hearts of dogs.

(Jugdutt 274: Appendix 38)

Relevance: This essential first step confirmed published data from other laboratories and the reproducibility and limitations of 2D-Echo for the assessment of regional and global LV dysfunction and topography after MI in my laboratory.

5.3.1.2. Phase 2: Feasibility and detection of asynergy

Background: Although some publications had appeared (15-18,230) on the feasibility of assessing asynergy using quantitative 2D-Echo, and others were just appearing (231,235,236,241,242,339), it was necessary to establish my own expertise and database. The second priority was therefore to establish the feasibility of our systematic 2D-Echo imaging approach (Figure 5) in patients with ischaemic heart disease, including acute and remote MI and other diseases. This was done in the 3500 consecutive patients who were studied between 1980 and 1985 in my clinical adult 2D-Echo laboratory (book in preparation).

Methods/Results: Serial systematic tomographic images (in parasternal long-axis, apical 4-chamber and parasternal short-axis views at mitral, chordal and papillary muscle levels), which were adequate for detailed analysis of endocardial wall motion and visual assessment of systolic thickening, were obtained in 85% of the patients. Asynergy was subsequently defined as akinesis (no motion, no thickening) and/or dyskinesis (paradoxical motion and systolic thickening). Hypokinesis was not included on the basis of the findings in previous reports (62,233) and difficulty with accurate visual quantification of hypokinesis.

In a subsequent clinical research study (only abstracts presented), the predictive value of an early 2D-Echo in acute MI, performed at 2 days by the bedside, was evaluated in 40 consecutive patients with a first MI. On ECG, 31 patients had transmural or Q-wave MI and 9 had subendocardial or non-Q-wave MI. The ECG location was inferior in 16, anterior in 20, posterior in 2 and uncertain in 2. The conclusions of that study were as follows:

i) The early 2D-Echo detected LV asynergy, defined as akinesis and/or dyskinesis in all patients (100%).

ii) The location of LV asynergy on 2D-Echo agreed with the ECG location of acute MI in all patients.

iii) Anterior LV asynergy in 4 of 21 patients was associated with apical right ventricular asynergy, and posterior LV asynergy in 6 of 12 patients was associated with right ventricular free wall asynergy.

iv) The early 2D-Echo detected LV thrombus in 13 of 21 patients with anterior LV asynergy and 2 of 16 patients with posterior LV asynergy, suggesting that thrombi are more frequent with anterior infarcts.

v) An estimate of the extent of LV asynergy, by summation of abnormal segment lengths as percent circumference (range 5-50%) from all short–axis views, correlated with peak CK levels ($r=0.88$, $P<0.001$).

vi) The location and extent of asynergy on 2D-Echo predicted early complications and detected late complications: acute ventricular septal defect in 2 patients; papillary muscle dysfunction in 3 patients or rupture in 1 patient; infarct extension in 3 patients and infarct expansion in 8 patient.

Relevance: The overall findings indicated that serial 2D-Echo after MI was feasible, provided reproducible diagnostic data in the early stages of infarction, and could detect unsuspected RV dysfunction and complications after acute MI.

5.3.2. The natural history of LV asynergy after acute MI by 2D-Echo

Background: There was a paucity of data on the natural history of LV asynergy after MI using 2D-Echo.

Methods/Results: Clinical and 2D-Echo data were collected on 89 consecutive patients with a first acute anterior MI (only abstract presented). The 63 patients with adequate and quantitative initial 2D-Echo were entered in a longitudinal 1-year follow-up study. The echocardiograms were coded for double-blind, detailed analysis by two experienced observers (the author and a trained assistant).

On the basis of the extent of LV asynergy as percent of LV circumference on images at the papiliary muscle level, and serial data over the first 3 months, the patients with first anterior infarcts could be classified into 3 groups (Figure 26):

1. Patients with a small area of LV asynergy initially had very small or no detectable asynergy at 3 months. These patients had subendocardial non-Q-wave infarcts on ECG and were in Killip class I on admission. They were in New York Heart Association (NYHA) functional class I at 3 months. These patients showed no regional or global LV dilatation.

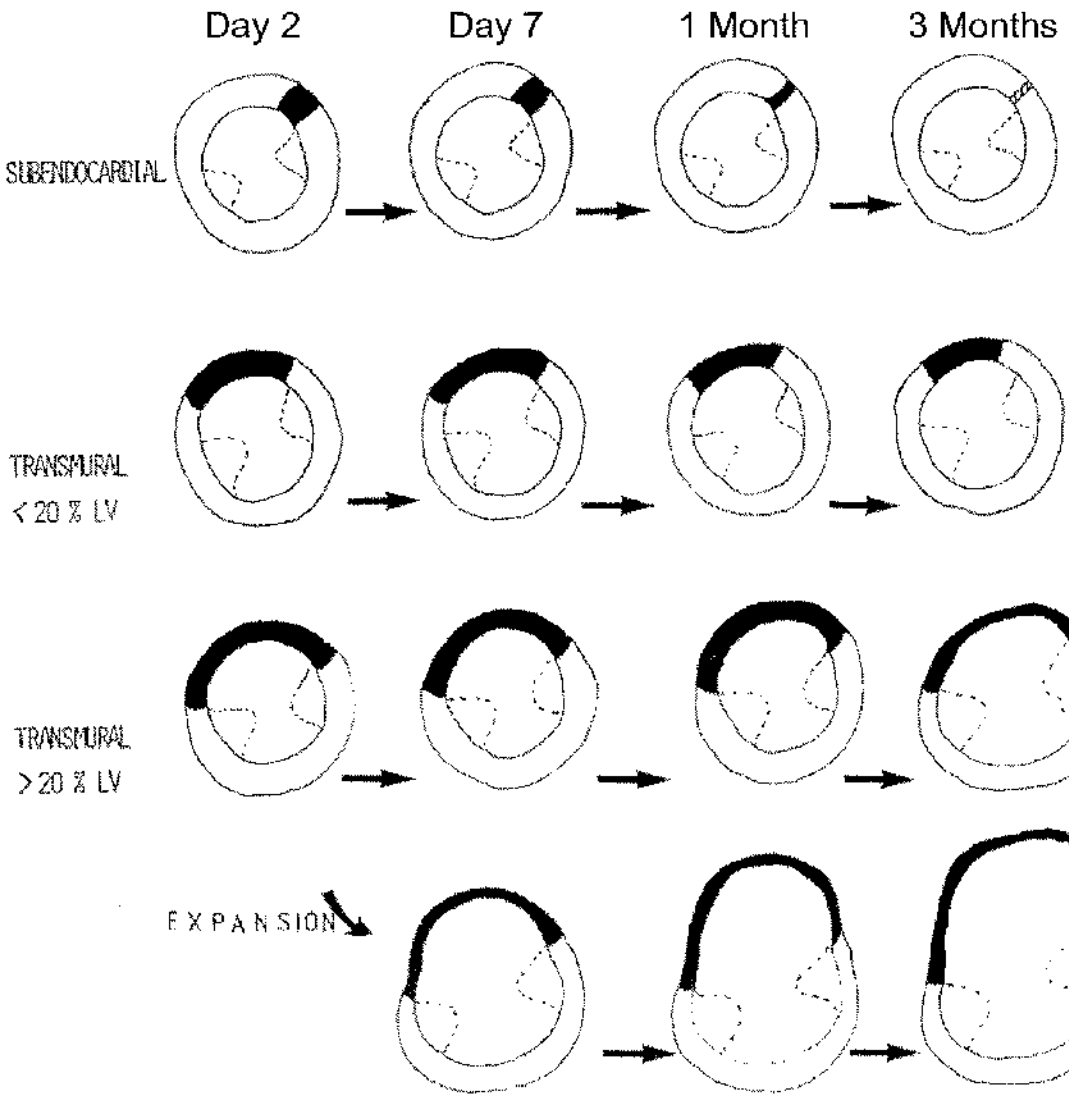

Figure 26. Natural history of LV geometry in survivors of a first anterior infarction over 3 months by 2D-Echo

Three main groups of patients after a first Q wave MI on the basis of asynergy on the baseline study on day 2. Average LV outlines at 4 time intervals over 3 months are shown. Dark segments = asynergic zone (akinesis + dyskinesis).

2. Patients with initial LV asynergic areas of 5-20% had persistent but slightly smaller areas of asynergy by 3 months, no significant change in LV cavity size or diastolic wall thinning. They had transmural or Q-wave infarcts on ECG and were in Killip class I to II on admission. At 3 months, they were in NYHA class I-II. These patients showed very mild RSD and progressive LV dilatation.

3. Patients with initial LV asynergic areas of 20-30% had persistent asynergy at 3 months but showed significant dilatation in LV cavity size and wall thinning in diastole with paradoxical motion in systole. An example of expansion with 18% LV circumferential asynergy at the papillary level on the baseline 2D-Echo is shown (Figure 27). A proportion of these patients, especially those with >30% LV asynergy, had developed infarct expansion between days 6 and 10. All had been in Killip class III-IV initially, with transmural, Q-wave infarcts on ECG. They were in NYHA class III at 3 months. These patients showed marked RSD and early aneurysm formation over the 3 months.

Relevance: The overall findings suggested that the extent of LV asynergy on an initial 2D-Echo in acute anterior MI can predict outcome at 3 months and 1 year. This study first unmasked the problem of RSD in quantifying total LV asynergy and volumes in patients with moderate to large MI.

5.3.3. Detailed analysis of 2D-Echo data and regional shape distortion (19: Appendix 1)

Background: Detailed analysis of 2D-Echo data was time consuming. However, the circumferential extent of LV asynergy in papillary and chordal short-axis sections and apical 4- and 2-chamber views could be quickly assessed at the bedside. Measurement of the extent of LV asynergy by manual contouring of these selected views could be made in 10 to 15 minutes.

Over the 1980's, my laboratory used: i) multiple to and fro video playbacks, ii) manual contouring of endocardial outlines and digitization using the HP digitizer, rather than the light pen system on the Varian system, iii) visual assessment of systolic thickening, as done by Gibson et al. (339), together with measurements of regional thicknesses on adequate images. It is important to

Patient A.G., age 58 years;1980

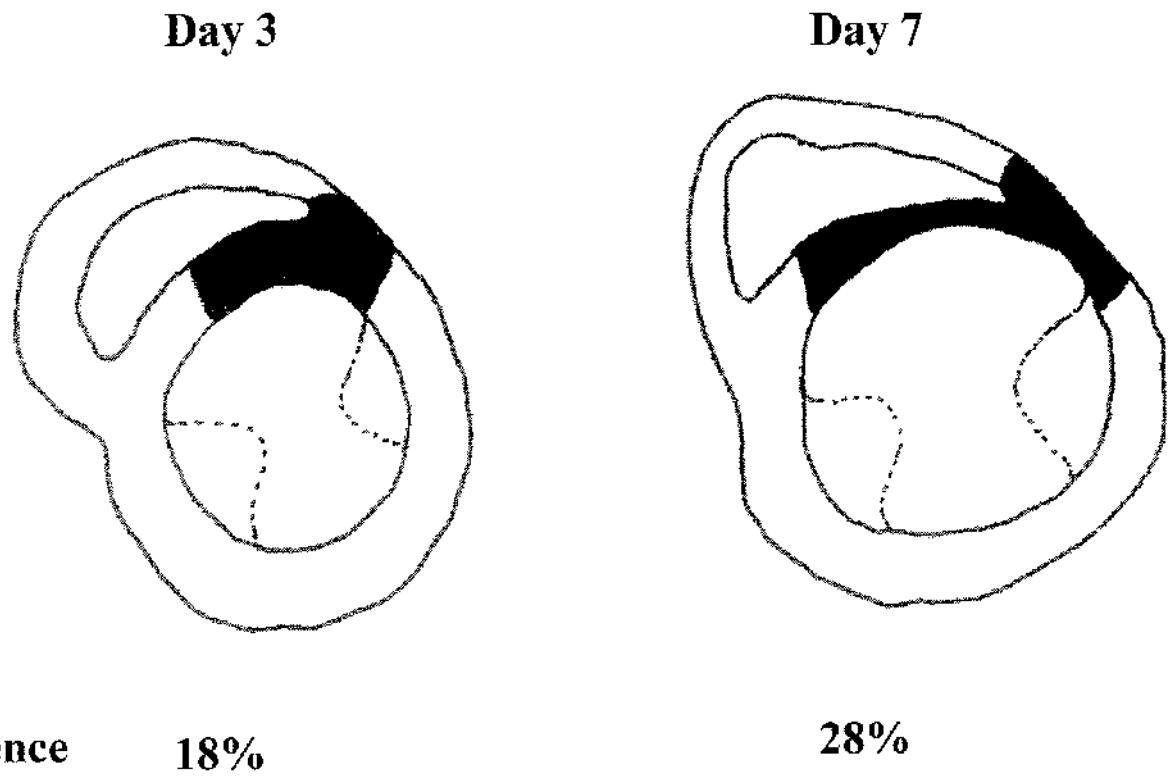

Figure 27. Acute infarct expansion after anteroseptal MI

Illustrative example from one patient showing computer-generated end-diastolic outlines of transverse sections at the short-axis papillary level on 2D-Echo. Dark segments = asynergic zone (akinesis + dyskinesis).

remember that in 1981, when this work began, commercial systems for analysis of 2D-Echo images were not available for off-line analysis of 2D-Echo images.

Methods/Results: As a first step towards more rapid analysis of 2D-Echo images, with the assistance of a computer assistant working in my laboratory and in consultation with the Information Systems, I explored the feasibility of acquiring digital images via the video recordings of the Varian system. I realized that a time-base corrector, a video-digitizer and software development were needed. These were implemented between 1984 and 1985. Digital images from selected patients were initially acquired via the digital RS-232 output port of the Varian system. Storage of a single frame on computer took 3 minutes (4800 BAUD), which was impractical from a therapeutic viewpoint although useful data could be obtained. Images were stored on floppy discs for additional processing on a larger computer (Computer Sciences). Subsequently, a Grinnel system with a frame-grabber was tested and found to be time consuming.

Manually contoured short-axis images were used for quantifying RSD (19; Figure 10) and wall thickness after MI (Figure 14). Transformation of 'manual contours' into the computer-generated graphical representation facilitated storage of large volumes of data on videotapes and rapid acquisition of meaningful data for comparison with subsequent studies.

The characterization of RSD on diastolic short-axis 2D-Echo images (19), using the traditional index ($P^2/4\pi A$), with perimeter (P) and area (A), as described by Holt and Marjoram (340), yielded similar values for distorted LV outlines from patients with MI and normal outlines from controls (1.042 versus 1.047, P=NS). In contrast, the 5 new indices of shape distortion, after the excision of the distorted segment (Figure 28), were markedly sensitive in detecting shape distortion of the asynergic regions in end-diastolic contours as well as greater distortion in end-systole (Table 8, Figure 28). The new indices include the peak (P_k) of the angular distribution and the first four moments (M_1, M_2, M_3 and M_4) of the distance distribution between the risk segment of LV asynergy and the computed ideal segment of a circle (19). These new RSD indices at end-diastole in infarct patients compared to normals were as follows: P_k, 6.0 versus 0.7 mm, P<0.001; M_1 (average), 3.8 versus 1.0 mm, P<0.001; M_2 (variance), 20.0 versus 0 mm^2, P<0.025; M_3 (skewness), -216.8 versus 0 mm^3, P<0.025; M_4 (kurtosis), 19576.0 versus 0 mm^4, P<0.05.

TABLE 8. Traditional and new primary shape distortion indices in systole and diastole in the infarct group*

Parameter	Diastole	Systole	P value
$P^2/4\pi A$	1.0402 ± 0.0266	1.0811 ± 0.0591	< 0.001
P_k (mm)	4.447 ± 4.300	9.0175 ± 6.580	< 0.001
M_1 (mm)	2.556 ± 2.438	5.597 ± 4.307	< 0.001
M_2 (mm^2)	4.1053 ± 7.6071	13.8832 ± 20.2275	< 0.001
M_3 (mm3)	-1.2304 ± 14.518	-23.787 ± 59.307	< 0.005
M_4 (mm^4)	129.550 ± 39.324	1050.200 ± 2851.000	< 0.025

Values as mean ± standard deviation.
* N = 58 sections

Relevance: Three points need emphasis:

First, in this method, RSD is measured directly and is applicable to MI at any location. The expansion index, which is based on the ratio of infarct to non-infarct segment lengths, gives very different (reciprocal) values for anterior and posterior MI. In addition, it depends on anatomic landmarks that may shift with expansion after infarction of antero-septal, infero-septal or postero-lateral regions.

Second, the distorted asynergic segment is replaced by a derived risk segment, which is a more accurate measure of the original segment of the LV wall that underwent infarction. The alternative approach of deriving the mass of the asynergic segment from its area required clear definition of both endocardial and epicardial borders. The epicardial border was less adequately visualized on 2D-Echo systems in the 1980's.

Third, in subsequent studies, the derived risk segment was used to compute LV asynergy, and the distorted native segment to quantify infarct expansion and RSD. Since the derivation of the new indices of RSD was time-consuming using the developed computer system, the depth and area of the RSD were used in later studies and found to be more practical.

A.

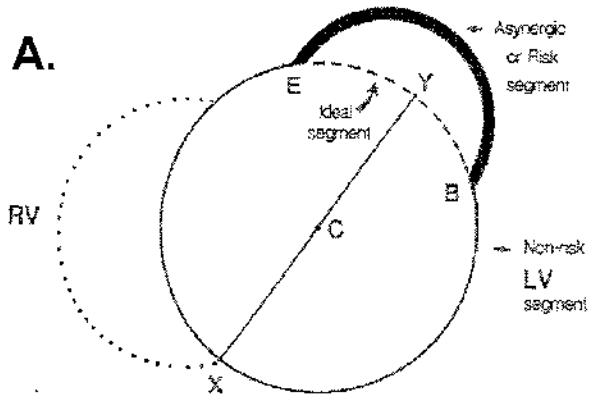

RV = right ventricle LV = left ventricle
X,Y = reference points C = center of ideal contour
B,E = beginning and end of asynergic segment

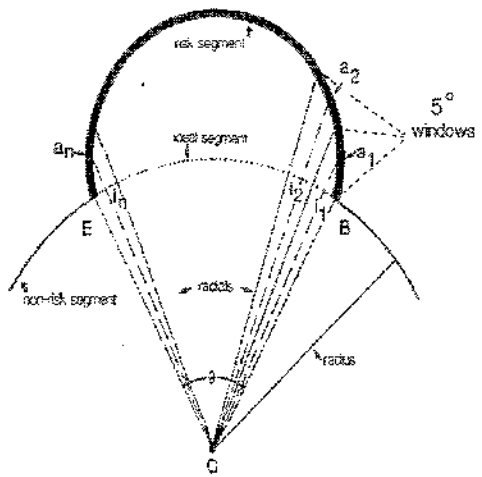

$a_1, i_1, \ldots, a_n, i_n$ = average radial distances, within 5° windows, between pairs of corresponding points at intersections of radials with risk and ideal segments, respectively

Figure 28.
Measurement of regional shape distortion after MI

A. Isolation and characterization of the distorted segment. The angular distribution is used to measure the peak distortion, P_k.

B. The traditional shape index ($P^2/4\pi A$) and the new indexes of regional shape distortion.
From Jugdutt et al. (19: Appendix 1)

B.

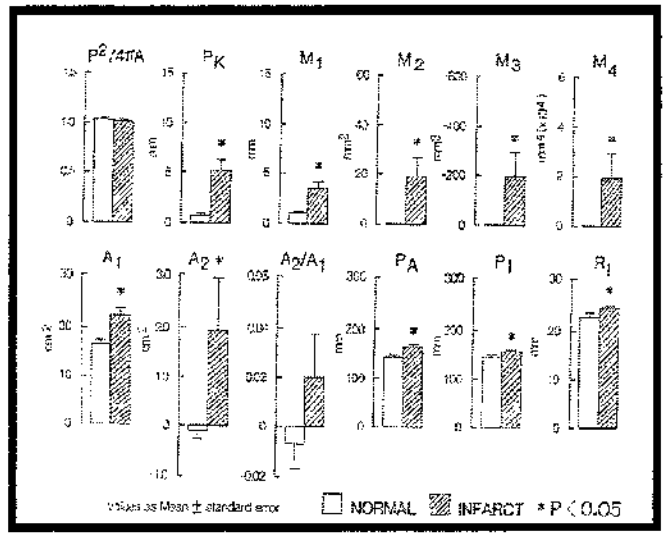

C. **TABLE 8. Traditional and new primary shape distortion indices in systole and diastole in the infarct group***

Parameter	Diastole	Systole	P value
$P^2/4\pi A$	1.0402 ± 0.0266	1.0811 ± 0.0591	< 0.001
P_k (mm)	4.447 ± 4.300	9.0175 ± 6.580	< 0.001
M_1 (mm)	2.555 ± 2.438	5.597 ± 4.307	< 0.001
M_2 (mm^2)	4.1953 ± 7.6871	13.8832 ± 20.2275	< 0.001
M_3 (mm3)	-1.2304 ± 14.518	-23.787 ± 59.307	< 0.005
M_4 (mm^4)	129.550 ± 39.324	1050.200 ± 2851.000	< 0.025

Values as mean ± standard deviation.
* N = 58 sections

5.3.4. Regional shape distortion as a predictor of adverse remodelling after MI (20: Appendix 2; 21: Appendix 3)

Background: Early detection of potential expanders (patients who develop clinically significant infarct expansion with acute regional LV dilatation and LV failure but no additional necrosis) after MI (18) is necessary in order to apply preventive therapy. Although stretching and thinning of the infarct segment had been used as measures of infarct expansion on 2D-Echo (18,31,32), direct measurement of RSD or dilatation of the infarct zone had only just been attempted in my laboratory (19,20). The hypothesis that the degree of RSD on an early 2D-Echo after acute MI may allow identification of patients prone to infarct expansion was therefore tested (21).

Methods/Results: To determine whether the degree of RSD or dilatation on early 2D-Echo after acute MI can identify potential expanders, serial clinical and 2D-Echo data were studied prospectively in 244 consecutive patients with a first Q-wave MI (Tables 9A, 9B). Initial (mean 2 days) and final (mean 10 days) echocardiograms were compared for regional LV asynergy (Figure 10), RSD (Figure 29) and conventional indices of expansion (Figure 11) measured on endocardial diastolic outlines of mid-LV short-axis sections.

Analysis of clinical and 2D-Echo data revealed 51 expanders and 193 non-expanders (Tables 9A, 9B, 10, 11). Expanders showed greater LV dysfunction and more in-hospital deaths (27% versus 8%, $P<0.001$) compared to non-expanders (Table 9B). Conventional indices of expansion showed more marked increase between initial and final 2D-Echo in expanders, but initial indices were not predictive. In contrast, the new RSD index P_k, a measure of outward bulge (Figure 29D), was markedly greater in expanders than non-expanders on both initial (16.5 versus 2.4 mm, $P<0.001$) and final echo (Table 11). Furthermore, expanders with $\geq$ 30% increase in P_k (to 21 mm) developed rupture of the ventricular septum (n=10) or free wall (n=2). Also, 50 of 51 expanders compared to 3 of 193 non-expanders had a $P_k \geq 10$ mm on the initial echo. A simpler index, the depth of RSD (r_d), provided similar discrimination as Pk (Table 12, Figure 30). The overall findings suggested that the degree of diastolic RSD on an early 2D-Echo after acute MI can identify potential expanders.

The relation between RSD and rupture of the ventricular septum was demonstrated in a parallel study (20: **Appendix 2**; Figure 31).

A, B. Regional diastolic shape distortion on 2D-Echo. Shortaxis images at low chordal level in end-diastole. Arrow = bulge in asynergic zones. A, anterior infarction; B, inferior infarction.

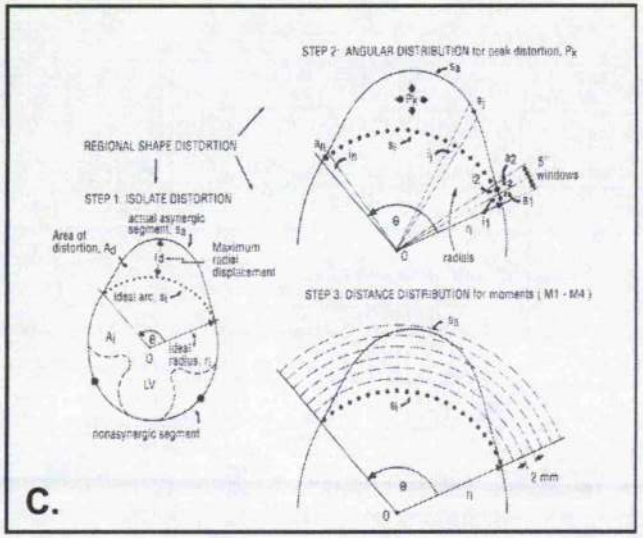

C. Methods of quantifying RSD. In step 1, actual distorted segment (s_a) is replaced by the ideal arc (s_i) so that the area of the bulge (Ad) and maximum radial displacement (rd) can be measured. In step 2, the bulge is characterized by the peak (P_k) of the angular distribution. In step 3, the bulge is characterized by the first 4 moments of the distance distribution. O = computed center of ideal circular contours: r_i = ideal radius.

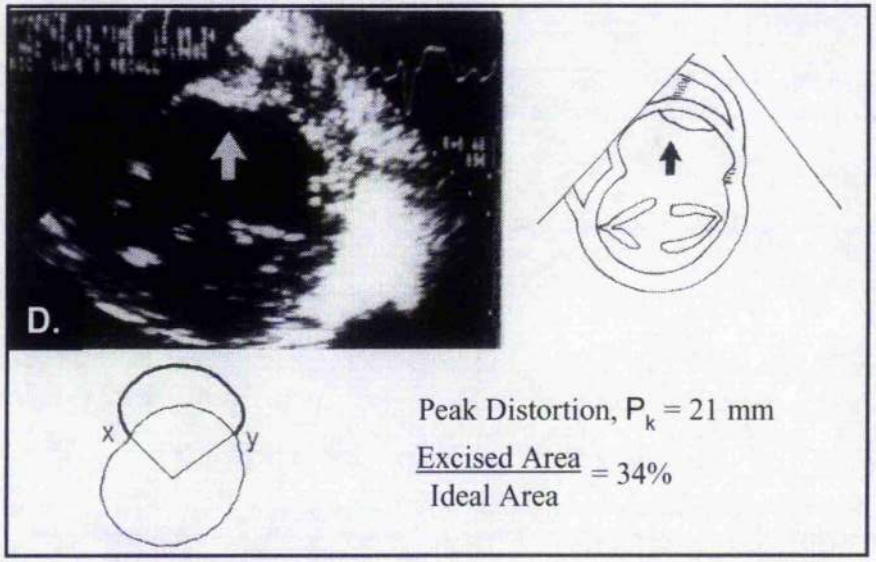

Figure 29. Regional shape distortion (RSD) and expanders

D. Anteroseptal RSD.
A, 2D-Echo image at chordal level woth diastolic bulge in asynergic zone.
B, Line drawing of image in A. Arrows = angulation caused by bulge.
C, Digitized contour with computer isolation of the distortion. D, Computed peak distortion and area of distortion normalized to the ideal area.
From Jugdutt (21: Appendix 3)

Table 9A. Initial patient data

Characteristic	Expanders (n=51)	Nonexpanders (n=193)	p Value
Age (yr)	60±12	57±14	NS
Sex (% male)	73%	78%	NS
Body surface area (m^2)	1.9±0.2	1.9±0.2	NS
History of hypertension (n)	13 (25%)	42 (22%)	NS
History of angina (n)	17 (33%)	69 (36%)	NS
Anterior MI (n)	31 (61%)	109 (56%)	NS
Heart rate (beats/min)	82±20	77±20	NS
Systolic BP (mmHg)	129±25	130±24	NS
Diastolic BP (mmHg)	83±17	85±15	NS
Mean BP (mmHg)	98±19	99±17	NS
RPP (mmHg × beats/min × 10^2)	8.0±2.2	7.8±2.6	NS
Killip class score	2.1±0.8	1.6±0.7	0.025
ΣST: anterior MI (mV)	11.4±7.0	8.1±5.0	0.005
ΣST: inferior MI (mV)	7.0±5.0	3.0±3.0	0.001
Peak CK level (IU/l)	2445±1574	1756±1412	0.01
CK infarct size (gEq)	72±60	43±30	0.005
Total asynergy (%)	29±7	20±9	0.001
Ejection fraction (%)	34±9	43±9	0.001

Abbreviations: BP=blood pressure; CK=creatine kinase; MI=myocardial infarction; ΣST=sum of ST-segment elevations; RPP=heart rate × mean blood pressure product.

Table 9B. Pertinent clinical findings and drugs during hospitalization

Parameter	Expanders (n=51)	Nonexpanders (n=193)	p Value
In-hospital deaths (n)	14 (27%)	15 (8%)	0.001
Maximum Killip score	3.3±0.8	2.2±0.9	0.001
Asynergy at 10 days (%)	25±8	18±9	0.001
Ejection fraction at 10 days (%)	42±10	47±8	0.005
Infarct extension (n)	9 (18%)	17 (9%)	NS
Cardiogenic shock (n)	10 (20%)	8 (4%)	0.001
Cardiac arrest (n)	7 (14%)	16 (8%)	NS
Free wall rupture (n)	2 (4%)	0	NS
Ventricular septal rupture (n)	10 (20%)	0	0.0005
Congestive failure (n)	37 (73%)	70 (36%)	0.0005
Pericarditis (n)	24 (47%)	20 (10%)	0.0005
Drugs			
Indomethacin (n)	19 (37%)	27 (14%)	0.0005
Ibuprofen (n)	9 (18%)	22 (11%)	NS
Prednisone (n)	0	3 (2%)	NS
Nitroglycerin, oral/paste (n)	40 (78%)	164 (85%)	NS
Captopril (n)	5 (10%)	0	0.0005
Beta-blocker (n)	20 (39%)	65 (34%)	NS
Calcium-blocker (n)	9 (18%)	31 (16%)	NS
Diuretic (n)	39 (76%)	95 (49%)	0.001
Inotrope (n)	30 (59%)	65 (34%)	0.005
Antiarrhythmic (n)	38 (75%)	125 (65%)	NS
Anticoagulant (n)	49 (96%)	161 (83%)	0.05
Antiplatelet drug (n)	8 (16%)	28 (15%)	NS

From Jugdutt (21: Appendix 3)

TABLE 10. Changes in topographic and functional parameters

	Expanders (n=51)		Nonexpanders (n=193)	
	Initial	Final	Initial	Final
ASL (cm)				
Anterior MI	10.4±3.0[a]	16.0±4.0[b]	9.9±1.7[a]	10.5±2.1
Inferior MI	6.7±0.9[a]	9.8±3.0[b]	6.9±1.2[a]	7.8±1.6
NASL (cm)				
Anterior MI	7.0±1.3[a]	7.9±1.1	6.8±1.2	6.9±1.3
Inferior MI	9.6±1.8[a]	10.7±2.0	9.6±1.5	9.8±1.7
Expansion index				
Anterior MI	1.50±0.36[a]	2.28±0.43[b]	1.48±0.30	1.52±0.30
Inferior MI	0.70±0.11[a]	1.01±0.46[b]	0.73±0.12[a]	0.81±0.17
Thinning ratio				
Anterior MI	0.76±0.15[a]	0.51±0.15[b]	0.76±0.19[a]	0.68±0.21
Inferior MI	0.74±0.11[a]	0.46±0.14[b]	0.74±0.14[a]	0.63±0.17
All	0.75±0.14[a]	0.49±0.14[b]	0.75±0.17[a]	0.66±0.19
$LVID_D$ (mm)				
Anterior	55±5[a,b]	58±7[b]	50±6[a]	52±5
Inferior	53±7[a,b]	58±9[b]	50±6[a]	54±8
All	54±6[a,b]	58±8[b]	50±6[a]	53±9
LVEDV (cm^3)				
Anterior	126±40[a]	165±61[b]	127±38[a]	138±38
Inferior	117±44[a]	168±78[b]	120±36[a]	131±36
All	122±41[a]	166±67[b]	124±37[a]	135±37
LV asynergy (%)				
Anterior MI	29±8[a,b]	24±9[b]	20±9[a]	18±9
Inferior MI	29±7[a,b]	25±6[b]	21±9[a]	19±8
All	29±7[a,b]	25±8[b]	20±9[a]	18±9
LVEF (%)				
Anterior MI	33±10[a,b]	41±12[b]	42±8[a]	47±8
Inferior MI	36±7[a,b]	45±6	43±10[a]	47±8
All	34±9[a,b]	42±10[b]	43±9[a]	47±8

[a]$p \leq 0.05$, significance of difference comparing date at 2 and 10 days within groups (ANOVA).
[b]$p \leq 0.05$, significance of difference comparing expander with nonexpander groups at corresponding times.
Abbreviations: ASL = infarct-containing segment length; NASL = non-infarct-containing segment length; LV = left ventricular; LVEF = left ventricular ejection fraction; $LVID_D$ = left ventricular internal diastolic dimension; LVEDV = left ventricular end-diastolic volume.

TABLE 11. Indices of global and regional diastolic shape distortion

Parameter	Timing	Expanders (n=51)	Nonexpanders (n=193)	p Value
Traditional global shape index				
$P^2/4\ \pi A$	a	1.06±0.08	1.03±0.03	0.025
	b	1.06±0.09	1.03±0.03	0.025
Regional shape distortion indices				
Peak distortion, P_k (mm)	a	16.5±6.1[a]	2.4±2.6[a]	0.001
	b	5.7±6.1	3.4±4.9	0.001
M_1, Average (mm)	a	10.8±10.6[a]	1.6±1.6[a]	0.005
	b	4.8±5.6	2.3±4.4	0.005
M_2, Variance (mm^2)	a	50.7±111[a]	1.9±3.9[a]	0.025
	b	19.9±57	3.7±9.2	0.05
M_3, Skewness (mm^3)	a	−21.2±78.8	−1.1±4.7	NS
	b	−65.3±421.6	−11.0±114.4	NS
M_4, Kurtosis (mm^4)	a	2531±8795	35±122	0.05
	b	1047±3443	260±2165	NS
Normalized distortion, P_k/r_i	a	0.71±0.34[a]	0.09±0.10[a]	0.001
	b	0.21±0.24	0.13±0.18	0.05
Ideal area, A_i (cm^2)	a	21.4±7.0[a]	22.2±7.8	NS
	b	24.8±12.6	22.6±7.7	NS
Area of distortion, A_d (cm^2)	a	5.2±2.6[a]	0.9±1.2[a]	0.001
	b	2.3±2.8	1.2±1.7	0.01
Area ratio, A_d/A_i	a	0.28±0.16[a]	0.05±0.13	0.001
	b	0.10±0.12	0.06±0.14	0.05
Actual asynergic segment, s_a (cm)	a	5.6±2.6	4.4±2.0	0.005
	b	5.6±2.7	4.5±4.6	NS
Depth of distortion, r_d (mm)	a	16.6±7.3[a]	2.3±2.8[a]	0.001
	b	5.8±5.7	3.1±4.4	0.005

[a]$p < 0.05$, significance of difference between initial (a) and final (b) echocardiograms.

From Jugdutt (21: Appendix 3)

TABLE 12. Ranking of echocardiographic parameters by ability to distinguish expanders from non-expanders using multivariate analysis of variance

	F value
Overall discrimination	
F ratio	$F_{0.05}$ (20,223) = 56.81
Critical F ratio	$F_{0.05}$ (20,200) = 1.62
Univariate discrimination	
Peak distortion, P_k	603.14[a]
Normalized distortion, P_k/r_j	485.20[a]
Depth of distortion, r_d	483.34[a]
Area of distortion, A_d	315.44[a]
M_1, Average	120.95[a]
Area ratio, A_d/A_j	110.94[a]
Infarct-containing segment length	59.77[a]
Total LV asynergy	48.77[a]
M_2, Variance	38.87[a]
Global LV ejection fraction	36.16[a]
Global shape index, $P^2/4\pi A$	25.71[a]
M_4, Kurtosis	15.71[a]
M_3, Skewness	12.88[a]
Actual asynergic segment, s_a	12.45[a]
Perimeter, P	10.06[a]
Long-axis height, h	1.66
Ideal asynergic segment, s_i	0.55
Expansion index	0.31
LV end-diastolic volume	0.18
Thinning ratio	0.04
Critical F ratio	$F_{0.05}$ (1,200) = 3.89

[a]Strongest discriminators; level of F test set at 95% confidence limits ($p < 0.05$).

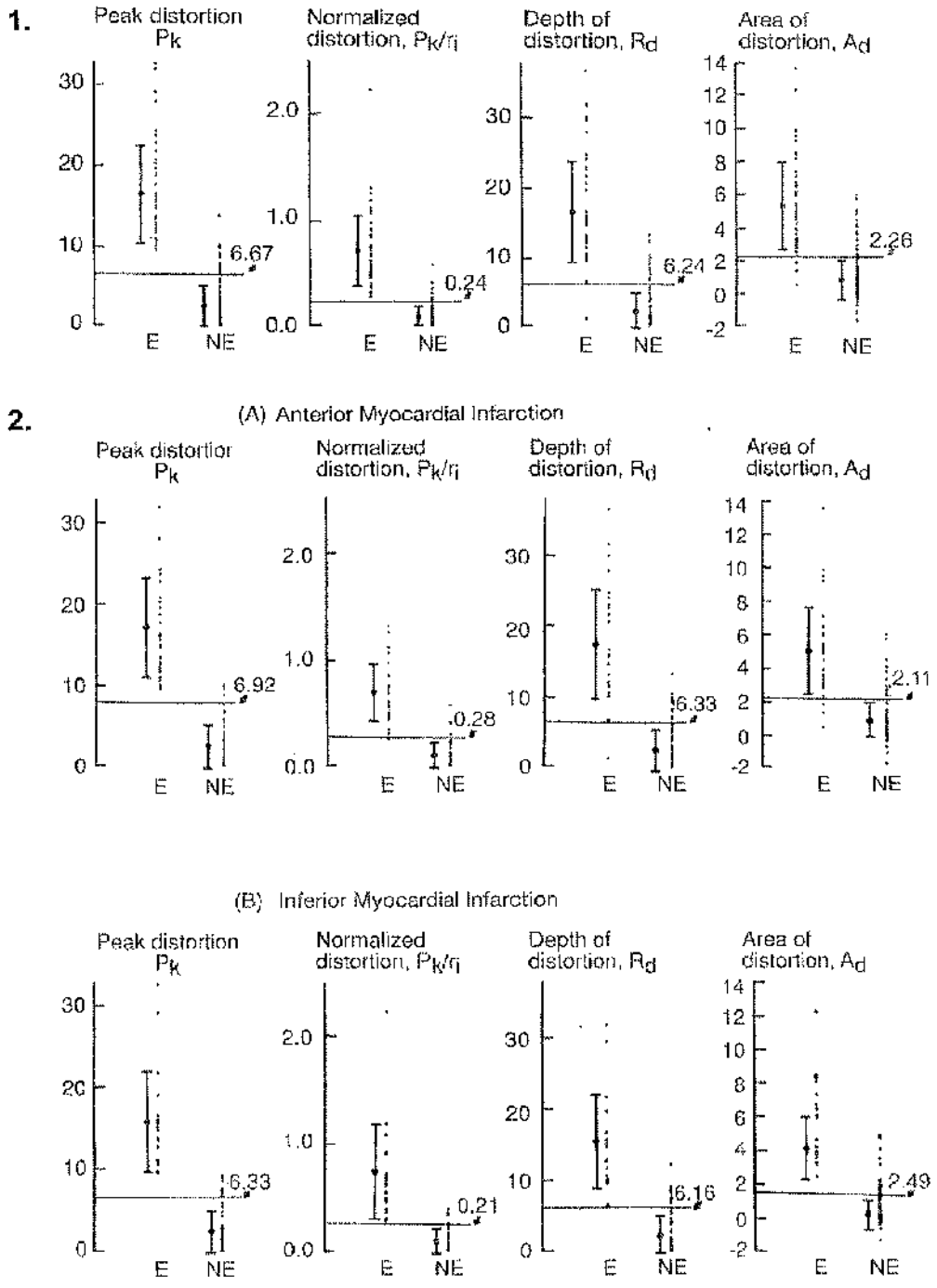

Figure 30. Discriminators of expanders and non-expanders by the degree of RSD

1. Four highest ranking discriminators of expanders (E) and non-expanders (NE).
2. Discriminators of expanders (E) and non-expanders (NE) in anterior and inferior MI subgroups. Dotted lines and arrow indicate cutoff values. P_k and R_d in mm, A_d in cm^2.

Jugdutt (21: Appendix 3)

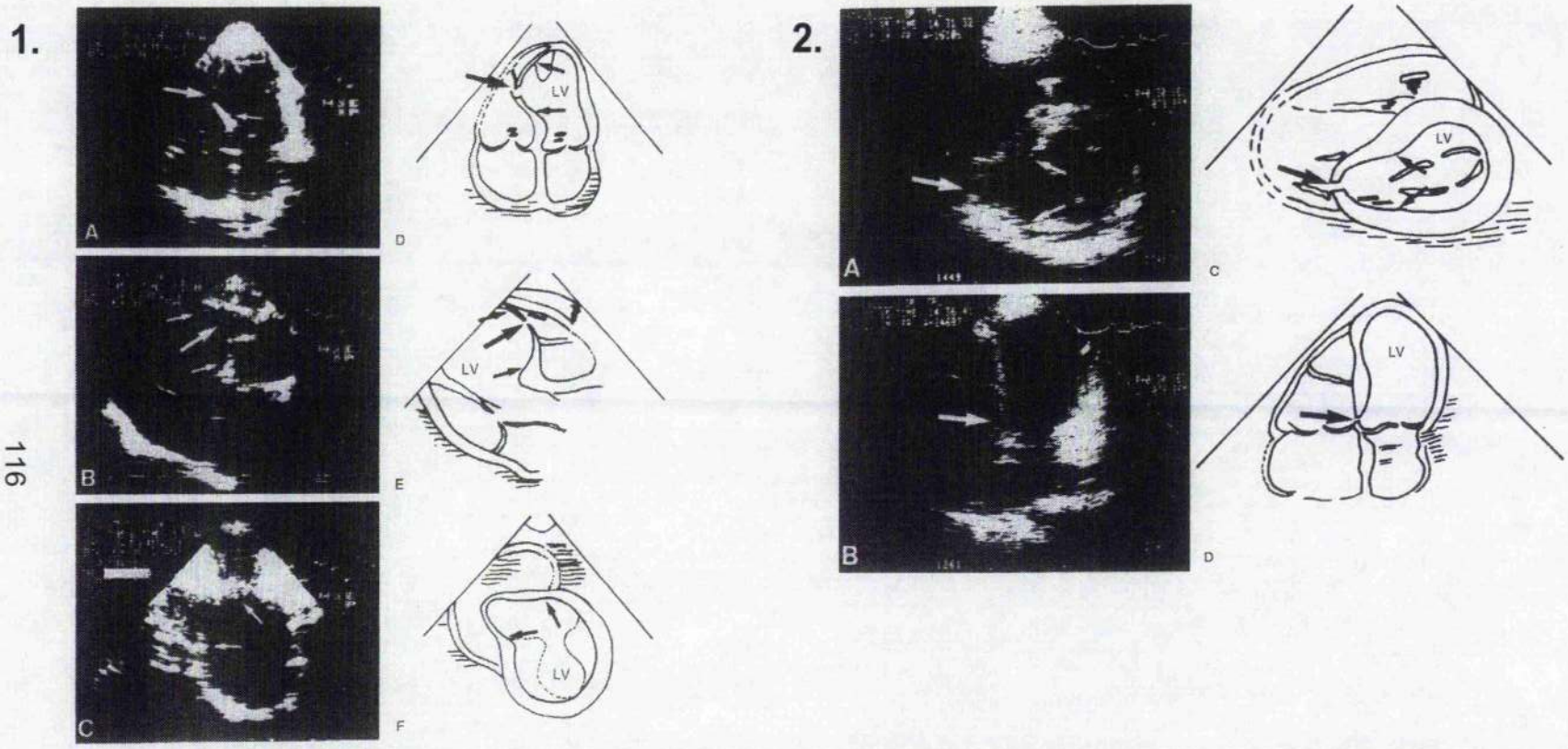

Figure 31. Regional shape distortion (RSD) and rupture of the ventricular septum

Panel 1. Acute ventricular septal rupture associated with marked anterior infarct expansion and RSD in a patient with anterior infarction. 2D-Echo images are shown on the left and corresponding diagrams on the right. A, D: apical 4-chamber view; B,E: parasternal long-axis view; C, F: parasternal short-axis at the papillary muscle level. Large arrow indicates site of septal rupture; small arrows indicate RSD and septal angulation.

Panel 2. Marked posterior infarct expansion and RSD associated with ventricular septal rupture in a patient with inferior myocardial infarction. 2D-Echo images are shown on the left and corresponding diagrams on the right. A, C: short-axis view at the mitral valve level; B, D: apical 4-chamber view. Large arrow indicates site of septal rupture; small arrows indicate RSD.

From Jugduttet al. (20: Appendix 2)

Relevance: Three points need emphasis:

First, the early detection of RSD might permit rational therapy for limiting adverse LV remodelling after MI and the objective assessment of the effects of therapy during healing after MI.

Second, a practical estimate of early RSD or diastolic bulging using the depth of distortion, r_d, might be useful in clinical studies to assess the efficacy of interventions.

Third, it may be possible to stratify patients on the basis of their topographic status after MI using RSD on 2D-Echo, in addition to their clinical and haemodynamic profiles.

5.3.5. The effect of a cardiac rehabilitation programme on 2D-Echo LV asynergy and RSD (34: Appendix 8)

Background: Enthusiasm about cardiac rehabilitation early after MI coincided with the introduction of various exercise programs in many clinics. However, the effects on LV remodelling, infarct topography and RSD in high-risk patients with anterior Q-wave MI undergoing exercise training had not been determined.

Methods/Results: A prospective pilot study was undertaken to determine the effect of a cardiac rehabilitation programme on LV asynergy by 2D-Echo in 20 patients surviving acute MI (10 subendocardial, 10 transmural). Resting 2D-Echo and exercise testing were done before and at the end of the program (6 weeks and 3 months). The rehabilitation programme, was conducted under the supervision of the director of the cardiac rehabilitation and exercise laboratory. The programme consisted of a 10-minute voluntary exercise at home (jogging) and participation in a group (volleyball once a week). At the beginning of the program, LV asynergy ranged between 5-15% in the subendocardial group versus 16-30% in the transmural group. After 3 months, 16 patients had improved exercise tolerance: 10 patients with subendocardial MI and 6 patients with transmural MI had initial LV asynergy between 16 and 24%. However, 4 patients with initial LV asynergy between 25 and 30% were in NYHA class II on medications (digoxin and diuretic) showed evidence of regional LV dilatation (Figure 32). The findings suggested that 2D-Echo might be useful in the selection and follow-up of patients on the post-infarction rehabilitation program.

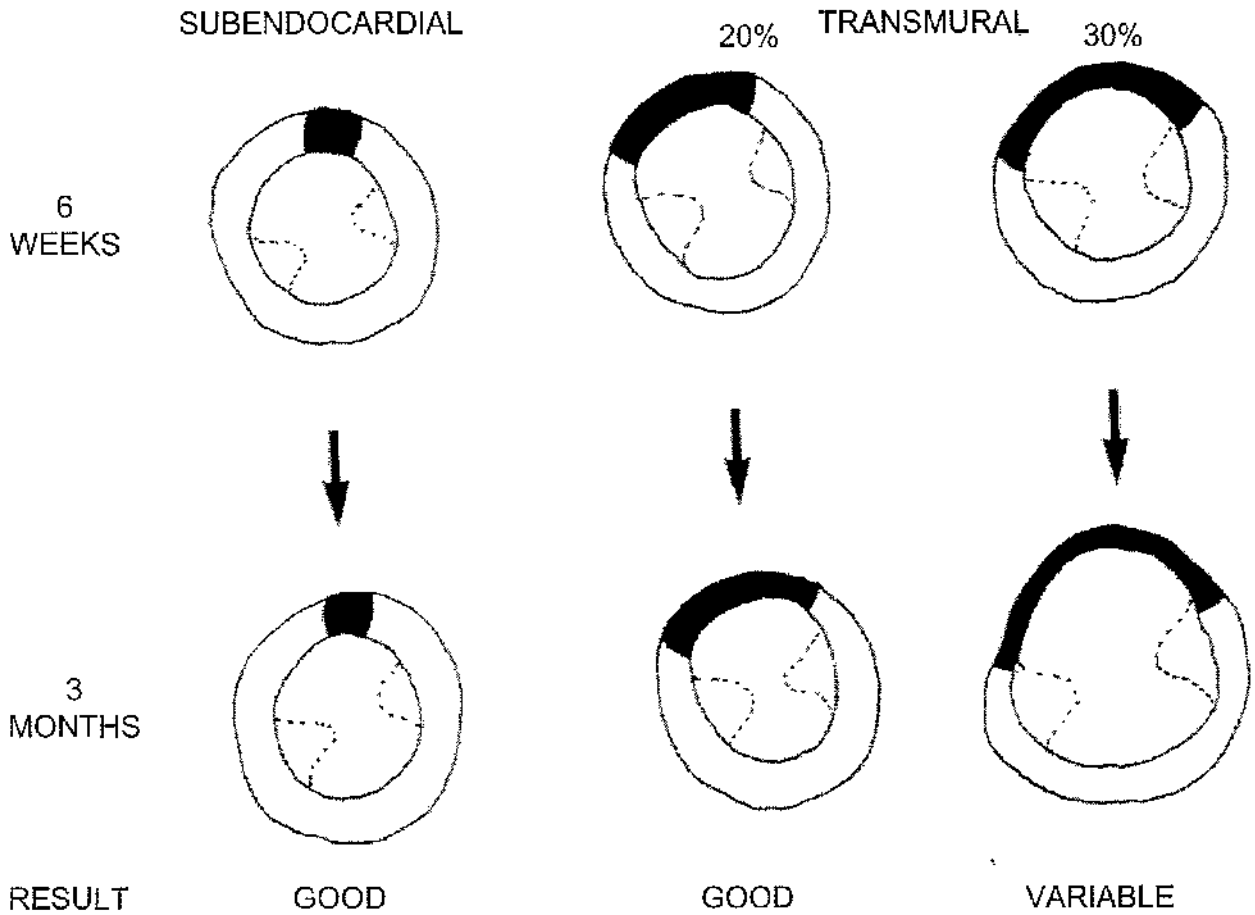

Figure 32. Pilot study. Evidence of topographic deterioration with exercise during a low exercise cardiac rehabilitation program

Note LV dilatation and increase in patients with 30% asynergy.

A subsequent prospective study was therefore undertaken to determine whether the extent of LV dysfunction and degree of RSD might predict outcome in survivors of moderate anterior Q-wave MI who underwent exercise training 15 weeks after MI (34). Left ventricular function and RSD were measured by 2D-Echo before and after 12 weeks of the low level exercise programme in 13 patients with MI (begun 15 weeks post MI) and 12 weeks apart in 24 matched MI patients without training (controls). The exercised MI patients were stratified on the basis of the response to exercise. Compared to baseline, the NYHA functional class score at the end of exercise training increased from 2.25 to 2.67 ($P<0.005$) in 6 patients (group 2) but did not change in 7 (group 1). Further discrimination of groups 1 and 2 was provided by an initial asynergy (akinesis or dyskinesis, or both) < 18% or ≥ 18%. Compared to group 1, group 2 had greater initial asynergy (32 versus 6%, $P<0.001$), expansion index (asynergic/normal endocardial segment length: 1.8 versus 1.6, $P<0.025$), and peak RSD index (12.2 versus 1.0 mm, $P<0.005$) but lower LV ejection fraction (43 versus 59%, $P<0.05$) and thinning ratio (asynergic/normal wall thickness: 0.61 versus 0.74, $P<0.05$).

These variables did not change with training in group 1. However, in group 2, training caused significant increase in asynergy (from 32 to 40%, $P<0.05$), expansion index (from 1.8 to 2.0, $P<0.01$) and peak RSD (from 12.2 to 20.9 mm, $P<0.05$) associated with a decrease in thinning ratio (from 0.61 to 0.51, $P<0.001$) and ejection fraction (from 43 to 30%, $P<0.005$). Initial values for these variables were similar for corresponding control groups but did not change over the 12 weeks. Thus, patients with ≥ 18% LV asynergy on the initial 2D-Echo showed more RSD, expansion and thinning before exercise training and developed further functional and topographic deterioration with training.

Relevance: These studies suggest that survivors of MI may be stratified before starting exercise programs on the basis of LV asynergy and RSD on a screening 2D-Echo. Patients with Q-wave MI, LV asynergy greater than 18% and significant RSD might be at risk of topographic deterioration during exercise training.

In a large study in the reperfusion era, Giannuzzi et al reported that exercise training, initiated 4-8 weeks after anterior Q-wave MI and continued for 6 months, did not appear to cause further LV dilatation or dysfunction (341). In contrast, a study in rats showed that endurance training after large MI results in

more adverse remodelling with severe global LV dilatation, LV shape distortion, and scar thinning, and decreased survival (342). The reasons for the disparate findings are not clear. It is possible that reperfusion played a role in Giannuzzi's study (341). Moreover, none of those studies evaluated infarct expansion or RSD.

5.3.6. Importance of early regional shape distortion in progressive LV dilatation after MI

5.3.6.1. Progressive changes in regional and global LV dilatation during remodelling after MI

Background: There was a paucity of data on the relation between early RSD and late global LV dilatation after MI.

Methods/Results: To determine the relation between early bulging of the asynergic zone and late global LV dilatation after MI, serial 2D-Echo studies from 800 patients with a first Q-wave MI, between 1980 and 1988, were analyzed (274). Four shape algorithms (rocket, bullet, grenade, spaceship) were systematically applied for calculating LV endocardial surface area, area of LV asynergy (akinesis + dyskinesis) and volumes from 4 short-axis and one base to apex image (Figure 25), with special attention being given to regional diastolic bulging (274: **Appendix 38**; only abstract presented; book chapter in preparation).

Analyses were done by 2 observers who were blinded to patient data. Areas and volumes computed using the 4 algorithms differed by < 6% and 11%, respectively. Results from the first 2D-Echo in 43 patients (28 anterior, 15 inferior) with CK infarct size data and 11 normal controls showed no difference in CK infarct size (45 versus 44 g-Eq) and mean LV asynergy 31% versus 37% surface area) for anterior and inferior MI. In contrast, mean LV surface area (133 versus 94 cm^2, P<0.001) and mean LV volume (155 versus 92 mL, P<0.001) were greater for anterior than inferior MI. The controls had no LV asynergy and normal mean LV volumes (111 mL) and surface area (124 cm^2).

Despite similar infarct size and asynergy on the initial 2D-Echo post-MI, the surface areas and volumes were greater in anterior than inferior groups indicating marked remodelling in the anterior but not the inferior group. Importantly, serial 2D-Echo revealed a progressive decrease in the bulge as global LV dilatation developed over 6 weeks and I year. The smoother LV outline of the dilated

ventricles after anterior MI was associated with increased sphericity, remodelling of apical shape from a gothic to a roman arch, and global thinning.

Relevance: This study underscores the important role of early RSD in subsequent global LV dilatation in survivors of moderately sized MI and more severe remodelling after anterior MI. Since estimates of infarct size from LV dysfunction by 2D-Echo tend to summate circumferential extents on diastolic short-axis images without attention to regional bulging, this important aspect of the pathophysiology of LV remodelling post-MI may be overlooked. Improved 2D-Echo systems with harmonic imaging allow changes in regional and global dilatation as well as dysfunction to be more easily appreciated and quantified. In addition, LV opacification with injection of Echo-contrast material may be used to enhance endocardial deformation at the LV apex in difficult cases.

5.3.6.2. Overestimation of infarct size on 2D-Echo due to RSD of the asynergic zone (36: Appendix 10)

Background: On 2D-Echo imaging, the infarcted area is detected by the extent of regional LV asynergy, and infarct expansion results in an increase ('expansion') of the asynergic area and dilatation. Since estimation of infarct size is based on the circumferential extent or surface area of LV asynergy, outward bulging of the infarct zone might be expected to result in overestimation of infarct size by 2D-Echo.

The effect of early RSD or bulging of infarct zones due to infarct expansion on estimates of regional LV dysfunction and infarct size by 2D-Echo imaging was therefore studied (36).

Methods/Results: Quantitative 2D-Echo's from patients with a first Q-wave MI and CK infarct size data, and normal subjects, were subjected to detailed analysis of regional LV dysfunction and RSD in short-axis images. Regional LV asynergy (akinesis and dyskinesis) and RSD indices [e.g. peak (P_k)/radius (r_i)] were measured on endocardial diastolic outlines of short-axis images in 43 post-MI patients (28 anterior and 15 inferior, 5.9 hours after onset of symptoms) and 11 normal subjects (controls). In the infarction group, the endocardial surface area of asynergy was calculated by 3D-reconstruction of the images and infarct size from serial CK blood levels.

Diastolic bulging of asynergic zones was found in all infarction patients. The RSD indices characterizing the area between the 'actual' bulging asynergic segment and the derived 'ideal' circular segment (excluding the bulge) on indexed sections were greater in infarct than control groups (P_k/r_i 0.31 ± 0.23 versus 0.03 ± 0.02, P<0.001) and greater in anterior than inferior infarction sub-groups (P_k/r_1 0.39 versus 0.16, P<0.001). Importantly, the degree of RSD correlated with overestimation of asynergy (r=0.89, P<0.001) (Figure 33), and the relation between infarct size and total 'ideal' asynergy showed a leftward shift from that with 'actual' asynergy.

Relevance: Early regional diastolic bulging of the infarct zone results in overestimation of regional ventricular dysfunction, especially when assessing effects of therapy on infarct size, remodelling and dysfunction using tomographic imaging.

5.3.6.3. Volume of RSD by 3D reconstruction of 2D-Echo images (33: Appendix 7)

Background: Several laboratories, including mine, were interested in 3D-reconstruction of 2D-Echo images. These algorithms were tested for volumes and the surface area of LV asynergy in my laboratory (Figure 25). The volume of LV global RSD may be estimated using 3D-reconstruction.

Methods/Results: The hypothesis that 3D reconstruction of 2D-Echo images can be used to estimate the volume of RSD was therefore tested (33). Accepted models of LV geometry that assume circular endocardial outlines in the short-axis and elliptical outlines in the long-axis give erroneous estimates of regional and global LV asynergy and LV volume in the presence of RSD after acute MI.

However, LV models reconstructed on computer from digitized 2D-Echo images in which the distorted segments have been excised and replaced with ideal circular (or elliptical) segments give improved correlation between total LV asynergy and CK infarct size (Figure 34). The distortion can be quantified and normalized to allow comparisons among treatment populations. RSD indices [area of distortion (A_d), peak distortion (P_k), depth (r_d)] measured on 2D-Echo images, and global RSD parameters (volume of distortion) measured on 3D reconstructions allow correction of infarct size estimates based on the endocardial

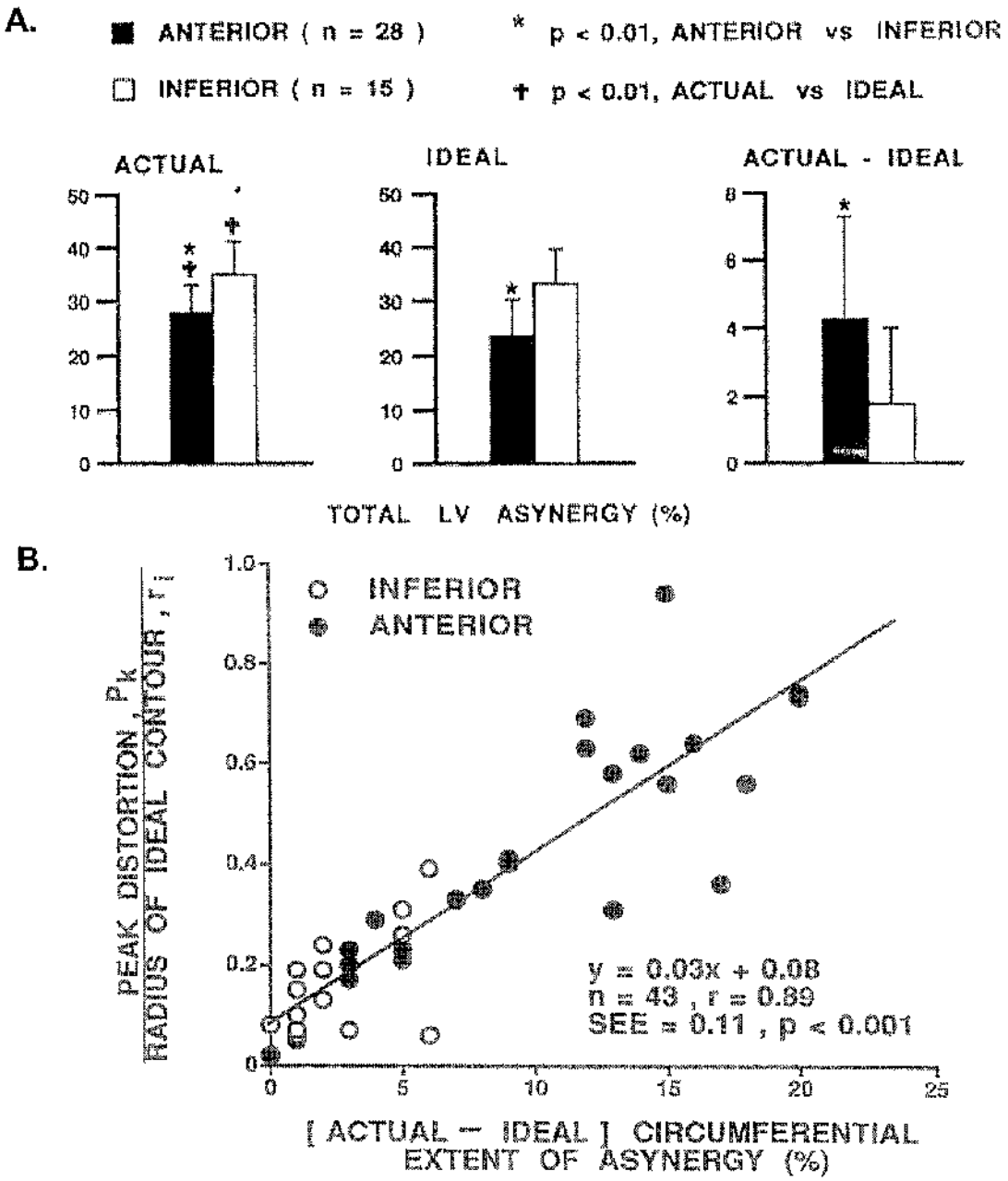

Figure 33. Overestimation of infarct size on 2D-Echo due to remodelling of the infarct zone

A. Actual and ideal left ventricular (LV) asynergy
B. Relation between the degree of distortion and the degree of overestimation of asynergy. SEE = standard error of estimate.

From Johnston and Jugdutt (36: Appendix 10)

1.

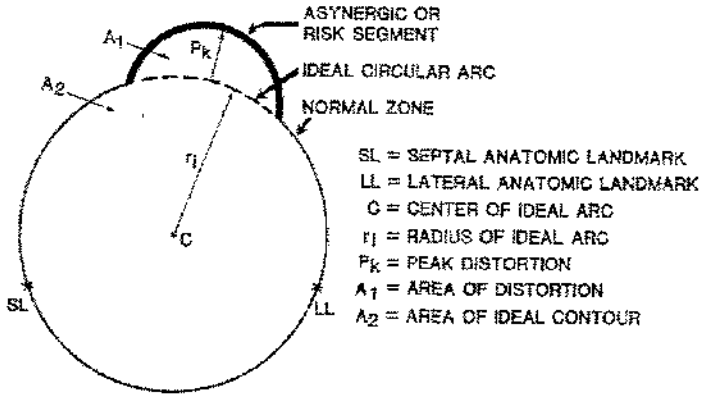

1. The regional shape distortion (RSD) algorithm was also applied to the control group. Each short-axis outline was subdivided into six sectors of 60 degrees. RSD data were obtained on each sector by considering the sector's endocardial border as an asynergic segment, with the remaining sectors comprising the normal endocardium.

3.

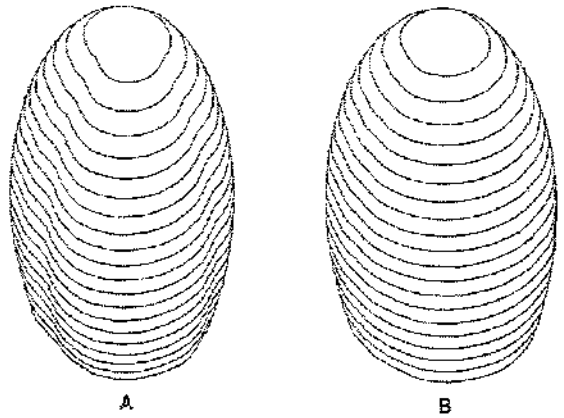

3. Computed and fitted volumes using 3D-recostruction

2.

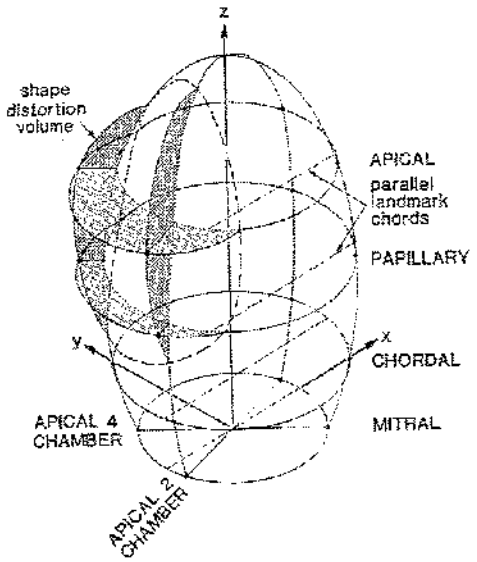

Figure 34. The regional shape distortion (RSD) algorithm

2. Model for quantifying global RSD by combining regional data in short-axis and long-axis 2D-Echo images. Shaded areas depict distorted zones. The elliptical surface fitting procedure was applied to both the ideal and distorted short-axis contours. The individual asynergic segments were used to compute global LV asynergy. The difference between actual and ideal asynergy was taken as a measure of the degree of overestimation.
From Maidens and Jugdutt (33: Appendix 7)

TABLE 13. Comparison of computed and ellipse fitted volumes in computer generated synthetic data

Model #	Volume (cm^3) computed	ellipse fit	% difference
	Actual (Distorted)		
1	88.6	87.9	-0.80
2	476.2	474.0	-0.45
3	82.3	81.8	-0.55
4	232.0	230.4	-0.69
5	78.4	77.8	-0.78
	Ideal		
1	84.8	86.3	+1.74
2	462.4	460.4	+1.77
3	75.1	76.1	+1.39
4	211.6	215.3	+1.76
5	74.5	76.0	+2.05

area of LV asynergy (Figure 34).

This approach was applied to 39 subjects (28 with a first Q-wave anterior MI; 11 normal controls). 2D-Echo's were recorded at a mean of 7 days post-MI. The computed and fitted volumes were in close agreement (Table 13, Figure 34).

This approach was applied to 39 subjects (28 with a first Q-wave anterior MI; 11 normal controls). 2D-Echo's were recorded at a mean of 7 days post-MI. The computed and fitted volumes were in close agreement (Table 13, Figure 37).

Relevance: The approach can be applied to compute the volume of RSD from various forms of tomographic cardiac imaging.

Other approaches have been proposed previously and are more cumbersome (343).

TABLE 13. Comparison of computed and ellipse fitted volumes in computer generated synthetic data

Model #	Volume (cm^3) computed	ellipse fit	% difference
	Actual (Distorted)		
1	88.6	87.9	-0.80
2	476.2	474.0	-0.45
3	82.3	81.8	-0.55
4	232.0	230.4	-0.69
5	78.4	77.8	-0.78
	Ideal		
1	84.8	86.3	+1.74
2	452.4	460.4	+1.77
3	75.1	76.1	+1.39
4	211.6	215.3	+1.76
5	74.5	76.0	+2.05

Jugdutt (33: Appendix 7)

5.4. CLINICAL STUDIES: MODIFICATION BY PHARMACOLOGICAL AGENTS

5.4.1. The effect of short-term anti-inflammatory therapies after acute MI on LV geometry and function during early healing (35: Appendix 9)

Background: The fact that acute infarct expansion and pericarditis are both common complications of high-risk patients with transmural or Q-wave MI provided the opportunity to the assess the effects of two NSAIDs, that were commonly prescribed for pericarditis, on LV remodelling.

Methods/Results: Evidence of acute infarct expansion on serial 2D-Echo and the frequency of the acute infarct expansion syndrome occurring at 2 days or more after a first Q-wave MI were therefore studied in 221 consecutive patients (100 anterior, 121 inferior) (35).

Patients with symptomatic pericarditis were treated with indomethacin (group 1, n=73) or ibuprofen (group 2, n=49) and those without symptomatic pericarditis received neither drug (group 3, n=99). The patients were followed for 1 year.

The overall frequency of the acute infarct expansion syndrome was 13%, and 69% of these were among the pericarditis groups. The infarct expansion syndrome was significantly more frequent in group 1 (22%) than group 2 (8%) ($P<0.05$) or group 3 (9%) ($P<0.025$).

Serial 2D-Echo (day 2, day 10) revealed more expansion with greater percentage increase in the infarct containing segment length in group 1 than groups 2 or 3 (18% versus 9% versus 9%, $P<0.005$). However, the decreases in infarct segment thickness were similar in group 1 (24%) and group 2 (25%) but greater ($P<0.001$) than in group 3 (7%).

Despite similar infarct size and infarct thinning in groups 1 and 2, the degree of infarct expansion on 2D-Echo was greater and the infarct expansion syndrome more frequent in group 1. However, when allowance was made for the potential protective effect of prior use of intravenous NTG and concomitant use of nifedipine, indomethacin and ibuprofen had similar effects on expansion.

The frequency of LV aneurysms was greater with indomethacin (group 1) than in groups 2 or 3 (33% versus 20% versus 17%, $\chi^2 = 6.09$, $P<0.05$). RSD was also more marked in group 1 patients.

Relevance: The overall findings suggested that indomethacin or ibuprofen should be used with caution after Q-wave infarction so as to avoid further infarct expansion. The fact that short-term use of other drugs might modify infarct remodelling should be considered in studies attempting to assess efficacy of one particular drug.

The possibility exists that the difference in remodelling in that study may have reflected the fact that patients with pericarditis had larger transmural infarcts than those without symptoms of pericarditis. Thus, although all patients had transmural or Q-wave MI, the CK infarct size was larger ($P < 0.05$) in patients receiving indomethacin (51.2 g-Eq) and ibuprofen (52.4 g-Eq) compared to the non-pericarditis group. Magnetic resonance imaging which allows the measurement of infarct transmurality may help to resolve the problem. Although new cyclo-oxygenase-2 (COX-2) inhibitors may be an alternative to NSAIDs for the treatment of pericardial pain, they have recently received increased publicity for increasing cardiovascular events.

5.4.2. Therapeutic interventions in acute myocardial infarction

Initial studies focused on LV unloading after MI using low-dose intravenous NTG. Patients with angina were studied before embarking on studies in acute MI.

5.4.2.1. Preliminary study of NTG infusions during pacing-induced angina in the cardiac catheterization laboratory

Background. There was a paucity of data on the effect of low-dose NTG infusion on LV asynergy assessed by 2D-Echo.

Methods/Results: To determine whether a 10 minute intravenous NTG infusion would decrease LV asynergy induced by atrial pacing in patients with chronic stable angina (< 6 months duration and no LV asynergy on a resting baseline 2D-Echo), asynergy was measured after atrial pacing to the angina threshold, or a maximum rate of 150 bpm, on biplane LV angiograms after 10 minute infusions of saline and again after 10 minute infusions of NTG (n=10).

NTG was infused in doses of 35 to 200 μg/min, to produce a detectable decrease in mean arterial pressure by 5%. In a control group, the second infusion also consisted of saline (control, n=10). In all patients receiving NTG, the LV filling pressure and pulmonary vascular resistance decreased before a decrease

in systemic vascular resistance was detected. Angiographic LV asynergy after NTG was less or absent compared to saline infusions. There was no improvement in LV asynergy in the control group. The improvement after NTG appeared to be related to i) decreased filling pressure, ii) decrease LV size (and wall stress), iii) the mild decrease in afterload (< 5%), and iv) possibly improved collateral blood flow.

Analysis of haemodynamic recordings, the time course of changes in LV filling pressure, arterial pressure, cardiac indices and vascular resistances, suggested that LV filling pressure might be a better guide for therapy in MI. In these studies, 2D-Echo recorded simultaneously as the LV angiograms confirmed the effects on LV asynergy. Similar effects were found in 6 patients given prostacyclin (PGI_2, gift from Upjohn). No significant RSD was detected in these patients.

The dose of NTG required to produce a 5-10% reduction in mean systolic blood pressure (but not below 100 mm Hg) varied widely in patients after acute MI, the range being 35 μg/min to 180 μg/min. Some patients were resistant to dropping arterial pressure despite high doses, while others were very sensitive in that respect. The pulmonary capillary wedge pressure decreased promptly in all patients.

Relevance: The findings of these preliminary studies (data not published) provided the basis for low-dose NTG infusions in subsequent studies.

5.4.2.2. Preliminary study of short-term low-dose NTG infusions during acute MI in the CCU (232: Appendix 36)

Background: Whether acute short-term low-dose NTG infusions in acute MI decreased measures of infarct size and LV asynergy on 2D-Echo had not been determined.

Methods/Results: Twenty-two patients with a first acute anterior MI and no contraindications were randomized between control and NTG therapy over 2 days (232). All patients had complete haemodynamic monitoring, praecordial ST-segment mapping, CK-MB and serial 2D-Echo studies (days 1, 2, 4 and 10). Haemodynamic measurements and cardiac index improved in all despite a 5% reduction in mean arterial pressure. The LV filling pressure decreased markedly

from a mean of 18 mm Hg to 5 mm Hg. The sum of ST segment elevations (or ΣST) on 16 lead praecordial maps decreased sharply. Cumulative CK infarct size also decreased. Four short-axis 2D-Echo views were analyzed. The extent of LV asynergy decreased in all. LV chamber size also decreased. The incidence of arrhythmias and complications over the acute phase were less in these NTG treated patients. The decrease in LV asynergy on 2D-Echo was persistent at 10 days (232).

Relevance: In that study (232), early low-dose NTG infusion for 39 hours after acute MI decreased LV asynergy, infarct size and complications. Retrospective analysis suggested that NTG also decreased RSD. The study also underscored the effect of the acute decrease in volume during NTG therapy on the assessment of RSD and infarct expansion. Additionally, the study led to the recognition of RSD with dilatation, stretching and thinning of the infarcted segment but no clinically evident 'infarct expansion'. This suggested that pathologic expansion of the infarcted segment was common, and that there might be a threshold beyond which acute dilatation, aneurysm and/or rupture occur.

5.4.3. The effect of short-term NTG infusion therapy during acute MI on LV geometry and function during healing after MI and beyond (28: Appendix 6)

Background: Until 1988, eight randomized clinical trials had clearly shown that low-dose intravenous NTG in acute MI i) improves haemodynamics, ii) decreases CK infarct size, iii) is more beneficial in early MI, iv) decreases LV asynergy, v) decreases remodelling, and vi) decreases other infarct related complications including mortality. These early studies of short-term low-dose intravenous NTG in acute MI have been reviewed (100**[Appendix 21]**,101,250**[Appendix 37]**). The effect of low-dose NTG infusion after a first Q-wave MI on measures of infarct size, infarct-related complications, and LV asynergy and remodelling on 2D-Echo had not been studied.

Methods/Results: The effect of timing, dosage and infarct location on the response to intravenous NTG therapy during acute MI was therefore studied in 310 patients: 154 NTG, 156 controls (28).

Several points in this study (28) need emphasis.

First, it was a prospective single-blinded study of 310 patients with acute MI randomized to NTG or placebo. NTG was titrated to lower mean blood pressure by 10% in normotensives and 30% in hypertensives (but not below 80 mm Hg) and was maintained for a mean of 39 hours. Measurements included clinical variables, CK infarct size, and indexes of LV function and expansion on 2D-Echo.

Compared to placebo, NTG: i) reduced overall CK infarct size [41 versus 55 g-Eq (gram-equivalent), $P<0.001$] and in both anterior (44 versus 58 g-Eq, $P<0.05$) and inferior infarction (39 versus 53 g-Eq, $P<0.025$) sub-groups, with greater benefit if given early (< 4 hours) and if average mean blood pressure was above 80 mm Hg in the first 12 hours; ii) decreased regional LV dysfunction, improved LV ejection fraction and decreased infarct expansion and thinning (Figure 35); iii) improved clinical functional status and haemodynamics; iv) decreased in-hospital complications, including the infarct expansion syndrome (2% versus 15%, $P<0.0005$), cardiogenic shock (5% versus 15%, $P<0.005$), LV thrombus (5% versus 22%, $P<0.0005$), and infarct extension (11% versus 22%, $P<0.025$); and v) decreased mortality in the acute anterior infarction sub-group, in-hospital (14% versus 26%, $P<0.01$), at 3 months (16% versus 28%, $P<0.025$) and at one-year (21% versus 31%, $P<0.05$).

Second, in that study (28), short-term NTG therapy after MI decreased both the frequency of clinically significant expansion (as manifested by the clinical syndrome and marked evidence on 2D-Echo) and purely echocardiographic expansion itself (2D-Echo measurements of infarct stretching, thinning and RSD). NTG therapy also decreased LV size.

Third, nitrate tolerance was detected in less than 25% of patients but did not result in significant loss of efficacy (28,118).

Fourth, these findings support the concept that the application of appropriate expansion-limiting therapy in the very early phase of healing, during and after MI, and before significant collagen deposition, might have greater potential for limiting remodelling and aneurysm formation (28,118).

Fifth, the greatest benefit from low-dose NTG was seen in the early sub-group with mean arterial pressure >80 mm Hg and > 30% improvement in ΣST, LV asynergy and LV ejection fraction during the early stages of therapy, regardless of the infarct location.

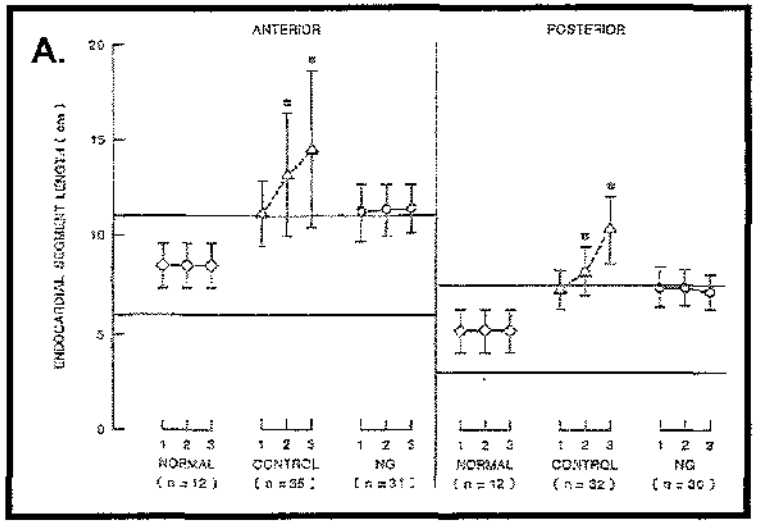

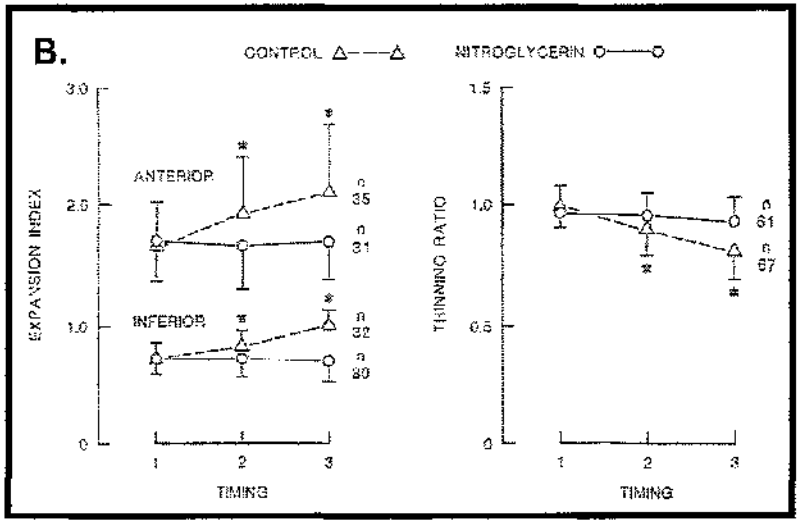

A. Changes in endocardial segment lengths in normal, control and nitroglycerin (NG) groups. Left panel: anterior segment data for anterior MI subgroups and normals. Right panel: Posterior segment data for inferior MI subgroups and normals. *P≤0.05,significance of difference comparing values at 2-3 days (2) and 7-10 daya (3) to baseline (1). Horizontal lines in the panels are two standard deviations from the mean value for normals.

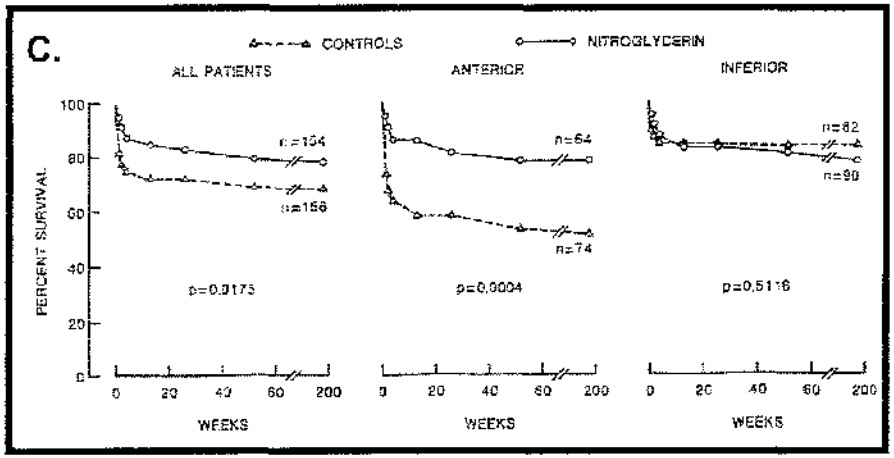

Figure 35. Beneficial effects of nitroglycerin therapy after acute MI

B. Changes in expansion index (left panel) and thinning ratio (right panel) for control and nitroglycerin groups. Expansion index is shown separately for anterior and inferior infarct subgroups. *P≤0.05,significance of difference comparing values at 2-3 days (2) and 10 daya (3) with baseline (1).

C. Actuarial curves for nitroglycerin and control groups. Data over the 43 months or 186 weeks of the long-term follow-up are shown. Left panel: All patients. Middle panel: Anterior subgroups. Right panel: Inferior subgroups.

From Jugdutt et al. (28: Appendix 6)

Relevance: This study (28) was the largest randomized trial of low-dose intravenous NTG in acute MI. It established that early and prolonged (≥ 48 hours) low-dose NTG infusions can be given safely to patients with MI to limit infarct size and also to improve LV function and geometry. Both infarct expansion and mortality were reduced in the high-risk group with Q-wave anterior MI (Figure 35). A meta-analysis of the pooled data from all 9 studies confirmed that NTG therapy decreased mortality, with a 35% reduction in the odds of death ratio (2P<0.001) (344).

5.4.4. The effects of prolonged NTG therapy, given during acute infarction and healing phases after acute MI, on LV geometry and function (105[Appendix 24],109[Appendix 26])

Background: Following the demonstration of the benefits of that low-dose intravenous NTG infusion, given over the first 48 hours after acute MI, on infarct size and LV remodelling, the next logical step was to study the effect of this intervention applied during the entire healing phase after MI. There was no published data on LV remodelling during the entire healing phase at the time.

Methods/Results: The hypothesis that prolonged NTG therapy, given throughout the infarction and healing phases after acute MI, may further limit deterioration of LV topography, reduce infarct expansion, improve LV function, and prevent aneurysm formation was therefore tested as the next step (104-107,109). Whether the beneficial effects persisted up to one year after therapy was also studied (106,107).

Briefly, to determine whether the effect of prolonged NTG therapy (low-dose infusion for the first 48 hours followed by buccal NTG for 6 weeks) versus placebo was studied in 43 patients with a first acute anterior Q-wave MI (Table 14, Figure 36). Buccal NTG (1-3 mg) was given every five hours with a daily 8-hour washout period to avoid the development of vascular tolerance. Left ventricular function and topography were assessed by serial 2D-Echo over 12 weeks. Prolonged NTG therapy decreased infarct expansion, thinning and RSD, improved haemodynamics, decreased LV volume and asynergy, and increased LV ejection fraction compared to placebo.

The overall findings suggested that prolonged LV unloading with low-dose NTG limited LV remodelling and improved LV function and clinical parameters when initiated early after MI (data not fully published; book chapter in preparation).

TABLE 14. Patient characteristics in the BNTG and placebo groups

Parameter	BNTG Group (n=23)	Placebo Group (n=20)	P Value
Sex	20 M, 5 F	20 M, 5 F	NS
Age (yr)	59 ± 10	57 ± 7	NS
Body surface area (m^2)	1.9 ± 0.2	1.9 ± 0.2	NS
Pain to admission	10 ± 13	10 ± 14	NS
Adm. to first 2D-Echo (h)	24 ± 18	22 ± 18	NS
Pain to NTG infusions (h)	12 ± 15	12 ± 14	NS
Dose: Average (µg/min)	71 ± 53	77 ± 65	NS
Range (µg/min)	5 - 232	10 - 220	NS
Duration of NTG infusion (h)	61 ± 19	66 ± 29	NS
History of:			
Hypertension (n)	7	8	NS
Heart failure (n)	0	0	NS
Infarction (n)	0	0	NS
2-day BP (mmHg):			
systolic	111 ± 13	115 ± 17	NS
diastolic	74 ± 9	74 ± 11	NS
mean	87 ± 10	88 ± 12	NS
2-day HR (bpm)	84 ± 10	87 ± 10	NS
2-day RPP			
(mmHg x bpm x 10^3)	7.6 ± 1.5	8.0 ± 1.9	NS
Admission Killip Class	2.2 ± 0.3	2.1 ± 0.2	NS
Creatine kinase:			
Peak (IU/L)	2583 ±1664	2174 ± 1791	NS
Infarct size (g-Eq)	52 ± 60	46 ± 33	NS
NYHA at: 24 weeks	1.3 ± 0.4	1.8 ± 0.6	0.005
52 weeks	1.4 ± 0.5	2.0 ± 0.3	0.001
Deaths at 52 weeks	0	0	NS

Abbreviations: BNTG, buccal nitrate; BP, blood pressure; bpm, beats per minute; F, female; M, male; RPP, rate pressure product; NYHA, New York Heart Association.

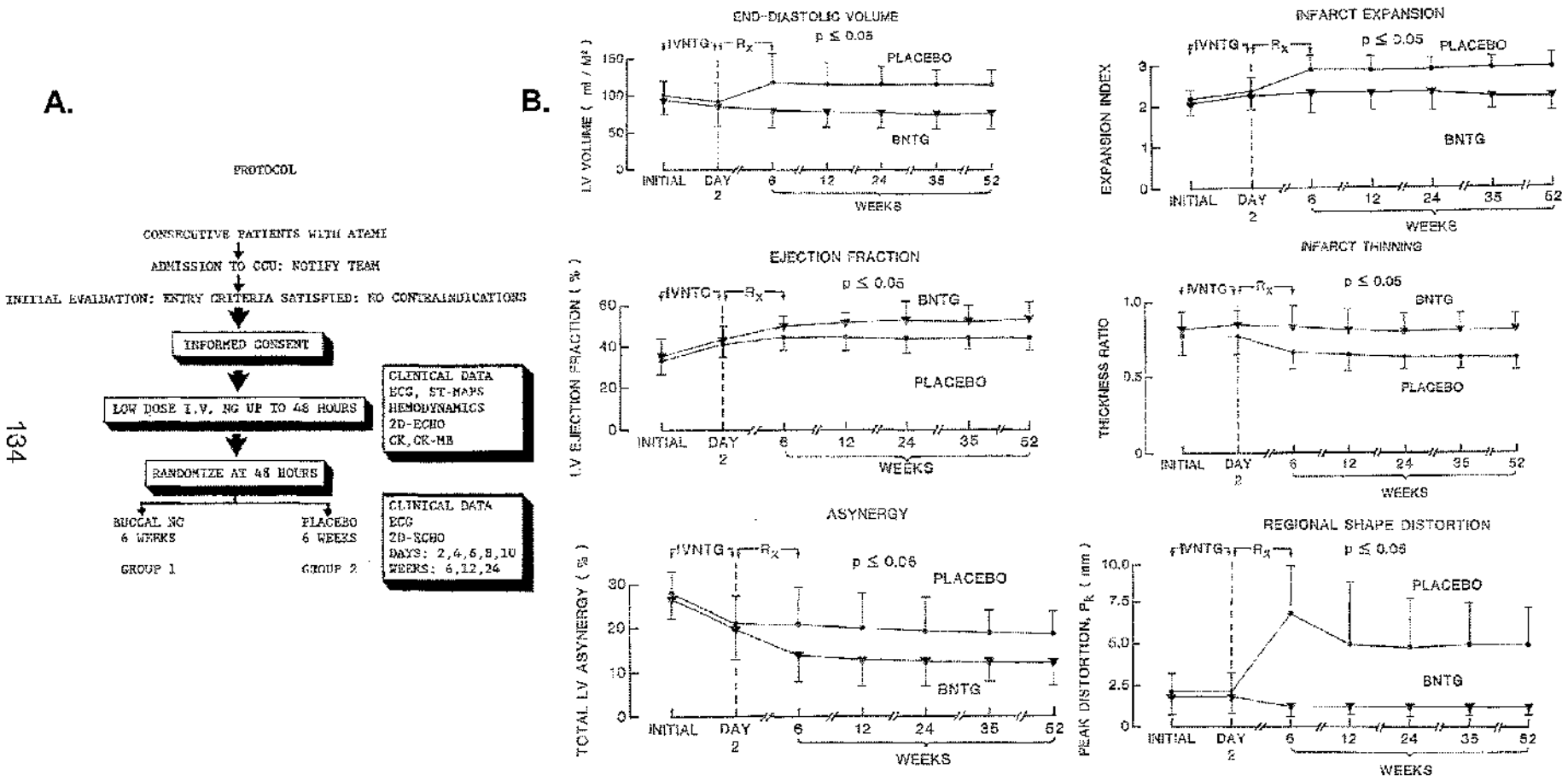

Figure 36. Protocol and results of the ATAMI study on the prolonged effects of nitrate therapy during healing post-MI

A. Protocol. **B.** Effects on diastolic volume, ejection fraction, total asynergy and infarct expansion, thinning and bulging. CK, creatine kinase; CCU, coronary care unit; ECG, electrocardiogram; 2D-Echo, two-dimensional echocardiogram; NG, nitroglycerin

From Jugdutt et al. (105: Appendix 24).

Relevance: Four points need emphasis. **First**, the beneficial effects of prolonged NTG therapy on early and late remodelling in that study suggested that therapy may have interrupted the vicious cycle leading to LV aneurysm, LV dilatation and congestive heart failure.

Second, low-dose intravenous NTG therapy was rapidly becoming routine therapy for the management of acute MI (345). Although NTG is widely used for the treatment of angina (346), low-dose NTG was proposed for the limitation of infarct size and early remodelling (28) and not for the relief of continuing chest pain as in unstable angina where high doses are used.

Third, although prolonged nitrate therapy for angina, especially at high doses, is associated with the development of nitrate tolerance (117), tolerance was not significant with low-dose NTG after MI (118: **Appendix 27**).

Fourth, since tolerance during chronic nitrate therapy for angina can be partially combated by intermittent or eccentric dosing and new formulations that permit a low nitrate interval beyond the first 48 hours (337), an eccentric regimen was used in this study. This precaution was also justified by the mechanisms that were proposed for tolerance at the time, namely: i) a cellular mechanism involving depletion of sulfhydryl groups or alteration of the guanylyl cyclase pathway (117), and ii) a systemic mechanism, whereby haemodynamic changes trigger off a counter-regulatory neurohumoral activation with stimulation of the renin-angiotensin pathway and fluid retention (346). Importantly, the eccentric NTG dosing regimen used in that study was associated with beneficial anti-remodelling effects.

5.4.5. The effects of prolonged NTG and captopril therapy, given during healing after acute MI, on LV geometry and function (108: Appendix 25;298: Appendix 41)

Background: On the basis of data available in the mid-1980's, two major approaches could be formulated to combination therapy for the limitation of remodelling after MI. **The first approach** was to use low-dose intravenous NTG acutely followed by either prolonged nitrate or prolonged ACE-inhibition therapy. **The second approach** was to use a combination of nitrate and an ACE inhibitor in the chronic therapy phase. In theory, sulfhydryl-containing ACE inhibitors such captopril could donate these groups as well as block neurohumoral activation, and thereby reduce nitrate tolerance. The combination of ACE inhibitors with

vasodilators such as nitrates in the management of congestive heart failure had already been suggested to be effective in inhibiting vasodilator-induced vasoconstriction (346). It should be noted that although chronic continuous nitrate therapy resulted in tolerance with attenuation of the anti-anginal effect, eccentric dosing was believed to provide protection against painful ischaemia (337).

Several significant advances brought nitrates into prominence in the late 1980's. Endothelium-derived relaxing factor (EDRF), one of the most active endogenous vasodilators (347), was identified as nitric oxide (NO) by Palmer et al. in 1987 (348) and proposed to represent endogenous nitrate. Nitrates were thought of as NO donors. It was proposed that NO might also act as a free radical scavenger and explain the beneficial effect of NTG during reperfusion. However, Myers et al. (326) suggested that the vasorelaxant property of EDRF more closely resembled S-nitroso-cysteine than NO.

Methods/Results: As the logical next step, the hypothesis that prolonged anti-remodelling therapy with acute NTG over 48 hours followed by the combination of NTG and captopril, might be more beneficial than monotherapy with NTG or captopril was tested in patients after Transmural Acute MI or TAMI (108: **Appendix 25**;298:**Appendix 41**).

Between 1989 and 1991, 160 consecutive patients who were admitted to the CCU with a potential first anterior or inferior TAMI and were treated with standard therapy consisting of thrombolysis followed by intravenous low-dose NTG infusion for 48 hours, and had an adequate 2D-Echo and evidence of Q-wave MI on ECGs at 48 hours were entered into the prospective, double-blind, placebo-controlled randomized study (Figure 37).

A factorial design (n=20/cell) was used and the patients with anterior (ATAMI) or inferior (ITAMI) TAMI were started on 6 weeks of oral placebo, captopril (25 mg t.i.d.), NTG (buccal 3 mg t.i.d., 5-hourly with an 8-hour washout) or NTG+captopril. The patients were followed for 1 year after therapy, with serial complete quantitative 2D-Echo. The 2D-Echo remodelling indices at 2 days, 6 weeks, 6 months, and 1 year as well as serial clinical data (complications, cardiovascular events and other drugs as per questionnaire) and ECGs were recorded (Figure 37).

At randomization, the demographic and clinical data for the 4 groups were similar (Table 15A). Average values were: 88% male gender; age 57 years;

TABLE 15 A. PATIENT CHARACTERISTICS (Mean ± SEM)

PARAMETER	PL (n=40)	CL (n=40)	NG (n=40)	CL+NG (n=40)
Sex (% Male)	96	91	76	88
Age (Years)	59±2	57±2	53±2	57±2
Weight (kg)	81±2	81±2	82±2	84±2
BSA (M^2)	1.9±0.02	1.9±0.02	1.9±0.02	1.9±0.02
Anterior (%)	50	50	50	50
Killip Class: Admission	1.6±0.08	1.7±0.06	1.7±0.09	1.7±0.08
Killip Class: Day 2	2.1±0.03	2.2±0.03	2.1±0.05	2.2±0.03
Peak CK (IU/L)	2060±233	2767±303	2138±218	2756±332
CK Infarct Size (gEq)	44±7	57±9	42±7	67±11
Thrombolysis (%)	43	43	52	55
Systolic BP (mmHg)	103±2	108±3	110±2	108±3
Diastolic BP (mmHg)	67±2	69±2	70±2	69±2
Mean BP (mmHg)	79±2	82±2	83±1	83±2
Heart Rate (bpm)	77±2	78±2	72±2	77±3
RPP (mmHgxbpmx10^3)	6.1±0.2	6.4±0.3	6.0±0.2	6.3±0.2
NTG Infusion (%)	100	100	100	100
Dose (mg/min)	75±9	68±9	77±10	71±8
Past Hx: Hypertension (%)	25	27	30	28
Past Hx: Infarction (%)	0	0	0	0
Past Hx: Heart Failure (%)	0	0	0	0

P = NS for all comparisons

Abbreviations: BP, blood pressure; BSA, body surface area; CK, creatine kinase; CL, captopril; Hx, history; NG, nitrate; PL, placebo; RPP, rate pressure product

TABLE 15 B. FOLLOW-UP DATA (10 years: 1990-2000)

	ATAMI Group (n = 80)					ITAMI Group (n = 80)				
	PL	CL	NG	NG+CL	ALL %)	PL	CL	NG	NG+CL	ALL (%)
PTCA	7	8	7	3	25 (31)	8	8	3	10	29 (36)
Rec MI	0	1	1	2	4 (5)	2	2	0	2	6 (8)
CHF	5	2	1	4	12 (15)	1	1	1	3	6 (8)*
CABG	3	2	4	4	13 (16)	7	3	5	7	22 (28)*
Death	4	3	2	6	15 (19)	0	1	0	1	2 (3)*
HTx	0	1	0	0	1 (1)	0	0	0	0	0 (0)
ACE-I†	3	3	2	5	13 (16)	3	1	3	4	11 (14)
BB	3	6	4	3	16 (20)	6	7	4	9	26 (33)*

*P < 0.05 (χ^2 Test); † (after 2 – 5 years)

Abbreviations: ACE-I, ACE-inhibitor; BB, beta blocker; CABG, coronary artery bypass graft; CHF, congestive heart failure; CL, captopril; HTx, history; NG, nitrate; PL, placebo; PTCA, percutaneous transluminal coronary intervention; Rec MI, recurrent MI.

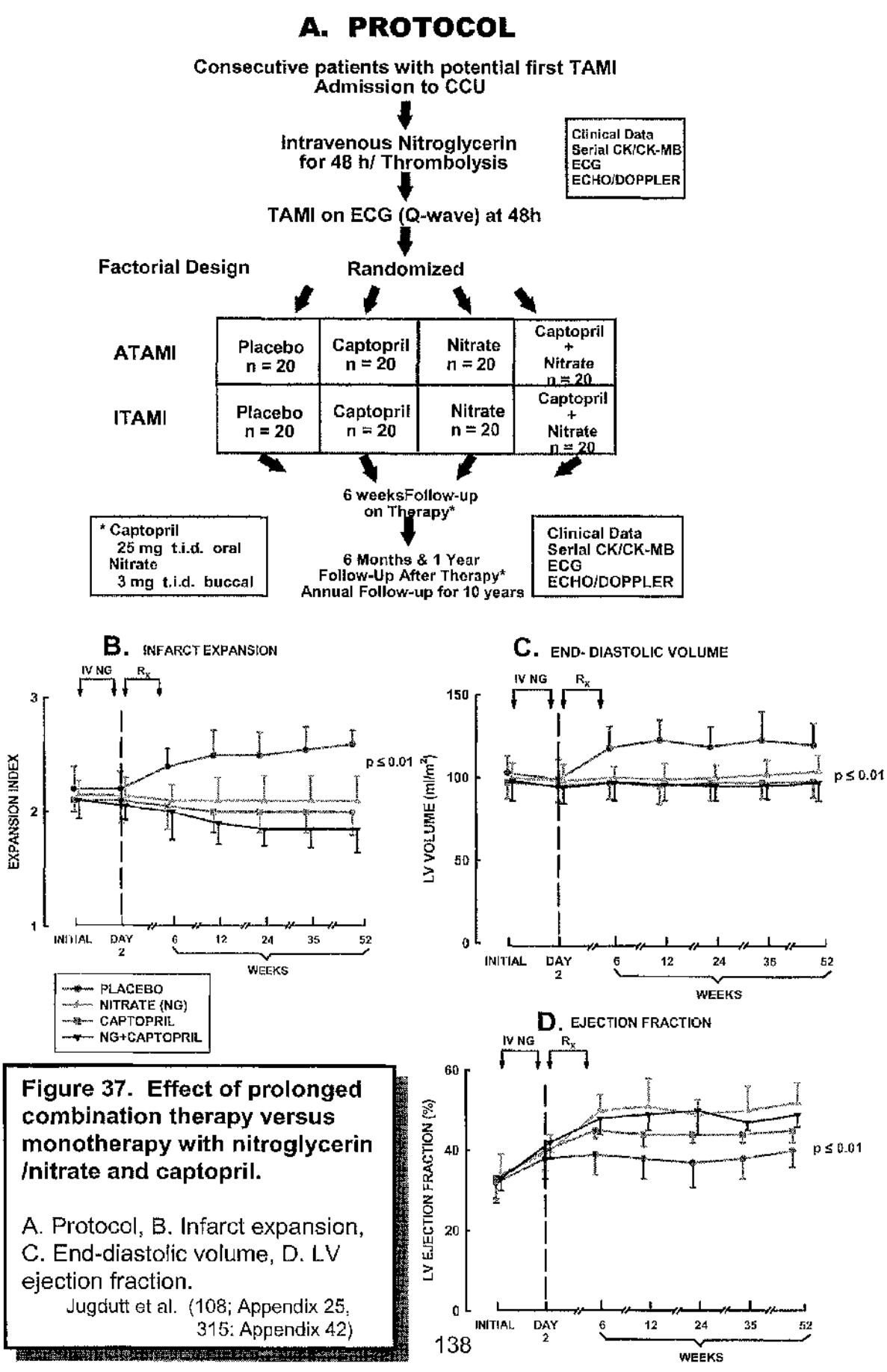

Figure 37. Effect of prolonged combination therapy versus monotherapy with nitroglycerin /nitrate and captopril.

A. Protocol, B. Infarct expansion, C. End-diastolic volume, D. LV ejection fraction.

Jugdutt et al. (108; Appendix 25, 315; Appendix 42)

weight 82 kg; 50% ATAMI; Killip class 2.1 ± 0.03; peak CK 2430 IU/L; CK infarct size 53 ± 8 g-Eq; thrombolytics 48%; mean blood pressure 82 ± 2 mm Hg. Compared to the placebo group, all active therapy groups showed preservation of global LV ejection fraction and limitation of remodelling (as assessed by the infarct expansion index, wall thinning ratio, RSD, and diastolic and systolic volumes) between 6 weeks and 1 year (Figure 37). Follow-up data at 10 years (Table 15B) showed that most of these patients survived 10 years (book chapter in preparation).

The sample sizes in the cells of the factorial template were carefully calculated for the 2D-Echo end-points on the basis of previous 2D-Echo data in my laboratory which was dedicated to research on remodelling after MI in humans (19-21,28,33-36,50,104-107,109,118,130,180,220,232,245,251-253,274,298) and the dog model (48,55,62,73,74,96,103,126-129,131,181,222,283,318,319). Feinstein's method was used (320) for calculation of sample size considering beta error (322). Defining a significant change for in-vivo LV function as a 25% increase in ejection fraction, or 25% improvement in remodeling parameters (LV end-diastolic volume), a doubly significant sample size (N) calculated after correcting for the chance of falsely accepting the null hypothesis due to sampling error, was n = 6 for $\alpha = 0.05$, $\beta = 0.1$. This was trebled to allow for inter-observer error and other factors.

Relevance: Monotherapy and combination therapy with NTG (eccentric dosing) and captopril, given during healing after transmural MI, produced similar anti-remodelling effects which persisted up to one year. It is clear from the pathophysiologic determinants of remodelling (Figure 7; Table 3) and the stages of remodelling (Figure 6; Table 2) that therapy applied very early and throughout the early phase of healing before collagen deposition, and continued throughout the late phase of healing and beyond, might result in greater benefits in the absence of negative factors. Potential therapies, reviewed previously (67; Figure 21), included nitrates, ACE inhibitors and beta-blockers and were included in management guidelines (345). While the beneficial effects of long-term therapy with ACE inhibitors in post-MI survivors are established (27), long-term therapy with nitrates is not recommended in post-MI survivors.

6. DISCUSSION

The period between 1980 and 1988, during which the studies outlined in this thesis were conducted and/or initiated, were exciting years in the development of the novel concepts of adverse remodelling after MI and its potential modification by anti-remodelling strategies. Importantly, that period witnessed the development of 2D-Echo as a powerful tool for the assessment of the dynamic changes in LV geometry and function after MI and the effects of potential therapeutic interventions. The studies have contributed to knowledge of the pathophysiology of healing and gross mechanisms of LV remodelling after MI (21,22) that triggered several clinical trials of potential anti-remodelling agents post-MI (23).

Rapid progress and developments during that period (1980-1988) made changes in the initial objectives and approaches necessary, with several to-and-fro leaps from bench to bedside research. Three landmark advances during that period triggered changes in the protocols for studies in this thesis. The first was the discovery that coronary thrombosis was the major culprit causing acute coronary occlusion in MI (349), which led to the use of widespread early thrombolytic therapy. The second was the discovery that LV unloading and inhibition of the renin-angiotensin pathway with ACE-inhibition limited progressive LV dilatation after MI (77), which led to the widespread use of ACE inhibitors after MI. The third was the discovery that reperfusion induced damage to the ECM (164), which rekindled previous interest in the role of the ECM (277) and collagen in cardiac remodelling (277,295) and also led to the concept of anti-fibrotic therapy in cardiovascular disease (295), with implications for MI.

6.1. Major findings

There are five major findings stemming from the studies in this thesis that are pertinent to the topic of 'modification of LV geometry and function during healing after acute MI' and might have profound therapeutic implications still pertinent in the 2000's.

First, the LV remodelling process is complex, involving multiple determinants and diverse mechanisms that are potentially modifiable (21,28,37,39, 50,103,126), and quantitative 2D-Echo and 3D reconstruction can be applied to measure the in-vivo regional and global structural, geometric and functional changes associated with LV remodelling post-MI (19-22,28,34,67,102,103,283). The

sequence of acute MI followed by early regional and subsequent progressive global LV dilatation and progressive LV dysfunction suggested that **bad remodelling outweighs the good**, a concept that is now generally accepted.

Second, **LV remodelling and infarct healing are dynamic processes that progress in parallel over time** (22) and the effects of interventions on LV remodelling during healing after MI can be tracked by serial quantitative 2D-Echo.

The studies showed that remodelling spans phases of infarction and healing, before and after infarct collagen deposition reaches a plateau, to scar formation (22,39,41,55) and anti-remodelling therapies can influence healing (22). The results supported the concept that organized collagen deposition and scar formation in the infarct zone and cardiomyocyte hypertrophy in the non-infarct zone are important for preserving structural and functional integrity after MI, especially since **cardiomyocyte regeneration is insufficient to compensate for its loss**. Studies of the rupture threshold indicated that the left ventricle after MI is mechanically weaker and more susceptible to distension (102,283). The results also indicated that therapy targeted at one mechanism or phase might be unsuitable for another and have unexpected effects that might be potentially deleterious (22). This was illustrated in the studies with NTG (122), anti-inflammatory agents (35,102), and ACE inhibitors (127-129,131).

Third, ECM and collagen deposition in the infarct zone protect against LV remodelling (41,74,279,284,291) and interventions that disrupt the ECM or decrease IZ collagen may promote adverse remodelling.

Since early reperfusion causes ECM disruption (164) and late reperfusion after 2 hours of occlusion causes more structural disruption of ECM than permanent occlusion (160), induces myocardial stunning and reperfusion injury whereby salvage of muscle and geometry might not salvage function (158,159,161), the possibility of **another double-edged sword** was a concern. However, the overall benefits of early reperfusion are undeniable and late reperfusion was shown to limit acute expansion in dogs and limit RSD on 2D-Echo despite slightly lower infarct collagen (49). Late reperfusion also acceierates healing (46) which appears to be beneficial. Taken together, **the final outcome of reperfusion appears to depend on a balance of effects**. Importantly, NTG infusion after late reperfusion resulted in earlier recruitment of LV function and preserved LV geometry in patients after MI (50).

Since angiotensin II mediates remodelling and failure (350) and stimulates fibroblast proliferation, ECM and collagen deposition, myocyte hypertrophy and fibrosis, thereby leading to increased resistance to LV distension, hypertrophic remodelling and impaired diastolic function (295), decreased angiotensin II formation with ACE-inhibition was expected to decrease ECM and collagen deposition, and decrease hypertrophy. A subsequent report showed decreased collagen with ACE-inhibition after MI in rats (351). Captopril was found to limit LV dysfunction and hypertrophy in patients with anterior Q-wave MI (130). Clearly ACE inhibitor-induced limitation of LV dilatation, hypertrophy and heart failure is beneficial.

However, the possibility that early ACE-inhibition after MI might decrease ECM and collagen deposition in the infarct zone and thereby promote infarct expansion, regional and global LV distension, impair IZ healing and act as a **double-edged sword**, was actively pursued. Although the ACE inhibitors were found to markedly decrease collagen in the infarct zone (127,128,129,131) and to a lesser extent in the non-infarct zone (129), and showed increased RSD on ex-vivo LV sections and in-vivo quantitative 2D-Echo in some studies, overall beneficial effects on global LV remodelling and function were found in survivors with small to moderate MI (108,130,298). Since late coronary reperfusion can damage ECM (160), whether reperfusion and ACE-inhibition might potentially result in **double jeopardy** raised concern. However, this was not found to be the case in survivors with small to moderate MI (108,130,298). Another study found that ACE inhibitors given early after reperfusion were beneficial (352), although RSD and detailed data on remodelling were not available.

Other researchers have shown that ACE inhibitors (338) and ARBs (353) block collagen deposition in the non-infarct zone in rats. Since ACE inhibitors also block bradykininase (354) (Figure 38), thereby increasing bradykinin, PGI_2 and NO which contribute to LV unloading, anti-trophic and other pleiotropic effects, **the final outcome may represent a balance of effects.** The recent finding that volume overload in dogs, where chymase dominates over ACE, results in loss of the collagen weave that is not attenuated by ACE-inhibition (355), suggests that chymase-induced ECM degradation (356) may be an important factor during ACE-inhibition.

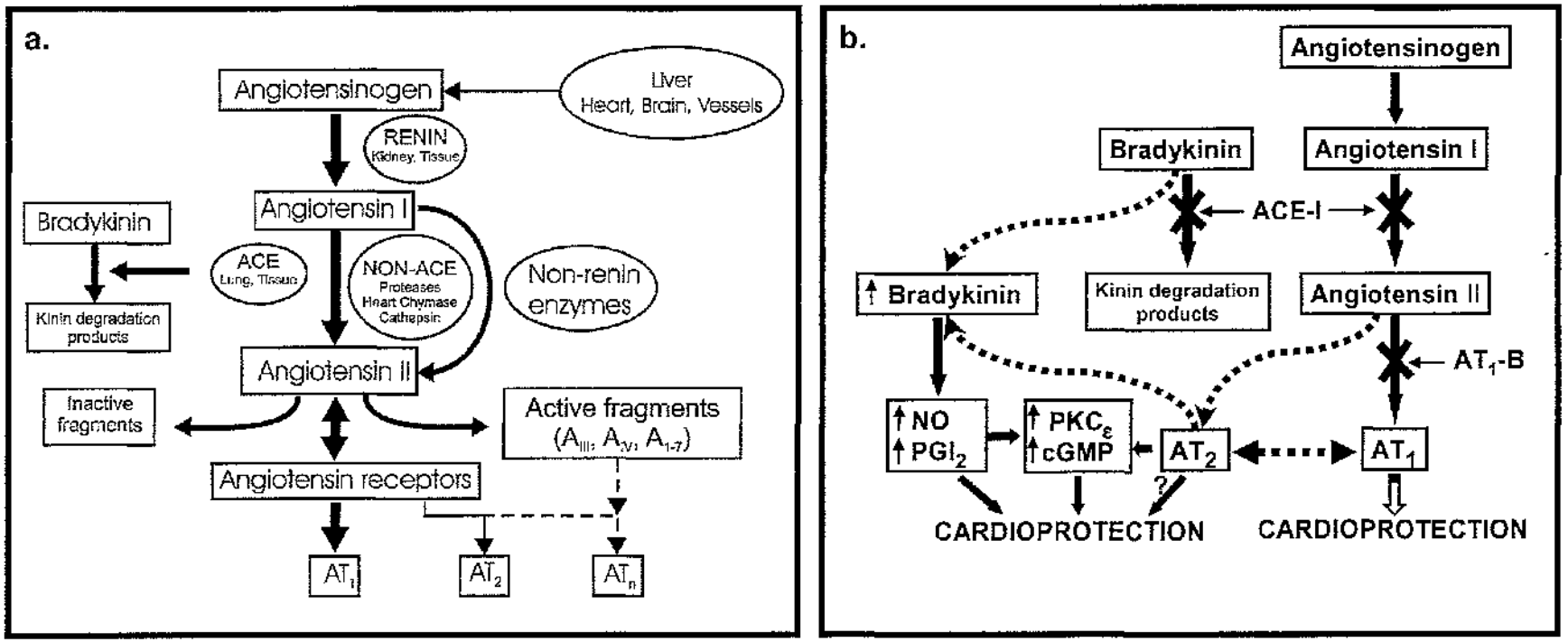

Figure 38. The angiotensin system.

a. Current view of the angiotensin system.

b. Postulated mechanism of benefits after combined ACE inhibition (ACE-I) and AT_1-blockade (AT_1-B).

A, angiotensin; ACE, angiotensin-converting enzyme; AT, angiotensin subtype receptor; cGMP, cyclic guanylate monophosphate; NO, nitric oxide; PGI_2, prostaglandin ; PKCε, protein kinase Cε .

From Jugdutt (363; Appendix 45)

Although acute administration intravenous low-dose NTG for 48 hours was effective in reducing infarct size and LV remodelling and dysfunction after MI (28), and prolonged NTG in eccentric dosing during healing after MI also limited LV remodelling and dysfunction (104-109) without decreasing infarct collagen or impairing healing (55,102,103,131), large clinical trials did not show a significant survival benefit (135-137). This negative result may have been due to the use of long-acting nitrates such as ISDN acutely, use of higher doses acutely often to control chest pain, continuous oral dosing subsequently resulting in the development of tolerance, and the administration of nitrates to other groups resulting in flawed statistics. A subsequent study showed benefit with prolonged transdermal NTG patch therapy (357).

Fourth, infarct size and transmurality are major determinants of adverse early and late remodelling after MI. Moderate transmural MI was shown to induce marked RSD and adverse remodelling after MI in the dog and patients. In addition, infarct location influenced the severity of early remodelling whereby the degree of RSD and severity of LV dysfunction was greater with anterior than inferior MI.

In the 1970's, limitation of infarct size was the therapeutic strategy of choice for reducing cardiovascular deaths because pump failure was directly related to infarct size (312). By the late 1980's, the increasing use of thrombolytic agents with or without PTCA, beta-blockers and nitrates had decreased early post-MI deaths to nearly 7% (28,121,134-141). The improved therapies increased the number of survivors but many still remain at risk of further adverse LV remodelling and its consequences (22). These include infarct expansion and thinning, LV aneurysm, LV dilatation, LV rupture, heart failure, LV volume overload, LV hypertrophy, arrhythmias and death.

Several studies in the 1980's, including those presented in this thesis, indicated that acute infarct expansion, LV dilatation, LV dysfunction, disability and death are directly related to infarct size and infarct transmurality (21-23,28,88). The 2D-Echo studies of MI in the dog and humans indicated that infarcting tissue undergoes early remodelling, with an expansion (stretching, thinning, and bulging) that **sets the stage for further adverse LV remodelling** (21,28,34,35,102,103, 127-131,283). In dogs, LV unloading with nitrates over the first 6 weeks produced greater benefit on LV dilatation and LV mass than over the first 2 weeks (103). **Early and prolonged anti-remodelling therapy after MI therefore seems to be**

a logical therapeutic strategy (22). Because patients with large anterior transmural (or Q-wave) MI are at highest risk for early expansion and LV remodelling (18,21-23,28,34,35,67,78,102,283), this **high-risk anterior MI group should be targeted for therapy.**

Studies with different pulses of anti-remodelling agents, such as captopril (22,23,121,126,132,134-141,145,318) and nitrates (28,55,102,103,318,357) in dog and human MI, support the idea that **salvage of geometry, function and lives might be greater with exposure to LV unloading throughout healing post-MI.** ACE inhibitor trials after MI showed a further small decrease in mortality ($\leq$ 7%) and morbidity in **selected patients** (121,125,134-141,145). Comparison of captopril and nitrate in dogs showed benefit on LV dilatation, mass and function with both agents, but infarct collagen was less with captopril and thinning less with nitrate (131). Also in dogs, enalapril decreased infarct collagen more than captopril (129) and made the scars flatter (131). This finding suggested that all ACE inhibitors were not equal.

There is general agreement that hypotension should be avoided when using vasodilators for LV unloading during MI (28,122,123). A **paradoxical J-curve effect** was demonstrated with high doses of NTG (100,122). This may also be important for salvage of muscle and healthy healing after MI. The concept that a border zone is potentially salvageable if flow is restored (149), or oxygen demands are decreased, or cellular and metabolic factors are improved (87), is still pertinent since early therapy is needed to optimize myocardial salvage during MI (153) and attenuate early expansion (22,23,67).

The negative results of the CONSENSUS II trial (123), the lack of early separation of survival curves in other trials with ACE inhibitors (121,135,136), the persistent LV dysfunction after early captopril in rats (338), and the persistent mortality after captopril in rats with large MI (77), might have been related to negative effects of early ACE-inhibition on blood pressure and collagen and ECM deposition in the infarct zone (55,354,358).

Fifth, the timing of anti-remodelling therapy relative to the infarct collagen plateau is an important factor for outcome during healing after MI.

The progressive and dynamic nature of the remodelling process during healing after MI suggests that timing and duration of therapy is important (22,338). The remodelling substrate also changes drastically during healing. The results presented in this thesis suggested that early and prolonged therapy should be used

(21). Early short-term therapy was shown to exert profound late effects on remodelling via effects on infarct size and early healing (28,55,103). Several reports in the 1990's indicated disease progression while on ACE-inhibition and favoured prolonged therapy beyond healing (26). Others suggested higher doses of ACE inhibitors.

The pathophysiological data presented in this thesis suggest that anti-remodelling therapy, applied before and after the infarct collagen plateaus, may produce different outcomes by modifying the determinants of remodelling and/or the substrate (22), such as the infarct size, healing process, deformation forces, LV loading conditions and wall tension. It may also modify the process during very early (first 24 h) and early remodelling (first 2 weeks) before infarct collagen plateaus, and late remodelling (3 to 6 weeks) after infarct collagen plateaus in dogs. Processes occurring before the collagen plateau include ECM degradation, infarct expansion, myocyte slippage, inflammation and fibroblast proliferation. After the collagen plateau, processes include compaction of infarct collagen, scar thinning, hypertrophy, formation of connections between collagen fibrils in the infarct and myocytes in the non-infarct zones (284) and fibroblast transformation to myofibroblasts containing actin filaments that mediate scar contraction (359).

6.2. Caution with the use of anti-fibrotic agents after MI

The aim of anti-fibrotic therapy is to inhibit or reverse cardiac fibrosis and its adverse effects on LV function (278). Potential approaches have been reviewed elsewhere (278). Anti-fibrotic therapy may be beneficial for non-infarcted hearts with chronic LV pressure overload (278) and possibly for ischaemic cardiomyopathy and the non-infarct zone after remote MI (360). However, caution might be advisable in idiopathic dilated cardiomyopathy without MI, because of the altered MMP/TIMP balance with increased MMPs and decreased TIMPs, and reduced cross-linking (277). Collective evidence emerging from experimental and clinical studies using anti-remodelling strategies after MI suggest that careful attention should also be given to timing, especially because **anti-fibrotic agents exert global actions that can affect both the infarct and non-infarct zones**. Experimental data on the temporal evolution of healing and ECM remodelling (22, 278,291) suggest that these agents could potentially enhance adverse ECM remodelling in the infarct zone **during the highly vulnerable periods of very early**

and early stages of healing after MI. It might also be prudent to exercise caution during the phase beyond scar formation (27).

6.3. Protecting the ECM in the infarct zone after MI

There is now consensus that LV remodelling after MI contributes significantly to LV dilatation and dysfunction, disability and death (23). Two paradigms, pertinent to anti-remodelling therapy, have evolved over the last 3 decades (27). The first paradigm, that LV remodelling is a major mechanism for disability and death (22,23) has received a great deal of attention. In contrast, paradigm 2, that remodelling of the ECM plays a major role in LV remodelling (277,278,291,293), whereby decrease, disruption and/or defective composition of the ECM promote LV dilatation and rupture (277-279,293) has received little attention. This is despite acknowledgement that myocardial collagen and the supporting ECM play protective roles in adverse LV remodelling during healing after MI (22,23,41,73,74, 129,164,277,294,295,308,) and should be preserved (22,23,27).

Many clinical trials have shown that ACE inhibitors with or without aldosterone antagonists, ARBs, beta-adrenergic blockers or reperfusion improve outcome in survivors of MI (134,308,361). However, the anti-fibrotic action of ACE inhibitors, aldosterone antagonists and ARBs on ECM in the infarct zone and non-infarct zone (277,278,295,308) and the reperfusion-induced damage to the ECM in the infarct zone (164,278,293) still need to be reconciled with the benefits (49,134,308,361). Although growth hormone was shown to stimulate post-MI repair, increase IZ scar collagen and reduce LV aneurysm formation (278), such approaches have not been actively pursued. Strategies to protect the ECM after MI, especially in the infarct zone, might further limit post-MI morbidity and mortality. Several factors could be targeted (27,278). In contrast to global approaches that target both the infarct and non-infarct zones with systemic delivery of adjunctive agents, **regional strategies could be applied to selectively protect the infarct zone against adverse ECM remodelling.** Monitoring using protein markers could be systematically applied to detect potentially adverse ECM remodelling during therapy (27,278). In addition, on the basis of the results presented in this thesis, **monitoring of the RSD and other LV remodelling indices by serial 2D-Echo may be helpful.**

6.4. Merits and limitations

There are several merits of the studies described in this thesis. A major strength is that the studies spanned the eras before and after the introduction of reperfusion therapy. They contain valuable data on moderate and large transmural MI that are less often seen in the 2000's. However, a significant number of patients still do not benefit from early reperfusion and optimal therapy as suggested in the latest ACC/AHA management guidelines (362), and present with large transmural MI or ST-elevation MI (STEMI), cardiogenic shock and significant RSD on 2D-Echo. Many patients receiving reperfusion therapy show RSD on endocardial contours and sub-epicardial aneurysms.

The results provide improved understanding of the pathophysiological mechanisms of LV remodelling during healing after MI. They also provide the rationale for the timing of anti-remodelling therapy. Importantly, they indicate that the effects of anti-remodelling therapy may be objectively assessed using non-invasive quantitative 2D-Echo imaging. 2D-Echo may also be used to stratify patients according to their topographic status and select high-risk patients for aggressive therapy.

As with all studies, there were several limitations in the research studies described in this thesis, but four deserve mention. **First**, it was necessary to select patients with a first MI for evaluation by 2D-Echo. **Second**, the 2D-Echo methods need to be applied in large clinical trials of potential anti-remodelling therapies. However, this has not been possible to date due to the lack of funds and support from the pharmaceutical industry, although the data from the studies were made available to the executive committees of several megatrials (23). **Third**, the computer software for the rapid analysis of quantitative 2D-Echo for the remodelling indices including RSD needs to be converted for general use. Despite the ability of 2D-Echo to provide quantitative data of robust remodelling indices, several trials have used areas to assess benefit (132), and have not taken advantage of the full potential of 2D-Echo imaging (125). **Fourth**, we focused on gross mechanisms of remodelling of LV shape and function between 1980 and 1988. Further studies are needed to address the biology of remodelling involving cells, proteins and molecules (27,190, 278).

6.5. Advances pertinent to the thesis

To place the thesis in perspective with current knowledge, it is necessary to consider pertinent advances that have impacted current strategies to limit, prevent or reverse remodelling after MI over nearly two decades. These advances may be considered under 3 headings: i) RAAS-inhibition; ii) nitrates and nitric oxide; and iii) novel concepts, approaches and technologies.

6.5.1. RAAS-inhibition

As mentioned previously, survivors of MI are at risk for death and disability. This is largely due to infarct-related complications such as adverse LV remodelling with progressive LV dilatation, dysfunction, heart failure, hypertrophy, and arrhythmias. Since heart failure is the end result of adverse remodelling among post-MI survivors and this group is increasing as a result of improved therapies for acute MI, the frequency of heart failure is also increasing. Finding improved therapies for heart failure in chronic MI is therefore an important goal (27).

The pertinent aspects of RAAS-inhibition in post-MI remodelling have been reviewed (363). As discussed before (pages 18-22, section 2.5.3.), angiotensin II, the primary effector molecule of the RAAS, is a major contributor to post-MI complications. Cumulative evidence indicates that angiotensin II is produced in both the circulation and tissues via ACE and non-ACE pathways (Figure 38), and has important physiological as well as pathophysiological actions, such as activation of other neurohumoral agonists including norepinephrine, aldosterone, endothelin and vasopressin that can be harmful (Figure 39). Although angiotensin II acts on both the angiotensin II type 1 (AT_1) and type 2 (AT_2) receptors (363,364), most of its effects are mediated through the AT_1 receptor (350). However, under certain conditions such as MI, healing post MI, heart failure, myocardial hypertrophy and vascular injury, the AT_2 receptor is up-regulated and may mediate some important cardiovascular effects of angiotensin II (363).

6.5.1.1. ACE inhibitor Trials

The original rationale for using ACE inhibitors was to inhibit ACE and thereby decrease angiotensin II formation (Figure 38a). This was supported by experimental studies in rats showing that chronic captopril therapy reduced LV dysfunction, LV remodelling and mortality in chronic MI (120).

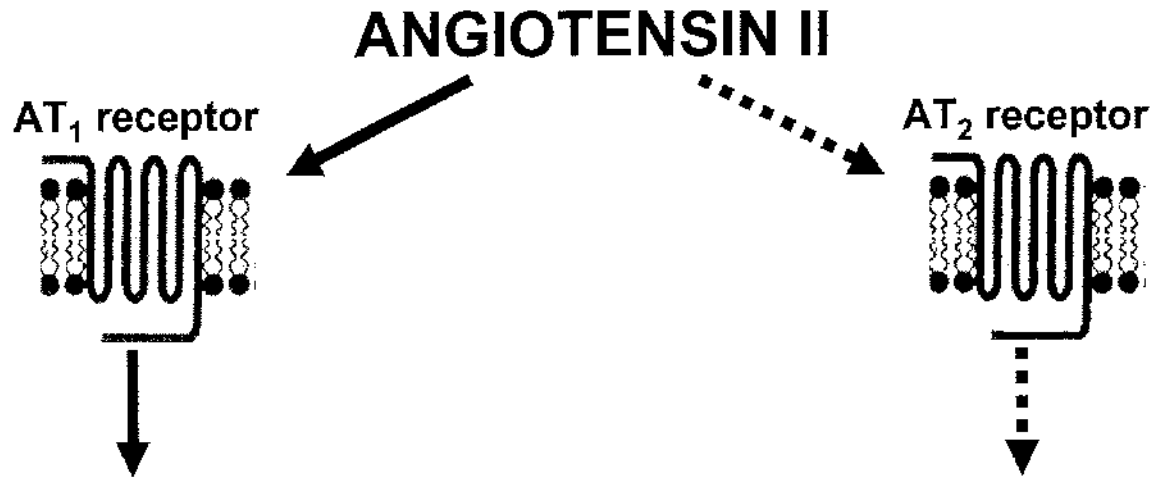

Vasoconstriction, direct and indirect
- Hypertension
- Increased LV impedance

Renal sodium resorption, volume expansion

Growth and Proliferation
- Hypertrophy
- Cardiac and vascular remodeling
- Fibrosis, collagen deposition
- Apoptosis

Activation of neurohumoral agonists
- Aldosterone
- Norepinephrine (sympathetic stimulation)
- Endothelin
- Vasopressin

Arrhythmogenic effects

Increased ischemia-reperfusion injury

Stimulate inflammation & oxidative stress in atherosclerosis
- Stimulate NADPH oxidase, superoxide
- Stimulate adhesion and chemo-attractant molecules
- Stimulate cytokines, matrix metalloproteinases
- Stimulate matrix expansion and fibrosis

Embryogenesis and development

Antigrowth, antiproliferation, antifibrosis

Apoptosis (vascular; myocyte)

Vasodilation

Cardioprotection during AT_1 blockade
- Stimulate kinin release and B_1/B_2 receptors
- Stimulate nitric oxide
- Stimulate prostaglandins
- Stimulate endothelin-derived hyperpolarizing factor
- Stimulate tissue plasminogen activator

Healing

Collagen synthesis

Ischemia-reperfusion injury

Figure 39. Major cardiovascular effects of angiotensin II.

Abbreviations as in text and pages xxi-xxiii. Updated from Jugdutt (363; Appendix 45)

Over the last two and a half decades, several randomized clinical trials have established ACE inhibitors for the treatment of MI, heart failure, and hypertension. Several trials (Table 16) showed that ACE inhibitors improve the survival of patients with MI (121,122,125,134,135,137-139,365, 366) and heart failure (122,142,143,145). The ACE inhibitor trials showed a survival benefit in over 100,000 patients with acute (367) and chronic (368) MI. The greatest benefits were found in the high-risk patients with LV dysfunction (369). ACE inhibitors in the SAVE (121,368), AIRE (139) and TRACE (365) trials reduced all-cause mortality, non-fatal cardiovascular events such as hospitalization for heart failure and recurrent MI, providing strong evidence that ACE inhibitors reduce mortality and morbidity in post-MI survivors.

TABLE 16. Trials of ACE inhibitors in heart failure and myocardial infarction

Year (Reference)	Trial	Number of patients	ACE-inhibitor	Disease
1987 (142)	CONSENSUS	253	Enalapril	HF
1991 (143)	SOLVD, symptomatic	2,569	Enalapril	HF
1992 (145)	SOLVD, asymptomatic	4,228	Enalapril	HF
1992 (123)	CONSENSUS II	6,090	Enalapril	MI
1992 (121)	SAVE	512	Captopril	MI
1993 (139)	AIRE	2,006	Ramipril	MI
1994 (136)	GISSI-3	19,394	Lisinopril	MI
1995 (135)	ISIS-4	58,050	Captopril	MI
1995 (140,365)	TRACE	6,676	Trandolapril	MI
1995 (137)	CCS-1	13,634	Captopril	MI
1995 (138)	SMILE	1,556	Zofenopril	MI
1996 (366)	GISSI-3	19,394	Lisinopril	MI
1997 (124,125)	HEART	352	Ramipril	MI

Abbreviations: HF, heart failure; MI, myocardial infarction. Other abbreviations as in the text and Abbreviation List (pages xxi to xxiii).

6.5.1.2. ARB Trials

The rationale for using ARBs was that they provide specific and selective blockade of angiotensin II at the AT_1 receptor. In view of the previously established benefits of ACE inhibitors, three other reasons were subsequently put forward for using an ARB. These included: i) more complete blockade of the effects of angiotensin II derived from all sources; ii) absence of inhibition of kininase II or increase in bradykinin which cause side-effects associated with ACE inhibitors, such as cough, angio-oedema, and hypotension; and iii) unopposed stimulation of the AT_2 receptor that may augment its beneficial effects (Figure 39).

Subsequent studies revealed that the cardioprotective effects of ACE-inhibition are not only related to blockade of angiotensin II formation via ACE but also the inhibition of breakdown of bradykinin via kininase II activity (Figure 38b). Thus during ACE-inhibition, the amount of angiotensin II presented to AT_1 and AT_2 receptors is decreased, at least initially, so that decreased AT_1 and AT_2 effects would be expected. However, the increase in bradykinin stimulates NO, PGI_2, EDHF, and tissue-thromboplastin activator (t-PA), thereby contributing to the vasodilatation, cardiovascular protection and other favourable vascular effects associated with ACE-inhibition (370). Of note, increased bradykinin during ACE-inhibition may also contribute to the hypotensive effect of ACE inhibitors.

In contrast, the cardioprotective effect of ARBs is mediated largely by AT_1 blockade and only partly via AT_2 receptor activation and via release of kinins and stimulation of kinin B_1 and B_2 receptors (371,372) or direct AT_2-mediated signaling via protein kinase C (PKC_ε), NO, and cGMP (373-375) (Figure 38b). Evidence to date suggests that this bradykinin-dependent protective pathway involving NO and PGI_2 is quantitatively greater with ACE inhibitors than ARBs.

The finding that angiotensin II levels persist during long-term therapy with ACE inhibitors (376,377) drew attention to the fact that ACE inhibitors do not block the formation of angiotensin II from angiotensin I via chymase or other non-ACE enzymes, or that from angiotensinogen via non-renin pathways (Figure 38). This finding promoted the idea that the combination of an ACE inhibitor and an ARB may achieve more complete blockade of the deleterious effects of angiotensin II and produce greater benefits. Some support for this concept was provided by experimental (378) and clinical (379) studies in heart failure.

Over the last nearly two decades, several randomized clinical trials (Table 17) have investigated the benefits of blocking the effects of angiotensin II via the AT_1 receptor using selective AT_1 receptor blockers (ARBs) in patients with MI (380,381), heart failure (382-387), and hypertension (388-390). Because ARBs were introduced after ACE inhibitors had been shown to be beneficial, it became necessary to demonstrate that ARBs were either superior to ACE inhibitors or equally effective in patients who were intolerant to ACE inhibitors and receiving other background therapies rather than relative to a true placebo group.

TABLE 17. Trials of ARBs in heart failure and myocardial infarction

Year (Reference)	Trial	Number of patients	ARB	Disease
1997 (382)	ELITE	722	Losartan	HF
1999 (392)	RESOLVD	768	Candesartan	HF
2000 (383)	ELITE II	3,152	Losartan	HF
2001 (361)	Val-HeFT	5,010	Valsartan	HF
2002 (380)	OPTIMAAL	5,477	Losartan	MI
2003 (384)	CHARM-Overall	7,601	Candesartan	HF
2003 (385)	CHARM-Added	2,548	Candesartan	HF
2003 (386)	CHARM-Alternative	2,028	Candesartan	HF
2003 (387)	CHARM-Preserved	3,023	Candesartan	HF
2003 (381)	VALIANT	14,703	Valsartan	MI

Abbreviations: HF, heart failure; MI, myocardial infarction. Other abbreviations as in the text and Abbreviation List (pages xxi to xxiii).

6.5.1.3. ELITE and CHARM

In the evaluation of 'losartan in the elderly' (ELITE) study of chronic heart failure patients (382), losartan showed an unexpected reduction in the secondary end-point of all-cause mortality by 46% relative to captopril. Although the study was small and not designed to assess mortality, this effect was felt to be due primarily to a reduction in sudden cardiac death. However, the ELITE II heart failure trial

(383), which was designed to assess superiority of losartan over captopril in reducing mortality, showed similar survival rates.

In the large 'candesartan in heart failure assessment of reduction in mortality and morbidity' (CHARM) trials (384-387), the ARB candesartan improved cardiovascular death or heart failure hospitalization in patients taking ACE inhibitors as well as those intolerant to ACE inhibitors. Importantly, compared to placebo in patients not receiving ACE inhibitors, candesartan reduced the composite primary end-point of cardiovascular death or admission for heart failure (P=0.001) although overall mortality did not improve (P=0.11) (386). In a sub-study of patients with low LV ejection fraction (≤ 40%) in the CHARM trial, candesartan reduced all-cause mortality, cardiovascular death and heart failure hospitalizations (391).

6.5.1.4. RESOLVD pilot study

In the 'randomized evaluation of strategies for left ventricular dysfunction' (RESOLVD) pilot study, candesartan was compared to enalapril and the combination (392). This small study suggested that combined therapy more effectively prevented LV remodelling than monotherapy. However, the study was prematurely terminated because of an early trend in increased mortality and heart failure hospitalization (secondary end-point) in the candesartan and combined therapy groups (392).

6.5.1.5. OPTIMAAL

In the 'optimal therapy in myocardial infarction with the angiotensin II antagonist losartan' (OPTIMAAL) trial (380), which was designed to test for superiority of an ARB on survival and other major cardiovascular outcomes in high-risk post-MI heart failure patients with captopril as comparator, losartan did not show superiority over captopril. Cardiovascular death was clearly less with captopril (P=0.035) while other outcomes were similar in the two groups. However, a non-significant trend favoured captopril for the primary end-point of all-cause mortality (P=0.069) but did not satisfy the criteria for non-inferiority.

6.5.1.6. VALIANT

In the 'valsartan in acute myocardial infarction trial, (VALIANT) (381), which was designed to assess superiority of the ARB valsartan over the ACE inhibitor

captopril as comparator on top of background therapy, the efficacy and safety of long-term treatment with valsartan, captopril and their combination was compared in 14,703 high-risk patients with MI and LV systolic dysfunction (ejection fraction < 40%) and/or heart failure (381). The patient selection matched that in the SAVE, AIRE and TRACE studies. The patients were randomized 0.5 to 10 days after acute MI and followed for a median period of 24.7 months. There was no difference in the primary end-point of all-cause mortality. Comparing valsartan with captopril, the upper limit of one-sided 97.5% confidence interval was within the pre-specified margin for non-inferiority for mortality (P=0.004) and the composite end-point of fatal and non-fatal events (P<0.001). Thus, valsartan was non-inferior to captopril. However, adverse events were greater with the combination of valsartan and captopril. Valsartan monotherapy was associated with more hypotension and renal dysfunction, and captopril monotherapy with cough, rash and taste disturbance.

This study established quite conclusively that valsartan was as effective as captopril in reducing mortality in high-risk patients after MI. However, the authors also performed a statistical comparison of the VALIANT results with those of SAVE, AIRE and TRACE using an imputed placebo, and showed that the 25% risk reduction in all-cause mortality in VALIANT was comparable to those in the ACE inhibitor trials.

The finding that the valsartan plus captopril combination increased adverse events including hypotension underscores the need for careful monitoring of blood pressure when combining RAAS inhibitors after MI and supports the caveat regarding vasodilator-induced hypotension in acute MI.

An interesting finding in VALIANT was the disproportionately high rates of heart failure, re-infarction, and stroke which accounted for more than 50% of the early mortality (381). In a sub-study (393), 21.5% of the 14,703 patients were elderly (age ≥ 75 years) and their outcomes remained poor. In fact, with increasing age in 4 sub-groups, the 3-year mortality quadrupled, composite end-points doubled, and heart failure admissions tripled. Adverse events from captopril and valsartan, or both, were also more common in the elderly. In another sub-study (394), 1.5% of patients with post-MI heart failure developed stroke and the stroke victims had greater in-hospital mortality (27.2 versus 6.5%, P<0.001) and more frequently had atrial fibrillation.

6.5.1.7. Val-HeFT

In Val-HeFT (361), which randomized 5,010 patients with heart failure to treatment with valsartan or placebo on top of standard therapy consisting of ACE inhibitors (93%), digoxin (67%), beta-blockers (35%), and the aldosterone blocker spironolactone (5%), valsartan did not reduce the primary end-point of all-cause mortality. However, valsartan reduced the composite end-point of mortality and morbidity, improved clinical signs and symptoms of heart failure, and decreased heart failure hospitalizations.

A post-hoc analysis of the combined end-point revealed that valsartan had a favourable effect in patients who did not receive ACE inhibitors or beta-blockers, but an adverse effect in the 30% of patients who received the combination of valsartan, ACE inhibitor and beta-blocker (361). In a sub-study of Val-HeFT (395), valsartan improved LV size and ejection fraction in all groups except those taking valsartan together with an ACE inhibitor and a beta-blocker.

However, this negative finding with triple therapy differs from those of the CHARM trials (384-387) and should not detract from the important benefits in Val-HeFT. For example, valsartan decreased mortality by 33% (P=0.017) and the combined end-point by 44% (P<0.001) in patients not taking ACE inhibitors, (395), supporting the use of valsartan as an alternative in patients intolerant to ACE inhibitors. Valsartan also improved the secondary end-points in Val-HeFT.

Sub-studies of Val-HeFT provided further support for RAAS-inhibition. In one sub-study (396), the addition of valsartan on top of background therapy for heart failure including beta-blockers and ACE inhibitors, was associated with a 37% reduction in atrial fibrillation, which has been linked to adverse atrial remodelling and poor clinical outcome. In another sub-study (397), valsartan reduced levels of brain natriuretic peptide (BNP) and plasma norepinephrine, which have been linked to poor outcome. Another sub-study showed that valsartan reduced aldosterone in all sub-groups despite different outcomes (398). In yet another sub-study, valsartan decreased plasma aldosterone and norepinephrine in chronic heart failure patients, and those receiving 4 weeks of standard ACE inhibitor therapy had "physiologically active levels of angiotensin II" which did not rise with co-administration of valsartan (399).

6.5.1.8. RALES and EPHESUS

The rationale for using aldosterone blockade in heart failure is two-fold. First, angiotensin II stimulates the release of aldosterone (Figure 39), thereby activating the mineralo-corticoid receptor. Second, activation of the mineralo-corticoid receptor persists despite the use of ACE inhibitors, ARBs and beta-blockers (400).

Apart from increasing sodium retention and potassium loss, aldosterone causes myocardial and vascular fibrosis, vascular damage and baroreceptor dysfunction, and inhibits myocardial norepinephrine uptake (400). Aldosterone also generates oxygen free radicals and aldosterone blockade decreases vascular NADPH oxidase activity and reactive oxygen species, and improves availability of NO and endothelial function (400). Aldosterone blockade has been shown to limit LV remodelling, fibrosis, MMP activation and angiogenesis in the coronary embolization model of heart failure in dogs (401), and limit collagen synthesis and LV remodelling as assessed by LV volumes on 2D-Echo in post-MI patients (402).

Two large trials have shown that aldosterone blockade reduces total mortality and hospitalization for heart failure in post-MI patients with LV systolic dysfunction (310). In the 'randomized aldactone evaluation study' (RALES), 1,663 patients with chronic heart failure (LV ejection fraction $\leq$ 35%) received the aldosterone blocker spironolactone or placebo on top of background therapy with an ACE inhibitor, diuretic, digoxin and beta-blocker (403). This trial was prematurely terminated due to the finding of a 30% reduction in all-cause mortality ($P<0.001$). In the 'eplerenone post acute MI efficacy and survival study' (EPHESUS), 6,642 patients with acute MI, LV ejection fraction $\leq$ 40% and heart failure were randomized to receive the selective aldosterone blocker, eplerenone or placebo on top of optimal background therapy (310). Eplerenone reduced all-cause mortality by 15 % ($P = 0.008$) and cardiovascular mortality by 17% ($P = 0.005$). Although serious hyperkalemia increased by 1% and 1.6%, respectively, in these studies, this did not result in deaths.

In a sub-study of RALES (308), spironolactone was associated with increased levels of markers of cardiac fibrosis or collagen synthesis, suggesting that limitation of excessive ECM turnover may have contributed to the benefits. In a sub-study of EPHESUS (404), eplerenone begun at a mean of 7.3 days after acute MI was shown to reduce the 30-day all-cause mortality, supporting the initiation of eplerenone in hospital.

6.5.1.9. RAAS-inhibition and prevention of LV remodelling in trials

The discovery that LV remodelling leads to progressive LV dilatation, a major determinant of post-MI survival and outcome that can be limited by RAAS-inhibition, represented a major paradigm shift that triggered several large randomized clinical trials. Despite these trials, however, there is to date (January 2006) a paucity of comprehensive data on effects of anti-remodelling agents on regional and global changes in topography, structure and function using 2D-Echo or other cardiac imaging modalities. Some reasons for this discrepancy have been the lack of funding and rapid methods for quantification.

Several post-MI trials, such as SAVE and HEART, used 2D-Echo evidence of a decrease in LV size (dimensions, areas, volumes) and increase in LV ejection fraction to support the beneficial effect of ACE inhibitors on LV remodelling (121,124,125,132,405). Thus, in a sub-study of SAVE (512 patients), 2D-Echo measures of LV cavity areas and the change in cavity area were shown to be predictors of adverse cardiovascular events and captopril decreased these areas and improved outcome (132). In HEART (312 patients), 2D-Echo measures of LV cavity area and volume ejection fraction improved with ramipril (125).

In a recently published sub-study of VALIANT (610 patients), 2D-Echo data showed similar changes in LV volume, ejection fraction, combined cavity areas, and infarct segment length over 20 months in groups receiving an ARB, ACE inhibitor or both (406). Importantly, baseline measures of LV volume, ejection fraction, and infarct segment length predicted outcome. To date (January 2006) and to the best of the author's knowledge, no 2D-Echo data on post-MI LV structural remodelling from RALES or EPHESUS have been published.

Several heart failure trials have reported beneficial effects of therapy on LV structural remodelling. In the 'vasodilator-heart failure trials' (V-HeFT) I and II (407), the mitral E-point septal separation (EPSS), LV internal diameter in systole (LVIDs), and the systolic radius to wall thickness ratio (Rs/THs) on 2D-Echo steered M-mode Echo in 642 patients were shown to predict mortality and reflect treatment effects in heart failure. These ACE inhibitor studies supported the use of the combination of a decrease in LV size and an increase in LV ejection fraction as a marker of regression of LV remodelling.

In Val-HeFT sub-studies (395,408), ARBs were suggested to limit adverse LV remodelling in heart failure on the basis of LV internal dimensions (2D-Echo steered M-mode Echo) and volume ejection fraction. Thus, in 5,010 patients with

moderate heart failure, valsartan added to an ACE inhibitor or beta-blocker was associated with improvement in LV size and function but this benefit was not found in patients taking valsartan and both ACE inhibitor and beta-blocker (395). Also in Val-HeFT, patients with the most LV dilatation (LV end-diastolic dimension ≥ 7.5 cm) and worse ejection fraction (less than 22%) benefited the most from the anti-remodelling effect of valsartan (408).

In RESOLVD, data on LV volumes and ejection fraction using radionuclide angiography in 768 patients with heart failure showed that the combination of candesartan and enalapril more effectively prevented LV remodelling (392).

To date (January 2006) and to the best of the author's knowldege, no 2D-Echo data on LV structural remodelling in heart failure from sub-studies of CHARM in heart failure have been published.

6.5.1.10. Expanding the RAAS-inhibition paradigm

In addition to infarct-related complications and progressive LV remodelling (27,37,247), post-MI survivors are at risk for further vascular remodelling, progressive atherosclerosis, myocardial ischaemia, recurrent MI, restenosis after coronary artery bypass surgery, metabolic syndrome and type II diabetes mellitus, peripheral artery disease, ventricular arrhythmias, ventricular dyssynchrony, atrial fibrillation and stroke. This risk may be partly due to genetic factors and continued exposure to the cardiovascular risk factors so that comprehensive secondary prevention is an important aspect of long-term therapy in survivors of MI.

Fifteen years ago, the treatment and prevention arms of SOLVD established that RAAS-inhibition with the ACE inhibitor enalapril offers protection against the development and progression of heart failure (143,145). Collective evidence from HOPE-TOO (409), the 'extension of the Heart outcomes protection evaluation' (HOPE) study (410), the 12 year extension of prevention SOLVD or 'SOLVD follow-up' (X-SOLVD) study (411), the 'extension of the AIRE' (AIREX) study (412), the 'losartan intervention for end-point reduction in hypertension' (LIFE) study (413) and its sub-study (414), suggest that prolonged RAAS-inhibition with ACE inhibitors and ARBs can effectively prolong life expectancy (415).

6.5.1.11. Summary and future directions

The totality of the evidence, from randomized clinical trials to 2005, supports the use RAAS-inhibition in post-MI survivors, with ACE inhibitors as first line therapy and ARBs and aldosterone antagonists as proven life-saving alternatives or add-ons. For patients intolerant to ACE inhibitors, results of trials support the use of valsartan and candesartan for post-MI and heart failure patients, respectively. Other potential indications for RAAS-inhibition include: i) limiting LV and atrial remodelling in MI survivors; ii) preventing atrial fibrillation and stroke, especially in MI survivors; iii) improving blood pressure control, cardiovascular protection and outcomes in hypertensive patients with LV hypertrophy; iv) reducing new onset diabetes and insulin resistance; v) preventing progression of atherosclerosis and its complications. Aggressive measures, including comprehensive RAAS-inhibition with ACE inhibitors, ARBs and aldosterone antagonists or on top of approved background therapies, may be needed for reducing risk in high-risk patients who do not achieve treatment targets recommended by evidence-based guidelines.

6.5.2. Nitrates and nitric oxide

Nitrates have formed part of cardiovascular therapeutics eversince Sir Lauder Brunton used amyl nitrate for therapy of angina pectoris in 1867. Nearly 12 decades later, work by Furchgott, Palmer, Ignarro, Moncada and others clarified that nitrates were NO donors and NO was the biological messenger that causes dilatation of coronary arteries. It was proposed that activation of NO synthase (NOS) leads to synthesis of endogenous NO from L-arginine whereas organic nitrates release NO via intracellular bioconversion. In that concept, NO then activates guanylyl cyclase, thereby increasing intracellular cGMP which mediates smooth muscle relaxation. In 1998, Nobel Prizes in Medicine were awarded to Furchgott, Ignarro and Murad for the discovery of NO as a signalling molecule in the cardiovascular system.

6.5.2.1. Nitrates in myocardial infarction and heart failure

The story of nitrates and NO is fraught with reports of both beneficial and deleterious effects (416,417). The evidence for the anti-ischaemic and cardioprotective effects of nitrates and the pathobiology of NO have been reviewed (38,100,101,333,418) and discussed (pages 17; 130-139) in this thesis.

In 1888, Stewart (419) first reported a case of nitrate tolerance in a patient who needed 20 grains of NTG to achieve the same decrease in blood pressure as induced by an initial dose of 1/100 grain, representing a 2000-fold increase. In 1932, Prodger (420) warned that too much nitrate resulted in hypotension. Currently, there is consensus that short-term nitrates are effective for the treatment of myocardial ischaemia and acute MI (100,101,333,418) but efficacy is markedly reduced with long-term nitrates due to the development of tolerance (333). This nitrate tolerance is partly related to continuous dosing, high dosage and potency of the preparation.

Experimentally, nitrate given in low dose and eccentric dosing with a nitrate-free interval has been shown to be beneficial after MI (48,103). Clinically, chronic nitrate in low dose was shown to be effective in one published trial (357,421), one published study presented in this thesis (105-107,109) and one unpublished study described in this thesis (109,298). In all these studies, the nitrates improved LV function and prevented remodelling post MI (105-109,298). Also clinically, low-dose intravenous NTG infusion for 48 hours in high-risk patients reduced LV dysfunction, acute infarct expansion, subsequent adverse LV remodelling, infarct-related complications and one-year mortality after acute MI (28). This effect was dose, blood pressure and preparation sensitive (28,118,122). A meta-analysis of various randomized clinical trials in MI using different nitrate preparations confirmed the benefits (344).

However, subsequent comparison of various nitrates and ACE inhibitors after MI in large trials did not show significant lasting benefit (135-137), probably because of hypotension and nitrate tolerance. In addition, a study of 1,002 patients with 'healed' MI (> 7 days post MI) treated with long-term sublingual or intravenous ISDN as well as NTG showed an increase in cardiac events (422). A meta-analysis suggested that nitrates might be harmful post MI (423). In a study of transdermal NTG in patients with angina pectoris, NTG reduced anginal attacks but did not prevent silent ischaemia (424). In the 'transderm-nitro trial' of chronic angina, some patients experienced increased angina during the patch-off intervals (425). Collectively, these studies suggest that the long-term nitrates as primary therapy after MI and a daily nitrate-free interval might not be prudent.

6.5.2.2. Mechanisms of nitrate action and tolerance

Our understanding of nitrate action and tolerance has increased over the last

decade (see 426 for review). In the prevalent NTG/NO hypothesis, NTG-induced vascular relaxation is due, in sequence, to activation of soluble guanylyl cyclase, increase in cGMP, activation of cGMP-dependent protein kinases and/or cyclic nucleotide-gated ion channels (427). NTG and other nitrates appear to share the same signalling pathway as NO generated via NOS. Although NTG bioconversion appears to be essential for cGMP formation, precisely how NTG activates guanylyl cyclase remains controversial.

The studies that favoured the NTG/NO hypothesis used very high NTG concentrations. Recent studies from Munzel's group (426) suggest that NTG activates the guanylyl cyclase/c-GMP protein kinase pathway independently of bioconversion to NO. Importantly, different activation pathways seem to be involved for low (therapeutic) and high (pharmacological) concentrations of NTG. The pathway used at the low anti-ischaemic and vasodilating concentrations generates low amounts of NO. At the low concentrations, the biotransformation of NTG appears to involve the mitochondrial isoform of aldehyde dehydrogenase (ALDH-2) (428). In contrast, high doses of high potency nitrates, such as NTG, and low potency nitrates, such as ISDN and ISMN, generate higher and measurable amounts of NO (426). Recently, Moncada's group used confocal microscopy to observe endothelium-synthesized NO and suggested that high concentrations of NTG do not release free NO, so that the action of NTG may not be related to its bioconversion to NO but rather to a different species that does not inhibit oxygen consumption by vascular mitochondria (429). The authors speculated that this may explain 'the long clinical success' of NTG (429).

Munzel's group has made various major contributions to the understanding of nitrate tolerance (426). Until a decade ago, two mechanisms of nitrate tolerance were recognized: i) neurohumoral counter-regulation, or 'pseudotolerance', associated with short-term treatment and involving increased intravascular volume and levels of catecholamines, vasopressin, renin, angiotensin II, and aldosterone; and ii) vascular or intrinsic tolerance, associated with chronic treatment and involving increased sensitivity to receptor-dependent vasoconstrictors such as endothelin-1 and big endothelin-1, which activate protein kinase C (PKC). Subsequently proposed mechanisms include increased activity of phosphodiesterase 1A1, desensitization of soluble guanylyl cyclase, increased production of reactive oxygen species, and impairment of nitrate biotransformation. Sydow in Munzel's group proposed another mechanism

involving NTG-induced mitochondrial production on reactive oxygen species and inhibition of ALDH-2 (which bioactivates NTG) (430). A major contributor to vascular tolerance is superoxide (O_2^-), a physiologically reactive free radical. Increased vascular superoxide reacts with vascular NO to form peroxynitrite ($ONOO^-$), which in turn leads to uncoupling of NOS and inhibition of soluble guanylyl cyclase and PGI_2 synthase. Although NO interacts readily with superoxide, providing detoxification, the resulting peroxynitrite may damage blood vessels and oxidize lipids. This oxidative stress hypothesis may explain why anti-oxidants reduce nitrate tolerance.

6.5.2.3. Biology of nitric oxide in the cardiovascular system

This topic has been reviewed (416-418). Nitric oxide ($NO^\cdot$ or NO) is a ubiquitous molecule that can have beneficial and deleterious effects depending on conditions. In nature, NO is a poisonous gas that is formed by oxidation of ammonia and is generated by incomplete combustion of gasoline in exhausts. In physiologic solutions, NO has a short half-life. In tissues, NO is a physiological regulator that plays key roles in signal transduction and cytotoxicity and participates in physiological functions, such as vasodilation, neurotransmission, and elimination of pathogens. Being an uncharged molecule, NO diffuses freely across cell membranes. NO also plays a major role in the pathophysiology of several diseases in the cardiovascular and other systems.

The biological actions of NO in the cardiovascular system are quite complex. Since NO is a free radical with an unpaired electron in the π molecular orbital, this electronic configuration imparts high reactivity to the molecule. Collective evidence indicates that NO acts by several mechanisms, including activation of soluble guanylyl cyclase, S-nitrosylation of thiols, and formation of peroxynitrite.

Whether NO is cytotoxic or cytoprotective depends on the form of delivery or transport and the quantity. Three NOSs have been cloned. Constitutive endothelial eNOS and neuronal nNOS release small amounts of NO transiently while inducible iNOS releases large amounts for prolonged periods. NO is protective in small amounts but toxic in excess. Low dose NO increases cardiac contractility while high dose NO reduces contractility. Increased angiotensin II inactivates NO, forms peroxynitrite and produces cardiotoxicity. NO produces post-translational modification of several effector molecules. S-nitrosylation may

be key in regulating myocardial performance and vascular tone.

The interaction between NO and superoxide, referred to as the nitroso-redox balance, plays a critical role in cardiovascular disease. Physiologically, the levels and location of NO and the production of superoxide are balanced within the cell. This facilitates post-translational modification of the effector proteins. Pathophysiologically, as in heart failure, the level and location of NO synthesis and excessive superoxide production result in interruption of effector signalling, leading to vasoconstriction, decreased contractility, cellular dysfunction and cell injury or cell death. Increased angiotensin II after ischaemia-reperfusion may contribute to injury by inactivating NO and forming peroxynitrite. Therapies that enhance NO bioavailability by increasing eNOS may be beneficial after ischaemia-reperfusion. This may explain the reports of beneficial effects of low-dose intravenous NTG (50) and ACE inhibitors (352) or ARBs (373-375) in reperfused acute MI.

Genetic mouse models of NOS deletion and over-expression have been studied. In rats, eNOS expression is decreased after MI. In mice, eNOS deletion is associated with increased mortality and over-expression with improved survival and limitation of LV dysfunction and remodelling after MI. In 2005, nNOS deficiency in mice was also reported to increase mortality and remodelling (431) and functional deterioration (432) after MI.

Several studies have underscored the cardioprotective role of NO in coronary artery disease, ischaemic preconditioning, ischaemia-reperfusion and heart failure (see 433 for review: **Appendix 46**). After ischaemia-reperfusion, low levels of NO are beneficial but high levels are harmful and contribute to reperfusion injury. Thus, reperfusion of ischaemic myocardium triggers the release of oxygen free radicals and a cascade involving endothelial dysfunction, decreased eNOS and eNOS-derived NO, neutrophil activation, increased cytokines, further increase in oxygen free radicals, increased iNOS and high levels of iNOS-derived NO, increased peroxynitrite, and cellular injury.

6.5.2.4. Hydralazine and prevention of nitrate tolerance

Agents with anti-oxidant properties might prevent nitrate tolerance (426). Potential agents include ACE inhibitors, ARBs, statins, L-arginine, tetra-hydrobiopterin (BH_4, co-factor for eNOS), ascorbic acid, ebselen and uric acid

(which decrease mitochondrial production of reactive oxygen species and preserve ALDH-2), and hydralazine.

Hydralazine interacts favourably with nitrates in several ways. It not only inhibits superoxide production but also iNOS and cyclo-oxygenase-2 (COX-2). It is also pro-angiogenic. The rationale proposed for combining ISDN and hydralazine is that ISDN stimulates the NO pathway (eNOS) while hydralazine inhibits superoxide production and iNOS, so that together they may restore the balance between NO and superoxide production.

Experimentally, hydralazine combined with ISDN was shown to prevent nitrate tolerance and improve mortality (434). The combination also improved mortality in patients with heart failure (144). In the recent 'African-American heart failure trial' (A-HeFT), the addition of ISDN and hydralazine on top of standard therapy increased survival in the African-Americans with advanced heart failure (435). This beneficial effect of hydralazine appears to involve its anti-oxidant properties, with inhibition of the activation of membrane-bound NADH oxidase (436) and inhibition of superoxide generation. The venodilatory effect of nitrate complements the arteriolar dilatory effect of hydralazine (86, 437). A sub-study of A-HeFT showed that the fixed-dose combination of ISDN and hydralazine reduced hospitalizations and was cost-effective in African-Americans (438). Another sub-study underscored the importance of considering ethnicity in clinical trials (439).

In summary, studies presented in this thesis illustrate the general principle that ventricular unloading therapy yields maximal benefit when it is begun very early and is prolonged, spans the infarct-healing process and extends beyond. The overall evidence to date does not favour long-term nitrates. However, the combination with hydralazine is beneficial in African-Americans. The caveat concerning avoidance of hypotension and the paradoxical J-curve effect with early unloading therapy after MI still applies (100,122,123, 440). Irrespective of the therapeutic approach that is selected, outcome depends critically on the timing and duration of therapy, and attention to the pathological processes.

6.5.3. Novel concepts, approaches and technologies

New knowledge of the biology of remodelling after MI underscores its complexity and the participation of various molecules, including cytokines, growth factors and hormones as well as various cellular responses and signalling pathways (27,278). Numerous new therapies are being proposed to modify and modulate these

processes in efforts to optimize outcome. New approaches to limit remodelling after MI include application of novel pharmacological interventions that target the damaged myocardium, the supporting ECM or both.

6.5.3.1. Myocardial salvage and cardioprotection

Advances were made in five major areas.

First, improved reperfusion strategies, with thrombolytic and anti-platelet agents and percutaneous coronary intervention (PCI), have impacted positively on outcome post MI. However, despite extensively documented overall benefits of reperfusion, ACE inhibitors, beta-blockers, statins, aspirin, ARBs and aldosterone antagonists after MI, cardiac enlargement and heart failure remain problematic (441), especially in survivors of ST-segment elevation MI (STEMI) (442). A challenge after reperfused STEMI is reperfusion injury, with myocardial stunning and persistent LV dysfunction, inflammation and cellular responses linked with healing, increased MMPs, ECM damage, decreased infarct collagen, decreased density of collagen cross-links, increased ruptures, necrosis and apoptosis, and no-reflow (27,442,443). Adjunctive therapies to protect against early ECM damage and decrease reperfusion injury in STEMI are therefore being studied. Combining regional therapy with a selective MMP inhibitor and an ARB during PCI plus stenting and abciximab very early after STEMI, might provide the opportunity to preserve more myocardium and ECM, and thereby improve outcome.

Second, novel drugs aimed at protecting the ischaemic myocardium have been developed for potential clinical application. One approach involves the use of metabolic modulators. Perhexiline, an anti-anginal drug that augments glucose metabolism by blocking mitochondrial free fatty acid uptake, has been shown to improve peak exercise oxygen consumption, LV ejection fraction, other measures of function, and skeletal muscle energetics in patients with heart failure (444). Whether metabolic modulators might improve remodelling needs study.

Third, stem cell therapy aimed at myocardial regeneration is being developed to repair injured hearts. In one report in 2005 (445), the granulocyte-colony-stimulating factor (G-CSF) was given after reperfusion (primary PCI/ stenting and abciximab) in patients with acute STEMI. G-CSF mediates mobilization of CD34+ mononuclear blood stem cells (MNC^{CD34+}). The patients showed improvement in metabolism (^{18}F-deoxyglucose uptake) in the infarct

zone, and LV ejection fraction and decrease in LV diastolic dimension on Echo, suggesting prevention of remodelling.

Fourth, inhibitors of apoptosis or programmed cell death (190) may prevent more myocardium and prevent remodelling. Until recently, cardiologists endorsed the dogma that the heart is terminally differentiated with no regenerative capacity and opposed the concept of apoptosis (446). Evidence from experimental and clinical studies indicate that cardiomyocyte cell death early after the onset of acute MI involves apoptosis followed by necrosis (188,190,447). In addition, low-grade apoptosis contributes to LV remodelling in chronic MI (448). The application of confocal microscopy (449), the use of biochemical markers (449), and the application of in-vivo imaging techniques for apoptosis using annexin-V (450,451) have advanced apoptosis research (190). Importantly, early interventions have been shown to prevent necrosis (452) as well as apoptosis (453,454) after acute ischaemia or ischaemia-reperfusion and long-term interventions have been shown to prevent apoptosis and adverse remodelling (455,456). Although these interventions involved RAAS inhibitors (454,456) and broad-spectrum caspase inhibitors (453,456), more selective anti-apoptotic agents are being developed. It might therefore be possible to target early apoptosis and necrosis in acute MI as well as long-term apoptosis in chronic MI, and quantify the effects using in-vivo imaging of apoptosis in studies aimed at preventing post-MI remodelling.

Fifth, therapies targeted at cytokines and the inflammatory process have been tested. Agents such as tumor necrosis factor-α (TNF-α) antagonists and endothelin antagonists were studied in clinical trials of heart failure and found not to be beneficial despite their benefit in experimental studies (457). Recently, large randomized clinical trials of COX-2 inhibitors (rofecoxib, celecoxib, and valdecoxib) for various indications confirmed cardiovascular toxicity (458,459).

6.5.3.2. Protecting the supporting extracellular matrix

Several approaches have been proposed.

First, MMP-inhibition is aimed at preventing ECM damage. The rationales (27,278) include: i) the ECM plays a critical role in both early and late LV remodelling after MI; ii) activation of MMPs that degrade the ECM has been linked to adverse LV remodelling; iii) a fine balance between MMPs and TIMPs is essential for maintaining ECM integrity and optimal structural support; and iv)

selective MMP inhibitors are becoming available. The inflammatory and healing responses elicited by acute MI involve inflammatory, fibroblast and vascular cells as well as growth factors, bioactive proteins and cytokines. In addition, a sharp rise in MMP above that of TIMP drives rapid ECM degradation, myocyte slippage and acute infarct expansion (early remodelling). Subsequently, MMP and TIMP levels subside but chronically higher MMP than TIMP in some hearts favour continued matrix degradation, thereby contributing to progressive, global LV dilatation. In contrast, higher TIMP than MMP levels and activities in remote MI contribute to increased ECM deposition and interstitial fibrosis. Release of growth factors (such as TGF-β) (460) and cytokines (including angiotensin II, TNF-α and interleukin-10) (443) into the interstitial space seem to modulate MMP/TIMP expression and ECM degradation or interstitial fibrosis.

To date, over 20 MMPs and 4 TIMPs have been described (27). MMPs are synthesized by many cells in a latent form (pro-MMP) and activated by proteolytic cleavage or conformational changes. Several MMPs, including MMP-2 and MMP-9, are associated with adverse LV remodelling after MI. Substrates for MMP-2 and MMP-9 include the three major collagen types I, II, and III that are involved in scar formation and fibrosis during healing after MI. However, the MMP-2 is constitutive while MMP-9 is inducible (461). In brief ischaemia-reperfusion, where inflammatory cells are absent, the major source of increased myocardial MMP-2 appears to be the myocyte. In contrast, the major source of increased myocardial MMP-9 during reperfused MI, where inflammation is enhanced, is the neutrophil and most likely involves MMP-9 induction. MMP-2 is the main MMP reported increased in rodents (462), whereas MMP-9 is the MMP reported increased in dogs with reperfused MI (461), suggesting differences among species.

All TIMPs may bind and inactivate MMPs, including MMP-2 and MMP-9. Decreased TIMP-3 is associated with adverse remodelling in human heart failure (463). Experimental studies using genetic mice or other models have implicated MMP activation in adverse remodelling after MI (303,304,464-468). For example, targeted deletion of MMP-9 attenuated LV dilation after MI in mice (303,464). Broad-spectrum MMP-inhibition limited late infarct expansion after MI in dogs (467). Data in MMP-2 and MMP-9 knock-out mice suggest that high MMP-2 and/or MMP-9 contribute to LV rupture after MI (464,469,470).

The recent PREMIER trial, using the broad-spectrum MMP-inhibitor PG-116,800 that was designed to target MMP-13 and MMPs 2, 3, 8, 9, and 14, did not

show limitation of LV remodelling in patients after STEMI (471). However, potential confounders in that study included late initiation of therapy with PCI within 29 hours and oral PG-116800 within 48 hours, background therapies with potential pleiotropic effects in both treatment arms, and the lack of selective MMP inhibition. This study did not measure RSD.

Second, other drugs used after MI may exert pleiotropic effects on MMP/TIMP balance. For example, RAAS-inhibition which induces cardio-protection in reperfused MI may improve the MMP/TIMP balance. In the dog model of reperfusion after prolonged ischaemia, valsartan given 30 minutes before ischaemia normalized the balance between MMP-9 and TIMP-3, improved LV contractile function, and limited acute infarct remodelling and infarct size (461). In the same model, valsartan reversed the changes in metabolic, functional and structural proteins induced by post-ischemic reperfusion (472,473). These studies suggest that the ARB valsartan not only limits reperfusion injury but also improves remodelling by matrix modulation.

Third, supporting structures have been targeted in an attempt to decrease the regional bulging and global dilatation after MI by applying external restraint (22,39,278). Some experimental studies have used a mesh over the infarct zone. The 'Acorn' cardiac support device, designed to provide diastolic support to the heart and thereby decrease LV diastolic wall stress and limit LV dilatation, has been shown to be effective in animal models of heart failure as well as patients with heart failure (474).

Fourth, alternative approaches have been targeted at improving ventricular function and limiting dilatation. These include ventricular reduction surgery (Batista procedure) (475), dynamic cardiomyoplasty (476), and implantation of pacing devices to control electrical/mechanical asynchrony and produce resynchronization (477). Of these, cardiac resynchronization is the only approach that is widely used in heart failure.

Fifth, cardiac tissue engineering is an innovative approach for creating a muscle patch and is undergoing investigation (478). Several scaffolds, cardiomyocyte-populated gelatin and alginate gelatin grafts have been tested in animals. It is being combined with stem cell transplantation enhanced with growth factors and angiogenic factors to achieve myocardial regeneration.

Sixth, local drug or gene delivery that separately target the infarct and non-infarct zones is undergoing evaluation. Gene therapy using various growth factors

such as the vascular endothelial growth factor (VEGF) has been studied, with some favourable effects reported on angiogenesis and ventricular function although controversy exists.

6.5.3.3. Novel approaches and concepts

Four major points need to be considered.

First, markers of immune reactions, collagen turnover, and MMPs can be used to monitor adverse ECM and cardiac remodelling. Since post-MI survivors who develop heart failure on therapy have a 10-fold greater risk of dying (441), a plasma marker that can identify those at high risk of adverse LV remodelling would be useful. Currently available surrogate markers of adverse outcome after MI include BNP (479), C-reactive protein (CRP) (480) and TNF-α (481). MMPs and TIMPS have been proposed. Thus, increased plasma MMP-9 after MI is a fairly consistent finding (482) that may reflect a spillover. Several studies have documented increased plasma MMP-9 (483,484), or both MMP-9 and MMP-2 levels (485,486), after acute (483,485,486) and remote (484) MI, increased plasma MMP-9 in acute coronary syndromes including MI (482,485), and increased plasma MMP-9 in heart failure (487,488). In one study, both plasma MMP-9 and TIMP-1 were increased in acute MI (482). Importantly, Squire et al (486) found that after MI, plasma MMP-9 levels correlated with LV dysfunction whereas plasma MMP-2 correlated inversely with LV volumes. Squire (486) also found that MMP-9 levels did not differ for anterior and inferior MI whereas MMP-2 levels were higher in anterior MI and TIMP-1 levels were higher in inferior MI. In one study that measured plasma MMP levels serially over 6 months after MI, increases in MMP-9 and TIMP-1 were most marked in moderate to large MI (483). In another study, MMP-9 correlated with cardiovascular risk (489). A potential confounder in acute MI studies is that increased plasma MMP-9 also correlated with plaque rupture (482,485). In remote MI, plasma MMP-9 was a predictor of MI but also reflected inflammation and atherosclerosis progression (484).

In a broader perspective, plasma markers of collagen turnover (307,490-494) or the connective tissue growth factor (CTGF) gene can be used to monitor anti-fibrotic effects of drugs (495). Other proteins and cells can be used to monitor the effects of drugs on inflammation and healing (496). Markers of immune reactions (497), adverse remodelling (498), phenotypes of responders to ACE

inhibitors and beta-blockers (499,500), and pharmacogenomic (501) approaches can all be applied to further improve outcome of survivors after MI.

Second, several novel imaging techniques are applicable for clinical studies of post-MI remodelling. Improved Echo imaging techniques include tissue Doppler imaging for diastolic function, tissue characterization imaging, myocardial strain and strain rate imaging based on Doppler, myocardial contrast imaging for perfusion/function mismatch, and 3D-Echo (502). Recently, speckle tracking for LV torsion (or twist) and LV systolic function was reported (503). Magnetic resonance imaging (MRI) tagging is also available but its use has been limited by its cost and complexity. It uses more transverse tomographic sections than is possible with 2D-Echo and the images are superior. The combination of data from first-pass and delayed contrast-enhanced imaging can predict functional recovery in reperfused MI (504). However, MRI cannot be easily applied to study high-risk patients with acute MI although it is well suited for studies of post-MI survivors. MMP-targeted radio-tracers have been developed for imaging the localization of MMP activation and tracking MMP-mediated remodelling post MI (505). Imaging of apoptosis is also being evaluated (450,451).

Third, polypharmacy is common in post-MI and heart failure patients. The use of RAAS inhibitors on top of background therapy increases the possibility of interactions. The pleiotropic effects of the drugs are becoming important. Experimental studies suggest that combination therapy is often more beneficial than monotherapy. In atrial pacing-induced heart failure in the pig, the combination of valsartan and the endothelin blocker bosentan resulted in additive beneficial effects on loading, neurohumoral activity and LV performance (506). In the rat model of post-MI heart failure, the combination of valsartan and the ACE inhibitor fosinopril resulted in suppression of histopathological changes associated with remodelling, such as normalization of collagen I, macrophages and myofibroblasts (507).

Although the effects of ACE inhibitors and ARBs on LV structural remodelling in post-MI survivors initially emphasized the haemodynamic mechanism (decreased blood pressure, preload and afterload and wall stress), the importance of the non-haemodynamic mechanism ('beyond decreasing blood pressure') involving inhibition of angiotensin II–induced growth, hypertrophy and apoptosis was later appreciated (27,508,509). AT_2 receptor stimulation was suggested to explain vasculoprotective effects of RAAS-inhibition with ACE

inhibitors and ARBs (372). In both dog and rat models of post-ischaemic reperfusion, ARB-induced cardioprotection was associated with enhanced AT_2 receptor expression (510,511). However, evidence suggests that AT_2 receptor stimulation may enhance acute ischaemia-reperfusion injury under certain conditions (512,513), and promote cardiac hypertrophy and vascular fibrosis, and reduce neo-vascularization in ischemic tissues (514). These negative effects of AT_2 stimulation may explain why ARBs are not found to be superior to ACE inhibitors in clinical trials.

A potential source of concern with the combination of ACE inhibitors, ARBs and aldosterone antagonists, is that they both very effectively decrease collagen and interstitial fibrosis. Although the anti-fibrotic effect of RAAS-inhibition results in improvement of LV diastolic function that may be beneficial in patients with post-MI hypertrophy and interstitial fibrosis, the possibility remains that over-aggressive reduction in collagen matrix may increase LV distensibility on the long-term and contribute to deterioration, especially in patients with large transmural MI (27). In 2005), a new mechanism for the anti-fibrotic effect of ACE inhibitors was identified. This involves the inhibition of the hydrolysis of N-acetyl-seryl-aspartyl-lysyl- proline (Ac-SDKP), resulting in decreased cardiac cell proliferation (possibly fibroblasts), inflammatory cell infiltration, expression of transforming growth factor-β (TGF-β), activation of Smad2 (the mediator of effects of TGF-β) and collagen deposition (515). Further studies linking markers of ECM and LV remodelling are therefore needed.

Fourth, it has been suggested that attention to differences in genetics, RAAS/ACE polymorphisms, race and age may further improve outcome in MI survivors. Pharmacogenetics and identification of the phenotypes of responders to ACE inhibitors (and beta-blockers) may be applied to select high-risk sub-groups. For example, ACE gene polymorphism is associated with higher levels of angiotensin II (516) and increased risk of cardiovascular disease (517) and MI (518). Several trials suggested that ACE gene polymorphism might influence the response to ACE inhibitors, with carriers of the DD genotype being associated with a more favourable effect, but controversy persists since chronic ACE inhibitor therapy increases angiotensin II levels. However, the ACE ID polymorphism is associated with higher ACE activity that may result in more favourable response to ACE inhibitors. In one study, only quinapril (not the ARB losartan, the calcium channel blocker amlodipine, or enalapril) was associated with a significant

improvement in brachial artery flow-mediated vasodilatation and this effect was related to the presence of ACE ID and II genotypes (519). In another study, ACE inhibitors did not increase re-stenosis after coronary stenting in patients with the ACE DD phenotype, irrespective of their tissue ACE affinity (520).

Recently, RAAS gene polymorphisms were linked to non-familial structural atrial fibrillation, providing further rationale for RAAS-inhibition with ACE inhibitors and ARBs to suppress atrial fibrillation in survivors of MI (521). RAAS-inhibition and genetics needs further study.

Whether pharmacotherapy should be based on racial background is controversial. The response to heart failure therapy is suboptimal in African-American patients (361,522-524), possibly due to a relative resistance to ACE inhibitors secondary to low renin (522). The A-HeFT (435) suggested that the ethnic background might influence the response to therapy with ISDN and hydralazine (439). Differences in response to RAAS-inhibition due to race needs further study.

6.6. Conclusions

The potential for preventing aneurysm formation and progressive LV dilatation and dysfunction after acute MI, by pharmacological limitation of early RSD and infarct expansion, is an exciting and achievable goal. The improved understanding of the early and late phases of the healing process after MI and the concurrent adverse ventricular remodelling process will permit the design of more rational therapy to prevent topographic deterioration and congestive heart failure. The early prediction of patients at high risk for infarct expansion, by measuring RSD and other robust remodelling indices using non-invasive imaging with 2D-Echo or other imaging modalities, such as MRI, will permit earlier intervention.

Collective evidence suggests that successful myocardial reperfusion therapy prevents transmural or Q-wave infarction and acute expansion, and subsequent prolonged pharmacotherapy provides additional benefit. Since late reperfusion can experimentally reduce expansion and thinning, adjunctive therapies may widen the window for salvaging LV shape and function. Clearly current pharmacotherapy after MI is not ideal, since ventricles continue to enlarge and the number of patients with LV dysfunction waiting for transplantation has not decreased.

The overall results of the studies in this thesis indicate that, after an acute MI, progressive regional and global changes in ventricular topography occur throughout the healing phase over a period of several weeks. This remodelling, which is most marked with large transmural and anterior infarction, involves a sequence of early remodelling with expansion of the infarcted zone (stretching, thinning, regional dilatation), collagen deposition into the already thinned and stretched infarct segments, followed by further late remodelling with more infarct wall thinning, aneurysm formation with a firm inelastic scar, and further progressive dilatation of the non-infarct segment. The early regional remodelling initiates a vicious cycle of LV dysfunction, decreased cardiac output, more cardiac dilatation, cardiac failure, neurohumoral activation and decreased survival. Major factors influencing remodelling include infarct size and transmurality, afterload, preload, wall stress, contractile function of adjacent normal myocardium, collateral blood flow and the healing process itself.

Pharmacological therapy, with intravenous low-dose NTG in the early phase followed by prolonged therapy with nitrates (eccentric dosing) or ACE inhibitors were effective for limiting LV regional remodelling, limiting global dilatation, preserving function and potentially improving survival after MI. Thrombolytic therapy also limited remodelling but only preserved muscle and function if performed very early. NTG and ACE inhibitors appeared to be effective as adjunctive therapy after reperfusion, although subsequent large clinical trials over the last decade only showed significant survival benefit with ACE inhibitors. The measurement of RSD and other indices of LV remodelling by quantitative 2D-Echo might be potentially important for assessing the effects of anti-remodelling strategies on the infarct zone during healing after MI and identifying patients at high risk for LV aneurysm and rupture. The relation of ECM disruption to RSD, as unmasked in the studies using 2D-Echo, may be applied for assessing future anti-remodelling therapies. Other imaging modalities such as MRI may be applied to detect RSD in future.

7. BIBLIOGRAPHY

1. Burton AC. The importance of the shape and size of the heart. Am Heart J 1957;54:801-810.
2. Dodge HT, Sandler H, Ballew DW, Lord JD, Jr. The use of biplane angiocardiography for the measurement of left ventricular volume in man. Am Heart J 1960;60:762-776.
3. Gould KL, Lipscomb K, Hamilton GW, Kennedy SW. Relation of left ventricular shape, function and wall stress in man. Am J Cardiol 1974;34: 627-634.
4. Dodge HT, Stewart DK, Frimer M. Implications of shape, stress, and wall dynamics in clinical heart disease. In: Fishman AP, editor. Heart Failure. Washington, Hemisphere, 1978;43-54.
5. Rogers EW, Feigenbaum H, Weyman AE. Echocardiography for quantitation of cardiac chambers. In: Goodwin JF, editor. Progress in Cardiology. Philadelphia: Lea & Febiger, 1979:1-28.
6. Shanoff HM, Little JA, Csima A, Yano R. Heart size and ten-year survival after uncomplicated myocardial infarction. Am Heart J 1969;78:608-614.
7. Ross J Jr, Sonnenblick EH, Taylor RR, Spotnitz HM, Covell JW. Diastolic geometry and sarcomere lengths in the chronically dilated canine left ventricle. Circ Res 1971;28:49-61.
8. Kostuk WJ, Kazamias TM, Gander MP, Simon AL, Ross J Jr. Left ventricular size after acute myocardial infarction. Serial changes and their prognostic significance. Circulation 1973;47:1174-1179.
9. Battler A, Karliner JS, Higgins CB, Slutsky R, Gilpin EA, Froelicher VF, et al. The initial chest x-ray in acute myocardial infarction. Prediction of early and late mortality and survival. Circulation 1980;61:1004-1009.
10. Janz RF, Kubert BR, Pate EF, Moriarty TF. Effect of shape on pressure-volume relationships of ellipsoidal shells. Am J Physiol 1980;238:H917-H926.
11. Borow KM, Lang RM, Neumann A, Carroll JD, Rajfer SI. Physiologic mechanisms governing hemodynamic responses to positive inotropic therapy in patients with dilated cardiomyopathy. Circulation 1988;77:625-637.

12. Lamas GA, Vaughan DE, Parisi AF, Pfeffer MA. Effects of left ventricular shape and captopril therapy on exercise capacity after anterior wall acute myocardial infarction. Am J Cardiol 1989;63:1167-1173.
13. Laskey WK, Sutton MS, Zeevi G, Hirshfeld JW Jr, Reichek N. Left ventricular mechanics in dilated cardiomyopathy. Am J Cardiol 1984;54: 620-625.
14. Herman MV, Gorlin R. Implications of left ventricular asynergy. Am J Cardiol 1982;23:538-547.
15. Weyman AE, Peskoe SM, Williams ES, Dillon JC, Fiegenbaum H. Detection of left ventricular aneurysms by cross-sectional echocardiography. Circulation 1976;54:936-944.
16. Kisslo JA, Robertson D, Gilbert BW, von Ramm O, Behar VS. A comparison of real-time, two dimensional echocardiography and cineangiography in detecting left ventricular asynergy. Circulation 1977; 55:134-141.
17. Heger JT, Weyman AE, Wann LS, Dillon JC, Feigenbaum H. Cross-sectional echocardiography in acute myocardial infarction: detection and localization of regional left ventricular asynergy. Circulation 1979;60:531-538.
18. Eaton LW, Weiss JL, Bulkley BH, Garrison JB, Weisfeldt ML. Regional cardiac dilatation after acute myocardial infarction: recognition by two-dimensional echocardiography. N Engl J Med 1979;300:57-62.
19. Jugdutt BI, Cahn RL, Basualdo CA, Rossall RE. Measurement of left ventricular shape distortion. In, Ripley, KL, editor. Computers in Cardiology. Los Angeles: IEEE Computer Society Press, 1984:47-52. [**Appendix 1**]
20. Jugdutt BI, Michorowski BL. Role of infarction expansion in rupture of the ventricular septum after acute myocardial infarction. A Two-Dimensional Echocardiographic study. Clin Cardiol 1987;10:641-652. [**Appendix 2**]
21. Jugdutt BI. Identification of patients prone to infarct expansion by the degree of regional shape distortion on an early two-dimensional echocardiogram after myocardial infarction. Clin Cardiol 1990;13:28-40. [**Appendix 3**]
22. Jugdutt BI. Prevention of ventricular remodelling post myocardial infarction: timing and duration of therapy. Can J Cardiol 1993;9:103-114. [**Appendix 4**]

23. Pfeffer MA, Braunwald E. Ventricular remodeliing after myocardial infarction. Experimental observations and clinical implications. Circulation 1990;81:1161-1172.

24. Cohn JN, Ferrari R, Sharpe N, on behalf of an International Forum on Cardiac Remodeling. Cardiac remodeling--concepts and clinical implications: a consensus paper from an international forum on cardiac remodeling. J Am Coll Cardiol 2000;35:569-582.

25. Sutton MG, Sharpe N. Left ventricular remodeling after myocardial infarction: pathophysiology and therapy. Circulation 2000;101:2981-2988.

26. Gaudron P, Eilles C, Kugler I, Ertl G. Progressive left ventricular dysfunction and remodeling after myocardial infarction. Potential mechanisms and early predictors. Circulation 1993;87:755-763.

27. Jugdutt BI. Ventricular remodeling postinfarction and the extracellular collagen matrix. When is enough enough? Circulation 2003;108:1395-1403. **[Appendix 5]**

28. Jugdutt BI, Warnica JW. Intravenous nitroglycerin therapy to limit myocardial infarct size, expansion and complications: effect of timing, dosage and infarct location. Circulation 1988;78:906-919. [**Appendix 6**]

29. Sharpe N, Murphy J, Smith H, Hannon S. Treatment of patients with symptomless left ventricular dysfunction after myocardial infarction. Lancet 1988;1:255-259.

30. Pfeffer MA, Lamas GA, Vaughan DE, Parisi AF, Braunwald E. Effect of captopril on progressive ventricular dilation after anterior myocardial infarction. N Engl J Med 1988;319:80-86.

31. Erlebacher JA, Weiss JL, Eaton LW, Kallman C, Weisfeldt ML, Bulkley BH. Late effects of acute infarct dilation on heart size: A two-dimensional echocardiographic study. Am J Cardiol 1982;49:1120-1126.

32. Erlebacher JA, Weiss JL, Weisfeldt ML, Bulkley BH. Early dilation of the infarcted segment in acute transmural myocardial infarction: Role of infarct expansion in acute left ventricular enlargement. J Am Coll Cardiol 1984;4:201-208.

33. Maidens JM, Blinston GE, Jugdutt BI. Computer-assisted measurement of regional and global left ventricular shape distortion after myocardial infarction. In, Computers in Cardiology. Los Angeles: IEEE Computer Society Press, 1987:413-416. [**Appendix 7**]

34. Jugdutt BI, Michorowski BL, Kappagoda TC. Exercise training after anterior Q wave myocardial infarction: importance of regional left ventricular function and topography. J Am Coll Cardiol 1988;12: 362-372. [**Appendix 8**]

35. Jugdutt BI, Basualdo CA. Myocardial infarct expansion during indomethacin and ibuprofen therapy for symptomatic post-infarction pericarditis: Effect of other pharmacologic agents during early remodelling. Can J Cardiol 1989;5:211-221. [Appendix 9]

36. Johnston BJ, Blinston GE, Jugdutt BI. Overestimation of myocardial infarct size on two-dimensional echocardiograms due to remodeling of the infarct zone. Can J Cardiol 1994;10:77-86. [**Appendix 10**]

37. Jugdutt BI. Prevention of ventricular remodeling after myocardial infarction and in congestive heart failure. Heart Failure Reviews 1996;1:115-129. [**Appendix 11**]

38. Jugdutt BI. The use of intravenous nitroglycerin and ACE-inhibitors for ventricular remodeling after myocardial infarction. Pharmacology (Life Science Advances) 1990;9:697-716.

39. Jugdutt BI. Modification of left ventricular remodelling after myocardial infarction. In: Dhalla NS, Beamish RE, Nagano M, editors. The Failing Heart. New York: Raven Press, 1995:231-245.

40. Fishbein MC, Maclean D, Maroko PR. The histopathologic evolution of myocardial infarction. Chest 1978;73:843-849.

41. Jugdutt BI, Amy RW. Healing after myocardial infarction in the dog: changes in infarct hydroxyproline and topography. J Am Coll Cardiol 1986;7:91-102. [**Appendix 12**]

42. Jugdutt BI. Extracellular matrix and remodeling. In: Villarreal FJ, editor. Interstitial Fibrosis in Heart Failure. New York: Springer Science+Business Media, Inc., 2004: 23-55.

43. Kloner RA, Fishbein MC, Lew H, Maroko PR, Braunwald E. Mummification of the infarcted myocardium by high dose corticosteroids. Circulation 1978;57:56-63.

44. Mallory GK, White PD, Salcedo-Salgar J. The speed of healing of myocardial infarction: a study of the pathologic anatomy in 72 cases. Am Heart J 1939;18:647-671.

45. Reimer KA, Lowe JE, Rasmussen MM, Jennings RB. The wavefront phenomenon of ischemic cell death. 1. Myocardial infarct size vs duration of coronary occlusion in dogs. Circulation 1977;56:786-794.

46. Boyle MP, Weisman HF. Limitation of infarct expansion and ventricular remodeling by late reperfusion. Circulation. 1993;88:2872-2883.

47. Hochman JS, Choo H. Limitation of myocardial infarct expansion by reperfusion independent of myocardial salvage. Circulation 1987;75:299-306.

48. Jugdutt BI, Khan MI, Jugdutt SJ, Blinston GE. Impact of left ventricular unloading after late reperfusion of canine anterior myocardial infarction on remodeling and function using isosorbide-5-mononitrate. Circulation 1995;92:926-934. [**Appendix 13**]

49. Jugdutt BI. Effect of reperfusion on ventricular mass, topography and function during healing of anterior infarction. Am J Physiol 1997;272:H1205-1211. [**Appendix 14**]

50. Jugdutt BI, Schwarz-Michorowski BL, Tymchak WJ, Burton JR. Prompt improvement of left ventricular function and topography with combined reperfusion and intravenous nitroglycerin in acute myocardial infarction. Cardiology 1997;88:170-179. [**Appendix 15**]

51. Hammerman H, Kloner RA, Hale S, Schoen FJ, Braunwald E. Dose-dependent effects of short-term methylprednisolone on myocardial infarct extent, scar formation, and ventricular function. Circulation 1983;68:446-452.

52. Hammerman H, Kloner RA, Schoen FJ, Brown EJ Jr, Hale S, Braunwald E. Indomethacin-induced scar thinning after experimental myocardial infarction. Circulation 1983;67:1290-1295.

53. Hammerman H, Schoen FJ, Braunwald E, Kloner RA. Drug-induced expansion of infarct: morphologic and functional correlations. Circulation 1984;69:611-617.

54. Brown EJ Jr, Kloner RA, Schoen FJ, Hammerman H, Hale S, Braunwald E. Scar thinning due to ibuprofen administration after experimental myocardial infarction. Am J Cardiol 1983;51:877-883.

55. Jugdutt BI. Delayed effects of early infarct-limiting therapies on healing after myocardial infarction. Circulation 1985;72:907-914. [**Appendix 16**]

56. Jugdutt BI, Hutchins GM, Bulkley BH, Pitt B, Becker LC. Effect of indomethacin on collateral blood flow and infarct size in the conscious dog. Circulation 1979;59:734-743.

57. Jugdutt BI, Hutchins GM, Bulkley BH, Becker LC. Salvage of ischemic myocardium by ibuprofen during infarction in the conscious dog. Am J Cardiol 1980 I;46:74-82.

58. Cannon RO 3rd, Rodriguez ER, Speir E, et al. Effect of ibuprofen on the healing phase of experimental myocardial infarction in the rat. Am J Cardiol 1985;55:1609-1613.

59. Hutchins GM, Bulkley BH. Infarct expansion versus extension: two different complications of acute myocardial infarction. Am J Cardiol 1978;41:1127-1132.

60. Schuster EH, Bulkley BH. Expansion of transmural myocardial infarction. A pathophysiologic factor in cardiac rupture. Circulation. 1979;60:1532-1538.

61. Reid PR, Taylor DR, Kelly DT, et al. Myocardial-infarct extension detected by precordial ST-segment mapping. N Engl J Med 1974;290:123-128.

62. Lieberman AN, Weiss JL, Jugdutt BI, et al. Two-dimensional echocardiography and infarct size: relationship of regional wall motion and thickening to the extent of myocardial infarction in the dog. Circulation 1981;63:739-746.

63. Michorowski B, Senaratne PJM, Jugdutt BI. Myocardial infarct expansion. Cardiovasc Rev and Reports 1987;8:42-47. [**Appendix 17**]

64. Weisman HF, Healy B. Myocardial infarct expansion, infarct extension, and reinfarction: pathophysiologic concepts. Prog Cardiovasc Dis 1987;30:73-110.

65. Tennant R, Wiggers CJ. The effect of coronary occlusion on myocardial infarction. Am J Physiol 1935;112:351-361.

66. Weisman HF, Bush DE, Mannisi JA, Weisfeldt ML, Healy B. Cellular mechanisms of myocardial infarct expansion. Circulation 1988;78:186-201.

67. Michorowski B, Senaratne PJM, Jugdutt BI. Deterring myocardial infarct expansion. Cardiovasc Rev and Reports 1987;8:55-62. [**Appendix 18**]

68. Theroux P, Ross J Jr, Franklin D, Covell JW, Bloor CM, Sasayama S. Regional myocardial function and dimensions early and late after myocardial infarction in the unanesthetized dog. Circ Res 1977;40:158-165.

69. Parmley WW, Chuck L, Kivowitz C, Matloff JM, Swan HJ. In vitro length-tension relations of human ventricular aneurysms. Relation of stiffness to mechanical disadvantage. Am J Cardiol 1973;32:889-894.

70. Eaton LW, Bulkley BH. Expansion of acute myocardial infarction: its relationship to infarct morphology in a canine model. Circ Res 1981;49:80-88.

71. Hochman JS, Bulkley BH. Expansion of acute myocardial infarction: an experimental study. Circulation 1982;65:1446-1450.

72. Hochman JS, Bulkley BH. Pathogenesis of left ventricular aneurysms: an experimental study in the rat model. Am J Cardiol 1982;50:83-88.

73. Jugdutt BI, Khan MI. Impact of increased infarct transmurality on remodeling and function during healing after anterior myocardial infarction in the dog. Can J Physiol Pharmacol 1992;70:949-958. [**Appendix 19**]

74. Jugdutt BI, Tang SB, Khan MI, Basualdo CA. Functional impact on remodeling during healing after non-Q-wave versus Q-wave anterior myocardial infarction in the dog. J Am Coll Cardiol 1992;20:722-731. [**Appendix 20**]

75. Pfeffer MA, Pfeffer JM, Fishbein MC, et al. Myocardial infarct size and ventricular function in rats. Circ Res 1979;44:503-512.

76. Fletcher PJ, Pfeffer JM, Pfeffer MA, Braunwald E. Left ventricular diastolic pressure-volume relations in rats with healed myocardial infarction. Effects on systolic function. Circ Res 1981;49:618-626.

77. Pfeffer MA, Pfeffer JM, Steinberg C, Finn P. Survival after an experimental myocardial infarction: beneficial effects of long-term therapy with captopril. Circulation 1985;72:406-412.

78. Stone PH, Raabe DS, Jaffe AS, et al., for the MILIS Group. Prognostic significance of location and type of myocardial infarction: independent adverse outcome associated with anterior location. J Am Coll Cardiol 1988;11:453-463.

79. Pirolo JS, Hutchins GM, Moore GM. Infarct expansion: pathologic analysis of 204 patients with a single myocardial infarct. J Am Coll Cardiol 1986; 7:349-354.

80. Role L, Bogen D, McMahon TA, Abelmann WH. Regional variations in calculated diastolic wall stress in rat left ventricle. Am J Physiol 1978; 235:H247-H250.

81. Hammerman H, Schoen FJ, Kloner RA. Short-term exercise has a prolonged effect on scar formation after experimental acute myocardial infarction. J Am Coll Cardiol 1983;2:979-982.

82. Kloner RA, Kloner JA. The effect of early exercise on myocardial infarct scar formation. Am Heart J. 1983;106:1009-1013.

83. Hochman JS, Bulkley BH. Effect of exercise on acute myocardial infarction in rats. J Am Coll Cardiol 1986;7:126-132.

84. Hammerman H, Kloner RA, Alker KJ, Schoen FJ, Braunwald E. Effects of transient increased afterload during experimentally induced acute myocardial infarction in dogs. Am J Cardiol 1985;55:566-570.

85. Flaherty JT, Becker LC, Weiss JL, et al. Results of a randomized prospective trial of intraaortic balloon counterpulsation and intravenous nitroglycerin in patients with acute myocardial infarction. J Am Coll Cardiol 1985;6:434-446.

86. Raya TE, Gay RG, Aguirre M, Goldman S. Importance of venodilatation in prevention of left ventricular dilatation after chronic large myocardial infarction in rats: a comparison of captopril and hydralazine. Circ Res 1989;64:330-337.

87. Maroko PR, Kjekshus JK, Sobel BE, et al. Factors influencing infarct size following experimental coronary artery occlusions. Circulation 1971;43:67-82.

88. Braunwald E. Introductory remarks. In, Protection of the ischemic myocardium. Circulation1976;53(Suppl 1):1.

89. Gottlieb SO, Becker LC, Weiss JL, et al. Nifedipine in acute myocardial infarction: an assessment of left ventricular function, infarct size, and infarct expansion. A double blind, randomised, placebo controlled trial. Br Heart J 1988 59:411-418.

90. Baker JT, Bramlet DA, Lester RM, Harrison DG, Roe CR, Cobb FR. Myocardial infarct extension: incidence and relationship to survival. Circulation 1982;65:918-923.

91. Marmor A, Geltman EM, Schechtman K, Sobel BE, Roberts R. Recurrent myocardial infarction: clinical predictors and prognostic implications. Circulation 1982;66:415-421.

92. Meizlish JL, Berger HJ, Plankey M, Errico D, Levy W, Zaret BL. Functional left ventricular aneurysm formation after acute anterior transmural

myocardial infarction. Incidence, natural history, and prognostic implications. N Engl J Med 1984;311:1001-1006.

93. Roberts CS, Maclean D, Braunwald E, Maroko PR, Kloner RA. Topographic changes in the left ventricle after experimentally induced myocardial infarction in the rat. Am J Cardiol 1983;51:872-876.

94. Roberts CS, Maclean D, Maroko P, Kloner RA. Early and late remodeling of the left ventricle after acute myocardial infarction. Am J Cardiol 1984; 54:407-410.

95. Lerman RH, Apstein CS, Kagan HM, , et al. Myocardial healing and repair after experimental infarction in the rabbit. Circ Res 1983;53:378-388.

96. Jugdutt BI, Joljart MJ, Khan MI. Rate of collagen deposition during healing after myocardial infarction in the rat and dog models: mechanistic insights into ventricular remodeling. Circulation 1996;94:94-101.

97. Maclean D, Fishbein MC, Braunwald E, Maroko PR. Long-term preservation of ischemic myocardium after experimental coronary artery occlusion. J Clin Invest 1978;61:541-551.

98. Jugdutt BI, Becker LC, Hutchins GM, Bulkley BH, Reid PR, Kallman CH. Effect of intravenous nitroglycerin on collateral blood flow and infarct size in the conscious dog. Circulation 1981;63:17-28.

99. Jugdutt BI, Hutchins GM, Bulkley BH, Becker LC. Dissimilar effects of prostacyclin, prostaglandin E1, and prostaglandin E2 on myocardial infarct size after coronary occlusion in conscious dogs. Circ Res 1981;49:685-700.

100. Jugdutt BI. Intravenous nitroglycerin unloading in acute myocardial infarction. Am J Cardiol. 1991;68:52D-63D. [**Appendix 21**]

101. Jugdutt BI. Role of Nitrates after acute myocardial infarction. Am J Cardiol 1992;70:82B-87B.

102. Jugdutt BI. Effect of nitroglycerin and ibuprofen on left ventricular topography and rupture threshold during healing after myocardial infarction in the dog. Can J Physiol Pharmacol 1988;66:385-395. [**Appendix 22**]

103. Jugdutt BI, Khan MI. Effect of prolonged nitrate therapy on left ventricular remodeling after canine acute myocardial infarction. Circulation 1994;89: 2297-2307. [**Appendix 23**]

104. Michorowski BL, Tymchak WT, Jugdutt BI. Improved left ventricular function and topography by prolonged nitroglycerin therapy after acute myocardial infarction. (Abstract) Circulation 1987;76: IV-128.

105. Jugdutt BI, Michorowski BL, Tymchak WJ. Improved left ventricular function and topography by prolonged nitroglycerin therapy after acute myocardial infarction. Z Kardiol 1989;78: Suppl 2; 127-129. [**Appendix 24**]

106. Humen DP, McCormick L, Jugdutt BI. Chronic reduction of left ventricular volumes at rest and exercise in patients treated with nitroglycerin following anterior MI. (Abstract). J Am Coll Cardiol 1989;13:25A.

107. Jugdutt BI, Neiman JC, Michorowski BL, Tymchak WJ, Genge TJ, Fitzpatrick LK. Persistent improvement in left ventricular geometry and function by prolonged nitroglycerin therapy after anterior transmural acute myocardial infarction. (Abstract) J Am Coll Cardiol 1990;15:214A.

108. Jugdutt BI, Tymchak W, Humen D, Gulamhusein S, Hales M. Prolonged nitroglycerin versus captopril therapy on remodeling after transmural myocardial infarction. (Abstract) Circulation 1990;82 (Suppl III):III-442. [**Appendix 25**]

109. Jugdutt BI, Michorowski BL, Tymchak WJ. Improved left ventricular geometry and function by prolonged nitroglycerin therapy after acute myocardial infarction. In, Lewis BS and Kimchi A, editors. Chronic Heart Failure - Mechanisms and Management. I. Quality of Life, II Nitrate Therapy. New York: Springer-Verlag, 1990:266-271. [**Appendix 26**]

110. Cohn JN. New concepts in the mechanisms and treatment of congestive heart failure. Am J Cardiol 1985;55:1A-2A.

111. Cody RJ. Clinical and hemodynamic experience with enalapril in congestive heart failure. Am J Cardiol 1985;55:36A-40A.

112. Michorowski B, Ceremuzynski L. The renin-angiotensin-aldosterone system and the clinical course of acute myocardial infarction. Eur Heart J 1983;4: 259-264.

113. McAlpine HM, Morton JJ, Leckie B, Rumley A, Gillen G, Dargie HJ. Neuroendocrine activation after acute myocardial infarction. Br Heart J. 1988;60:117-124.

114. Vaughan DE, Lamas GA, Pfeffer MA. Role of left ventricular dysfunction in selective neurohumoral activation in the recovery phase of anterior wall acute myocardial infarction. Am J Cardiol 1990;66:529-532.

115. Parmley WW. Pathophysiology of congestive heart failure. Am J Cardiol 1985;56:7A-11A.

116. Fouad FM, Tarazi RC, Bravo EL, Hart NJ, Castle LW, Salcedo EE. Long-term control of congestive heart failure with captopril. Am J Cardiol 1982; 49:1489-1496.

117. Fung HL, Chong S, Kowaluk E. Mechanisms of nitrate action and vascular tolerance. Eur Heart J 1989;10(Suppl A):2-6.

118. Jugdutt BI, Warnica JW. Tolerance with low dose intravenous nitroglycerin therapy in acute myocardial infarction. Am J Cardiol 1989;64:581-587. **[Appendix 27]**

119. Ertl G, Kloner RA, Alexander RW, Braunwald E. Limitation of experimental infarct size by an angiotensin-converting enzyme inhibitor. Circulation 1982;65:40-48.

120. Pfeffer JM, Pfeffer MA, Braunwald E. Influence of chronic captopril therapy on the infarcted left ventricle of the rat. Circ Res 1985;57:84-95.

121. Pfeffer MA, Braunwald E, Moyé LA et al on behalf of the SAVE Investigators. Effect of captopril on mortality and morbidity in patients with left ventricular dysfunction after myocardial infarction. N Engl J Med 1992;327:669-677.

122. Jugdutt BI. Myocardial salvage by intravenous nitroglycerin in conscious dogs: loss of beneficial effect with marked nitroglycerin-induced hypotension. Circulation 1983;68:673-684. **[Appendix 28]**

123. Swedberg K, Held P, Kjekshus J, et al. on Behalf of the Consensus Study Group. Effects of the early administration of enalapril on mortality in patients with acute myocardial infarction. Results of the Cooperative New Scandinavian Enalapril Survival Study II (CONSENSUS II) N Engl J Med 1992;32):678-684.

124. Pfeffer MA, Hennekens CH, for the HEART Study Executive Committee. When a question has an answer: rationale for our early termination of the HEART Trial. Am J Cardiol 1995;75:1173-1175.

125. Pfeffer MA, Greaves SC, Arnold JM, et al. Early versus delayed angiotensin-converting enzyme inhibition therapy in acute myocardial infarction. The healing and early afterload reducing therapy trial. Circulation 1997;95:2643-2651.

126. Jugdutt BI, Michorowski BL, Khan MI. Effect of long-term captopril therapy on left ventricular remodeling and function during healing and canine myocardial infarction. J Am Coll Cardiol 1992;19:713-723. [**Appendix 29**]

127. Jugdutt BI, Khan MI, Jugdutt SJ, Blinston GE. Effect of enalapril on ventricular remodeling and function during healing after anterior myocardial infarction in the dog. Circulation 1995;91:802-812. [**Appendix 30**]

128. Jugdutt BI. Effect of captopril and enalapril on left ventricular geometry, function and collagen during healing after anterior and inferior myocardial infarction in the dog. J Am Coll Cardiol 1995;25:1718-1725. [**Appendix 31**]

129. Jugdutt BI, Lucas A, Khan MI. Effect of angiotensin-converting-enzyme inhibition on infarct collagen and remodeling during healing after transmural canine myocardial infarction. Can J Cardiology 1997;13:657-668. [**Appendix 32**]

130. Jugdutt BI, Humen DP. Limitation of left ventricular hypertrophy and dysfunction by ACE inhibition after anterior Q-wave myocardial infarction. Cardiology 1998; 89:283-290.

131. Jugdutt BI, Khan MI, Jugdutt SJ, Blinston GE. Combined captopril and isosorbide dinitrate during healing after myocardial infarction. Effect on remodeling, function, mass and collagen. J Am Coll Cardiol 1995;25:1089-1096. [**Appendix 33**]

132. Sutton M St.J, Pfeffer MA, Plappert T, et al. for the SAVE Investigators. Quantitative two-dimensional echocardiographic measurements are major predictors of adverse cardiovascular events after acute myocardial infarction. The protective effects of captopril. Circulation 1994;89:68-75.

133. Ertl G, Jugdutt BI. ACE inhibition after myocardial infarction: Can megatrials provide answers? Lancet 1994;344:1068-1069.

134. Latini R, Maggioni AP, Flather M, Sleight P, Tognoni G, for the meeting participants. ACE inhibitor use in patients with myocardial infarction. Summary of evidence from clinical trials. Circulation 1995;92:3132-3137.

135. ISIS-4 (Fourth International Study of Infarct Survival) Collaborative Group. ISIS-4: a randomised factorial trial assessing early oral captopril, oral mononitrate, and intravenous magnesium sulphate in 58,050 patients with suspected acute myocardial infarction. Lancet 1995;345:669-685.

136. Gruppo Italiano per lo Studio della Sopravvivenza nell'infarto Miocardico. GISSI-3: effects of lisinopril and transdermal glyceryl trinitrate singly and

together on 6-week mortality and ventricular function after acute myocardial infarction. Lancet 1994;343:1115-1122.

137. Chinese Cardiac Study Collaborative Group. Oral captopril versus placebo among 13,634 patients with suspected acute myocardial infarction: interim report from the Chinese Cardiac Study (CCS-1). Lancet 1995;345:686-687.

138. Ambrosioni E, Borghi C, Magnani B, for the Survival of Myocardial Infarction Long-Term Evaluation (SMILE) Study Investigators. The effect of the angiotensin-converting-enzyme inhibitor zofenopril on mortality and morbidity after anterior myocardial infarction. N Engl J Med 1995;332:80-85.

139. The Acute Infarction Ramipril Efficacy (AIRE) Study Investigators. Effect of ramipril on mortality and morbidity of survivors of acute myocardial infarction with clinical evidence of heart failure. Lancet 1993;342:821-828.

140. The Trace Study Group. The TRAndolapril Cardiac Evaluation (TRACE) study: rationale, design, and baseline characteristics of the screened population. Am J Cardiol 1994;73:44C-50C.

141. Kingma JH, van Gilst WH, Peels CH, Dambrink JH, Verheugt FW, Wielenga RP. Acute intervention with captopril during thrombolysis in patients with first anterior myocardial infarction. Results from the Captopril and Thrombolysis Study (CATS). Eur Heart J 1994;15:898-907.

142. The CONSENSUS Trial Study Group. Effects of enalapril on mortality in severe congestive heart failure: results of the Cooperative North Scandinavian Enalapril Survival Study (CONSENSUS). N Engl J Med. 1987;316:1429-1435.

143. The SOLVD Investigators. Effect of enalapril on survival in patients with reduced left ventricular ejection fractions and congestive heart failure. N Engl J Med 1991;325:293-302.

144. Cohn JN, Johnson G, Ziesche S, et al. A comparison of enalapril with hydralazine-isosorbide dinitrate in the treatment of chronic congestive heart failure. N Engl J Med 1991;325:303-310.

145. The SOLVD Investigators. Effect of enalapril on mortality and the development of heart failure in asymptomatic patients with reduced left ventricular ejection fractions. N Engl J Med 1992;327:685-691.

146. Lowe JE, Reimer KA, Jennings RB. Experimental infarct size as a function of the amount of myocardium at risk. Am J Pathol 1978;90:363-379.

147. Jugdutt BI, Hutchins GM, Bulkley BH, Becker LC. Myocardial infarction in the conscious dog: Three-dimensional mapping of infarct, collateral flow and region at risk. Circulation 1979;60:1141-1150.

148. Reimer KA, Jennings RB. The 'wavefront phenomenon' of myocardial ischemic cell death. II: transmural progression of necrosis within the framework of ischemic bed size (myocardium at risk) and collateral flow. Lab Invest 1979;40:633-644.

149. Jugdutt BI, Becker LC, Hutchins GM. Early changes in collateral blood flow during myocardial infarction in conscious dogs. Am J Physiol 1979;237: H371-380.

150. Jennings RB, Ganote CE. Mitochondrial structure and function in acute myocardial ischemic injury. Circ Res 1976;38:I80-I91.

151. Reimer KA, Lowe JE, Rasmussen MM, Jennings RB. The wavefront phenomenon of ischemic cell death. 1. Myocardial infarct size vs duration of coronary occlusion in dogs. Circulation 1977;56:786-794.

152. Milavetz JJ, Giebel DW, Christian TF, Schwartz RS, Holmes DR Jr, Gibbons RJ. Time to therapy and salvage in myocardial infarction. J Am Coll Cardiol 1998;31:1246-2451.

153. Hillis LD, Fishbein MC, Braunwald E, Maroko PR. The influence of the time interval between coronary artery occlusion and the administration of hyaluronidase on salvage of ischemic myocardium in dogs. Circ Res 1977; 41:26-31.

154. Flaherty JT, Becker LC, Bulkley BH, et al. A randomized prospective trial of intravenous nitroglycerin in patients with acute myocardial infarction. Circulation 1983;68:576-588.

155. Mathey D, Bleifeld W, Buss H, Hanrath P. Creatine kinase release in acute myocardial infarction: correlation with clinical, electrocardiographic, and pathological findings. Br Heart J 1975;37:1161-1168.

156. Kagen L, Scheidt S, Butt A. Serum myoglobin in myocardial infarction: the "staccato phenomenon." Is acute myocardial infarction in man an intermittent event? Am J Med 1977;62:86-92.

157. Mills RM Jr, Young E, Gorlin R, Lesch M. Natural history of S-T segment elevation after acute myocardial infarction. Am J Cardiol 1975;35:609-14.

158. Braunwald E, Kloner RA. The stunned myocardium: prolonged, postischemic ventricular dysfunction. Circulation 1982;66:1146-1149.

159. Ambrosio G, Becker LC, Hutchins GM, Weisman HF, Weisfeldt ML. Reduction in experimental infarct size by recombinant human superoxide dismutase: insights into the pathophysiology of reperfusion injury. Circulation 1986;74:1424-1433.

160. Przyklenk K, Kloner RA. Superoxide dismutase plus catalase improve contractile function in the canine model of the stunned myocardium. Circ Res 1986;58:148-156.

161. Ellis SG, Topol EJ, Gallison L, et al. Predictors of success for coronary angioplasty performed for acute myocardial infarction. J Am Coll Cardiol 1988;12:1407-1415.

162. Becker LC, Jeremy RW, Schaper J, Schaper W. Ultrastructural assessment of myocardial necrosis occurring during ischemia and 3-h reperfusion in the dog. Am J Physiol 1999;277: H243-H252.

163. Bolli R. Mechanism of myocardial stunning. Circulation 1990;82:723-738.

164. Zhao M, Zhang H, Robinson TF, Factor SM, Sonnenblick EH, Eng C. Profound structural alterations of the extracellular collagen matrix in postischemic dysfunctional ("stunned") but viable myocardium. J Am Coll Cardiol. 1987;10:1322-1334.

165. Takahashi S, Barry AC, Factor SM. Collagen degradation in ischaemic rat hearts. Biochem J. 1990;265:233-241.

166. Charney RH, Takahashi S, Zhao M, Sonnenblick EH, Eng C. Collagen loss in the stunned myocardium. Circulation 1992;85: 1483-1490.

167. Hale SL, Kloner RA. Left ventricular topographic alterations in the completely healed rat infarct caused by early and late coronary artery reperfusion. Am Heart J 1988;116:1508-1513.

168. Morita M, Kawashima S, Ueno M, Kubota A, Iwasaki T. Effects of late reperfusion on infarct expansion and infarct healing in conscious rats. Am J Pathol 1993;143: 419-430.

169. Theroux P, Ross J Jr, Franklin D, Kemper WS, Sasayama S. Coronary arterial reperfusion. III. Early and late effects on regional myocardial function and dimensions in conscious dogs. Am J Cardiol 1976;38:599-606.

170. Lavallee M, Cox D, Patrick TA, Vatner SF. Salvage of myocardial function by coronary artery reperfusion 1, 2, and 3 hours after occlusion in conscious dogs. Circ Res 1983;53:235-247.

171. Bush LR, Buja LM, Samowitz W, et al. Recovery of left ventricular segmental function after long-term reperfusion following temporary coronary occlusion in conscious dogs. Comparison of 2- and 4-hour occlusions. Circ Res 1983;53:248-263.

172. Kambayashi M, Miura T, Oh BH, et al. Myocardial cell hypertrophy after myocardial infarction with reperfusion in dogs. Circulation 1992;86:1935-1944.

173. Richard V, Murry CE, Reimer KA. Healing of myocardial infarcts in dogs. Effects of late reperfusion. Circulation 1995;92:1891-1901.

174. Roberts CS, Schoen FJ, Kloner RA. Effect of coronary reperfusion on myocardial hemorrhage and infarct healing. Am J Cardiol 1983;52:610-614.

175. Geft IL, Fishbein MC, Hashida J, et al. Effects of late coronary artery reperfusion after myocardial necrosis is complete. Am Heart J 1984;107: 623-629.

176. Connelly CM, Vogel WM, Wiegner AW, et al. Effects of reperfusion after coronary artery occlusion on post-infarction scar tissue. Circ Res 1985; 57:562-577.

177. Hirayama A, Adachi T, Asada S, et al. Late reperfusion for acute myocardial infarction limits the dilatation of left ventricle without the reduction of infarct size. Circulation 1993;88:2565-2574.

178. Hammerman H, O'Boyle JE, Cohen C, Kloner RA, Parisi AF. Dissociation between two-dimensional echocardiographic left ventricular wall motion and myocardial salvage in early experimental acute myocardial infarction in dogs. Am J Cardiol 1984;54:875-879.

179. Horwitz LD, Fennessey PV, Shikes RH, Kong Y. Marked reduction in myocardial infarct size due to prolonged infusion of an antioxidant during reperfusion. Circulation 1994;89:1792-1801.

180. Tymchak WJ, Michorowski BL, Burton JR, Jugdutt BI. Preservation of left ventricular function and topography with combined reperfusion and intravenous nitroglycerin in acute myocardial infarction. (Abstract) J Am Coll Cardiol 1988;11:90A.

181. Jugdutt BI, Wang S, Demare J, et al. Preservation of myocardial function and topography by late reperfusion and superoxide dismutase. (Abstract) J Am Coll Cardiol 1989;13:109a.

182. Jugdutt BI. Adjunctive Pharmacologic therapies in acute myocardial infarction. In, Brown DL, editor. Cardiac Intensive Care. Philadelphia: WB Saunders Company Publishers, 1998:181-186.

183. Roth A, Barbash GI, Hod H, et al. Should thrombolytic therapy be administered in the mobile intensive care unit in patients with evolving myocardial infarction? A pilot study. J Am Coll Cardiol 1990;15:932-936.

184. Force T, Kemper A, Leavitt M, Parisi AF. Acute reduction in functional infarct expansion with late coronary reperfusion: assessment with quantitative two-dimensional echocardiography. J Am Coll Cardiol 1988; 11:192-200.

185. Gruppo Italiano per lo Studio della Streptochinasi nell'Infarto Miocardico (GISSI). Effectiveness of intravenous thrombolytic treatment in acute myocardial infarction. Lancet 1986;1:397-402.

186. ISIS-2 (Second International Study of Infarct Survival) Collaborative Group. Randomised trial of intravenous streptokinase, oral aspirin, both, or neither among 17,187 cases of suspected acute myocardial infarction: ISIS-2. Lancet 1988;2:349-360.

187. ISIS-2 (Second International Study of Infarct Survival) Collaborative Group. Randomized trial of intravenous streptokinase, oral aspirin, both, or neither among 17,187 cases of suspected acute myocardial infarction: ISIS-2. J Am Coll Cardiol 1988;12(6 Suppl A):3A-13A.

188. Kajstura J, Cheng W, Reiss K, et al. Apoptotic and necrotic myocyte cell deaths are independent contributing variables of infarct size in rats. Lab Invest 1996;74:86-107.

189. Ohno M, Takemura G, Ohno A, Misao J, Hayakawa Y, Minatoguchi S, Fujiwara T, Fujiwara H. 'Apoptotic' myocytes in infarct area in rabbit hearts may be oncotic myocytes with DNA fragmentation: analysis by immunogold electron microscopy combined with In situ nick end-labeling. Circulation 1998;98:1422-1430.

190. Jugdutt BI, Idikio H. Apoptosis and oncosis in acute coronary syndromes: Assessment and implications. Mol and Cell Biochem 2005;270:177-200.

191. Dumont EA, Reutelingsperger CP, Smits JF, et al. Real-time imaging of apoptotic cell-membrane changes at the single-cell level in the beating murine heart. Nat Med 2001;7:1352-1355.

192. Hofstra L, Liem IH, Dumont EA, et al. Visualization of cell death in vivo in patients with acute myocardial infarction. Lancet 2000;356:209-212.

193. Thimister PW, Hofstra L, Liem IH, et al. In vivo detection of cell death in the area at risk in acute myocardial infarction. J Nucl Med 2003;44:391-396.

194. McKay RG, Pfeffer MA, Pasternak RC, et al. Left ventricular remodeling after myocardial infarction: a corollary to infarct expansion. Circulation 1986;74:693-702.

195. Seals AA, Pratt CM, Mahmarian JJ, et al. Relation of left ventricular dilation during acute myocardial infarction to systolic performance, diastolic dysfunction, infarct size and location. Am J Cardiol 1988;61:224-229.

196. Oldroyd KG, Pye MP, Ray SG, et al. Effects of early captopril administration on infarct expansion, left ventricular remodeling and exercise capacity after acute myocardial infarction. Am J Cardiol 1991;68:713-718.

197. Golia G, Marino P, Rametta F, et al. Reperfusion reduces left ventricular dilatation by preventing infarct expansion in the acute and chronic phases of myocardial infarction. Am Heart J 1994;127:499-509.

198. Chareonthaitawee P, Christian TF, Hirose K, Gibbons RJ, Rumberger JA. Relation of initial infarct size to extent of left ventricular remodeling in the year after acute myocardial infarction. J Am Coll Cardiol 1995;25:567-573.

199. Peels KH, Visser CA, Dambrink JH, et al. Left ventricular wall motion score as an early predictor of left ventricular dilation and mortality after first anterior infarction treated with thrombolysis. The CATS Investigators Group. Am J Cardiol 1996;77:1149-1154.

200. Destro G, Marino P, Barbieri E, et al. Postinfarctional remodeling: increased dye intensity in the myocardial risk area after angioplasty of infarct-related coronary artery is associated with reduction of ventricular volumes. J Am Coll Cardiol 2001;37:1239-1245.

201. Solomon SD, Glynn RJ, Greaves S, et al. Recovery of ventricular function after myocardial infarction in the reperfusion era: the healing and early afterload reducing therapy study. Ann Intern Med 2001;134:451-458.

202. Gregg DE, Patterson RE. Functional importance of the coronary collaterals. N Engl J Med 1980;303:1404-1406.

203. Baroldi G, Mantero O, Scomazzoni G. The collaterals of the coronary arteries in normal and pathologic hearts. Circ Res 1956;4:223-229.

204. Schaper W. The collateral circulation of the heart. In, Black DAK, editor. Clinical Studies. Amsterdam, North-Holland. 1971.

205. Blumgart HL, Schlesinger MJ, Davis D. Studies on reaction of clinical manifestations of angina pectoris, coronary thrombosis, and acute myocardial infarction to pathologic findings: with particular reference to the significance of collateral circulation. Am Heart J 1940;19:1-91.

206. Hirzel HO, Nelson GR, Sonnenblick EH, Kirk ES. Redistribution of collateral blood flow from necrotic to surviving myocardium following coronary occlusion in the dog. Circ Res 1976;39:214-222.

207. Gregg DE. The natural history of coronary collateral development. Circ Res 1974;35:335-344.

208. Levin DC. Pathways and functional significance of the coronary collateral circulation. Circulation 1974;50:831-837.

209. Jeremy RW, Hackworthy RA, Bautovich G, Hutton BF, Harris PJ. Infarct artery perfusion and changes in left ventricular volume in the month after acute myocardial infarction. J Am Coll Cardiol 1987;9:989-995.

210. Hirai T, Fujita M, Nakajima H, et al. Importance of collateral circulation for prevention of left ventricular aneurysm formation in acute myocardial infarction. Circulation 1989;79:791-796.

211. Dzavik V, Carere RG, Mancini GB, et al. for the Total Occlusion Study of Canada Investigators. Predictors of improvement in left ventricular function after percutaneous revascularization of occluded coronary arteries: a report from the Total Occlusion Study of Canada (TOSCA). Am Heart J 2001; 142:301-308.

212. Reimer KA, Rasmussen MM, Jennings RB. Reduction by propranolol of myocardial necrosis following temporary coronary artery occlusion in dogs. Circ Res 1973;33:353-363.

213. Jugdutt BI, Lee SJK. Intravenous therapy with propranolol in acute myocardial infarction: Effects on changes in the S-T segment and hemodynamics. CHEST 1978;74: 514-521.

214. The MIAMI Trial Research Group. Metoprolol in acute myocardial infarction (MIAMI). A randomised placebo-controlled international trial. Eur Heart J 1985;6:199-226.

215. Herlitz J, Waldenstrom J, Hjalmarson A. Infarct size limitation after early intervention with metoprolol in the MIAMI Trial. Cardiology 1988;75:117-22.

216. Herlitz J, Hjalmarson A, Karlson BW. Prognosis during one year for patients with myocardial infarction in relation to the development of Q waves: experiences from the MIAMI trial. Clin Cardiol 1990;13:261-264.

217. Breisblatt WM, Waldo DA, Burns MJ, Spaccavento LJ. Hemodynamic effects of intravenous metoprolol in acute myocardial infarction: the role of anatomic subsets in predicting patient response. Am Heart J 1988;116:44-49.

218. Zmudka K, Aubert A, Dubiel J, et al. Early intravenous administration of metoprolol enhances myocardial salvage by thrombolysis with recombinant tissue-type plasminogen activator after thrombotic coronary artery occlusion in the dog by improvement of the collateral blood flow to the area at risk. J Am Coll Cardiol 1994;23:1499-1504.

219. Fishbein MC, Lei LQ, Rubin SA. Long-term propranolol administration alters myocyte and ventricular geometry in rat hearts with and without infarction. Circulation 1988;78:369-375.

220. Jugdutt B, Warnica JW. Improved left ventricular function with Metoprolol in acute myocardial infarction. (Abstract) Circulation 1987;76: IV-276.

221. Ellis SG, Muller DW, Topol EJ. Possible survival benefit from concomitant beta-but not calcium-antagonist therapy during reperfusion for acute myocardial infarction. Am J Cardiol 1990;66:125-128.

222. Jugdutt BI, Khan MI, Jugdutt SJ, Blinston GE. Effect of prolonged inotropic stimulation on ventricular remodeling during healing after myocardial infarction in the dog: Mechanistic insights. J Am Coll Cardiol 1996;27:1787-1795.

223. Fulton WFM. The coronary arteries. Arteriography, microanatomy, and pathogenesis of obliterative coronary artery disease. Springfield, Illinois: Charles C. Thomas, 1965.

224. Hales MR, Carrington CB. A pigmented gelatin mass for vascular injection. Yale J Biol Med 1971;43:257-270.

225. Reimer KA, Jennings RB, Cobb FR, et al. Animal models for protecting ischemic myocardium: results of the NHLBI Cooperative Study. Comparison of unconscious and conscious dog models. Circ Res 1985; 56:651-665.

226. Jugdutt BI. Effect of PGE_1, PGE_2, and PGI_2 on ventricular arrhythmias during myocardial infarction in conscious dogs: Relation to infarct size. Prostaglandins and Med 1981;7:431-455.

227. Jugdutt BI. Different relations between infarct size and occluded bed size in barbiturate-anesthetized versus conscious dog. J Am Coll Cardiol 1985;6: 1035-1046. [**Appendix 34**]

228. Jugdutt BI. Difference in the relation between infarct and occluded bed in pentobarbital-anesthetized and conscious dogs. Can J Physiol Pharmacol 1986;64: 254-262. [**Appendix 35**]

229. Jugdutt BI, Rogers MC, Hutchins GM, Becker LC. Increased myocardial infarct size by thiopental after coronary occlusion in the dog. Am Heart J 1986;112:485-494.

230. Tajik AJ, Seward JB, Hagler DJ, Mair DD, Lie JT. Two-dimensional real-time ultrasonic imaging of the heart and great vessels. Technique, image orientation, structure identification, and validation. Mayo Clin Proc 1978;53:271-303.

231. Visser CA, Lie KI, Kan G, Meltzer R, Durrer D. Detection and quantification of acute, isolated myocardial infarction by two dimensional echocardiography. Am J Cardiol 1981;47:1020-1025.

232. Jugdutt BI, Sussex BA, Warnica JW, Rossall RE. Persistent reduction in left ventricular asynergy in patients with acute myocardial infarction with infusion of nitroglycerin. Circulation 1983;68:1264-1273. [**Appendix 36**]

233. Falsetti HL, Marcus ML, Kerber RE, Skorton DJ. Quantification of myocardial ischemia and infarction by left ventricular imaging. Circulation 1981;63:747-751.

234. Baur HR, Daniel JA, Nelson RR. Detection of left ventricular aneurysm on two dimensional echocardiography. Am J Cardiol 1982;50:191-196.

235. Parisi AF, Moynihan PF, Folland ED, Strauss WE, Sharma GV, Sasahara AA. Echocardiography in acute and remote myocardial infarction. Am J Cardiol 1980;46:1205-1214.

236. Gueret P, Meerbaum S, Wyatt HL, Uchiyama T, Lang TW, Corday E. Two-dimensional echocardiographic quantitation of left ventricular volumes and ejection fraction. Importance of accounting for dyssynergy in short-axis reconstruction models. Circulation 1980;62:1308-1318.

237. Devereux RB, Reichek N. Echocardiographic determination of left ventricular mass in man. Anatomic validation of the method. Circulation 1977;55:613-618.

238. Eaton LW, Maughan WL, Shoukas AA, Weiss JL. Accurate volume determination in the isolated ejecting canine left ventricle by two-dimensional echocardiography. Circulation 1979;60:320-326.

239. Gibbons EF, Hogan RD, Franklin TD, Nolting M, Weyman AE. The natural history of regional dysfunction in a canine preparation of chronic infarction. Circulation 1985;71:394-402.

240. Choong CY, Gibbons EF, Hogan RD, et al. Relationship of functional recovery to scar contraction after myocardial infarction in the canine left ventricle. Am Heart J 1989;117:819-829.

241. Guyer DE, Foale RA, Gillam LD, Wilkins GT, Guerrero JL, Weyman AE. An echocardiographic technique for quantifying and displaying the extent of regional left ventricular dyssynergy. J Am Coll Cardiol 1986;8:830-835.

242. Guyer DE, Gibson TC, Gillam LD, et al. A new echocardiographic model for quantifying three-dimensional endocardial surface area. J Am Coll Cardiol 1986;8:819-829.

243. Picard MH, Wilkins GT, Ray PA, Weyman AE. Natural history of left ventricular size and function after acute myocardial infarction. Assessment and prediction by echocardiographic endocardial surface mapping. Circulation 1990;82:484-494.

244. Picard MH, Wilkins GT, Gillam LD, Thomas JD, Weyman AE. Immediate regional endocardial surface expansion following coronary occlusion in the canine left ventricle: disproportionate effects of anterior versus inferior ischemia. Am Heart J 1991;121:753-762.

245. Jugdutt BI, Sivaram CA. Prospective two-dimensional echocardiographic evaluation of left ventricular thrombus and embolism after mycocardial infarction. J Am Coll Cardiol 1989;13: 554-64.

246. Delemarre BJ, Visser CA, Bot H, Dunning AJ. Prediction of apical thrombus formation in acute myocardial infarction based on left ventricular spatial flow pattern. J Am Coll Cardiol 1990;15:355-360.

247. Jugdutt BI, Manyari DE, Humen DP. Detection of viability of dysfunctional myocardium in coronary heart disease. II. Echocardiography. Heart Failure Reviews 1998;2:207-233.

248. Nieminen M, Heikkila J. Echoventriculography in acute myocardial infarction. II: Monitoring of left ventricular performance. Br Heart J 1976;38: 271-281.

249. Rigo P, Murray M, Strauss HW, et al. Left ventricular function in acute myocardial infarction evaluation by gated scintiphotography. Circulation 1974;50:678-684.

250. Jugdutt BI. Intravenous nitroglycerin infusion in acute myocardial infarction: myocardial salvage. Cardiovasc Rev Rep 1984;5:1145-1163 and Master Teacher Award 1990;11:53-67. [**Appendix 37**]

251. Jugdutt BI, Sussex BA, Haraphongse M, Rossall RE. Right ventricular involvement in transmural inferior wall infarction: Two-dimensional echocardiographic and clinical correlations. Clin Invest Med 1983;6:261-273.

252. Jugdutt BI, Haraphongse M, Basualdo CA, Rossall RE. Evaluation of biventricular involvement in hypotensive patients with transmural inferior infarction by two-dimensional echocardiography. Am Heart J 1984;108: 1417-1426.

253. Jugdutt BI, Sussex BA, Sivaram CA, Rossall RE. Right ventricular infarction: A two-dimensional echocardiographic evaluation. Am Heart J 1984;107 505-518.

254. Ford LE. Heart size. Circ Res 1976;39:297-303.

255. Moriarty TF. The law of Laplace. Its limitations as a relation for diastolic pressure, volume, or wall stress of the left ventricle. Circ Res 1980;46:321-331.

256. Spotnitz HM, Sonnenblick EH, Spiro D. Relation of ultrastructure to function in the intact heart: sarcomere structure relative to pressure volume curves of intact left ventricles of dog and cat. Circ Res 1966;18:49-66.

257. Sandler H, Dodge HT. Left ventricular tension and stress in man. Circ Res 1963;13:91-104.

258. Streeter DD Jr, Hanna WT. Engineering mechanics for successive states in canine left ventricular myocardium. I. Cavity and wall geometry. Circ Res 1973;33:639-655.

259. Woods RH. A few applications of a physical theorem to membrane in the human body in a state of tension. J Anat Physiol 1892;26:362-370.

260. Yin FCP. Ventricular wall stress. Circ Res 1981;49:829-842.

261. Mirsky I. Review of various theories for the evaluation of left ventricular wall stress. In, Mirsky I, Ghista D, Sandler H, editors. Cardiac mechanics: Physiological, clinical, and mathematical considerations. New York: John Wiley & Sons, Inc., 1974:381-409.

262. Janz RF. Estimation of local myocardial stress. Am J Physiol 1982;242: H875-H881.

263. Tomlinson CW. Left ventricular geometry and function in experimental heart failure. Can J Cardiol 1987;3:305-310.

264. Douglas PS, Reichek N, Plappert T, Muhammad A, St John Sutton MG. Comparison of echocardiographic methods for assessment of left ventricular shortening and wall stress. J Am Coll Cardiol 1987;9:945-951.

265. Douglas PS, Morrow R, Ioli A, Reichek N. Left ventricular shape, afterload and survival in idiopathic dilated cardiomyopathy. J Am Coll Cardiol 1989; 13:311-315.

266. D'Cruz IA, Shroff SG, Janicki JS, Jain A, Reddy HK, Lakier JB. Differences in the shape of the normal, cardiomyopathic, and volume overloaded human left ventricle. J Am Soc Echocardiogr 1989;2:408-414.

267. Fischl SJ, Gorlin R, Herman MV. Cardiac shape and function in aortic valve disease: physiologic and clinical implications. Am J Cardiol 1977; 39:170-176.

268. Gibson DG, Brown DJ. Continuous assessment of left ventricular shape in man. Br Heart J 1975;37:904-910.

269. Kass DA, Traill TA, Keating M, Altieri PI, Maughan WL. Abnormalities of dynamic ventricular shape change in patients with aortic and mitral valvular regurgitation: assessment by Fourier shape analysis and global geometric indexes. Circ Res 1988;62:127-138.

270. Mancini GBJ, DeBoe SF, Gillon J, Simon SB, LeFree MT, Weymouth TE. Measurement of systolic and diastolic disorders of shape using frame-by-frame quantitative regional curvature analysis. Coronary Artery Disease 1991;2:179-187.

271. Sabbah HN, Kono T, Stein PD, Mancini GB, Goldstein S. Left ventricular shape changes during the course of evolving heart failure. Am J Physiol 1992;263:H266-H270.

272. Rogers EW, Feigenbaum H, Weyman AE. Echocardiography for quantification of cardiac chambers. In: Goodwin JF, editor. Progress in cardiology. Philadelphia: Lea & Febiger, 1979:1-72.

273. Visser CA, Kan G, Meltzer RS, Moulijn AC, David GK, Dunning AJ. Assessment of left ventricular aneurysm resectability by two-dimensional echocardiography. Am J Cardiol 1985;56:857-860.

274. Jugdutt BI, Khan MI, Johnston BJ, Jugdutt SJ, Blinston GE. Progressive changes in regional and global left ventricular dilation during remodeling post-myocardial infarction. (Abstract) J Am Coll Cardiol 1994;23:269A. **[Appendix 38]**

275. Bogen DK, Rabinowitz SA, Needleman A, McMahon TA, Abelmann WH. An analysis of the mechanical disadvantage of myocardial infarction in the canine left ventricle. Circ Res 1980;47:728-741.

276. Pouleur HG, Konstam MA, Udelson JE, Rousseau MF. Changes in ventricular volume, wall thickness and wall stress during progression of left ventricular dysfunction. The SOLVD Investigators. J Am Coll Cardiol 1993; 22(4 Suppl A):43A-48A.

277. Weber KT, Anversa P, Armstrong PW, et al. Remodeling and reparation of the cardiovascular system. J Am Coll Cardiol 1992;20:3-16.

278. Jugdutt BI. Remodeling of the myocardium and potential targets in the collagen degradation and synthesis pathways. Current Drug Targets, Cardiovascular & Haematological Disorders 2003;3:27-56. **[Appendix 39]**

279. Caulfield JB, Borg TK. The collagen network of the heart. Lab Invest 1979;40:364-372.

280. Tyagi SC, Kumar SG, Banks J, et al. Co-expression of tissue inhibitor and matrix metalloproteinase in myocardium. J Mol Cell Cardiol 1995;27:2177-2189.

281. Covell JW. Factors influencing diastolic function. Possible role of the extracellular matrix. Circulation 1990;81 (suppl III):III-115-III-158.

282. Honan MB, Harrell FE Jr, Reimer KA, et al. Cardiac rupture, mortality and the timing of thrombolytic therapy: a meta-analysis. J Am Coll Cardiol. 1990;16:359-367.

283. Jugdutt BI. Left ventricular rupture threshold during the healing phase after myocardial infarction in the dog. Can J Physiol Pharmacol 1987;65:307-316. [**Appendix 40**]

284. Whittaker P, Boughner DR, Kloner RA. Analysis of healing after myocardial infarction using polarized light microscopy. Am J Pathol. 1989; 134:879-893.

285. Linzbach AJ. Heart failure from the point of view of quantitative anatomy. Am J Cardiol. 1960;5: 370-382.

286. Bing OH, Fanburg BL, Brooks WW, et al. The effect of lathyrogen beta-amino proprionitrile (BAPN) on the mechanical properties of experimentally hypertrophied rat cardiac muscle. Circ Res. 1978;43:632-637.

287. Caulfield JB, Wolkowicz P. Inducible collagenolytic activity in isolated perfused rat hearts. Am J Pathol. 1988;131:199-205.

288. MacKenna DA, Omens JH, McCulloch AD, et al. Contribution of collagen matrix to passive left ventricular mechanics in isolated rat hearts. Am J Physiol. 1994;266:H1007-H1018.

289. Holmes JW, Yamashita H, Waldman LK, et al. Scar remodeling and transmural deformation after infarction in the pig. Circulation. 1994;90:411-420.

290. Cannon RO, Butany JW, McManus BM, et al. Early degradation of collagen after acute myocardial infarction in the rat. Am J Cardiol. 1983;52:390-395.

291. Olivetti G, Capasso JM, Sonnenblick EH, Anversa P. Side-to-side slippage of myocytes participates in ventricular wall remodeling acutely after myocardial infarction in rats. Circ Res 1990;67: 23-34.

292. Heymans S, Luttun A, Nuyens D, et al. Inhibition of plasminogen activators or matrix metalloproteinases prevents cardiac rupture but impairs therapeutic angiogenesis and causes cardiac failure. Nat Med. 1999;5:1135-1142.

293. Factor SM, Robinson TF, Dominitz R, et al. Alterations of the myocardial skeletal framework in acute myocardial infarction with and without ventricular rupture. Am J Cardiovasc Pathol. 1987;1:91-97 .

294. Tyagi SC. Proteinases and myocardial extracellular matrix turnover. Mol Cell Bioch 1997; 168:1-12.

295. Weber KT. Extracellular matrix remodeling in heart failure. A role for de novo angiotensin II generation. Circulation 1997;96:4065-4082.

296. Cleutjens JPM, Kandala JC, Guarda E, et al. Regulation of collagen degradation in the rat myocardium after infarction. J Mol Cell Cardiol 1995; 27:1281-1292.

297. Jordan JE, Zhao ZQ, Vinten-Johansen J. The role of neutrophils in myocardial ischemia-reperfusion injury. Cardiovasc Res. 1999;43:860 - 878.

298. Jugdutt BI, Balghith M. Diastolic dysfunction during remodeling after myocardial infarction: Natural history and effect of prolonged ACE inhibition and nitrate therapy. (Abstract) Circulation 2001;104:II-430. [**Appendix 41**]

299. Pfeffer JM, Pfeffer MA, Fletcher PJ, et al. Progressive ventricular remodeling in rat with myocardial infarction. Am J Physiol. 1991;260: H1406-1414.

300. Chandrashekhar Y, Sen S, Anway R, Shuros A, Anand I. Long-term caspase inhibition ameliorates apoptosis, reduces myocardial troponin-I cleavage, protects left ventricular function, and attenuates remodeling in rats with myocardial infarction. J Am Coll Cardiol 2004;43:295-301.

301. Lu L, Gunja-Smith Z, Woessner JF, Ursell PC, Nissen T, Galardy RE, Xu Y, Zhu P, Schwartz GG. Matrix metalloproteinases and collagen ultrastructure in moderate myocardial ischemia and reperfusion in vivo. Am J Physiol 2000;279: H601-H609.

302. Etoh T, Joffs C, Deschamps AM, Davis J, et al. Myocardial and interstitial matrix metalloproteinase activity after acute myocardial infarction in pigs. Am J Physiol 2001:281:H987-H994.

303. Ducharme A, Frantz S, Aikawa M, et al. Targeted deletion of matrix metalloprotienase-9 attenuates left ventricular enlargement and collagen accumulation after experimental myocardial infarction. J Clin Invest 2000; 106:55-62.

304. Rohde LE, Ducharme A, Arroyo LH, et al. Matrix metalloproteinase inhibition attenuates early left ventricular enlargement after experimental myocardial infarction in mice. Circulation 1999;99:3063-3070.

305. Kim CB, Braunwald E. Potential benefits of late reperfusion of infarcted myocardium. The open artery hypothesis. Circulation 1993;88:2426-2436.

306. LATE Study Group. Late Assessment of Thrombolytic Efficacy (LATE) study with alteplase 6-24 hours after onset of acute myocardial infarction. Lancet 1993;25;342:759-766.

307. Peuhkurinen KJ, Risteli L, Melkko JT, et al. Thrombolytic therapy with streptokinase stimulates collagen breakdown. Circulation 1991;83:1969-1975.

308. Zannad F, Alla F, Dousset B, et al. Limitation of excessive extracellular matrix turnover may contribute to survival benefit of spironolactone therapy in patients with congestive heart failure: insights from the randomized aldactone evaluation study (RALES). Rales Investigators. Circulation 2000;102:2700-2706.

309. Nguyen QT, Cernacek P, Calderoni A, et al. Endothelin A receptor blockade causes adverse left ventricular remodeling but improves pulmonary artery pressure after infarction in the rat. Circulation 1998;98:2323-2330.

310. Pitt B, Remme W, Zannad F, et al.; Eplerenone Post-Acute Myocardial Infarction Heart Failure Efficacy and Survival Study Investigators. Eplerenone, a selective aldosterone blocker, in patients with left ventricular dysfunction after myocardial infarction. N Engl J Med 2003;348:1309-1321.

311. Becker RC, Hochman JS, Cannon CP, et al. Fatal cardiac rupture among patients treated with thrombolytic agents and adjunctive thrombin antagonists: observations from the Thrombolysis and Thrombin Inhibition in Myocardial Infarction 9 Study. J Am Coll Cardiol 1999;33:479-487.

312. Harnarayan C, Bennett MA, Pentecost BL, Brewer DB. Quantitative study of infarcted myocardium in cardiogenic shock. Br Heart J 1970;32:728-732.

313. Levy RI. Introduction. Causes of the decrease in cardiovascular mortality. Am J Cardiol 1984;54:1C, 7C-13C.

314. Yusuf S, Thom T, Abbott RD. Changes in hypertension treatment and in congestive heart failure mortality in the United States. Hypertension 1989; 13(5 Suppl):I74-I79.

315. Balghith M, Jugdutt BI. Assessment of diastolic dysfunction after acute myocardial infarction using Doppler Echocardiography. Can J Cardiol 2002;18:69-77. [**Appendix 42**]

316. Douglas PS, Tallant B. Hypertrophy, fibrosis and diastolic dysfunction in early canine experimental hypertension. J Am Coll Cardiol 1991;17:530-536.

317. Bergman I, Loxley R. Two improved and simplified methods for the spectrophotometric determination of hydroxyproline. Anal Chem 1963;35: 1961-1965.

318. Jugdutt BI, Humen DP, Khan MI, Schwarz-Michorowski BL. Effect of left ventricular unloading with captopril on remodelling and function during healing of anterior transmural myocardial infarction in the dog. Can J Cardiol 1992;8:151-163. [**Appendix 43**]

319. Ford WR, Menon V, Bhambhani A, Liyanage R, Khan MI, Jugdutt BI. Changes in myocardial density during postinfarction healing: effect on estimation of in vivo left ventricular mass by echocardiographic imaging. Can J Physiol & Pharmacol 1997;75:1075-1082.

320. Feinstein AR. Clinical Biostatics. St. Louis:Mosby, 1977:329.

321. Shell WE, Kjekshus JK, Sobel BE. Quantitative assessment of the extent of myocardial infarction in the conscious dog by means of analysis of serial changes in serum creatine phosphokinase activity. Clin Invest 1971;50: 2614-2625.

322. Wallenstein S, Zucker CL, Fleiss JL. Some statistical methods useful in Circulation Research. Circ Res 1980;47:1-9.

323. Kass DA, Maughan WL, Ciuffo A, Graves W, Healy B, Weisfeldt ML. Disproportionate epicardial dilation after transmural infarction of the canine left ventricle: acute and chronic differences. J Am Coll Cardiol 1988;11: 177-185.

324. Vracko R, Thorning D, Frederickson RG. Connective tissue cells in healing rat myocardium. A study of cell reactions in rhythmically contracting environment. Am J Pathol 1989;134:993-1006.

325. Sun Y, Weber KT. Infarct scar: a dynamic tissue. *Cardiovasc Res.* 2000; 46:250-256.

326. Myers JH, Stirling MC, Choy M, Buda AJ, Gallagher KP. Direct measurement of inner and outer wall thickening dynamics with epicardial echocardiography. Circulation 1986;74:164-172.

327. Kaul S, Pandian NG, Okada RD, Pohost GM, Weyman AE. Contrast echocardiography in acute myocardial ischemia: I. In vivo determination of total left ventricular "area at risk". J Am Coll Cardiol 1984;4:1272-1282.

328. Kaul S, Gillam LD, Weyman AE. Contrast echocardiography in acute myocardial ischemia. II. The effect of site of injection of contrast agent on the estimation of area at risk for necrosis after coronary occlusion. J Am Coll Cardiol 1985;6:825-830.

329. Kaul S, Glasheen W, Ruddy TD, Pandian NG, Weyman AE, Okada RD. The importance of defining left ventricular area at risk in vivo during acute myocardial infarction: an experimental evaluation with myocardial contrast two-dimensional echocardiography. Circulation 1987;75:1249-1260.

330. Touchstone DA, Beller GA, Nygaard TW, Tedesco C, Kaul S. Effects of successful intravenous reperfusion therapy on regional myocardial function and geometry in humans: a tomographic assessment using two-dimensional echocardiography. J Am Coll Cardiol 1989;13:1506-1513.

331. Villanueva FS, Glasheen WP, Sklenar J, Kaul S. Assessment of risk area during coronary occlusion and infarct size after reperfusion with myocardial contrast echocardiography using left and right atrial injections of contrast. Circulation 1993;88:596-604.

332. Abrams J. Tolerance to organic nitrates. Circulation 1986;74:1181-1185.

333. Jugdutt BI. Nitrates as anti-ischemic and cardioprotective agents. In: Singh BN, Dzau VJ, Vanhoutte P, Woosley RL, editors. Cardiovascular Pharmacology and Therapeutics. New York: Churchill Livingston, 1993:449-465. [**Appendix 44**]

334. Needleman P, Jonhson EM Jr. Vasodilators and the treatment of angina. In, Gilman AG, Goodman LS, Gilman A, editors. Goodman and Gilman's The Pharmacological Basis of Therapeutics. New York: Macmillan Publishing, 1980:819-833.

335. De Caterina R, Giannessi D, Crea F, Chierchia S, Bernini W, Gazzetti P, L'Abbate A. Inhibition of platelet function by injectable isosorbide dinitrate. Am J Cardiol 1984;53:1683-1687.

336. Bassenge E, Busse R, Pohl U. [Inhibition of thrombocyte aggregation and adhesion by endothelium-derived relaxant factor (EDRF) and their pathophysiologic significance]. Z Kardiol 1989;78(Suppl 6):54-8.

337. Thadani U, Hamilton SF, Olson E, et al. Duration of effects and tolerance of slow-release isosorbide-5-mononitrate for angina pectoris. Am J Cardiol 1987;59:756-762.

338. Schoemaker RG, Debets JJ, Struyker-Boudier HA, Smits JF. Delayed but not immediate captopril therapy improves cardiac function in conscious rats, following myocardial infarction. J Mol Cell Cardiol 1991;23:187-197.

339. Gibson RS, Bishop HL, Stamm RB, Crampton RS, Beller GA, Martin RP. Value of early two dimensional echocardiography in patients with acute myocardial infarction. Am J Cardiol 1982;49:1110-1119.

340. Holt M, Marjoram DTE. Measurement of shape in geography. In: Heinemann, editor. Mathematics in a changing world. London: Walker, 1973:236.

341. Giannuzzi P, Tavazzi L, Temporelli PL, et al. Long-term physical training and left ventricular remodeling after anterior myocardial infarction: results of the Exercise in Anterior Myocardial Infarction (EAMI) trial. EAMI Study Group. J Am Coll Cardiol 1993;22:1821-1829.

342. Gaudron P, Hu K, Schamberger R, Budin M, Walter B, Ertl G. Effect of endurance training early or late after coronary artery occlusion on left ventricular remodeling, hemodynamics, and survival in rats with chronic transmural myocardial infarction. Circulation 1994;89:402-412.

343. Buck T, Hunold P, Wentz KU, Tkalec W, Nesser HJ, Erbel R. Tomographic three-dimensional echocardiographic determination of chamber size and systolic function in patients with left ventricular aneurysm: comparison to magnetic resonance imaging, cineventriculography, and two-dimensional echocardiography. Circulation 1997;96:4286-4297.

344. Yusuf S, Collins R, MacMahon S, Peto S. Effect of intravenous nitrates on mortality in acute myocardial infarction: an overview of the randomised trials. Lancet 1988;1:1088-1092.

345. Ryan TJ, Anderson JL, Antman EM, et al. ACC/AHA guidelines for the management of patients with acute myocardial infarction. A report of the American College of Cardiology/American Heart Association Task Force on

Practice Guidelines (Committee on Management of Acute Myocardial Infarction). J Am Coll Cardiol 1996;28:1328-1428.

346. Packer M, Meller J, Medina N, Gorlin R. Determinants of drug response in severe chronic heart failure. I. Activation of vasoconstrictor forces during vasodilator therapy. Circulation 1981;64:506-514.

347. Bassenge E, Busse R. Endothelial modulation of coronary tone. Prog Cardiovasc Dis 1988;30:349-380.

348. Palmer RM, Ferrige AG, Moncada S. Nitric oxide release accounts for the biological activity of endothelium-derived relaxing factor. Nature 1987;327:524-526.

349. DeWood MA, Spores J, Notske R, et al. Prevalence of total coronary occlusion during the early hours of transmural myocardial infarction. N Engl J Med 1980;303:897-902.

350. Timmermans PBMWM, Smith RD. Angiotensin II receptor subtypes: selective antagonists and functional correlates. Eur Heart J 1994;15(suppl D):79-87.

351. Michel JB, Lattion AL, Salzmann JL, et al. Hormonal and cardiac effects of converting enzyme inhibition in rat myocardial infarction. Circ Res 1988;62:641-650.

352. Nabel EG, Topol EJ, Galeana A, et al. A randomized placebo-controlled trial of combined early intravenous captopril and recombinant tissue-type plasminogen activator therapy in acute myocardial infarction. J Am Coll Cardiol 1991;17:467-473.

353. Smits JFM, van Krimpen C, Schoemaker RG, Cleutjens JPM, Daemen MJAP. Angiotensin II receptor blockade after myocardial infarction in rats: effects on hemodynamics, myocardial DNA synthesis, and interstitial collagen content. J Cardiovasc Pharmacol 1992;20:722-778.

354. Hall AS, Tan L-B, Ball SG. Inhibition of ACE/kininase-II, acute myocardial infarction, and survival. Cardiovasc Res 1994;28:190-198.

355. Dell'Italia LJ, Meng QC, Balcells IME, et al. Increased ACE and chymase-like activity in cardiac tissue of dogs with chronic mitral regurgitation. Am J Physiol 1995;269:H2065-H2073.

356. Saarinen J, Kalkkinen N, Welgus HG, Kovanen PT. Activation of human interstital procollagenase through direct cleavage of the ^{83}Leu-^{84}Thr bond by mast cell chymase. J Biol Chem 1994;269:18134-18140.

357. Mahmarian JJ, Moyé LA, Chinoy DA, et al. Transdermal nitroglycerin patch therapy improves left ventricular function and prevents remodeling after acute myocardial infarction. Results of a multicenter prospective randomized, double-blind, placebo-controlled trial. Circulation 1998;97: 2017-2024.

358. Furberg CD, Campbell RWF, Pitt B. ACE inhibitors after myocardial infarction. N Engl J Med 1993;328:967.

359. Willems IEMG, Havenith MG, De Mey JGR, Daemen MJAP. The α-smooth muscle actin-positive cells in healing human myocardial scars. Am J Pathol 1994; 145:868-875.

360. Beltrami CA, Finato N, Rocco M, et al. Structural basis of end-stage failure in ischemic cardiomyopathy in humans. Circulation 1994;89:151-163.

361. Cohn JN, Tognoni G; for the Valsartan Heart Failure Trial Investigators. A randomized trial of the angiotensin-receptor blocker valsartan in chronic heart failure. N Engl J Med 2001;345:1667-1675.

362. Ryan TJ, Antman EM, Brooks NH, et al. 1999 update: ACC/AHA guidelines for the management of patients with acute myocardial infarction. A report of the American College of Cardiology/American Heart Association Task Force on Practice Guidelines (Committee on Management of Acute Myocardial Infarction). J Am Coll Cardiol 1999;34:890-911.

363. Jugdutt BI. Angiotensin II receptor blockers. In M.H. Crawford, editor. 1998 Cardiology Clinics Annual of Drug Therapy. Philadelphia: W.B. Saunders Publishers, 1998;Vol 2:1-17. [**Appendix 45**]

364. Dzau VJ. Theodore Cooper Lecture: Tissue angiotensin and pathobiology of vascular disease: a unifying hypothesis. Hypertension 2001;37:1047-1052.

365. Kober L, Torp-Pedersen C, Carlsen JE, et al. A clinical trial of the angiotensin-converting-enzyme inhibitor trandolapril in patients with left ventricular dysfunction after myocardial infarction. Trandolapril Cardiac Evaluation (TRACE) Study Group. N Engl J Med 1995;333:1670-1676.

366. The GISSI-3 trial. Gruppo Italiano per lo Studio della Sopravvivenza nell'Infarto Miocardico. Six-month effects of early treatment with lisinopril and transdermal glyceryl trinitrate singly and together withdrawn six weeks after acute myocardial infarction. J Am Coll Cardiol 1996;27:337-344.

367. ACE Inhibitor Myocardial Infarction Collaborative Group. Indications for ACE inhibitors in the early treatment of acute myocardial infarction: systematic overview of individual data from 100,000 patients in randomized trials. Circulation 1998;97:2202-2212.

368. Flather MD, Yusuf S, Kober L, et al. ACE-Inhibitor Myocardial Infarction Collaborative Group. Long-term ACE-inhibitor therapy in patients with heart failure or left-ventricular dysfunction: a systematic overview of data from individual patients. Lancet 2000;355:1575-1581.

369. Pfeffer MA. ACE inhibitors in acute myocardial infarction: patient selection and timing. Circulation 1998;97:2192-2194.

370. Drexler H. Endothelial dysfunction in heart failure and potential for reversal by ACE inhibition. Br Heart J 1994:72(3 Suppl):S11-S14.

371. Seyedi N, Xu X, Nasjletti A, et al. Coronary kinin generation mediates nitric oxide release after angiotensin receptor stimulation. Hypertension 1995;26:164-170.

372. Liu YH, Yang XP, Shesely EG, et al. Role of angiotensin II type 2 receptors and kinins in the cardioprotective effect of angiotensin II type 1 receptor antagonists in rats with heart failure. J Am Coll Cardiol 2004;43: 1473-1480.

373. Xu Y, Menon V, Jugdutt BI. Cardioprotection after angiotensin II type 1 blockade involves angiotensin II type 2 receptor expression and activation of protein kinase C-epsilon in acutely reperfused myocardial infarction in the dog. Effect of UP269-6 and losartan on AT_1 and AT_2-receptor expression and IP_3 receptor and PKCε proteins. J Renin Angiotensin Aldosterone Syst 2000;1:184-195.

374. Jugdutt BI, Balghith M. Enhanced regional AT_2-receptor and PKCε expression during cardioprotection induced by AT_1-receptor blockade after reperfused myocardial infarction. J Renin Angiotensin Aldosterone Syst 2001;2:134-140.

375. Jugdutt BI, Xu Y, Balghith M, et al. Cardioprotection induced by AT_1R blockade after reperfused myocardial infarction: association with regional increase in AT_2R, IP_3R and PKCε proteins and cGMP. J Cardiovasc Pharmacol Ther 2000;5:301-311.

376. Kawamura M, Imanashi M, Matsushima Y, et al. Circulating angiotensin II levels under repeated administration of lisinopril in normal subjects. Clin Exp Pharmacol Physiol 1992;19:547-553.

377. Jorde UP, Ennezat PV, Lisker J, et al. Maximally recommended doses of angiotensin-converting enzyme (ACE) inhibitors do not completely prevent ACE-mediated formation of angiotensin II in chronic heart failure. Circulation 2000;101:844-846.

378. Spinale FG, de Gasparo M, Whitebread S, et al. Modulation of the renin-angiotensin pathway through enzyme inhibition and specific receptor blockade in pacing-induced heart failure: I. Effects on left ventricular performance and neurohormonal systems. Circulation 1997;96:2385-2396.

379. Hamroff G, Katz SD, Mancini D, et al. Addition of angiotensin II receptor blockade to maximal angiotensin-converting enzyme inhibition improves exercise capacity in patients with severe congestive heart failure. Circulation 1999;99:990-992.

380. Dickstein K, Kjekshus J; OPTIMAAL Steering Committee of the OPTIMAAL Study Group. Effects of losartan and captopril on mortality and morbidity in high-risk patients after acute myocardial infarction: the OPTIMAAL randomised trial. Optimal Trial in Myocardial Infarction with Angiotensin II Antagonist Losartan. Lancet 2002;360:752-760.

381. Pfeffer MA, McMurray JJ, Velazquez EJ, et al. for the Valsartan in Acute Myocardial Infarction Trial Investigators. Valsartan, captopril, or both in myocardial infarction complicated by heart failure, left ventricular dysfunction, or both. N Engl J Med 2003;349:1893-1906.

382. Pitt B, Segal R, Martinez FA, et al. Randomised trial of losartan versus captopril in patients over 65 with heart failure (Evaluation of Losartan in the Elderly Study, ELITE). Lancet 1997;349:747-752.

383. Pitt B, Poole-Wilson PA, Segal R, et al. Effect of losartan compared with captopril on mortality in patients with symptomatic heart failure: randomised trial--the Losartan Heart Failure Survival Study ELITE II. Lancet 2000;355: 1582-1587.

384. Pfeffer MA, Swedberg K, Granger CB, et al. for the CHARM Investigators and Committees. Effects of candesartan on mortality and morbidity in patients with chronic heart failure: the CHARM-Overall programme. Lancet 2003;362:759-766.

385. McMurray JJ, Ostergren J, Swedberg K, et al. for the CHARM Investigators and Committees. Effects of candesartan in patients with chronic heart failure and reduced left-ventricular systolic function taking angiotensin-converting-enzyme inhibitors: the CHARM-Added trial. Lancet 2003;362: 767-771.

386. Granger CB, McMurray JJ, Yusuf S, et al. for the CHARM Investigators and Committees. Effects of candesartan in patients with chronic heart failure and reduced left-ventricular systolic function intolerant to angiotensin-converting-enzyme inhibitors: the CHARM-Alternative trial. Lancet 2003; 362:772-776.

387. Yusuf S, Pfeffer MA, Swedberg K, et al. for the CHARM Investigators and Committees. Effects of candesartan in patients with chronic heart failure and preserved left-ventricular ejection fraction: the CHARM-Preserved Trial. Lancet 2003;362:777-781.

388. Sever PS, Dahlof B, Poulter NR, et al. for the ASCOT Investigators. Prevention of coronary and stroke events with atorvastatin in hypertensive patients who have average or lower-than-average cholesterol concentrations, in the Anglo-Scandinavian Cardiac Outcomes Trial--Lipid Lowering Arm (ASCOT-LLA): a multicentre randomised controlled trial. Lancet 2003;361:1149-1158.

389. Dahlof B, Sever PS, Poulter NR, et al. for the ASCOT Investigators. Prevention of cardiovascular events with an antihypertensive regimen of amlodipine adding perindopril as required versus atenolol adding bendroflumethiazide as required, in the Anglo-Scandinavian Cardiac Outcomes Trial-Blood Pressure Lowering Arm (ASCOT-BPLA): a multicentre randomised controlled trial. Lancet 2005;366:895-906.

390. Poulter NR, Wedel H, Dahlof B, et al. for the ASCOT Investigators. Role of blood pressure and other variables in the differential cardiovascular event rates noted in the Anglo-Scandinavian Cardiac Outcomes Trial-Blood Pressure Lowering Arm (ASCOT-BPLA). Lancet 2005;366:907-913.

391. Young JB, Dunlap ME, Pfeffer MA, et al. for the Candesartan in Heart failure Assessment of Reduction in Mortality and morbidity (CHARM) Investigators and Committees. Mortality and morbidity reduction with Candesartan in patients with chronic heart failure and left ventricular

systolic dysfunction: results of the CHARM low-left ventricular ejection fraction trials. Circulation 2004;110:2618-2626.

392. McKelvie RS, Yusuf S, Pericak D, et al. Comparison of candesartan, enalapril, and their combination in congestive heart failure: randomized evaluation of strategies for left ventricular dysfunction (RESOLVD) pilot study. The RESOLVD Pilot Study Investigators. Circulation 1999;100: 1056-1064.

393. White HD, Aylward PE, Huang Z, et al. for the VALIANT Investigators. Mortality and morbidity remain high despite captopril and/or Valsartan therapy in elderly patients with left ventricular systolic dysfunction, heart failure, or both after acute myocardial infarction: results from the Valsartan in Acute Myocardial Infarction Trial (VALIANT). Circulation 2005;112:3391-3399.

394. Szummer KE, Solomon SD, Velazquez EJ, et al. for the VALIANT Registry. Heart failure on admission and the risk of stroke following acute myocardial infarction: the VALIANT registry. Eur Heart J 2005;26:2114-2119.

395. Wong M, Staszewsky L, Latini R, et al. for the Val-HeFT Heart Failure Trial Investigators. Valsartan benefits left ventricular structure and function in heart failure: Val-HeFT echocardiographic study. J Am Coll Cardiol 2002; 40:970-975.

396. Maggioni AP, Latini R, Carson PE, et al. for the Val-HeFT Investigators. Valsartan reduces the incidence of atrial fibrillation in patients with heart failure: results from the Valsartan Heart Failure Trial (Val-HeFT). Am Heart J 2005;149:548-557.

397. Latini R, Masson S, Anand I, et al. for the Valsartan Heart Failure Trial Investigators. Effects of valsartan on circulating brain natriuretic peptide and norepinephrine in symptomatic chronic heart failure: the Valsartan Heart Failure Trial (Val-HeFT). Circulation 2002;106:2454-2458.

398. Cohn JN, Anand IS, Latini R, et al. for the Valsartan Heart Failure Trial Investigators. 2003. Sustained reduction of aldosterone in response to the angiotensin receptor blocker valsartan in patients with chronic heart failure: results from the Valsartan Heart Failure Trial. *Circulation*, 108:1306-9.

399. Baruch L, Anand I, Cohen IS, et al. 1999. Augmented short- and long-term hemodynamic and hormonal effects of an angiotensin receptor blocker added to angiotensin converting enzyme inhibitor therapy in

patients with heart failure. Vasodilator Heart Failure Trial (V-HeFT) Study Group. *Circulation*, 99:2658-64.

400. Pitt B. Effect of aldosterone blockade in patients with systolic left ventricular dysfunction: implications of the RALES and EPHESUS studies. Mol Cell Endocrinol 2004;217:53-58.

401. Suzuki G, Morita H, Mishima T, et al. Effects of long-term monotherapy with eplerenone, a novel aldosterone blocker, on progression of left ventricular dysfunction and remodeling in dogs with heart failure. Circulation 2002;106:2967-2972.

402. Modena MG, Aveta P, Menozzi A, Rossi R. Aldosterone inhibition limits collagen synthesis and progressive left ventricular enlargement after anterior myocardial infarction. Am Heart J 2001;141:41-46.

403. Pitt B, Zannad F, Remme WJ, et al. The effect of spironolactone on morbidity and mortality in patients with severe heart failure. Randomized Aldactone Evaluation Study Investigators. N Engl J Med 1999;341:709-717.

404. Pitt B, White H, Nicolau J, et al. for the EPHESUS Investigators. Eplerenone reduces mortality 30 days after randomization following acute myocardial infarction in patients with left ventricular systolic dysfunction and heart failure. J Am Coll Cardiol 2005;46:425-431.

405. Aikawa Y, Rohde L, Plehn J, et al. Regional wall stress predicts ventricular remodeling after anteroseptal myocardial infarction in the Healing and Early Afterload Reducing Trial (HEART): an echocardiography-based structural analysis. Am Heart J 2001;141:234-242.

406. Solomon SD, Skali H, Anavekar NS, et al. Changes in ventricular size and function in patients treated with valsartan, captopril, or both after myocardial infarction. Circulation 2005;111:3411-3419.

407. Wong M, Johnson G, Shabetai R, et al. Echocardiographic variables as prognostic indicators and therapeutic monitors in chronic congestive heart failure. Veterans Affairs cooperative studies V-HeFT I and II. V-HeFT VA Cooperative Studies Group. Circulation 1993;87(6 Suppl):VI-65-70.

408. Wong M, Staszewsky L, Latini R, et al. Severity of left ventricular remodeling defines outcomes and response to therapy in heart failure: Valsartan heart failure trial (Val-HeFT) echocardiographic data. J Am Coll Cardiol 2004;43:2022-2027.

409. Lonn E, Bosch J, Yusuf S, et al. for the HOPE and HOPE-TOO Trial Investigators. Effects of long-term vitamin E supplementation on cardiovascular events and cancer: a randomized controlled trial. JAMA 2005;293:1338-1347.

410. Yusuf S, Sleight P, Pogue J, et al. Effects of an angiotensin-converting-enzyme inhibitor, ramipril, on cardiovascular events in high-risk patients. The Heart Outcomes Prevention Evaluation Study Investigators. N Engl J Med 2000;342:145-153.

411. Jong P, Yusuf S, Rousseau MF, et al. Effect of enalapril on 12-year survival and life expectancy in patients with left ventricular systolic dysfunction: a follow-up study. Lancet 2003;361:1834-1848.

412. Hall AS, Murray GD, Ball SG. Follow-up study of patients randomly allocated ramipril or placebo for heart failure after acute myocardial infarction: AIRE Extension (AIREX) Study. Lancet 1997;349:1493-1497.

413. Dahlof B, Devereux RB, Kjeldsen SE, et al. for the LIFE Study Group. Cardiovascular morbidity and mortality in the Losartan Intervention For Endpoint reduction in hypertension study (LIFE): a randomised trial against atenolol. Lancet 2002;359:995-1003.

414. Devereux RB, Roman MJ, Palmieri V, et al. Left ventricular wall stresses and wall stress-mass-heart rate products in hypertensive patients with electrocardiographic left ventricular hypertrophy: the LIFE study. Losartan Intervention For Endpoint reduction in hypertension. J Hypertens 2000;18: 1129-1138.

415. Lopez-Sendon J, Swedberg K, McMurray J, et al. for the Task Force on ACE-inhibitors of the European Society of Cardiology. Expert consensus document on angiotensin converting enzyme inhibitors in cardiovascular disease. The Task Force on ACE-inhibitors of the European Society of Cardiology. Eur Heart J 2004;25:1454-1470.

416. Jugdutt BI. Nitric oxide in heart failure: friend or foe. Heart Failure Reviews 2002;7:385-389.

417. Jugdutt BI. Nitric oxide and cardiovascular protection. Heart Failure Reviews 2003;8:29-34.

418. Jugdutt BI, comp. The Role of Nitric Oxide in Heart Failure. Norwell: Kluwer Academic Publishers, 2004. ISBN 1-4020-7736-X

419. Stewart DD. Remarkable tolerance to nitroglycerine. Philadelphia Polyclinic 1888;6:43.

420. Prodger SH, Ayman D. Harmful effects of nitroglycerin: With special reference to coronary thrombosis. Am J Med Sci 1932;184:480-491.

421. Pratt CM, Mahmarian JJ, Morales-Ballejo H, et al. for the Transdermal Nitroglycerin Investigators Group. [Named Investigator in List]. Design of a randomized, placebo-controlled multicenter trial on the long-term effects of intermittent transdermal nitroglycerin on left ventricular remodeling after acute myocardial infarction. Am J Cardiol 1998;81:719-724.

422. Ishikawa K, Kanamasa K, Ogawa I, et al. Long-term nitrate treatment increases cardiac events in patients with healed myocardial infarction. Secondary Prevention Group. Jpn Circ J 1996;60:779-788.

423. Nakamura Y, Moss AJ, Brown MW, Kinoshita M, Kawai C. Long-term nitrate use may be deleterious in ischemic heart disease: A study using the databases from two large-scale postinfarction studies. Multicenter Myocardial Ischemia Research Group. Am Heart J 1999;138:577-585.

424. Rossetti E, Luca C, Bonetti F, Chierchia SL. Transdermal nitroglycerin reduces the frequency of anginal attacks but fails to prevent silent ischemia. J Am Coll Cardiol 1993;21:337-342.

425. DeMots H, Glasser SP. Intermittent transdermal nitroglycerin therapy in the treatment of chronic stable angina. J Am Coll Cardiol 1989;13:786-795.

426. Munzel T, Daiber A, Mulsch A. Explaining the phenomenon of nitrate tolerance. Circ Res 2005;97:618-628.

427. Murad F. Cellular signaling with nitric oxide and cyclic GMP. Braz J Med Biol Res 1999;32:1317-1327.

428. Chen Z, Zhang J, Stamler JS. Identification of the enzymatic mechanism of nitroglycerin bioactivation. Proc Natl Acad Sci U S A 2002;99:8306-8311.

429. Nunez C, Victor VM, Tur R, et al. Discrepancies between nitroglycerin and NO-releasing drugs on mitochondrial oxygen consumption, vasoactivity, and the release of NO. Circ Res 2005;97:1063-1069.

430. Sydow K, Daiber A, Oelze M, et al. Central role of mitochondrial aldehyde dehydrogenase and reactive oxygen species in nitroglycerin tolerance and cross-tolerance. J Clin Invest 2004;113:482-489.

431. Saraiva RM, Minhas KM, Raju SV, et al. Deficiency of neuronal nitric oxide synthase increases mortality and cardiac remodeling after myocardial

infarction: role of nitroso-redox equilibrium. Circulation 2005;112:3415-3422.

432. Dawson D, Lygate CA, Zhang MH, Hulbert K, Neubauer S, Casadei B. nNOS gene deletion exacerbates pathological left ventricular remodeling and functional deterioration after myocardial infarction. Circulation 2005; 112:3729-3737.

433. Jugdutt BI. Nitric oxide and cardioprotection during ischemia-reperfusion. Heart Failure Reviews 2002;7:391-405. [**Appendix 46**]

434. Bauer JA, Fung HL. Concurrent hydralazine administration prevents nitroglycerin-induced hemodynamic tolerance in experimental heart failure. Circulation 1991;84:35-39.

435. Taylor AL, Ziesche S, Yancy C, et al. for the African-American Heart Failure Trial Investigators. Combination of isosorbide dinitrate and hydralazine in blacks with heart failure. N Engl J Med 2004;351:2049-2057.

436. Munzel T, Kurz S, Rajagopalan S, et al. Hydralazine prevents nitroglycerin tolerance by inhibiting activation of a membrane-bound NADH oxidase. A new action for an old drug. J Clin Invest 1996;98:1465-1470.

437. Nelson GI, Ahuja RC, Silke B, Hussain M, Taylor SH. Arteriolar or venous dilatation in left ventricular failure following acute myocardial infarction: a haemodynamic trial of hydralazine and isosorbide dinitrate. J Cardiovasc Pharmacol 1983;5:574-579.

438. Angus DC, Linde-Zwirble WT, Tam SW, et al. for the African-American Heart Failure Trial (A-HeFT) Investigators. Cost-effectiveness of fixed-dose combination of isosorbide dinitrate and hydralazine therapy for blacks with heart failure. Circulation 2005;112:3745-3753.

439. Taylor AL, Wright JT Jr. Should ethnicity serve as the basis for clinical trial design? Importance of race/ethnicity in clinical trials: lessons from the African-American Heart Failure Trial (A-HeFT), the African-American Study of Kidney Disease and Hypertension (AASK), and the Antihypertensive and Lipid-Lowering Treatment to Prevent Heart Attack Trial (ALLHAT). Circulation 2005;112:3654-3666.

440. Cruickshank JM. Coronary flow reserve and the J curve relation between diastolic blood pressure and myocardial infarction. BMJ 1988;297:1227-1230.

441. Lewis EF, Moye LA, Rouleau JL, et al. Predictors of late development of heart failure in stable survivors of myocardial infarction: the CARE study. J Am Coll Cardiol 2003 42:1446-1453.

442. Bolognese L, Neskovic AN, Parodi G, et al. Left ventricular remodeling after primary coronary angioplasty: patterns of left ventricular dilation and long-term prognostic implications. Circulation 106:2351-2357, 2002.

443. Frangogiannis NG, Smith CW, Entman ML. The inflammatory response in myocardial infarction. Cardiovasc Res 2002;53:31-47

444. Lee L, Campbell R, Scheuermann-Freestone M, et al. Metabolic modulation with perhexiline in chronic heart failure: a randomized, controlled trial of short-term use of a novel treatment. Circulation 2005; 112:3280-3288.

445. Ince H, Petzsch M, Kleine HD, et al. Preservation from left ventricular remodeling by front-integrated revascularization and stem cell liberation in evolving acute myocardial infarction by use of granulocyte-colony-stimulating factor (FIRSTLINE-AMI). Circulation 2005;112:3097-3106.

446. Anversa P, Nadal-Ginard B. Myocyte renewal and ventricular remodelling. Nature 2002;415:240-243.

447. Ohno M, Takemura G, Ohno A, et al. "Apoptotic" myocytes in infarct area in rabbit hearts may be oncotic myocytes with DNA fragmentation: analysis by immunogold electron microscopy combined with In situ nick end-labeling. Circulation 1998;98:1422-1430.

448. Haunstetter A, Izumo S: Apoptosis: basic mechanisms and implications for cardiovascular disease. Circ Res 1998;82:1111-1129.

449. Anversa P, Leri A, Kajstura J: Myocardial basis for heart failure: role of cell death. In: D. L. Mann,ed. Heart Failure. A Companion to Braunwald's Heart Disease. Pennsylvania: Saunders, 2004; 71-89

450. Dumont EA, Reutelingsperger CP, Smits JF, et al. Real-time imaging of apoptotic cell-membrane changes at the single-cell level in the beating murine heart. Nat Med 2001;7:1352-1355.

451. Narula J, Acio ER, Narula N, et al. Annexin-V imaging for noninvasive detection of cardiac allograft rejection. Nat Med 2001;7:1347-1352.

452. Jugdutt BI. Recruitment of ventricular function with adjunctive nitrate therapy after late reperfusion. In: Singal PK, Beamish RG, Dhalla NS, eds.

Mechanisms of Heart Failure. Boston: Kluwer Academic Publishers, 1995; 425-432.

453. Yaoita H, Ogawa K, Maehara K, Maruyama Y. Attenuation of ischemia/reperfusion injury in rats by a caspase inhibitor. Circulation 1998; 97:276-281.

454. Jugdutt BI, Menon V. AT_2 receptor and apoptosis during AT_1 receptor blockade in reperfused myocardial infarction in the rat. Mol and Cell Biochem 2004;262:203-214.

455. Goussev A, Sharov VG, Shimoyama H, et al. Effects of ACE inhibition on cardiomyocyte apoptosis in dogs with heart failure. Am J Physiol 1998;275: H626-H631.

456. Chandrashekhar Y, Sen S, Anway R, Shuros A, Anand I. Long-term caspase inhibition ameliorates apoptosis, reduces myocardial troponin-I cleavage, protects left ventricular function, and attenuates remodeling in rats with myocardial infarction. J Am Coll Cardiol 2004;43:295-301.

457. Louis A, Cleland JG, Crabbe S, et al. Clinical Trials Update: CAPRICORN, COPERNICUS, MIRACLE, STAF, RITZ-2, RECOVER and RENAISSANCE and cachexia and cholesterol in heart failure. Highlights of the Scientific Sessions of the American College of Cardiology. Eur J Heart Fail 2001;3:381-7.

458. Solomon SD, McMurray JJ, Pfeffer MA, et al. for the Adenoma Prevention with Celecoxib (APC) Study Investigators. Cardiovascular risk associated with celecoxib in a clinical trial for colorectal adenoma prevention. N Engl J Med 2005;352:1071-1080.

459. Drazen JM. COX-2 inhibitors--a lesson in unexpected problems. N Engl J Med 2005;352:1131-1132.

460. Weber KT. Extracellular matrix remodeling in heart failure. A role for de novo angiotensin II generation. Circulation 1997;96:4065-4082

461. Sawicki G, Menon V, Jugdutt BI. Improved balance between TIMP-3 and MMP-9 after regional myocardial ischemia-reperfusion during AT_1 receptor blockade. J Cardiac Failure 2004;10:442-449

462. Cheung P-Y, Sawicki G, Wozniak M, Wang W, Radomski MW, Schulz R. Matrix metalloproteinase-2 contributes to ischemia-reperfusion injury in the heart. Circulation 2000;101:1833-1839.

463. Li YY, Feldman AM, Sun Y, McTiernan CF. Differential expression of tissue inhibitors of metalloproteinases in the failing human heart. Circulation. 1998;98:1728-1734.

464. Heymans S, Luttun A, Nuyens D, et al. Inhibition of plasminogen activators or matrix metalloproteinases prevents cardiac rupture but impairs therapeutic angiogenesis and causes cardiac failure. Nat Med 1999;5:1135-1142

465. Peterson JT, Hallak H, Johnson L, et al. Matrix metalloproteinase inhibition attenuates left ventricular remodeling and dysfunction in a rat model of progressive heart failure. Circulation 2001;103:2303-2309

466. Mukherjee R, Brinsa TA, Dowdy KB, et al. Myocardial infarct expansion and matrix metalloproteinase inhibition. Circulation 2003;107:618-625

467. Yarbrough WM, Mukherjee R, Escobar GP, et al. Selective targeting and timing of matrix metalloproteinase inhibition in post-myocardial infarction remodeling. Circulation 2003;108:1753-1759

468. Mukherjee R, Parkhurst AM, Mingoia JT, et al. Myocardial remodeling after discrete radiofrequency injury: effects of tissue inhibitor of matrix metalloproteinase-1 gene deletion. Am J Physiol Heart Circ Physiol 2004; 286:H1242-H1247

469. Hayashidani S, Tsutsui H, Ikeuchi M, et al. Targeted deletion of MMP-2 attenuates early LV rupture and late remodeling after experimental myocardial infarction. Am J Physiol Heart Circ Physiol 2003;285:H1229-H1235

470. Matsumura S, Iwanaga S, Mochizuki S, Okamoto H, Ogawa S, Okada Y. Targeted deletion or pharmacological inhibition of MMP-2 prevents cardiac rupture after myocardial infarction in mice. J Clin Invest 2005;115:599-609

471. Gruberg L. Coverage of late breaking trials of the American College of Cardiology 2005 Annual Scientific Session. Weaver WD. PREMIER: Prevention of MI Early Remodeling-The Effects of PG-116800. Medscape 2005, http://www.medscape.com/ viewarticle/501553

472. Jugdutt BI, Sawicki G. AT_1 receptor blockade alters metabolic, functional and structural proteins after reperfused myocardial infarction. Detection using proteomics. Mol and Cell Biochem 2004;263:179-188.

473. Sawicki G, Jugdutt BI. Detection of changes in protein levels in the in vivo canine model of acute heart failure following ischemia-reperfusion injury – Functional proteomics studies. Proteomics 2004;4:2195-2202.

474. Starling RC, Jessup M. Worldwide clinical experience with the CorCap Cardiac Support Device. J Card Fail 2004;10(6 Suppl):S225-S233.

475. Batista RJ, Santos JL, Takeshita N, Bocchino L, Lima PN, Cunha MA. Partial left ventriculectomy to improve left ventricular function in end-stage heart disease. J Card Surg 1996;11:96-97.

476. Kass DA, Baughman KL, Pak PH, et al. Reverse remodeling from cardiomyoplasty in human heart failure. External constraint versus active assist. Circulation 1995;91:2314-2318.

477. St John Sutton MG, Plappert T, Abraham WT, et al. for the Multicenter InSync Randomized Clinical Evaluation (MIRACLE) Study Group. Effect of cardiac resynchronization therapy on left ventricular size and function in chronic heart failure. Circulation 2003;107:1985-1990.

478. Leor J, Cohen S. Myocardial tissue engineering: creating a muscle patch for a wounded heart. Ann N Y Acad Sci 2004;1015:312-319.

479. Anand IS, Fisher LD, Chiang YT, et al. for the Val-HeFT Investigators. Changes in brain natriuretic peptide and norepinephrine over time and mortality and morbidity in the Valsartan Heart Failure Trial (Val-HeFT). Circulation 2003;107:1278-1283.

480. Kinjo K, Sato H, Ohnishi Y, et al. for the Osaka Acute Coronary Insufficiency Study (OACIS)) Group. Impact of high-sensitivity C-reactive protein on predicting long-term mortality of acute myocardial infarction. Am J Cardiol 2003;91:931-935.

481. Bradham WS, Bozkurt B, Gunasinghe H, Mann D, Spinale FG. Tumor necrosis factor-alpha and myocardial remodeling in progression of heart failure: a current perspective. Cardiovasc Res 2002;53:822-830.

482. Inokubo Y, Hanada H, Ishizaka H, Fukushi T, Kamada T, Okumura K. Plasma levels of matrix metalloproteinase-9 and tissue inhibitor of metalloproteinase-1 are increased in the coronary circulation in patients with acute coronary syndrome. Am Heart J 2001;141:211-217

483. Kaden JJ, Demfle CE, Sueselbeck T, et al. Time-dependent changes in the plasma concentration of matrix metalloproteinase 9 after acute myocardial infarction. Cardiology 2003;99:140-14.

484. Renko J, Kalela A, Jaakkola O, et al. Serum matrix metalloproteinase-9 is elevated in men with a history of myocardial infarction. Scand J Clin Lab Invest 2004;64:255-261.

485. Kai H, Ikeda H, Yasukawa H, et al. Peripheral blood levels of matrix metalloproteases-2 and -9 are elevated in patients with acute coronary syndromes. J Am Coll Cardiol 1998;32:368-372.

486. Squire IB, Evans J, Ng LL, Loftus IM, Thompson MM. Plasma MMP-9 and MMP-2 following acute myocardial infarction in man: correlation with echocardiographic and neurohumoral parameters of left ventricular dysfunction. J Card Fail 2004;10:328-333.

487. Wilson EM, Gunasinghe HR, Coker MT, et al. Plasma matrix metalloproteinase and inhibitor profiles in patients with heart failure. J Card Fail 2002;8:390-398

488. Altieri P, Brunelli C, Garibaldi S, et al. Metalloproteinases 2 and 9 are increased in plasma of patients with heart failure. Eur J Clin Invest 2003;33:648-656

489. Sundstrom J, Evams JC, Benjamin EJ, et al. Relations of plasma matrix metalloproteinase-9 to clinical cardiovascular risk factors and echocardiographic left ventricular measures: the Framingham Heart Study. Circulation 2004;109:2850-2856

490. Zannad F, Alla F, Dousset B, et al. Limitation of excessive extracellular matrix turnover may contribute to survival benefit of spironolactone therapy in patients with congestive heart failure: insights from the randomized aldactone evaluation study (RALES). Rales Investigators. Circulation. 2000;102:2700-2706.

491. Uusimaa P, Risteli J, Niemela M, et al. Collagen scar formation after acute myocardial infarction: relationships to infarct size, left ventricular function, and coronary artery patency. Circulation. 1997;96:2565-72.

492. Sato Y, Kataoka K, Matsumori A, et al. Measuring serum aminoterminal type III procollagen peptide, 7S domain of type IV collagen, and cardiac troponin T in patients with idiopathic dilated cardiomyopathy and secondary cardiomyopathy. Heart 1997;78:505-508.

493. Host NB, Jensen LT, Bendixen PM, et al. The aminoterminal propeptide of type III procollagen provides new information on prognosis after acute myocardial infarction. Am J Cardiol 1995;76:869-873.

494. Klappacher G, Franzen P, Haab D, et al. Measuring extracellular matrix turnover in the serum of patients with idiopathic or ischemic dilated

cardiomyopathy and impact on diagnosis and prognosis. Am J Cardiol 1995;75:913-918.

495. Chen MM, Lam A, Abraham JA, et al. CTGF expression is induced by TGF-β in cardiac fibroblasts and cardiac myocytes: a potential role in heart fibrosis. J Mol Cell Cardiol. 2000;32:1805-1819.

496. Jugdutt BI. Monocytosis and adverse left ventricular remodeling after reperfused myocardial infarction. J Am Coll Cardiol. 2002;39:247-250.

497. Deswal A, Peterson NJ, Feldman AM, et al. Cytokines and cytokine receptors in advanced heart failure. An analysis of the cytokine database from the Vesnarinone Trial (VEST). Circulation. 2001;103:2055-2059.

498. Maekawa Y, Anzai T, Yoshikawa T, et al. Prognostic significance of peripheral monocytosis after reperfused acute myocardial infarction: a possible role for left ventricular remodeling. J Am Coll Cardiol. 2002;39:241-246.

499. Hoit BD, Suresh DP, Craft L, et al. β2-adrenergic receptor polymorphisms at amino acid 16 differentially influence agonist-stimulated blood pressure and peripheral blood flow in normal individuals. Am Heart J. 2000;139: 537-542.

500. Ueda S, Meredith PA, Morton JJ, et al. ACE (I/D) genotype as a predictor of the magnitude and duration of the response to an ACE inhibitor drug (enalaprilat) in humans. Circulation. 1998;98:2148-2153.

501. Rusnak JM, Kisabeth RM, Herbert DP, et al. Pharmacogenomics: A clinician's primer on emerging technologies for improved patient care. Mayo Clin Proc. 2001;76:299-309.

502. Feigenbaum H, Armstrong WF, Ryan T, comps. Specialized echocardiographic techniques and methods. In: Feigenbaum H, Armstrong WF, Ryan T, eds. Feigenbaum's Echocardiography. Philadelphia: Lippincott Williams & Wilkins, 2005;46-75.

503. Helle-Valle T, Crosby J, Edvardsen T, et al. New noninvasive method for assessment of left ventricular rotation: speckle tracking echocardiography. Circulation 2005;112:3149-3156.

504. Rogers WJ Jr, Kramer CM, Geskin G, et al. Early contrast-enhanced MRI predicts late functional recovery after reperfused myocardial infarction. Circulation 1999;99:744-750.

505. Su H, Spinale FG, Dobrucki LW, et al. Noninvasive targeted imaging of matrix metalloproteinase activation in a murine model of postinfarction remodeling. Circulation 2005;112:3157-167.

506. New RB, Sampson AC, King MK, et al. Effects of combined angiotensin II and endothelin receptor blockade with developing heart failure: effects on left ventricular performance. Circulation 2000;102:1447-1453.

507. Yu CM, Tipoe GL, Wing-Hon Lai K, et al. Effects of combination of angiotensin-converting enzyme inhibitor and angiotensin receptor antagonist on inflammatory cellular infiltration and myocardial interstitial fibrosis after acute myocardial infarction. J Am Coll Cardiol 2001;38:1207-1215.

508. Dzau VJ. Tissue renin-angiotensin system in myocardial hypertrophy and failure. Arch Intern Med 1993;153:937-942.

509. Leri A, Liu Y, Li B, et al. Up-regulation of AT_1 and AT_2 receptors in postinfarcted hypertrophied myocytes and stretch-mediated apoptotic cell death. Am J Pathol 2000;156:1663-1672.

510. Jugdutt BI, Menon V. Valsartan-induced cardioprotection involves angiotensin II type 2 receptor upregulation in dog and rat in vivo models of reperfused myocardial infarction. J Cardiac Failure 2004;10:74-82.

511. Jugdutt BI, Menon V. AT_1 receptor blockade limits myocardial injury and upregulates AT_2 receptors during reperfused myocardial infarction. Mol and Cell Biochem 2004;260:111-118.

512. Ford WR, Clanachan AS, Jugdutt BI. Opposite effects of angiotensin receptor antagonists on recovery of mechanical function after ischemia-reperfusion in isolated working rat hearts. Circulation 1996;94:3087-3089.

513. Xu Y, Clanachan AS, Jugdutt BI. Enhanced expression of AT_2R, IP_3R and PKC_ε during cardioprotection induced by AT_2R blockade. Hypertension 2000;36:506-510.

514. Levy BI. Can angiotensin II type 2 receptors have deleterious effects in cardiovascular disease? Implications for therapeutic blockade of the renin-angiotensin system. Circulation 2004;109:8-13.

515. Peng H, Carretero OA, Vuljaj N, et al. Angiotensin-converting enzyme inhibitors: a new mechanism of action. Circulation 2005;112:2436-2445.

516. Rigat B, Hubert C, Alhenc-Gelas F, Cambien F, Corvol P, Soubrier F. An insertion/deletion polymorphism in the angiotensin I-converting enzyme

gene accounting for half the variance of serum enzyme levels. J Clin Invest 1990;86:1343-1346.

517. Cambien F, Poirier O, Lecerf L, et al. Deletion polymorphism in the gene for angiotensin-converting enzyme is a potent risk factor for myocardial infarction. Nature 1992;359:641-644.

518. Agerholm-Larsen B, Nordestgaard BG, Tybjaerg-Hansen A. ACE gene polymorphism in cardiovascular disease: meta-analyses of small and large studies in whites. Arterioscler Thromb Vasc Biol 2000;20:484-492.

519. Anderson TJ, Elstein E, Haber H, et al. Comparative study of ACE-inhibition, angiotensin II antagonism, and calcium channel blockade on flow-mediated vasodilation in patients with coronary disease (BANFF study). J Am Coll Cardiol 2000;35:60-66.

520. Koch W, Mehilli J, von Beckerath N, Bottiger C, Schomig A, Kastrati A. Angiotensin I-converting enzyme (ACE) inhibitors and restenosis after coronary artery stenting in patients with the DD genotype of the ACE gene. J Am Coll Cardiol 2003;41:1957-1961.

521. Tsai CT, Lai LP, Lin JL, et al. Renin-angiotensin system gene polymorphisms and atrial fibrillation. Circulation 2004;109:1640-1646.

522. Weir MR, Gray JM, Paster R, et al. Differing mechanisms of action of angiotensin-converting enzyme inhibition in black and white hypertensive patients. The Trandolapril Multicenter Study Group. Hypertension 1995; 26:124-130.

523. Dries DL, Exner DV, Gersh BJ, et al. Racial differences in the outcome of left ventricular dysfunction. N Engl J Med 1999;340:609-616.

524. Exner DV, Dries DL, Domanski MJ, et al. Lesser response to angiotensin-converting-enzyme inhibitor therapy in black as compared with white patients with left ventricular dysfunction. N Engl J Med 2001;344:1351-1357.

APPENDIX

MODIFICATION OF LEFT VENTRICULAR GEOMETRY AND FUNCTION DURING HEALING AFTER ACUTE MYOCARDIAL INFARCTION

Bodh I.Jugdutt, MBChB, MSc

A thesis submitted in fulfillment of the requirements

for the degree of Doctor of Medicine (MD),

FACULTY OF MEDICINE, UNIVERSITY OF GLASGOW

The research was conducted in the Division of Cardiology,

Department of Medicine, Faculty of Medicine, University of Alberta,

Edmonton, Alberta, T6G 2R7, CANADA.

December 2004
Revised January 2006

LIST OF APPENDED ORIGINAL CONTRIBUTIONS
In order of citation in Volume 1

Appendix #
(Reference)

1 (19) Jugdutt BI, Cahn RL, Basualdo CA, Rossall RE. Measurement of left ventricular shape distortion. In, Ripley, KL, editor. Computers in Cardiology. Los Angeles: IEEE Computer Society Press, 1984:47-52.

2 (20) Jugdutt BI, Michorowski BL. Role of infarction expansion in rupture of the ventricular septum after acute myocardial infarction. A Two-Dimensional Echocardiographic study. Clin Cardiol 1987;10: 641-652.

3 (21) Jugdutt BI. Identification of patients prone to infarct expansion by the degree of regional shape distortion on an early two-dimensional echocardiogram after myocardial infarction. A prospective study. Clin Cardiol 1990;13: 28-40.

4 (22) Jugdutt BI. Prevention of ventricular remodelling post myocardial infarction: Timing and duration of therapy. Can J Cardiol 1993;9: 103-114.

5 (27) Jugdutt BI. Ventricular remodeling postinfarction and the extracellular collagen matrix. When is enough enough? Circulation 2003;108:1395-1403.

6 (28) Jugdutt BI, Warnica JW. Intravenous nitroglycerin therapy to limit myocardial infarct size, expansion and complications: effect of timing, dosage and infarct location. Circulation 1988;78:906-919.

7 (33) Maidens JM, Blinston GE, Jugdutt BI. Computer-assisted measurement of regional and global left ventricular shape distortion after myocardial infarction. In, Computers in Cardiology. Los Angeles: IEEE Computer Society Press, 1987:413-416.

8 (34) Jugdutt BI, Michorowski BL, Kappagoda TC. Exercise training after anterior Q wave myocardial infarction: importance of regional left ventricular function and topography. J Am Coll Cardiol 1988;12: 362-372.

9 (35) Jugdutt BI, Basualdo CA. Myocardial infarct expansion during indomethacin and ibuprofen therapy for symptomatic post-infarction pericarditis: Effect of other pharmacologic agents during early remodelling. Can J Cardiol. 1989;5:211-221.

10 (36) Johnston BJ, Blinston GE, Jugdutt BI. Overestimation of myocardial infarct size on two-dimensional echocardiograms due to remodeling of the infarct zone. Can J Cardiol 1994;10:77-86.

11 (37) Jugdutt BI. Prevention of ventricular remodeling after myocardial infarction and in congestive heart failure. Heart Failure Reviews 1996; 1:115-129.

12 (41) Jugdutt BI, Amy RW. Healing after myocardial infarction in the dog: changes in infarct hydroxyproline and topography. J Am Coll Cardiol 1986;7:91-102.

13 (48) Jugdutt BI, Khan MI, Jugdutt SJ, Blinston GE. Impact of left ventricular unloading after late reperfusion of canine anterior myocardial infarction on remodeling and function using isosorbide-5-mononitrate. Circulation 1995;92:926-934.

14 (49) Jugdutt BI. Effect of reperfusion on ventricular mass, topography and function during healing of anterior infarction. Am J Physiol 1997;272: H1205-1211.

15 (50) Jugdutt BI, Schwarz-Michorowski BL, Tymchak WJ, Burton JR. Prompt improvement of left ventricular function and topography with combined reperfusion and intravenous nitroglycerin in acute myocardial infarction. Cardiology 1997;88:170-179.

16 (55) Jugdutt BI. Delayed effects of early infarct-limiting therapies on healing after myocardial infarction. Circulation 1985;72: 907-914.

17 (63) Michorowski B, Senaratne PJM, Jugdutt BI. Myocardial infarct expansion. Cardiovasc Rev Rep 1987;8: 42-47.

18 (67) Michorowski B, Senaratne PJM, Jugdutt BI. Deterring myocardial infarct expansion. Cardiovasc Rev Rep 1987;8: 55-62.

19 (73) Jugdutt BI, Khan MI. Impact of increased infarct transmurality on remodeling and function during healing after anterior myocardial infarction in the dog. Can J Physiol Pharmacol 1992;70:949-958.

20 (74) Jugdutt BI, Tang SB, Khan MI, Basualdo CA. Functional impact on remodeling during healing after non-Q-wave versus Q-wave anterior myocardial infarction in the dog. J Am Coll Cardiol 1992;20:722-731.

21 (100) Jugdutt BI. Intravenous nitroglycerin unloading in acute myocardial infarction. Am J Cardiol. 1991;68:52D-63D.

22 (102) Jugdutt BI. Effect of nitroglycerin and ibuprofen on left ventricular topography and rupture threshold during healing after myocardial infarction in the dog. Can J Physiol Pharmacol 1988;66:385-395.

23 (103) Jugdutt BI, Khan MI. Effect of prolonged nitrate therapy on left ventricular remodeling after canine acute myocardial infarction. Circulation 1994;89:2297-2307.

24 (105) Jugdutt BI, Michorowski BL, Tymchak WJ. Improved left ventricular function and topography by prolonged nitroglycerin therapy after acute myocardial infarction. Z Kardiol 1989;78: Suppl 2; 127-129.

25 (108) Jugdutt BI, Tymchak W, Humen D, Gulamhusein S, Hales M. Prolonged nitroglycerin versus captopril therapy on remodeling after transmural myocardial infarction. (Abstract) Circulation 1990;82 (Suppl III):III-442.

26 (109) Jugdutt BI, Michorowski BL, Tymchak WJ. Improved left ventricular geometry and function by prolonged nitroglycerin therapy after acute myocardial infarction. In, Lewis BS and Kimchi A, editors. Chronic Heart Failure - Mechanisms and Management. I. Quality of Life, II Nitrate Therapy. New York: Springer-Verlag, 1990:266-271.

27 (118) Jugdutt BI, Warnica JW. Tolerance with low dose intravenous nitroglycerin therapy in acute myocardial infarction. Am J Cardiol 1989; 64:581-587.

28 (122) Jugdutt BI. Myocardial salvage by intravenous nitroglycerin in conscious dogs: loss of beneficial effect with marked nitroglycerin-induced hypotension. Circulation 1983;68:673-684.

29 (126) Jugdutt BI, Michorowski BL, Khan MI. Effect of long-term captopril therapy on left ventricular remodeling and function during healing of canine myocardial infarction. J Am Coll Cardiol 1992;19:713- 723.

30 (127) Jugdutt BI, Khan MI, Jugdutt SJ, Blinston GE. Effect of enalapril on ventricular remodeling and function during healing after anterior myocardial infarction in the dog. Circulation 1995;91:802-812.

31 (128) Jugdutt BI. Effect of captopril and enalapril on left ventricular geometry, function and collagen during healing after anterior and inferior myocardial infarction in the dog. J Am Coll Cardiol 1995;25:1718-1725.

32 (129) Jugdutt BI, Lucas A, Khan MI. Effect of angiotensin-converting-enzyme inhibition on infarct collagen and remodeling during healing after transmural canine myocardial infarction. Can J Cardiology 1997;13:657-668.

33 (131) Jugdutt BI, Khan MI, Jugdutt SJ, Blinston GE. Combined captopril and isosorbide dinitrate during healing after myocardial infarction. Effect on remodeling, function, mass and collagen. J Am Coll Cardiol 1995;25: 1089-1096.

34 (227) Jugdutt BI. Different relations between infarct size and occluded bed size in barbiturate-anesthetized versus conscious dog. J Am Coll Cardiol 1985;6:1035-1046.

35 (228) Jugdutt BI. Difference in the relation between infarct and occluded bed in pentobarbital-anesthetized and conscious dogs. Can J Physiol Pharmacol 1986;64: 254-262.

36 (232) Jugdutt BI, Sussex BA, Warnica JW, Rossall RE. Persistent reduction in left ventricular asynergy in patients with acute myocardial infarction by intravenous infusion of nitroglycerin. Circulation 1983;68:1264-1273.

37 (250) Jugdutt BI. Intravenous nitroglycerin infusion in acute myocardial infarction: myocardial salvage. Cardiovasc Rev Rep 1984;5:1145-1163 and Master Teacher Award 1990;11:53-67.

38 (274) Jugdutt BI, Khan MI, Johnston BJ, Jugdutt SJ, Blinston GE. Progressive changes in regional and global left ventricular dilation during remodeling post-myocardial infarction. (Abstract) J Am Coll Cardiol 1994;23:269A.

39 (278) Jugdutt BI. Remodeling of the myocardium and potential targets in the collagen degradation and synthesis pathways. Current Drug Targets, Cardiovascular & Haematological Disorders 2003;3:27-56.

40 (283) Jugdutt BI. Left ventricular rupture threshold during the healing phase after myocardial infarction in the dog. Can J Physiol Pharmacol 1987; 65:307-316.

41 (298) Jugdutt BI, Balghith M. Diastolic dysfunction during remodeling after myocardial infarction: Natural history and effect of prolonged ACE inhibition and nitrate therapy. (Abstract) Circulation 2001;104:II-430.

42 (315) Balghith M, Jugdutt BI. Assessment of diastolic dysfunction after acute myocardial infarction using Doppler Echocardiography. Can J Cardiol 2002;18:69-77.

43 (318) Jugdutt BI, Humen DP, Khan MI, Schwarz-Michorowski BL. Effect of left ventricular unloading with captopril on remodelling and function during healing of anterior transmural myocardial infarction in the dog. Can J Cardiol 1992;8:151-163.

44 (333) Jugdutt BI. Nitrates as anti-ischemic and cardioprotective agents. In: Singh BN, Dzau VJ, Vanhoutte P, Woosley RL, editors. Cardiovascular Pharmacology and Therapeutics. New York: Churchill Livingston, 1993:449-465.

45 (363) Jugdutt BI. Angiotensin II receptor blockers. In M.H. Crawford, editor. 1998 Cardiology Clinics Annual of Drug Therapy. Philadelphia: W.B. Saunders Publishers, 1998;Vol 2:1-17.

46 (433) Jugdutt BI. Nitric oxide and cardioprotection during ischemia-reperfusion. Heart Failure Reviews 2002;7:391-405.